BioMed Research International

Recent Advances in Understanding the Role of Genomic and Epigenomic Factors in Noncommunicable Diseases

Lead Guest Editor: Hossain U. Shekhar
Guest Editors: Sajib Chakraborty, Md. Kaiissar Mannoor, and Altaf H. Sarker

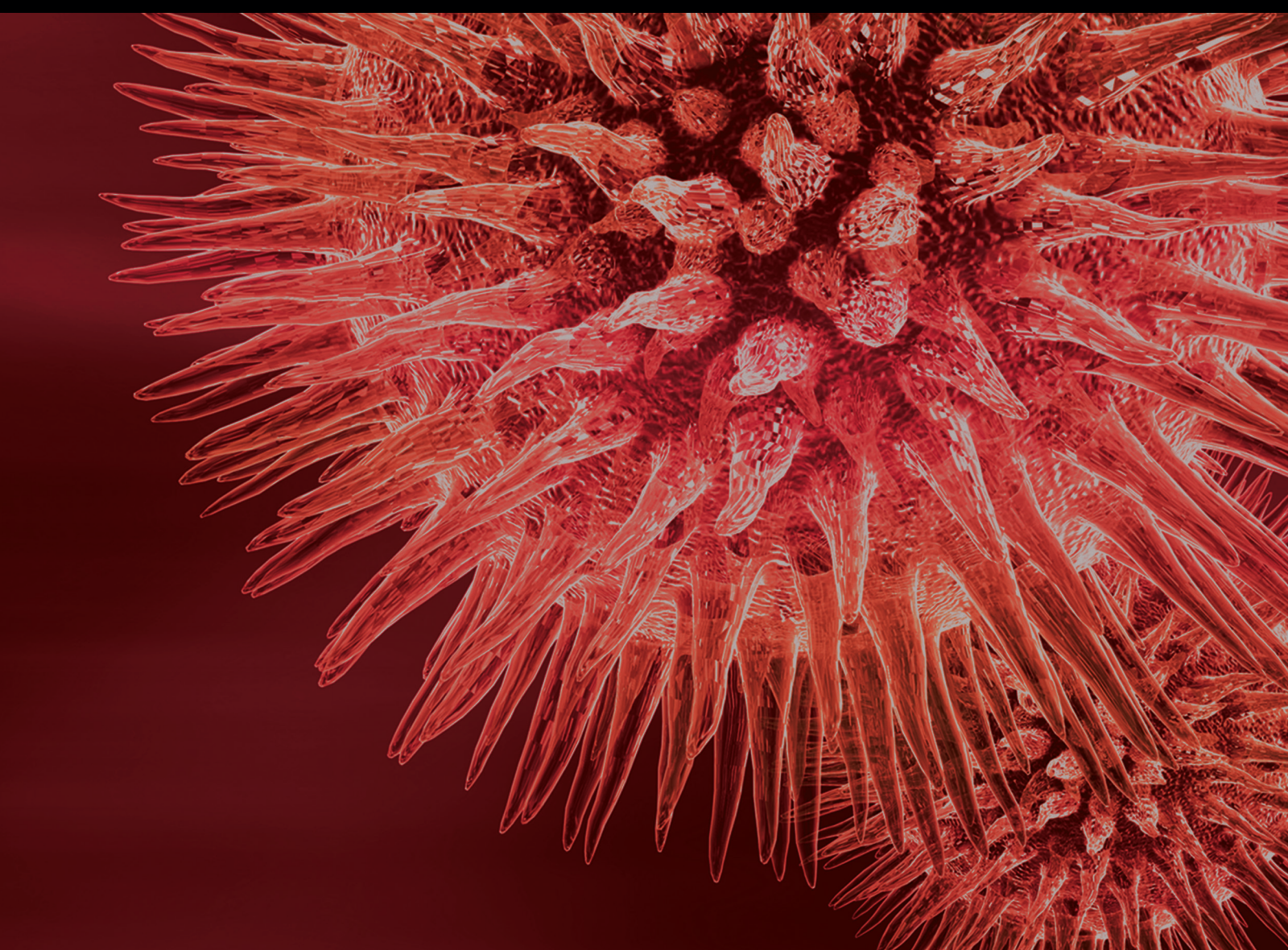

Recent Advances in Understanding the Role of Genomic and Epigenomic Factors in Noncommunicable Diseases

BioMed Research International

Recent Advances in Understanding the Role of Genomic and Epigenomic Factors in Noncommunicable Diseases

Lead Guest Editor: Hossain U. Shekhar
Guest Editors: Sajib Chakraborty, Md. Kaiissar Mannoor, and Altaf H. Sarker

Contents

Recent Advances in Understanding the Role of Genomic and Epigenomic Factors in Noncommunicable Diseases
Hossain U. Shekhar, Sajib Chakraborty, Kaiissar Mannoor, and Altaf H. Sarker
Editorial (2 pages), Article ID 1649873, Volume 2019 (2019)

Mutation Spectrum in TPO Gene of Bangladeshi Patients with Thyroid Dyshormonogenesis and Analysis of the Effects of Different Mutations on the Structural Features and Functions of TPO Protein through *In Silico* Approach
Mst. Noorjahan Begum, Md Tarikul Islam, Shekh Rezwan Hossain, Golam Sarower Bhuyan, Mohammad A. Halim, Imrul Shahriar, Suprovath Kumar Sarker, Shahinur Haque, Tasnia Kawsar Konika, Md. Sazzadul Islam, Asifuzzaman Rahat, Syeda Kashfi Qadri, Rosy Sultana, Suraiya Begum, Sadia Sultana, Narayan Saha, Mizanul Hasan, M. A. Hasanat, Hurjahan Banu, Hossain Uddin Shekhar, Emran Kabir Chowdhury, Abu A. Sajib, Abul B. M. M. K. Islam, Syed Saleheen Qadri, Firdausi Qadri, Sharif Akhteruzzaman, and Kaiissar Mannoor
Research Article (18 pages), Article ID 9218903, Volume 2019 (2019)

A Metabolomic Study on the Intervention of Traditional Chinese Medicine Qushi Huayu Decoction on Rat Model of Fatty Liver Induced by High-Fat Diet
Xiao-jun Gou, Shanshan Gao, Liang Chen, Qin Feng, and Yi-yang Hu
Research Article (14 pages), Article ID 5920485, Volume 2019 (2019)

Evaluation of Pathological Association between Stroke-Related QTL and Salt-Induced Renal Injury in Stroke-Prone Spontaneously Hypertensive Rat
Mohammad Farhadur Reza, Davis Ngarashi, Masamichi Koike, Masaki Misumi, Hiroki Ohara, and Toru Nabika
Research Article (7 pages), Article ID 5049746, Volume 2019 (2019)

Unveiling the Role of DNA Methylation in Kidney Transplantation: Novel Perspectives toward Biomarker Identification
Antonella Agodi, Martina Barchitta, Andrea Maugeri, Guido Basile, Matilde Zamboni, Giulia Bernardini, Daniela Corona, and Massimiliano Veroux
Review Article (8 pages), Article ID 1602539, Volume 2019 (2019)

Age-Specific Cut-off Values of Amino Acids and Acylcarnitines for Diagnosis of Inborn Errors of Metabolism Using Liquid Chromatography Tandem Mass Spectrometry
Suprovath Kumar Sarker, Md Tarikul Islam, Aparna Biswas, Golam Sarower Bhuyan, Rosy Sultana, Nusrat Sultana, Shagoofa Rakhshanda, Mst. Noorjahan Begum, Asifuzzaman Rahat, Sharmina Yeasmin, Mowshori Khanam, Asim Kumar Saha, Farjana Akther Noor, Abu A. Sajib, Abul B. M. M. K. Islam, Syeda Kashfi Qadri, Mohammod Shahidullah, Mohammad Abdul Mannan, A. K. M. Muraduzzaman, Tahmina Shirin, Sheikh Maksudur Rahman, Syed Saleheen Qadri, Narayan Saha, Sharif Akhteruzzaman, Firdausi Qadri, and Kaiissar Mannoor
Research Article (11 pages), Article ID 3460902, Volume 2019 (2019)

RNF213 Variant Diversity Predisposes Distinct Populations to Dissimilar Cerebrovascular Diseases
Jing Lin and Wenli Sheng
Review Article (7 pages), Article ID 6359174, Volume 2018 (2019)

Cutaneous Malignancy due to Arsenicosis in Bangladesh: 12-Year Study in Tertiary Level Hospital
Md. Iqbal Mahmud Choudhury, Nilufar Shabnam, Tazin Ahsan, S. M. Abu Ahsan, Md. Saiful Kabir, Rashed Md. Khan, Md. Abdal Miah, Mohd. Kamal Uddin, and Md. Aminur Rashid Liton
Research Article (9 pages), Article ID 4678362, Volume 2018 (2019)

Effect of Comorbidity on Lung Cancer Diagnosis Timing and Mortality: A Nationwide Population-Based Cohort Study in Taiwan
Shinechimeg Dima, Kun-Huang Chen, Kung-Jeng Wang, Kung-Min Wang, and Nai-Chia Teng
Research Article (9 pages), Article ID 1252897, Volume 2018 (2019)

Onco-Multi-OMICS Approach: A New Frontier in Cancer Research
Sajib Chakraborty, Md. Ismail Hosen, Musaddeque Ahmed, and Hossain Uddin Shekhar
Review Article (14 pages), Article ID 9836256, Volume 2018 (2019)

Complement System and Age-Related Macular Degeneration: Implications of Gene-Environment Interaction for Preventive and Personalized Medicine
Andrea Maugeri, Martina Barchitta, Maria Grazia Mazzone, Francesco Giuliano, and Antonella Agodi
Review Article (13 pages), Article ID 7532507, Volume 2018 (2019)

Polymorphisms of TNF-α -308 G/A and IL-8 -251 T/A Genes Associated with Urothelial Carcinoma: A Case-Control Study
Chia-Chang Wu, Yung-Kai Huang, Chao-Yuan Huang, Horng-Sheng Shiue, Yeong-Shiau Pu, Chien-Tien Su, Ying-Chin Lin, and Yu-Mei Hsueh
Research Article (8 pages), Article ID 3148137, Volume 2018 (2019)

Hindawi
BioMed Research International
Volume 2019, Article ID 1649873, 2 pages
https://doi.org/10.1155/2019/1649873

Editorial

Recent Advances in Understanding the Role of Genomic and Epigenomic Factors in Noncommunicable Diseases

Hossain U. Shekhar[1], **Sajib Chakraborty**[1], **Kaiissar Mannoor**[2] **and Altaf H. Sarker**[3]

[1]*Department of Biochemistry and Molecular Biology, University of Dhaka, Bangladesh*
[2]*Genetics and Genomics Laboratory Institute for Developing Science and Health Initiatives, Bangladesh*
[3]*Lawrence Berkeley Lab, USA*

Correspondence should be addressed to Sajib Chakraborty; sajib@du.ac.bd

Received 27 January 2019; Accepted 21 February 2019; Published 8 April 2019

The NGS based whole genome and exome sequencing endeavors have identified a plethora of mutations in the coding regions of the human genome that are held responsible as the causative factors for various human noncommunicable diseases including cancer. These mutations encompass various nonsynonymous nucleotide substitutions causing missense, nonsense, and frameshift changes in the protein-coding genes. For these types of mutations it is easier to establish a causal link between these mutations and disease phenotypes as they tend to change the amino acids in the proteins resulting in their loss-of-function (of tumor suppressor genes) or gain-of-function (of oncogenes) which might be directly responsible for the disease such as cancer. Apart from these disease-causing mutations, vast majority (more than 80%) of single-nucleotide polymorphisms were distributed throughout the human genome, mostly in the noncoding regions such as introns and intergenic regions [1]. Large body of evidence suggested that variants in the noncoding regions can be considered as genetic predisposition to many noncommunicable diseases including cancer [2]. For instance, genome-wide association studies (GWAS) have provided statistical evidence that numerous single-nucleotide variants/polymorphisms (SNVs/SNPs) in the noncoding regions are associated with increased risk of complex diseases [3]. The direct causal relationship between allelic variants originating from SNPs and disease phenotype becomes obscure when the variation occurs in noncoding regions. Initially it was suggested that the risk variants identified by GWAS may possibly be physically associated with a neighboring protein-coding gene that is the true causative variant. However another plausible explanation is that genetic variations residing in the functional but noncoding regions may have an impact on nearby genes. Recent GWAS studies have revealed that the SNPs that are associated with diseases are preferentially concentrated in the noncoding but functional genomic regions such as enhancer elements, DNase hypersensitivity regions, and epigenetically important chromatin marks [4]. A recent study highlighted the importance of the SNPs in the noncoding regions of human genome and their functional consequences in terms of genetic propensity to cancer. This seminal study conducted by Hua *et al.* sought to uncover the underlying mechanism of prostate cancer risk-associated SNP (rs11672691) in the promoter region of a long noncoding RNA (LncRNA) [5]. SNP-rs11672691 resides in the promoter region of the short isoform of the lncRNA-PCAT19 (PACT19-short). This short form of the lncRNA is encoded by the third intron of the long isoform of lncRNA-PCAT19 (PACT19-long) gene. The allelic risk-variant due to SNP-rs11672691 is typically associated with reduced and elevated expression of short and long isoforms, respectively. The region harboring the risk-SNP has both promoter and enhancers capability and thereby considered as bifunctional. The SNP-rs11672691 in this region hinders the physical interaction of the transcription factor NKX3.1 and YY1 to the promoter of PCAT19-short leading to the diminished promoter activity without losing its functional

capacity as enhancer for PCAT19-long. As a consequence the decreased and increased expression of PCAT19-short and PCAT19-long, respectively, occur in the individuals who are at risk of prostate cancer since PCAT19-long in concert with other genes transcriptionally induces certain cell cycle genes which in turn increase the risk of prostate cancer [5]. This study not only highlights the importance of the SNPs in the noncoding regions but also mechanistically shows how a single SNP can control the expression levels of two functional isoforms of lncRNAs.

This special issue underscored the roles of many genetic factors in the predisposition of variety of diseases including cancer, stroke, and cerebrovascular diseases and highlighted the influence of epigenetic modifications in kidney transplantation. For instance, *C.-C. Wu et al.* determined the genetic predisposition of urothelial carcinoma due to SNPs of inflammation associated genes, TNF-α and IL-8. Following the similar argument, in a review paper *J. Lin and W. Sheng* summarized the association of NF213 variant diversity with cerebrovascular diseases. Following the same line, Mst. N. Begum et al. revealed how the substitutions mutations (SNPs) in thyroid peroxidase (TPO) gene contribute to the thyroid dyshormonogenesis (TDH) in Bangladeshi patients. Apart from the uncovering the variations in genetic level, *A. Agodi* et al. emphasized the clinical potential of epigenetic modification in the form of DNA methylation in chronic kidney disease (CKD) and complications after kidney transplantation. In this review article the authors hypothesized that identifying DNA-methylation status in patients undergoing kidney transplantation has the potential to develop key strategies to prevent as well as treat the complications that typically arise from kidney transplantation procedure. In this special issue two of the published studies conducted by *S. K. Sarker* et al. and *X. Gou* et al. employed metabolomics methods to identify markers for inborn errors of metabolisms (IEMs) and drug-mechanism, respectively. Apart from these studies *M. F. Reza* et al. identified that a QTL region residing on chromosome 18 may play a role in modulating the response towards salt-induced renal injury in a blood pressure independent mechanism. *S. Dima* et al. conducted an epidemiological study to those lung cancer patients with preexisting comorbidity although it may result in the early diagnosis of lung cancer; adverse consequences of comorbidity may present a challenge in the treatment of older cancer patients. M. I. M. *Choudhury* et al. performed a similar epidemiological study to identify the incidence rate of cutaneous malignancy in Bangladesh. In a comprehensive review article, *A. Maugeri* et al. presented a detailed summary regarding the role of complement system and its genetic variants in "age-related macular degeneration (AMD)", emphasizing the modulatory role of the interplays between genetic and environmental factors and their consequences on AMD onset, progression, and therapeutic response. In a comprehensive review, *S. Chakraborty* et al. argued in favor of multi-OMICS approaches instead of single OMICS study for cancer research. In the article the authors highlighted several examples where multi-OMICS studies were used to dissect the cellular response to chemo- or immunotherapy as well as discover molecular candidates for cancer. In summary the authors focused on the application of different multi-OMICS approaches in the field of cancer research and discussed how these approaches are shaping the field of personalized oncomedicine.

In light of the published articles in this special issue, it can be safely assumed that genetic variants as well as epigenetic factors should be investigated in-depth to understand their biological functions in human noncommunicable diseases. Study of the factors in both genomic and epigenomic levels may facilitate the discovery of biomarkers to assess the risk, diagnosis, and prognosis of noncommunicable diseases.

Conflicts of Interest

The editors declare that they have no conflicts of interest regardingthe publication of this special issue.

Hossain U. Shekhar
Sajib Chakraborty
Kaiissar Mannoor
Altaf H. Sarker

References

[1] T. A. Manolio, F. S. Collins, N. J. Cox et al., "Finding the missing heritability of complex diseases," *Nature*, vol. 461, no. 7265, pp. 747–753, 2009.

[2] A. Sud, B. Kinnersley, and R. S. Houlston, "Genome-wide association studies of cancer: Current insights and future perspectives," *Nature Reviews Cancer*, vol. 17, no. 11, pp. 692–704, 2017.

[3] C. Q. Chang, A. Yesupriya, J. L. Rowell et al., "A systematic review of cancer GWAS and candidate gene meta-analyses reveals limited overlap but similar effect sizes," *European Journal of Human Genetics*, vol. 22, no. 3, pp. 402–408, 2014.

[4] F. Zhang and J. R. Lupski, "Non-coding genetic variants in human disease," *Human Molecular Genetics*, vol. 24, no. 1, pp. R102–R110, 2015.

[5] J. T. Hua, M. Ahmed, H. Guo et al., "Risk SNP-mediated promoter-enhancer switching drives prostate cancer through lncRNA PCAT19," *Cell*, vol. 174, no. 3, pp. 564.e18–575.e18, 2018.

Hindawi
BioMed Research International
Volume 2019, Article ID 9218903, 18 pages
https://doi.org/10.1155/2019/9218903

Research Article

Mutation Spectrum in TPO Gene of Bangladeshi Patients with Thyroid Dyshormonogenesis and Analysis of the Effects of Different Mutations on the Structural Features and Functions of TPO Protein through *In Silico* Approach

Mst. Noorjahan Begum[1,2] **Md Tarikul Islam**[1] **Shekh Rezwan Hossain**[1,3] **Golam Sarower Bhuyan**[4] **Mohammad A. Halim**[5] **Imrul Shahriar**[5] **Suprovath Kumar Sarker**[1,2] **Shahinur Haque**[6] **Tasnia Kawsar Konika**[6] **Md. Sazzadul Islam**[1,7] **Asifuzzaman Rahat**[4] **Syeda Kashfi Qadri**[8] **Rosy Sultana**[1,9] **Suraiya Begum**[10] **Sadia Sultana**[6] **Narayan Saha**[11] **Mizanul Hasan**[6] **M. A. Hasanat**[12] **Hurjahan Banu**[12] **Hossain Uddin Shekhar**[3] **Emran Kabir Chowdhury**[3] **Abu A. Sajib**[2] **Abul B. M. M. K. Islam**[2] **Syed Saleheen Qadri**[1,4] **Firdausi Qadri**[1,4,13] **Sharif Akhteruzzaman**[2] **and Kaiissar Mannoor**[1,4]

[1] *Laboratory of Genetics and Genomics, Institute for Developing Science and Health Initiatives (ideSHi), Mohakhali, Dhaka 1212, Bangladesh*
[2] *Department of Genetic Engineering and Biotechnology, University of Dhaka, Dhaka 1000, Bangladesh*
[3] *Department of Biochemistry and Molecular Biology, University of Dhaka, Dhaka 1000, Bangladesh*
[4] *Infectious Diseases Laboratory, Institute for Developing Science and Health Initiatives (ideSHi), Mohakhali, Dhaka 1212, Bangladesh*
[5] *The Red-Green Research Centre (RGRC), 218 Elephant Road, Dhaka 1205, Bangladesh*
[6] *Nuclear Medicine and Allied Sciences, Bangabandhu Sheikh Mujib Medical University (BSMMU), Shahbag, Dhaka 1000, Bangladesh*
[7] *Department of Biochemistry and Molecular Biology, Jagannath University, Dhaka, Bangladesh*
[8] *Department of Paediatric Medicine, KK Women's and Children's Hospital, 100 Bukit Timah Road, Singapore*
[9] *Bangladesh University of Health Sciences, Bangladesh*
[10] *Department of Peadiatrics Endocrinology, Bangabandhu Sheikh Mujib Medical University (BSMMU), Shahbag, Dhaka 1000, Bangladesh*
[11] *Pediatric Neurology, National Institute of Neurosciences & Hospital, Dhaka 1207, Bangladesh*
[12] *Department of Endocrinology, Bangabandhu Sheikh Mujib Medical University (BSMMU), Shahbag, Dhaka 1000, Bangladesh*
[13] *Department of Enteric and Respiratory Infectious Diseases, Infectious Diseases Division, International Centre for Diarrhoeal Disease Research, Mohakhali, Dhaka, Bangladesh*

Correspondence should be addressed to Kaiissar Mannoor; kaiissar@ideshi.org

Received 7 July 2018; Revised 3 January 2019; Accepted 10 January 2019; Published 24 February 2019

Academic Editor: Gerald J. Wyckoff

Although thyroid dyshormonogenesis (TDH) accounts for 10-20% of congenital hypothyroidism (CH), the molecular etiology of TDH is unknown in Bangladesh. Thyroid peroxidase (TPO) is most frequently associated with TDH and the present study investigated the spectrum of TPO mutations in Bangladeshi patients and analyzed the effects of mutations on TPO protein structure through *in silico* approach. Sequencing-based analysis of TPO gene revealed four mutations in 36 diagnosed patients with TDH including three nonsynonymous mutations, namely, p.Ala373Ser, p.Ser398Thr, and p.Thr725Pro, and one synonymous mutation p.Pro715Pro. Homology modelling-based analysis of predicted structures of MPO-like domain ($TPO_{142\text{-}738}$) and the full-length TPO

protein (TPO_{1-933}) revealed differences between mutant and wild type structures. Molecular docking studies were performed between predicted structures and heme. TPO_{1-933} predicted structure showed more reliable results in terms of interactions with the heme prosthetic group as the binding energies were -11.5 kcal/mol, -3.2 kcal/mol, -11.5 kcal/mol, and -7.9 kcal/mol for WT, p.Ala373Ser, p.Ser398Thr, and p.Thr725Pro, respectively, implying that p.Ala373Ser and p.Thr725Pro mutations were more damaging than p.Ser398Thr. However, for the $TPO_{142-738}$ predicted structures, the binding energies were -11.9 kcal/mol, -10.8 kcal/mol, -2.5 kcal/mol, and -5.3 kcal/mol for the wild type protein, mutant proteins with p.Ala373Ser, p.Ser398Thr, and p.Thr725Pro substitutions, respectively. However, when the interactions between the crucial residues including residues His239, Arg396, Glu399, and His494 of TPO protein and heme were taken into consideration using both TPO_{1-933} and $TPO_{142-738}$ predicted structures, it appeared that p.Ala373Ser and p.Thr725Pro could affect the interactions more severely than the p.Ser398Thr. Validation of the molecular docking results was performed by computer simulation in terms of quantum mechanics/molecular mechanics (QM/MM) and molecular dynamics (MD) simulation. In conclusion, the substitutions mutations, namely, p.Ala373Ser, p.Ser398Thr, and p.Thr725Pro, had been involved in Bangladeshi patients with TDH and molecular docking-based study revealed that these mutations had damaging effect on the TPO protein activity.

1. Introduction

Congenital hypothyroidism (CH) is defined as insufficient production of thyroid hormone at birth [1]. The global frequency of CH is 1 in 3000-4000 whereas a pilot study in Bangladesh reported an incidence rate of 1 in 1300 [2, 3]. Thyroid dyshormonogenesis (TDH) which results due to defect in the pathway of thyroid hormone biosynthesis accounts for 10 to 20% cases of CH [4]. Till now, mutations in seven genes, namely, NIS (sodium iodine symporter, SLC5A5), PDS (Pendrin or SLC26A4), TPO (thyroid peroxidase), TG (thyroglobulin), IYD (iodotyrosine deiodinase, DEHAL1), DUOX2, and DUOXA2 (dual oxidase), have been reported to be involved in pathogenesis of TDH [5]. However, mutations in TPO gene which may result in total iodide organification defect (TIOD) or partial iodide organification defect (PIOD) have been described as the most common forms of TDH, and to date more than 60 different mutations have been described [6, 7].

TPO is the major enzyme in thyroid hormone biosynthesis and it catalyzes both iodination and coupling of iodotyrosine residues in TG (thyroglobulin). It is a glycosylated hemeprotein of 110 kDa bound at the apical membrane of thyrocytes [8]. The single gene encoding TPO is located on chromosome 2p25 containing 17 exons and it spans at least 150 kb [9]. It is a homodimer protein (each monomer consists of 933 amino acid residues) and contains a peroxidase domain, three additional extracellular domains, a transmembrane helix, and a short C-terminal intracellular tail [10]. Although a low-resolution crystal structure of TPO has been reported, its high resolution structure remains to be determined [11, 12]. The closest known homologues of TPO are lactoperoxidase (LPO), myeloperoxidase (MPO), and eosinophil peroxidase (EPO) with a sequence identity of 48%, 47%, and 47%, respectively. X-ray crystallographic structures have been determined for MPO and LPO [13, 14], providing a platform for investigating the structural basis of TPO. Nevertheless, Sarah et al. investigated plausible modes of TPO structure and dimer organization through *in silico* approach [15]. However, how certain mutations affect the TPO protein structure and its enzyme activity is still unknown.

Investigation of mutational spectrum is paramount for genetic disorder study as it gives insight into the disease pathogenicity as well as severity. Screening and identification of mutational spectrum in the TPO gene of patients with TIOD and PIOD have been reported in different countries of the world like Argentina, Netherlands, Japan, Portugal, and China [6, 16–19]. In addition, changes in the TPO enzyme were assayed *in vitro* to compare mutant and wild type activities by several study groups and demonstrated mild to severe TPO enzyme inactivity for some mutations [20, 21]. Though the prevalence of CH is more than twice the global incidence rate in Bangladesh, molecular basis of CH is still unknown in this country. Moreover, the effects of different mutations in the TPO gene on enzyme activity have not been investigated. In this study, we investigated the spectrum of mutations in TPO gene of patients with TDH and explored the possible effect of these mutations on the structure of TPO protein and TPO's MPO-like domain through *in silico* approach such as homology modelling, molecular docking followed by qunatum mechanics/molecular mechanics (QM/MM) and molecular dynamics (MD) simulation.

2. Methods and Materials

2.1. Study Participants. A total of 36 confirmed cases of congenital hypothyroid patients with dyshormonogenesis were enrolled at the clinical care settings of National Institute of Nuclear Medicine and Allied Sciences (NINMAS) and department of Endocrinology, Bangabandhu Sheikh Mujib Medical University (BSMMU), Dhaka, for their follow-up examinations. Written informed consent was signed by the parents or guardians of the patients. 3 mL of blood was collected in an EDTA tube from each patient. Ethical clearance was obtained from the ethical committee of BSMMU and University of Dhaka.

2.2. DNA Isolation and Polymerase Chain Reaction (PCR) Amplification. Genomic DNA was isolated from the EDTA blood by using a Qiagen DNAeasy mini kit. The isolated DNA was then amplified by PCR using TPO gene specific primers that together covered from Exon 8 to Exon 14, since global data showed that most of the common mutations in the TPO gene of the patients with congenital hypothyroidism were confined in this region. The primer sequences are listed in Table 1.

To amplify the desired target sequence of TPO gene, PCR amplification was conducted on a thermal cycler (Bio-Rad, USA). The final reaction volume was 10 μl for each of

Table 1: List of primers for PCR amplification and Sanger sequencing of TPO gene.

Primer Name	Sequence (5′-3′)	Product size (base pair)
TPO_Ex8F	TCCAGAGTCTTACAAAGGGTGC	679
TPO_Ex8R	GTACCTGGGAGAGAGAAGCCAC	
TPO_Ex9F	GAGGTGCTGTCTCTTGCCACTG	568
TPO_Ex9R	GGAAGAGTTCATGGGGACCAGC	
TPO_Ex10F	TAGAACTGAGCCAAGAGCTGTC	292
TPO_Ex10R	CTAGCAGCAGGTTGCTAGCTCG	
TPO_Ex11F	GACCATGGCATGAGTGAGATGG	363
TPO_Ex11R	CTGCCTCTGTGCAGAACGTG	
TPO_Ex12F	GGTTCTCCATGCACTGTGACCT	1044
TPO_Ex13R	GATTCCACGTGCCTGTCCTGAG	
TPO_Ex14F	CCTCATCACCTTTTCGGATGTGC	512
TPO_Ex14R	CAGACAGCAGGCACACGAAGTG	

the reactions which contained 1 μL 10X PCR buffer, 0.3 μL 25 mM $MgCl_2$, 2 μL 5X Q-solution, 1.6 μL 2.5 mM dNTPs mixture, 0.2 μL 10 mM Forward and 0.2 μL Reverse primers, 0.05 μL Taq DNA Polymerase, and 50 ng of genomic DNA, and total reaction volume was made up to 10 μL by addition of nuclease free water. The thermal cycling condition included (a) initial denaturation at 95°C for 5 minutes, (b) 35 cycles of denaturation at 95°C for 40 seconds annealing at 58°C for 35 seconds and extension at 72°C for 40 seconds, and (c) final extension at 72°C for 5 minutes.

2.3. Sanger Sequencing of PCR Products. Prior to sequencing, PCR product was purified using a Qiagen PCR purification kit (Qiagen) according to manufacturer's instruction. The cycle sequencing PCR was then conducted using a BigDye Chain Terminator version 3.1 Cycle Sequencing Kit (Applied Biosystems, USA) following manufacturer's instructions. The thermal cycling profile included (a) initial denaturation at 94°C for 1 minute, (b) 25 cycles of denaturation at 94°C for 10 seconds, annealing at 58°C for 5 seconds and extension at 60°C for 4 minutes, and (c) final extension at 60°C for 10 minutes. Following completion of cycle sequencing PCR, purification of the product was performed using a BigDye XTerminator® Purification Kit (Applied Biosystems). Finally, sequencing of the purified cycle sequencing product was performed on the ABI PRISM 310 automated sequencer (Applied Biosystems, USA).

2.4. Sequencing Data Analysis. Sequencing data were collected using ABI PRISM 310 data collection software version 3.1.0 (Applied Biosystems). Collected FASTA format of sequencing data was used to identify substitution or deletion mutations in the *TPO* gene by alignment with the reference sequence (Accession number; NC_000002.12 retrieved from the NCBI database) using the basic local alignment search tool (BLAST). ExPASy translate tool was used to convert nucleotides sequence into corresponding amino acids.

2.5. Analysis of Effect of Three Nonsynonymous Mutations in the 3D Structure of TPO Protein

2.5.1. Prediction of 3D Structure through In Silico Approach. We found 4 mutations including three nonsynonymous mutations, namely, p.Ala373Ser; p.Ser398Thr and p.Thr725Pro and a synonymous mutation p.Pro725Pro in the $TPO_{1\text{-}933}$ gene. One of our primary goals was to investigate the effect of the nonsynonymous mutations on the 3D structure of MPO-like domain of the TPO protein. In addition, we aimed at seeing whether the mutations had any effects on the heme interactions with specific amino acid residues. The corresponding positions of the mutations, including p.Ala373Ser, p.Ser398Thr, and p.Thr725Pro in the MPO-like domain of $TPO_{142\text{-}738}$ were p.Ala232Ser, p.Ser257Thr, and p.Thr584Pro, designated as $TPO_{142\text{-}738}$MT1, $TPO_{142\text{-}738}$MT2, and $TPO_{142\text{-}738}$MT3, respectively. Since the crystallographic structure of TPO protein was available at lower resolution, to understand the effect of mutations in the structure of MPO-like domain of $TPO_{142\text{-}738}$, amino acid sequences of wild type and mutant proteins containing different nonsynonymous mutations were submitted to I-TASSER server in order to obtain the 3D structures [22–24]. We obtained 1 model for each structure based on C-score, Template Modelling (TM) score, and Root Mean Square Deviation (RMSD) score. In addition, we investigated the effects of the mutations on full-length TPO protein structure and functions in order to compare with the results with MPO-like domain to see if any changes were found. For this purpose, we also predicted the structures of whole TPO protein ($TPO_{1\text{-}933}$) for the wild type (TPO WT) and the mutants (TPO MT1, TPO MT2, and TPO MT3) by using the I-TASSER server and obtained 5 models for each. From the models, we selected the suitable ones based on the organization of its various domains such as myeloperoxidase- (MPO-) like domain (residues 142–738), complement control protein- (CCP-) like domain (residues 740–795) and epidermal growth factor- (EGF-) like domain (residues 796–846) of the whole protein according to published article [15].

2.5.2. Validation of the 3D Structures. The predicted 3D structures of $TPO_{142\text{-}738}$ WT, $TPO_{142\text{-}738}$MT1, $TPO_{142\text{-}738}$ MT2, $TPO_{142\text{-}738}$ MT3, $TPO_{1\text{-}933}$WT, $TPO_{1\text{-}933}$MT1, $TPO_{1\text{-}933}$MT2, and $TPO_{1\text{-}933}$MT3 were validated using 2 different web servers, namely, Verify3D server, and RAMPAGE server [25–27]. To validate the structure, the PDB format of the predicted

Table 2: Grid box center and grid box size for full-length $TPO_{1\text{-}933}$ WT, MT1, MT2, and MT3.

Proteins	Grid box center (Å)			Grid box size (Å)		
	X	Y	Z	X	Y	Z
$TPO_{1\text{-}933}$ WT	109.7751	128.9632	119.5649	24.5891	20.8773	31.4612
$TPO_{1\text{-}933}$ MT1	105.160	102.301	98.7798	25.0	25.0	25.0
$TPO_{1\text{-}933}$ MT2	99.6151	102.226	100.5057	25.0	25.0	25.0
$TPO_{1\text{-}933}$ MT3	102.196	124.345	113.7515	25.0	25.0	25.0

3D structure was submitted to both the servers. The result included the percentage of the amino acids having the average 3D-1D score of ≥ 0.2 for Verify3D server. The RAMPAGE webserver performs Ramachandran Plot Analysis by providing results including the percentages of the amino acid residues within the favored, allowed, and outlier regions. The results of the Verify3D and the RAMPAGE webservers were summarized in the results section.

2.5.3. Optimization of Heme Using Quantum Mechanical (QM) Calculations. Since TPO is a heme containing protein, we investigated the effect of mutation on binding affinity of heme with TPO and its interactions with specific amino acid residues. The initial structure of heme was obtained from the Protein Data Bank (PDB) database, (PDB ID: HEM). Quantum mechanics (QM) calculation had been used to optimize the heme. The QM calculation was conducted using density functional theory (DFT) method employing Becke's (B) exchange functional combining Lee, Yang, and Parr's (LYP) correlation functional, widely known as B3LYP density functional in Gaussian 09 program package [28–30]. SDD basis set had been used for optimization of the heme [31, 32].

2.5.4. Molecular Docking of Heme with the Predicted 3D Structures of TPO. For molecular docking, Autodock Vina [33, 34] protocol was employed. The molecular docking approach involved the prediction of the interaction between a small molecule and a protein at the atomic level, which provided us the opportunity to investigate the behavior of small molecules in the binding site of target proteins and to elucidate the fundamental biochemical processes. Before docking processes, knowing the location of ligand binding sites in the target protein could significantly increase the docking efficiency [35]. The binding sites of heme with TPO had been identified. It was found that Asp238, His239, Arg396, Glu399, and His494 were present in the active site of $TPO_{1\text{-}933}$; i.e. MPO-like domain and these amino acid residues were involved with heme interactions and thus the catalytic activity of TPO [36, 37]. But in the case of MPO-like domain of $TPO_{142\text{-}738}$, the corresponding position of Asp238, His239, Arg396, Glu399, and His494 would be Asp97, His98, Arg255, Glu258, and His353, respectively. Optimal confined search space had been selected for successful flexible molecular docking of heme with $TPO_{142\text{-}738}$ WT, $TPO_{142\text{-}738}$ MT1, $TPO_{142\text{-}738}$ MT2, and $TPO_{142\text{-}738}$ MT3. The center of the grid box for $TPO_{142\text{-}738}$ WT was set to 71.337 Å, 73.748 Å, and 72.888 Å; whereas they were set to 71.281 Å, 73.813 Å, and 73.314 Å for $TPO_{142\text{-}738}$ MT1; 73.115 Å, 74.888 Å, and 73.156 Å for $TPO_{142\text{-}738}$ MT2; and 73.273 Å, 75.433 Å, and 74.247 Å for $TPO_{142–738}$ MT3 in the x, y, and z directions, respectively. The grid box size was set to 25.0 Å, 25.0 Å, and 25.0 Å for $TPO_{142\text{-}738}$WT, MT1, MT2, and MT3 in the x, y, and z directions, respectively. Grid box value center and grid box size was also optimized for full-length $TPO_{1\text{-}933}$ (Table 2).

2.5.5. Visualization and Analysis of Docking Results. The molecular docking results of heme with $TPO_{142\text{-}738}$ WT, $TPO_{142\text{-}738}$ MT1, $TPO_{142\text{-}738}$ MT2, and $TPO_{142–738}$ MT3 and also for the whole protein $TPO_{1\text{-}933}$ were visualized and analyzed using the PyMol (version 2.0) and BIOVIA Discovery Studio 2017 software [38, 39]. The binding affinities of heme with wild type TPO (TPO WT) compared to 3 mutant proteins (TPO MT1, TPO MT2, and TPO MT3) were observed. Moreover, the corresponding non-bond interactions of amino acids with heme were also studied for wild type and mutant 3D structures.

2.5.6. QM/MM and Molecular Dynamics (MD) Simulation. To validate the molecular docking results, further analysis by quantum chemical method QM/MM and molecular dynamics (MD) simulations were employed for full-length TPO proteins (wild type, MT1, and MT3) since published data showed MT1 and MT3 had severe effect on enzyme activity than MT2. The QM/MM calculations of the selected protein-ligand complexes were performed by a two-layer ONIOM method available in the Gaussian09 software package [40–46], QM and MM regions have been shown in supplementary Figure 3. The heme molecule was included in the QM region and semiempirical PM6 level of theory [47] was considered due to large structure of the heme molecules. The regions of full-length protein were computed in the MM region and the Universal Force Field (UFF) was used for the energy minimization. The total ONIOM energy of the entire system is as follows: (see [48])

$$E^{ONIOM} = E^{real,MM} + E^{model,QM} - E^{model,MM} \quad (1)$$

The *real* system consists of all the atoms and is calculated only at the MM level. The *model* system consists of the part

Table 3: Mutation detection in the TPO gene of hypothyroid patients.

Sl no.	Exon	Nucleotide position	Amino acid position	Functional change (polarity)	Reference
1	8	c.1117G>T	p.Ala373Ser	Similar to non-enzymatic reaction rate	[20, 52]
2	8	c.1193G>C	p.Ser398Thr	Low enzymatic reaction rate	[20, 52]
3	12	c.2145C>T	p.Pro715Pro	Not applicable	[20, 52, 53]
4	12	c.2173A>C	p.Thr725Pro	Similar to non-enzymatic reaction rate	[20, 52, 53]

Table 4: Summary of the corresponding model numbers, C-score, TM-score, and the RMSD-score of the predicted 3D structures of $TPO_{142\text{-}738}$ WT, $TPO_{142\text{-}738}$ MT1, $TPO_{142\text{-}738}$ MT2, $TPO_{142\text{-}738}$ MT3, $TPO_{1\text{-}933}$ WT, $TPO_{1\text{-}933}$ MT1, $TPO_{1\text{-}933}$ MT2, and $TPO_{1\text{-}933}$ MT3.

Features	$TPO_{142\text{-}738}$ WT	$TPO_{142\text{-}738}$ MT1	$TPO_{142\text{-}738}$ MT2	$TPO_{142\text{-}738}$ MT3	$TPO_{1\text{-}933}$ WT	$TPO_{1\text{-}933}$ MT1	$TPO_{1\text{-}933}$ MT2	$TPO_{1\text{-}933}$ MT3
Model no.	01	01	01	01	02	01	05	01
C-score	2	2	1.99	1.99	−3.35	−3.23	−3.27	−2.9
TM-score	0.99 ± 0.04	0.99 ± 0.04	0.99 ± 0.04	0.99 ± 0.04	–	0.35 ± 0.12	–	0.38 ± 0.13
RMSD (Å)	3.5 ± 2.4	3.4 ± 2.4	3.6 ± 2.5	3.6 ± 2.5	–	17.2 ± 2.7	–	16.2 ± 3.1

C-score = confidence score range: [-5, 2]; TM-score = Template Modelling score, TM-score < 0.17 indicates random similarity and TM-score > 0.5 indicates correct similarity; RMSD = Root Mean Square Deviation. WT = wild type, MT1 = mutant 1 (p.Ala373Ser), MT2 = mutant 2 (p.Ser398Thr), and MT3 = mutant 3 (p.Thr725Pro).

of the system (such as heme) that is treated at the QM level [40].

For molecular dynamics simulation, YASARA dynamics program was employed and [48, 49]. AMBER14 force field was considered for all calculations. The size of the cubic simulation box was 167.17 Å∗ 167.17 Å ∗ 167.17 Å and 151,343 water molecules were added to maintain a solvent density of 1.0 g/ml. The total number of atoms in the system was 469,240. Due to the large size of the protein, we have performed 5000 ps MD simulation [50]. For short-range van der Waals and Coulomb interactions, a cut-off radius of 8.0 Å was considered. Long-range electrostatic interactions were taken into consideration using the Particle Mesh Ewald algorithm [50]. MD simulation was performed for 5000 ps at 310K having a time step of 1.25 fs and the simulation snapshots were saved at every 100 ps. To check whether the ligand stayed in the same binding pocket after 5000 ps of simulation, the heme ligands were retrieved from the simulated ligand-protein complexes and molecular docking was performed again using Autodock Vina protocol as mentioned earlier. The docked structures were analyzed using the same protocol as stated before.

3. Result

3.1. Demographic Information of the Study Participants. A total of 36 confirmed cases of congenital hypothyroidism with dyshormonogenesis were enrolled in this study. Among 36 patients, 15 (41.67%) and 21 (58.33%) were female and male, respectively, with an average age of 7.58 ± 4.56 years.

3.2. Analysis of TPO Gene for Identification of Molecular Basis of Hypothyroidism. As mutations in the TPO gene are commonly associated with thyroid dyshormonogenesis and related complications [18, 51], we opted to analyze the TPO gene to find whether there were mutations in this gene of the study participants. Upon Sanger sequencing of specimens from the patients with thyroid dyshormonogenesis targeting exon-8 to exon-14 which are commonly reported in TPO-associated thyroid dyshormonogenesis, mutations were detected in all 36 samples. A total of four mutations, namely, c.1117G>T (p.Ala373Ser), c.1193G>C (p.Ser398Thr), c.2145C>T (p.Pro715Pro), and c.2173A>C (p.Thr725Pro) were identified in the study participants (Table 3). The first two of these four mutations were detected in exon-8, whereas the remaining two mutations were detected in exon-12. Even though c.2145C>T (or p.Pro715Pro) of the four mutations is a synonymous point mutation and is innocuous, the other three nonsynonymous mutations, namely, p.Ala373Ser, p.Ser398Thr, and p.Thr725Pro, had previously been reported in the patients with thyroid dyshormonogenesis and the reaction kinetics catalyzed by the mutant TPO enzyme proved to be similar with nonenzymatic reaction rates by several other studies [20, 52, 53].

3.3. Prediction of 3D Structures of Myeloperoxidase- (MPO-) Like Domain ($TPO_{142\text{-}738}$) and Full-Length TPO Protein ($TPO_{1\text{-}933}$). The crystallographic structure of TPO protein is available with low resolution and the catalytic domain of $TPO_{142\text{-}738}$ is similar to human myeloperoxidase (MPO). Since the mutations that were identified in this present study were confined in the MPO-like domain of TPO protein, we investigated the effect of mutations on the 3D structure of MPO-like domain ($TPO_{142\text{-}738}$) of TPO protein. Also, we wanted to see whether the mutations caused any changes in the interactions of various amino acid residues with heme prosthetic group. We submitted the amino acid $TPO_{142\text{-}738}$ sequence for the wild type (WT), mutant- MT1, MT2, and MT3 to the I-TASSER server and obtained 3D structures with C-scores of 2, 2, 1.99, and 1.99 for $TPO_{142\text{-}738}$ WT, $TPO_{142\text{-}738}$ MT1, $TPO_{142\text{-}738}$ MT2, and $TPO_{142\text{-}738}$ MT3, respectively (Table 4 and Figure 1). To investigate the effects of the mutations on the full-length TPO protein structure and functions, we also predicted the 3D structures for

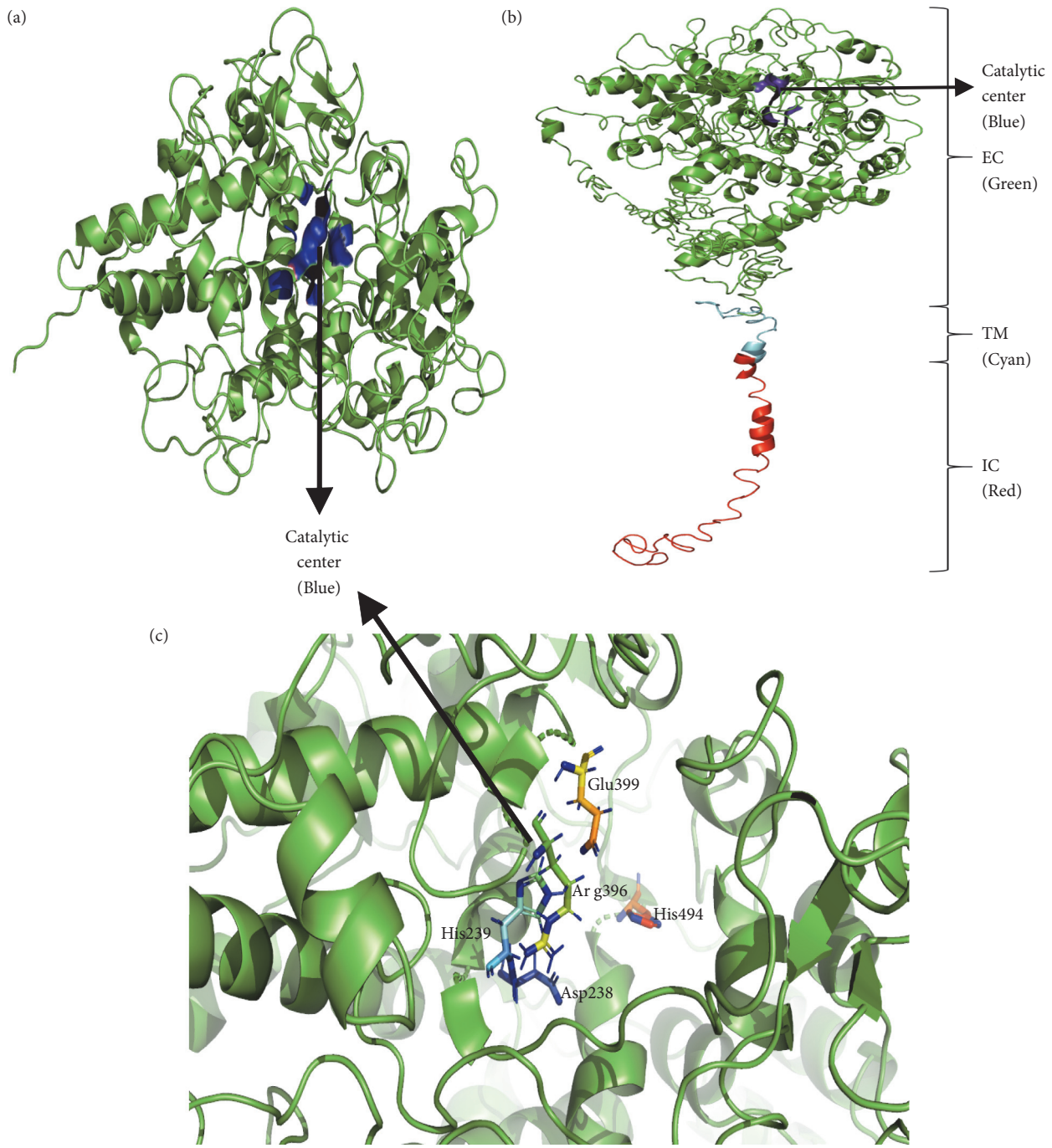

Figure 1: The predicted 3D structures of the proteins. (a) $TPO_{142-738}$ WT, (b) TPO_{1-933} WT, and (c) catalytic site of TPO with crucial amino acids Asp238, His239, Arg396, Glu399, and His494. The specific regions of the TPO_{1-933} WT structure are indicated with the corresponding color written in the brackets. EC = extracellular region shown in green color, TM = transmembrane region shown in cyan color, and IC = intracellular region shown in red color.

TPO_{1-933} WT, TPO_{1-933} MT1, TPO_{1-933} MT2, and TPO_{1-933} MT3 using the I-TASSER server and compared the results with the MPO-like domain. From the server, we obtained 5 models for each of TPO_{1-933} WT, TPO_{1-933} MT1, TPO_{1-933} MT2, and TPO_{1-933} MT3 and we chose the best model by analyzing the organization of the MPO-like domain (residues 142–738); complement control protein- (CCP-) like domain (residues 740–795); and epidermal growth factor- (EGF-) like domain (residues 796–846) if they were in correct arrangement [54–58] (Figure 1 and Supplementary Figure 2). The corresponding C-score, TM-score, and RMSD score of TPO_{1-933} WT, TPO_{1-933} MT1, TPO_{1-933} MT2, and TPO_{1-933} MT3 were summarized in Table 4.

Table 5: Summary of the Verify3D and RAMPAGE webserver results for the predicted 3D structures of $TPO_{142\text{-}738}$ WT, $TPO_{142\text{-}738}$ MT1, $TPO_{142\text{-}738}$ MT2, $TPO_{142\text{-}738}$ MT3, $TPO_{1\text{-}933}$ WT, $TPO_{1\text{-}933}$ MT1, $TPO_{1\text{-}933}$ MT2, and $TPO_{1\text{-}933}$ MT3 proteins.

		$TPO_{142\text{-}738}$ WT	$TPO_{142\text{-}738}$ MT1	$TPO_{142\text{-}738}$ MT2	$TPO_{142\text{-}738}$ MT3	$TPO_{1\text{-}933}$ WT	$TPO_{1\text{-}933}$ MT1	$TPO_{1\text{-}933}$ MT2	$TPO_{1\text{-}933}$ MT3
Verify3D		96.15%	89.78%	94.14%	94.64%	73.10%	70.74%	76.10%	76.63%
RAMP-AGE	Favored region	84.5%	84.4%	85.2%	81.2%	68.40%	69.60%	66.90%	69.80%
	Allowed region	11.6%	11.1%	10.4%	14.3%	17.20%	16.20%	18.40%	18.80%
	Outlier region	3.9%	4.4%	4.4%	4.5%	14.40%	14.20%	14.70%	11.40%

Verify3D: percentages of amino acids having the average 3D-1D score ≥ 0.2; RAMPAGE: percentages of the amino acid residues within the favored, allowed, and outlier regions. WT = wild type, MT1 = mutant 1 (p.Ala373Ser), MT2 = mutant 2 (p.Ser398Thr), and MT3 = mutant 3 (p.Thr725Pro).

3.4. Validation of the 3D Structures of $TPO_{142\text{-}738}$ WT, $TPO_{142\text{-}738}$ MT1, $TPO_{142\text{-}738}$ MT2, $TPO_{142\text{-}738}$ MT3, $TPO_{1\text{-}933}$ WT, $TPO_{1\text{-}933}$ MT1, $TPO_{1\text{-}933}$ MT2, and $TPO_{1\text{-}933}$ MT3 Proteins. We validated the 3D structures of TPO WT, MT1, MT2, and MT3 proteins by Verify3D server which measures the accuracy of the predicted 3D structure model with its respective residues (1D) by assigning a structural class based on its location and environment. In Verify3D, more than 80% amino acid residues had the average 3D-1D score of ≥ 0.2 which confers the validity of the 3D structures of $TPO_{142\text{-}738}$ WT (96.15%), $TPO_{142\text{-}738}$ MT1 (89.78%), $TPO_{142\text{-}738}$ MT2 (94.14%), and $TPO_{142\text{-}738}$ MT3 (94.64%) (Table 5). Moreover, validation of the structures by the RAMPAGE web server also provided the percentages of the amino acid residues within favored, allowed, and outlier regions. In case of $TPO_{142\text{-}738}$ WT, 84.5% residues were within the favored region, 11.6% were within the allowed region, and 3.9% were within the outlier region. For $TPO_{142\text{-}738}$ MT1, 84.4% residues were in the favored regions, 11.1% in the allowed region, and 4.4% in the outlier regions. On the one hand, for $TPO_{142\text{-}738}$ MT2, 85.2% residues were confined in the favored regions, 10.4% in the allowed region and 4.4% in the outlier regions and on the other hand, for $TPO_{142\text{-}738}$ MT3, 81.2% residues were confined in the favored region, 14.3% in the allowed region and 4.5% in the outlier regions (Table 5). The Verify3D results showed that the percentages of amino acid residues having average 3D-1D score of ≥ 0.2 for $TPO_{1\text{-}933}$ WT, $TPO_{1\text{-}933}$ MT1, $TPO_{1\text{-}933}$ MT2, and $TPO_{1\text{-}933}$ MT3 were 73.10%, 70.74%, 76.10%, and 76.63%, respectively. The results provided by RAMPAGE server for $TPO_{1\text{-}933}$ WT, $TPO_{1\text{-}933}$ MT1, $TPO_{1\text{-}933}$ MT2, and $TPO_{1\text{-}933}$ MT3 were summarized in Table 5.

3.5. Optimization of Heme. Density functional theory using B3LYP/SDD was employed for the optimization of the heme prosthetic group. Slight changes in bond distances and bond angles were observed between crystal and DFT structures which are presented in Table 6 and Supplementary Figure 1.

3.6. Molecular Docking, Visualization and Analysis of the Docking of Heme with the Predicted Structures of $TPO_{142\text{-}738}$ WT, $TPO_{142\text{-}738}$ MT1, $TPO_{142\text{-}738}$ MT2, $TPO_{142\text{-}738}$ MT3, $TPO_{1\text{-}933}$ WT, $TPO_{1\text{-}933}$ MT1, $TPO_{1\text{-}933}$ MT2, and $TPO_{1\text{-}933}$ MT3 Proteins. From the analysis, it was found that heme interacted with $TPO_{1\text{-}933}$ WT through a total of 21 non-bond interactions including interactions with Arg491, and Arg582 through hydrogen bonds, interactions with His239, Val400, Phe490, Arg491, His494, Ile497, Phe523, Leu560, Leu564, and Leu575 through hydrophobic interaction, and interactions with Arg396, Glu399, and Arg491 through electrostatic interactions (Table 7 and Figure 2). Moreover, similar to $TPO_{1\text{-}933}$ WT, when MPO-like domain ($TPO_{142\text{-}738}$) WT predicted structure was used for docking, 21 non-bond interactions of amino acids with heme were observed as well (Figure 3). However, not all of these 21 interactions for $TPO_{142\text{-}738}$ and $TPO_{1\text{-}933}$ were common. The $TPO_{142\text{-}738}$ WT interactions with heme included Arg582 and Arg586 through hydrogen bonds, His239, Val400, His494, Ile497, Phe523, Leu560, Leu564, Val566, Leu567, and Leu575 through hydrophobic interactions and Arg396, and Glu399 through electrostatic interactions. The common 11 interactions for $TPO_{1\text{-}933}$ WT and $TPO_{142\text{-}738}$ WT included His239, Arg396, Glu399, Val400, His494, Ile497, Phe523, Leu560, Leu564, Leu575, and Arg582. Moreover, of the aforementioned 11 residues, 4 residues including His239, Arg396, Glu399, and His494 had been reported to correspond to amino acid residues in MPO protein which were crucial for enzyme activity [36, 37].

For $TPO_{1\text{-}933}$ MT1, a total of 12 residues were found to interact with heme. Among those residues, 2 residues, namely, His239 and His494, interacted with heme through hydrogen bonds and 5 residues including His239, Phe243, Arg396, Phe524, and Leu567 interacted through hydrophobic interactions (Table 7, Figure 2 and Supplementary Table 2). Total number of interactions decreased significantly for $TPO_{1\text{-}933}$ MT1 compared to the $TPO_{1\text{-}933}$ WT and the Glu399 residue which is crucial for interaction was also absent in the $TPO_{1\text{-}933}$ MT1. On the other hand, when $TPO_{142\text{-}738}$ MT1 predicted structure was used for molecular docking, a total of 19 residues were found to interact with heme (Table 7, Figure 3 and Supplementary Table 1). Among those 19 residues, 4 residues including Met231, Gly234, Ser402, and Gly493 interacted with heme through hydrogen bonds, the residues Gly234, Gln235, Val400, Phe490, Arg491, Ile497, Phe523, Leu560, Leu564, and Leu575 interacted through hydrophobic interactions, and the residue Glu399 interacted through electrostatic interaction with the heme (Table 7). However, the crucial interactions of heme with His239, Arg396, and His494 were absent in the $TPO_{142\text{-}738}$ MT1. The structure-based docking of both $TPO_{1\text{-}933}$ and $TPO_{142\text{-}738}$ suggested that MT1 mutation was damaging for the TPO enzyme activity.

For $TPO_{1\text{-}933}$ MT2, a total of 20 amino acid residues were found to interact with the heme. Among those residues, 3

Table 6: Summarized data for the bond distances and bond angles of specific atoms of heme before and after optimization.

X-ray Structure		DFT structure		X-ray Structure		DFT Structure	
Atoms	Bond distance (nm)	Atoms	Bond distance (nm)	Atoms	Bond angle (degrees)	Atoms	Bond angle (degrees)
39N...43Fe	1.977	13N...43Fe	2.013	39N...43Fe...40N	82.23°	13N...43Fe...14N	89.78°
40N...43Fe	2.393	14N...43Fe	2.008	40N...43Fe...41N	80.66°	14N...43Fe...15N	89.97°
41N...43Fe	2.088	15N...43Fe	2.008	41N...43Fe...42N	94.79°	15N...43Fe...42N	90.04°
42N...43Fe	1.845	42N...43Fe	2.011	39N...43Fe...42N	98.39°	42N...43Fe...13N	90.22°

Table 7: Binding energy and non-bond interactions of heme with $TPO_{142-738}$ WT, $TPO_{142-738}$ MT1, $TPO_{142-738}$ MT2, $TPO_{142-738}$ MT3, TPO_{1-933} WT, TPO_{1-933} MT1, TPO_{1-933} MT2, and TPO_{1-933} MT3 proteins after flexible docking.

Protein type	Binding Affinity (kcal/mol)	Hydrogen bond	Hydrophobic bond	Electrostatic bond	Total interactions
$TPO_{142-738}$ WT	–11.9	Arg441(Arg582), Arg445(Arg586)	His98(His239), Val259(Val400), His353(His494), Ile356(Ile497), Phe382(Phe523), Leu419(Leu560), Leu423(Leu564), Val425(Val566), Leu426(Leu567), Leu434(Leu575)	Arg255(Arg396), Glu258(Glu399)	21
$TPO_{142-738}$ MT1	–10.8	Met90(Met231), Gly93(Gly234), Ser261(Ser402), Gly352(Gly493)	Gly93(Gly234), Gln94(Gln235), Val259(Val400), Phe349(Phe490), Arg350(Arg491), Ile356(Ile497), Phe382(Phe523), Leu419(Leu560), Leu423(Leu564), Leu434(Leu575)	Glu258(Glu399)	19
$TPO_{142-738}$ MT2	–2.5	Arg350(Arg491), Asn438(Asn579), Arg441(Arg582)	Phe102(Phe243),His 353(His494), Phe382(Phe523), Phe383(Phe524), Leu423(Leu564), Phe424(Phe565), Val425(Val566), Leu426(Leu567), Leu434(Leu575)	Glu258(Glu399)	20
$TPO_{142-738}$ MT3	–5.3	His98(His239), Arg255(Arg396), Arg350(Arg491), Arg441(Arg582)	Phe102(Phe243), Phe382(Phe523), Phe383(Phe524), Leu423(Leu564), Phe424(Phe565), Leu426(Leu567)Leu 434(Leu575)	Glu258(Glu399)	16
TPO_{1-933} WT	–11.5	Arg491, Arg582	His239, Val400, Phe490, Arg491, His494, Ile497, Phe523, Leu560, Leu564, Leu575	Arg396, Glu399, Arg491	21
TPO_{1-933} MT1	–3.2	His239, His494	His239, Phe243, Arg396, Phe524, Leu567	Not found	12
TPO_{1-933} MT2	–11.5	His239, Arg491, Arg582	His239, Val400, Arg491, His494, Ile497, Phe523, Leu564, Val566, Leu575	Arg396, Glu399	20
TPO_{1-933} MT3	–7.9	Gln246, Arg491, Ser568	Phe243, Val400, Arg491, His494, Ile497, Phe523, Phe524, Leu560, Leu564, Val566, Leu575	Glu399	21

The amino acid residues and their positions are designated as the three letter abbreviations and the corresponding number; in case of $TPO_{142-738}$ the amino acid outside the first bracket indicates the position in predicted structure for $TPO_{142-738}$ and the amino acid residues in first bracket indicates the real position in TPO_{1-933} protein; WT = wild type; MT1 = mutant 1 (p.Ala373Ser); MT2 = mutant 2 (p.Ser398Thr); MT3 = mutant 3 (p.Thr725Pro).

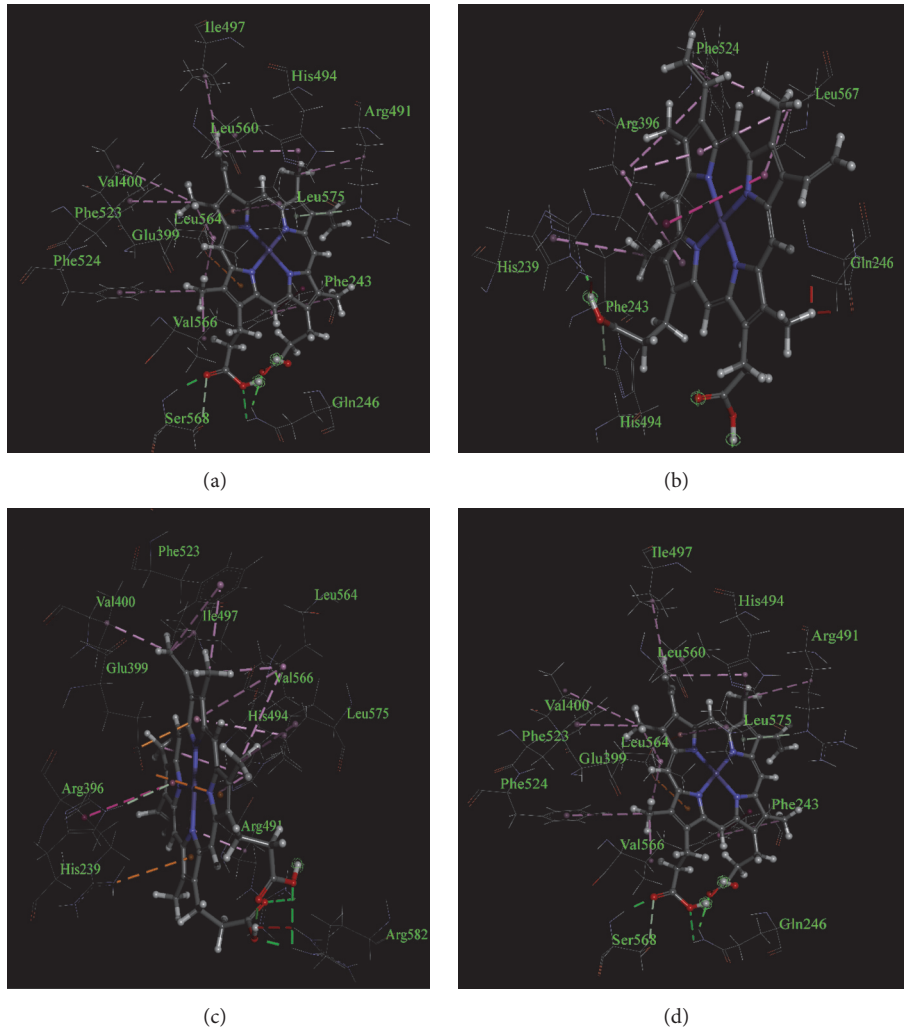

FIGURE 2: Non-bond interactions of heme with corresponding predicted structures as obtained using a BIOVIA Discovery Studio 2017. (a) $TPO_{1\text{-}933}$ WT, (b) $TPO_{1\text{-}933}$ MT1, (c) $TPO_{1\text{-}933}$ MT2, and (d) $TPO_{1\text{-}933}$ MT3. The amino acid residues and their positions are designated as the three letter abbreviations and the corresponding numbers.

residues including His239, Arg491, and Arg582 interacted with heme through hydrogen bonds, 9 residues including His239, Val400, Arg491, His494, Ile497, Phe523, Leu564, Val566, and Leu575 interacted through hydrophobic interactions, and 2 residues including Arg396 and Glu399 interacted through electrostatic interactions (Table 7, Figure 2 and Supplementary Table 2). All four crucial interacting residues, namely, His239, Arg396, Glu399, and His494, which are important for MPO-like domain activity in TPO enzyme, were found to interact with heme in $TPO_{1\text{-}933}$ MT2. On the other hand, when $TPO_{142\text{-}738}$ MT2 predicted structure was used for docking, a total of 20 residues were found to interact with heme. Among those 20 residues, 3 residues including Arg491, Asn579, and Arg582 interacted with heme through hydrogen bonds, the residues Phe243, His494, Phe523, Phe524, Leu564, Phe565, Val566, Leu567, and Leu575 interacted through hydrophobic interactions and the residue Glu399 interacted through electrostatic interaction (Table 7, Figure 3 and Supplementary Table 1). However, the crucial interactions of heme with residues His239 and Arg396 were absent in the $TPO_{142\text{-}738}$ MT2. The $TPO_{1\text{-}933}$ structure-based docking showed that the mutations did not result in any major changes in interactions and all major interacting residues were present, whereas the $TPO_{142\text{-}738}$ structure-based docking suggested result which was similar to $TPO_{1\text{-}933}$ except that the major interacting residues His239 and Arg396 were absent. Together, the docking results are indicative of the fact that this mutation might have an association with PIOD.

For $TPO_{1\text{-}933}$ MT3, a total of 21 residues were found to interact with the heme. Among those residues, 3 residues including Gln246, Arg491, and Ser568 interacted with heme through hydrogen bonds, 11 residues including Phe243, Val400, Arg491, His494, Ile497, Phe523, Phe524, Leu560, Leu564, Val566, and Leu575 interacted through hydrophobic interactions, and the residue Glu399 interacted through electrostatic interaction (Table 7, Figure 2 and Supplementary Table 2). Two crucial interacting residues, namely, His239 and Arg396 which are important for MPO-like domain activity

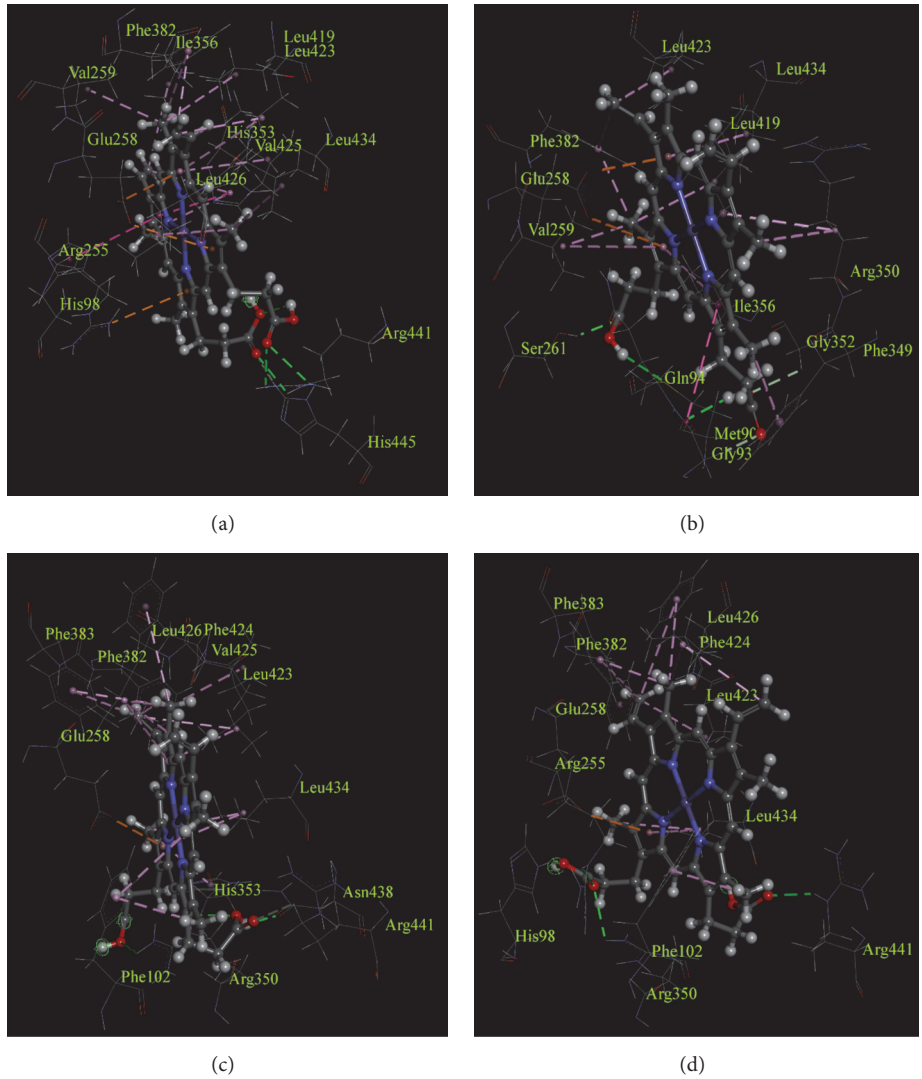

Figure 3: Non-bond interactions of heme with corresponding predicted structures as obtained using a BIOVIA Discovery Studio 2017. (a) $TPO_{142\text{-}738}$ WT, (b) $TPO_{142\text{-}738}$ MT1, (c) $TPO_{142\text{-}738}$ MT2, and (d) $TPO_{142\text{-}738}$ MT3. The amino acid residues and their positions are designated as the three letter abbreviations and the corresponding numbers.

in the TPO enzyme, were absent in $TPO_{1\text{-}933}$ MT3. On the other hand, when $TPO_{142\text{-}738}$ MT3 predicted structure was used for docking, a total of 16 residues were found to interact with heme. Among those 16 residues, 4 residues including His239, Arg396, Arg491, and Arg582 interacted with heme through hydrogen bonds, the residues Phe243, Phe523, Phe524, Leu564, Phe565, Leu567, and Leu575 interacted through hydrophobic interactions and the residue Glu399 interacted through electrostatic interaction (Table 7, Figure 3 and Supplementary Table 1). However, the crucial interactions of heme with His494 were absent in the $TPO_{142\text{-}738}$ MT3. Both $TPO_{1\text{-}933}$ and $TPO_{142\text{-}738}$ structure-based docking with heme suggested that MT3 mutation might have damaging effect to the TPO protein activity.

3.7. QM/MM and Molecular Dynamics (MD) Simulation. According to Guria et al. $TPO_{1\text{-}933}$ MT1 (p.Ala373Ser) and $TPO_{1\text{-}933}$ MT3 (p.Thr725Pro) showed more damaging effect on the catalytic activity of TPO protein [20] and our molecular docking-based study showed that full-length $TPO_{1\text{-}933}$ MT2 (p.Ser398Thr) structure interacted to all the crucial amino acids in the catalytic site of TPO; thus we selected these $TPO_{1\text{-}933}$ MT1 (p.Ala373Ser) and $TPO_{1\text{-}933}$ MT3 (p.Thr725Pro) mutant cases for further analysis to validate the molecular docking results and to compare the amino acid interactions with the wild type structure. The interactions between the amino acid residues of $TPO_{1\text{-}933}$ WT, $TPO_{1\text{-}933}$ MT1, and $TPO_{1\text{-}933}$ MT3 proteins and the heme groups were further studied by QM/MM and the mode of interactions is depicted in Figure 4. It was observed that the interacting residues were the same as obtained from the initial docking results.

To investigate the structural changes during molecular dynamics simulation, the protein-ligand complex after 5000 ps of simulation was superimposed on the initial docked protein-ligand complex. The superimposed structures of

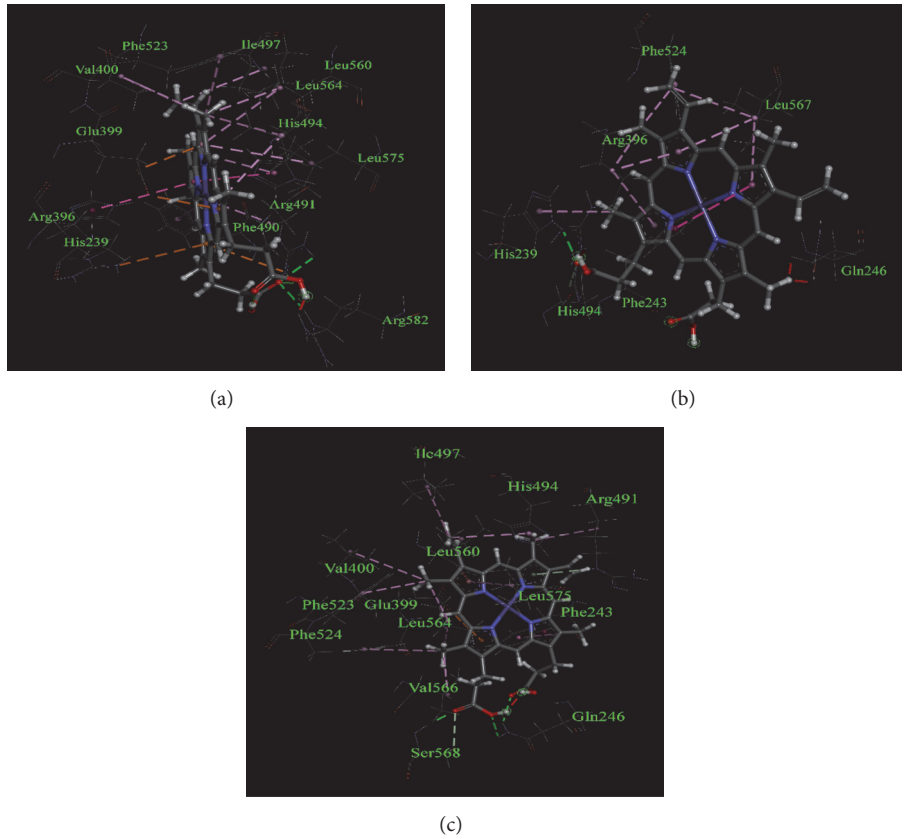

FIGURE 4: Non-bond interactions of heme with corresponding predicted structures as obtained using a BIOVIA Discovery Studio 2017, after QM/MM calculations of the structures with heme molecule in the active site performed at the ONIOM- (PM6: UFF) level of theory. (a) $TPO_{1\text{-}933}$ WT, (b) $TPO_{1\text{-}933}$ MT1, and (c) $TPO_{1\text{-}933}$ MT3. The amino acid residues and their positions are designated as the three letter abbreviations and the corresponding numbers.

$TPO_{1\text{-}933}$ WT, $TPO_{1\text{-}933}$ MT1 (p.Ala373Ser), and $TPO_{1\text{-}933}$ MT3 (p.Thr725Pro) proteins are depicted in Figure 5. It was observed that the heme ligand was found within the catalytic sites.

As protein flexibility can give rise to difference in binding interactions of a ligand with its target protein, the retrieved protein structure after 5000 ps simulation was again docked with the heme ligand and the results are depicted in Figure 6. From the analysis of molecular docking after performing molecular dynamics of the protein structures, we observed that although heme interacted with $TPO_{1\text{-}933}$ WT through all the crucial amino acids (Asp238, His239, Arg396, Glu399, and His494), while it interacted with $TPO_{1\text{-}933}$ MT1 and $TPO_{1\text{-}933}$ MT3 through Glu399 and His494 residues only. Thus in the mutant cases, there were no interactions for the other 3 amino acid residues, namely, Asp238, His239, and Arg396. As these 5 amino acid residues are important for the catalytic activity of the protein, the absence of interactions with one of these crucial amino acids could affect the functional activity of the protein.

4. Discussion

Though congenital hypothyroidism (CH) is the most common preventable disorder, newborn screening is not a regular practice in Bangladesh. Due to late initiation of treatment, many late-diagnosed hypothyroid patients experience various typical signs and symptoms of hypothyroidism even though they receive regular levothyroxine treatment. Although several genes have been reported to be involved in thyroid dyshormonogenesis (TDH), mutation in the TPO gene is frequently described with mild to severe repercussions resulting in partial iodine organification defect (PIOD) to total iodine organification defect (TIOD) [21]. In this present study, we investigated (a) the mutational spectrum in the TPO gene of TDH patients and (b) the influence of specific mutation on TPO protein structure by means of *in silico* approach. To the best of our knowledge, this is the first molecular investigation on genetic etiology of TDH in Bangladesh.

In this study, we analyzed exons 8-14 of TPO gene of the TDH patients as the previous studies had reported that this region was crucial for the enzymatic activity and mutations in this region may result in absence or reduction in TPO activity [20, 59]. Analysis of 36 specimens revealed three nonsynonymous mutations including p.Ala373Ser (TPO MT1), p.Ser398Thr (TPO MT2), and p.Thr725Pro (TPO MT3) and one synonymous mutation p.Pro715Pro. The identified nonsynonymous mutations had previously been reported to be pathogenic or disease-causing mutations [51, 53]. Moreover, a cloning-based study involving aforementioned mutations

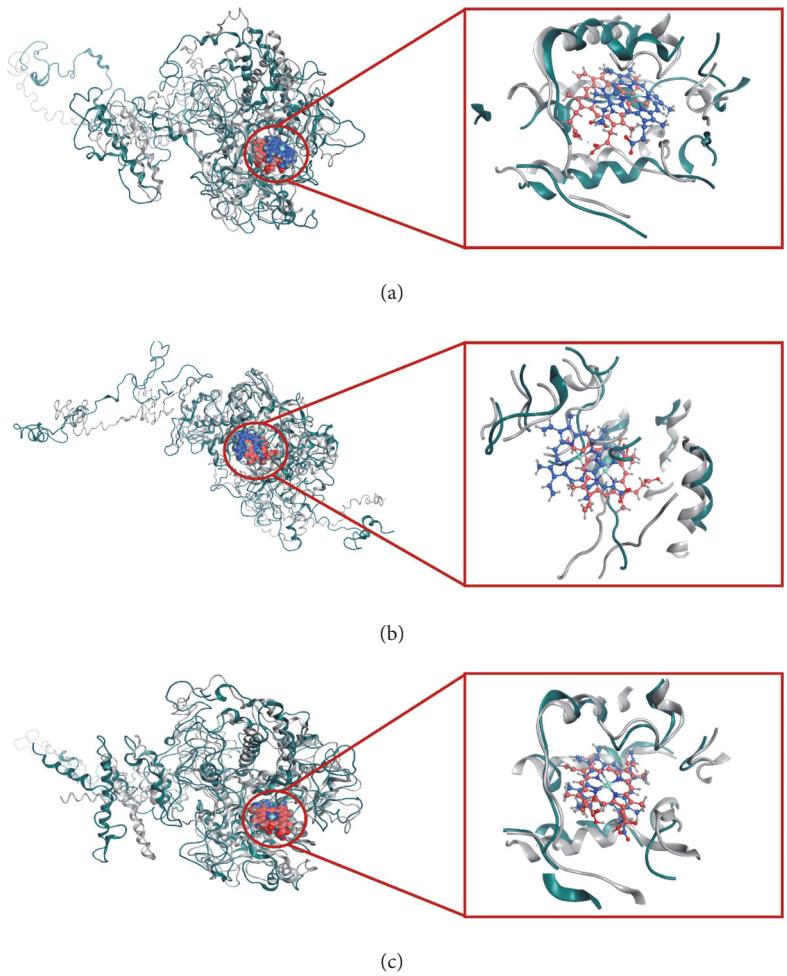

FIGURE 5: Superimposed structures of protein-ligand (heme) complexes before and after 5000 ps MD simulation. (a) $TPO_{1\text{-}933}$ WT, (b) $TPO_{1\text{-}933}$ MT1, and (c) $TPO_{1\text{-}933}$ MT3. Grey and blue colors indicate results before MD simulation whereas green and pink indicate results after MD simulation.

by Guria et al. reported that these mutations could result in low expression of TPO mRNAs as well as a reduction in TPO enzyme activity [20]. They also demonstrated that mutation p.Ala373Ser (TPO MT1) was more damaging than mutation p.Ser398Thr (TPO MT2). This phenomenon could be explained by a change in aliphatic amino acid to hydroxyl-containing amino acid at 373^{th} position of TPO protein, whereas the other mutation (p.Ser398Thr) did not result in such a shift from one group of amino acids to another. However, the mutation in exon-12, namely, p.Thr725Pro (TPO MT3), could result in a failure of TPO protein to shift to its active state as it is well reported that threonine is the phosphorylation site for protein activation [60, 61]. Moreover, p.Thr725Pro had been reported to be associated with autoimmune hypothyroidism [62]. As CH is genetically and phenotypically diverse, molecular studies may provide additional information for diagnosis, classification, and prognosis of the disease. Particularly, in patients with normal thyroid gland morphology, it could be difficult to distinguish between thyrotropin resistance and dyshormonogenesis; and molecular genetic studies may reveal true etiology of the disease in these cases. In this study, at least one of this three damaging mutations was found in a homozygous state or two of them were in a heterozygous state in each of the study participants. We previously reported a mutational hot-spot in the HBB gene and established a cost-effective molecular method (high resolution melting curve analysis) for screening of HBB gene mutations in Bangladesh [63]. Such a cost-effective approach can be adopted for TDH patients and carrier screening targeting the TPO genes in Bangladesh.

Substitution of an amino acid affects the shape, function, or binding properties of a given protein. With growing importance of genetics and genomics in health sector, considerable efforts have been devoted to linking human phenotypes to genotypic variations at the nucleotide level and associated changes in 3D protein structure [64, 65]. Since the identified mutations were pathogenic, we wanted to investigate how these mutations were related to dyshormonogenesis by affecting the structural integrity and function of TPO protein.

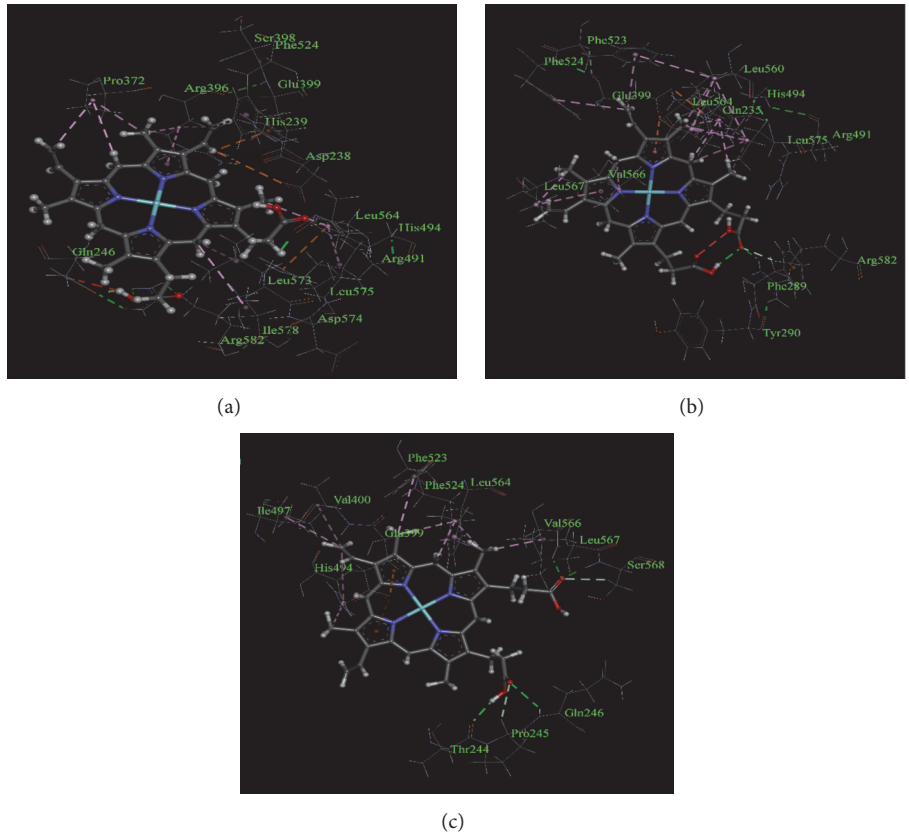

Figure 6: Non-bond interactions of heme with corresponding predicted structures as obtained after docking with the structures retrieved from the 5000 ps simulation using a BIOVIA Discovery Studio 2017. (a) $TPO_{1\text{-}933}$ WT, (b) $TPO_{1\text{-}933}$ MT1, and (c) $TPO_{1\text{-}933}$ MT3. The amino acid residues and their positions are designated as the three letter abbreviations and the corresponding numbers.

To date, there is no high resolution X-ray crystallographic structure for any of the TPO proteins (wild type or mutated) in the public databases. However, there were structures for closely related proteins, namely, myeloperoxidases (MPO) and lactoperoxidases (LPO) [11, 12]. Thus we predicted and validated the three dimensional (3D) structures of TPO (WT and MT) protein using various bioinformatics tools. We studied the effects of mutations on the structural integrity, arrangement of various domains, and folding patterns of the TPO protein. To further study mutational effects, we performed molecular docking of heme in the catalytic site of TPO to investigate how these mutations could affect the activity of TPO enzyme. We obtained the binding energies of heme for the wild type and the mutant structures of TPO protein and found a reduction in binding affinities in the mutant structures compared to the wild type one. Further, we analyzed the detailed results of molecular docking by observing the non-bond interactions of heme with specific amino acid residues to understand the effects of mutations on the functions of TPO protein.

In our study, we applied our bioinformatics approaches on the MPO-like domain of TPO ($TPO_{142\text{-}738}$) and full-length TPO protein ($TPO_{1\text{-}933}$) targeting the non-bond interactions between the heme group and amino acid residues as the mutations identified in this study were found in this region and this MPO-like domain was the catalytic site of TPO enzyme [54]. We obtained the predicted structures for the wild type and the mutant proteins from the I-TASSER server for $TPO_{142\text{-}738}$ and all the structures had significant confidence score (C-score) suggesting that the structures were valid for further studies [22]. However, I-TASSER predicted structures for $TPO_{1\text{-}933}$ had lower C-score value and the reasons may be due to prediction for a very large protein, because I-TASSER predicts structures which are based on iterative threading and also homology modelling and as TPO has no crystallographic structure, this still remains a challenge [22, 24]. We also verified the structures using the Verify3D and the RAMPAGE web servers and both of the servers gave satisfactory results [27, 66]. As heme is crucial for the catalytic activity of TPO, the molecular docking of heme with the wild type and the mutant TPO structures could help us to understand the effects of mutations on the functions of TPO protein. We observed a decrease in heme binding energies in the cases of mutant TPO proteins suggesting that the catalytic activity of mutant TPO might have been hampered. Further investigation gave us information about the heme interactions with specific amino acid residues of TPO protein. The heme prosthetic group of wild type structure interacted with all the important amino acid residues including His239, Arg396, Glu399 and His494 through non-bond interactions.

But in the cases of mutant structures, some of the important amino acid interactions were absent, suggesting that the mutations might have damaging effects on heme interactions and thereby affecting the catalytic activity of TPO enzyme. Guria et al. demonstrated that MT1 (p.Ala373Ser), MT2 (p.Ser398Thr), and MT3 (p.Thr725Pro) had damaging effect on TPO mRNA expression and enzyme activity [20]. However, MT1 (p.Ala373Ser) and MT3 (p.Thr725Pro) showed iodination reactions similar to the nonenzymatic reaction rate, suggesting that these two mutations were more damaging than the MT2 (p.Ser398Thr) which showed more efficient iodination reaction than MT1 and MT3 but less efficient than the wild type TPO protein [20]. This finding is consistent with our molecular docking-based study targeting both the MPO-like domain of TPO ($TPO_{142\text{-}738}$) and the full-length TPO protein ($TPO_{1\text{-}933}$) predicted structures. MT1 and MT3 had more enhanced influence on the interactions between several crucial residues and the heme group, whereas MT2 had less influence on the interaction between the TPO protein and the heme prosthetic group. Different studies showed that quantum chemical methods such as DFT or QM/MM can also be employed for investigating the intermolecular interactions [67–69]. Thus, to validate the results of molecular docking, we performed QM/MM calculations on the full-length wild type TPO protein and two mutant proteins (MT1 and MT3) that had severe damaging effect on the catalytic activity of TPO.

The heme group was treated using a semiempirical approach of calculations and the protein was treated using an approach of molecular mechanical calculations. The structures obtained after performing QM/MM calculations were taken into consideration for further analysis of the presence of non-bond interactions of the active site residues with the heme group. The interactions observed were exactly similar to those obtained from molecular docking, suggesting that the docking results obtained were valid.

In cellular environment, protein structures are always in a dynamic condition. To mimic the cellular environment, we performed molecular dynamics simulation in a cubic simulation box containing water molecules and NaCl and a pH of 7.4 was maintained. After performing 5000 ps simulation under the influence of AMBER14 force field, the final protein structures were superimposed on the corresponding docked protein structure. The results infer that the protein-ligand complexes studied were considerably stable over time as there was very small change in the coordinates of the heme group after the simulation. To observe the effect of protein dynamics, the protein structures were retrieved from the 5000 ps simulation snapshot and again docked with the heme ligand. The finding was rather interesting as the wild type protein was still found to be interacting with the crucial amino acid residues. However, these important interactions were found to be absent for the mutant proteins that might be a potential cause of a decrease in the enzymatic activity of TPO protein.

To understand the in-depth characteristics of TPO protein of both wild type and mutant forms, we performed *in silico* approach to mimic cellular environment. However, various computational chemistry-based approaches like IR and Raman spectroscopy can be used to identify the changes in molecular level with higher specificity [70, 71]. Such compositional analysis in various cellular conditions has become very popular for characterizing the biochemical changes in various disease conditions and also for the study on characterizing the spectrum of various hormones such as corticosteroids [70–72]. The study by Claudio et al. analyzed the molecular vibrational spectrum of thyroid tissues from normal and disease conditions which could ultimately represent the characteristics of secondary structures of proteins [73]. Although use of IR and Raman spectroscopy could offer more insights into the physiological conditions of TDH patients carrying mutations in the TPO gene, the present study was not subjected to such approaches because we did not have such facilities.

In this present study, we had used computational approaches such as molecular docking, QM/MM and molecular dynamics simulation to investigate the effect of mutations on TPO protein interactions. The present study could be useful for future studies including study of the effect of mutations on TPO dimer organization and how mutations in the TPO gene could lead to a change in the TPO protein conformation.

5. Conclusion

Our study investigated the genetic etiology of Bangladeshi patients with TDH, which may further help us to screen and categorize the disease. Three pathogenic mutations were observed in the patients with TDH including p.Ala373Ser, p.Ser398Thr, and p.Thr725Pro. *In silico* based study revealed that p.Ala373Ser and p.Thr725Pro mutations resulted in a significant change in interactions between the amino acid residues of TPO protein and the heme group, whereas the p.Ser398Thr mutation could affect the TPO protein to a lesser extent. The results of this study may help better understand the correlation between specific mutation in the TPO gene and altered biological activities of the TPO protein as well as disease severity among the TDH patients. Furthermore, future study on dimer formation of TPO protein and functional activity study of TPO enzyme in physiological condition is expected to shed light on how mutation in the TPO gene can affect thyroid hormone biosynthesis pathway and find a mutation-based better treatment strategy for individual patients.

Data Availability

The data used to support the findings of this study are included within the article.

Ethical Approval

This study was approved by the Ethical Review Board for Human Studies of BSMMU and University of Dhaka.

Conflicts of Interest

The authors declare that they have no conflicts of interest.

Authors' Contributions

Mst. Noorjahan Begum, Md Tarikul Islam, Golam Sarower Bhuyan, Suprovath Kumar Sarker, Shekh Rezwan Hossain, and Imrul Shahriar conducted the laboratory work, data analysis, and manuscript draft writing. Shahinur Haque, Tasnia Kawsar Konika, Asifuzzaman Rahat, Rosy Sultana, Hurjahan Banu, Narayan Saha, M. A. Hasanat, Mizanul Hasan, Abu A. Sajib, Emran Kabir Chowdhury, Hossain Uddin Shekhar, Abul B. M. M. K. Islam, Suraiya Begum, Md. Sazzadul Islam, and Sadia Sultana assisted in specimen and clinical information collection. Kaiissar Mannoor, Firdausi Qadri, Syed Saleheen Qadri, Mohammad A. Halim, Syeda Kashfi Qadri, and Sharif Akhteruzzaman designed the study plan and supervised the overall project. Md Tarikul Islam, Shekh Rezwan Hossain, and Golam Sarower Bhuyan contributed equally to this work. All authors have read and approved the paper for publication.

Acknowledgments

The authors are thankful to UGC for its generous support and also grateful to ideSHi, RGRC, and BSMMU. This study was supported by grant (CP-4029) from the Higher Education Quality Enhancement Project of the University Grant Commission (UGC) of Bangladesh.

Supplementary Materials

Supplementary Figure 1: Structural differences of heme before and after optimization from three different points of view. Supplementary Figure 2: The predicted 3D structures of the proteins. (A) $TPO_{1\text{-}933}$ WT, (B) $TPO_{1\text{-}933}$ MT1, (C) $TPO_{1\text{-}933}$ MT2, and (D) $TPO_{1\text{-}933}$ MT3. The specific regions of the structures are indicated with the corresponding color written in the brackets. EC = extracellular region shown in green color, TM = transmembrane region shown in cyan color, and IC = intracellular region shown in red color, catalytic center shown in blue color. Supplementary Figure 3: QM/MM ONIOM calculation set up for protein-ligand complexes, high level (ball and stick), and low level (line). Supplementary Table 1: Binding energies and non-bond interactions of heme with $TPO_{142\text{-}738}$ WT, $TPO_{142\text{-}738}$ MT1, $TPO_{142\text{-}738}$ MT2, and $TPO_{142\text{-}738}$ MT3 after flexible docking. Supplementary Table 2: Binding energies and non-bond interactions of heme with $TPO_{1\text{-}933}$WT, $TPO_{1\text{-}933}$MT1, $TPO_{1\text{-}933}$ MT2, and $TPO_{1\text{-}933}$ MT3 after flexible docking. *(Supplementary Materials)*

References

[1] M. V. Rastogi and S. H. LaFranchi, "Congenital hypothyroidism," *Orphanet Journal of Rare Diseases*, vol. 5, no. 1, article 17, 2010.

[2] D. A. Fisher, "Second international conference on neonatalthyroid screening: progress report," *Journal of Pediatrics*, vol. 102, no. 5, pp. 653-654, 1983.

[3] M. Hasan, N. Nahar, A. Ahmed, and F. Moslem, "Screening for congenital hypothyroidism-a new era in Bangladesh," *The Southeast Asian Journal of Tropical Medicine and Public Health*, vol. 34, pp. 162–164, 2004.

[4] C. C. Lee, F. Harun, M. Y. Jalaludin, C. Y. Lim, K. L. Ng, and S. Mat Junit, "Functional analyses of c.2268dup in thyroid peroxidase gene associated with goitrous congenital hypothyroidism," *BioMed Research International*, vol. 2014, Article ID 370538, 11 pages, 2014.

[5] H. Cangul, Z. Aycan, A. Olivera-Nappa et al., "Thyroid dyshormonogenesis is mainly caused by TPO mutations in consanguineous community," *Clinical Endocrinology*, vol. 79, no. 2, pp. 275–281, 2013.

[6] B. Bakker, H. Bikker, T. Vulsma, J. S. E. De Randamie, B. M. Wiedijk, and J. J. M. De Vijlder, "Two decades of screening for congenital hypothyroidism in the Netherlands: TPO gene mutations in total iodide organification defects (an update)," *The Journal of Clinical Endocrinology & Metabolism*, vol. 85, no. 10, pp. 3708–3712, 2000.

[7] F. S. Belforte, M. B. Miras, M. C. Olcese et al., "Congenital goitrous hypothyroidism: Mutation analysis in the thyroid peroxidase gene," *Clinical Endocrinology*, vol. 76, no. 4, pp. 568–576, 2012.

[8] A. Taurog, M. Dorris, and D. R. Doerge, "Evidence for a radical mechanism in peroxidase-catalyzed coupling. I. Steady-state experiments with various peroxidases," *Archives of Biochemistry and Biophysics*, vol. 315, no. 1, pp. 82–90, 1994.

[9] Y. Endo, S. Onogi, K. Umeki et al., "Regional localization of the gene for thyroid peroxidase to human chromosome 2p25 and mouse chromosome 12C," *Genomics*, vol. 25, no. 3, pp. 760-761, 1995.

[10] J. P. Banga, D. Mahadevan, G. J. Barton et al., "Prediction of domain organisation and secondary structure of thyroid peroxidase, a human autoantigen involved in destructive thyroiditis," *FEBS Letters*, vol. 266, no. 1-2, pp. 133–141, 1990.

[11] A. Gardas, M. K. Sohi, B. J. Sutton, A. M. McGregor, and J. P. Banga, "Purification and crystallisation of the autoantigen thyroid peroxidase from human Graves' thyroid tissue," *Biochemical and Biophysical Research Communications*, vol. 234, no. 2, pp. 366–370, 1997.

[12] E. Hendry, G. Taylor, K. Ziemnicka, F. Grennan Jones, J. Furmaniak, and B. Rees Smith, "Recombinant human thyroid peroxidase expressed in insect cells is soluble at high concentrations and forms diffracting crystals," *Journal of Endocrinology*, vol. 160, no. 3, pp. R13–R15, 1999.

[13] T. J. Fiedler, C. A. Davey, and R. E. Fenna, "X-ray crystal structure and characterization of halide-binding sites of human myeloperoxidase at 1.8 Å resolution," *The Journal of Biological Chemistry*, vol. 275, no. 16, pp. 11964–11971, 2000.

[14] A. K. Singh, N. Singh, S. Sharma et al., "Crystal Structure of Lactoperoxidase at 2.4 Å Resolution," *Journal of Molecular Biology*, vol. 376, no. 4, pp. 1060–1075, 2008.

[15] S. N. Le, B. T. Porebski, J. McCoey et al., "Modelling of thyroid peroxidase reveals insights into its enzyme function and autoantigenicity," *PLoS ONE*, vol. 10, no. 12, Article ID e0142615, 2015.

[16] C. M. Rivolta, S. A. Esperante, L. Gruñeiro-Papendieck et al., "Five novel inactivating mutations in the thyroid peroxidase gene responsible for congenital goiter and iodide organification defect," *Human Mutation*, vol. 22, no. 3, p. 259, 2003.

[17] T. Kotani, K. Umeki, J.-I. Kawano et al., "Partial iodide organification defect caused by a novel mutation of the thyroid peroxidase gene in three siblings," *Clinical Endocrinology*, vol. 59, no. 2, pp. 198–206, 2003.

[18] C. Rodrigues, P. Jorge, J. Pires Soares et al., "Mutation screening of the thyroid peroxidase gene in a cohort of 55 Portuguese patients with congenital hypothyroidism," *European Journal of Endocrinology*, vol. 152, no. 2, pp. 193–198, 2005.

[19] J.-Y. Wu, S.-G. Shu, C.-F. Yang, C.-C. Lee, and F.-J. Tsai, "Mutation analysis of thyroid peroxidase gene in Chinese patients with total iodide organification defect: identification of five novel mutations," *Journal of Endocrinology*, vol. 172, no. 3, pp. 627–635, 2002.

[20] S. Guria, B. Bankura, N. Balmiki et al., "Functional analysis of thyroid peroxidase gene mutations detected in patients with thyroid dyshormonogenesis," *International Journal of Endocrinology*, vol. 2014, Article ID 390121, 8 pages, 2014.

[21] H. Bikker, F. Baas, and J. J. M. De Vijlder, "Molecular analysis of mutated thyroid peroxidase detected in patients with total iodide organification defects," *The Journal of Clinical Endocrinology & Metabolism*, vol. 82, no. 2, pp. 649–653, 1997.

[22] Y. Zhang, "I-TASSER server for protein 3D structure prediction," *BMC Bioinformatics*, vol. 9, no. 1, article 40, 2008.

[23] A. Roy, A. Kucukural, and Y. Zhang, "I-TASSER: a unified platform for automated protein structure and function prediction," *Nature Protocols*, vol. 5, no. 4, pp. 725–738, 2010.

[24] J. Yang, R. Yan, A. Roy, D. Xu, J. Poisson, and Y. Zhang, "The I-TASSER Suite: protein structure and function prediction," *Nature Methods*, vol. 12, no. 1, pp. 7-8, 2015.

[25] J. U. Bowie, R. Luthy, and D. Eisenberg, "A method to identify protein sequences that fold into a known three-dimensional structure," *Science*, vol. 253, no. 5016, pp. 164–170, 1991.

[26] R. Luthy, J. U. Bowie, and D. Eisenberg, "Assesment of protein models with three-dimensional profiles," *Nature*, vol. 356, no. 6364, pp. 83–85, 1992.

[27] S. C. Lovell, I. W. Davis, W. B. Arendall et al., "Structure validation by Cα geometry: ϕ, ψ and Cβ deviation," *Proteins: Structure, Function, and Bioinformatics*, vol. 50, no. 3, pp. 437–450, 2003.

[28] A. D. Becke, "Density-functional exchange-energy approximation with correct asymptotic behavior," *Physical Review A: Atomic, Molecular and Optical Physics*, vol. 38, no. 6, pp. 3098–3100, 1988.

[29] C. Lee, W. Yang, and R. G. Parr, "Development of the Colle-Salvetti correlation-energy formula into a functional of the electron density," *Physical Review B: Condensed Matter and Materials Physics*, vol. 37, no. 2, pp. 785–789, 1988.

[30] M. Frisch, G. Trucks, and H. Schlegel, *GAUSSIAN 09, Gaussian 09, Revision D. 01*, Gaussian Inc, Wallingford, Conn, USA, 2009.

[31] M. Dolg, U. Wedig, H. Stoll, and H. Preuss, "Energy-adjusted ab initio pseudopotentials for the first row transition elements," *The Journal of Chemical Physics*, vol. 86, no. 2, pp. 866–872, 1986.

[32] D. Andrae, U. Haeussermann, M. Dolg, H. Stoll, and H. Preuss, "Energy-adjusted ab initio pseudopotentials for the second and third row transition elements," *Theoretical Chemistry Accounts*, vol. 77, no. 2, pp. 123–141, 1990.

[33] S. Dallakyan and A. J. Olson, "Small-molecule library screening by docking with PyRx," *Methods in Molecular Biology*, vol. 1263, pp. 243–250, 2015.

[34] O. Trott and A. J. Olson, "AutoDock Vina: improving the speed and accuracy of docking with a new scoring function, efficient optimization and multithreading," *Journal of Computational Chemistry*, vol. 31, no. 2, pp. 455–461, 2010.

[35] T. Lengauer and M. Rarey, "Computational methods for biomolecular docking," *Current Opinion in Structural Biology*, vol. 6, no. 3, pp. 402–406, 1996.

[36] P. G. Furtmüller, M. Zederbauer, W. Jantschko et al., "Active site structure and catalytic mechanisms of human peroxidases," *Archives of Biochemistry and Biophysics*, vol. 445, no. 2, pp. 199–213, 2006.

[37] A. Taurog, "Molecular evolution of thyroid peroxidase," *Biochimie*, vol. 81, no. 5, pp. 557–562, 1999.

[38] L. Schrödinger, "LLC2010The PyMOL Molecular Graphics System, Version 1.4. The PyMOL molecular graphics system," 2010.

[39] *BIOVIA DS, Discovery Studio Modeling Environment*, Dassault Systèmes, San Diego, Calif, USA, 2017.

[40] T. Vreven, K. S. Byun, I. Komáromi et al., "Combining quantum mechanics methods with molecular mechanics methods in ONIOM," *Journal of Chemical Theory and Computation*, vol. 2, no. 3, pp. 815–826, 2006.

[41] K. G. Vladimirovich, N. R. Nizamovich, T. N. Borisovna et al., "Improvement technology manufacturing poly radioprotective microbial poliantigen," *Research Journal of Pharmaceutical, Biological and Chemical Sciences*, vol. 7, no. 4, pp. 2193–2199, 2016.

[42] T. Vreven, M. J. Frisch, K. N. Kudin, H. B. Schlegel, and K. Morokuma, "Geometry optimization with QM/MM methods II: Explicit quadratic coupling," *Molecular Physics*, vol. 104, no. 5-7, pp. 701–714, 2006.

[43] T. Vreven and K. Morokuma, "On the Application of the IMOMO (integrated molecular orbital + molecular orbital) Method," *Journal of Computational Chemistry*, vol. 21, no. 16, pp. 1419–1432, 2000.

[44] S. Dapprich, I. Komáromi, K. S. Byun, K. Morokuma, and M. J. Frisch, "A new ONIOM implementation in Gaussian98. Part I. The calculation of energies, gradients, vibrational frequencies and electric field derivatives," *Journal of Molecular Structure: THEOCHEM*, vol. 461-462, pp. 1–21, 1999.

[45] F. Maseras and K. Morokuma, "IMOMM: A new integrated ab initio + molecular mechanics geometry optimization scheme of equilibrium structures and transition states," *Journal of Computational Chemistry*, vol. 16, no. 9, pp. 1170–1179, 1995.

[46] M. Frisch, G. Trucks, H. B. Schlegel et al., *Gaussian 09, revision a. 02, gaussian*, Gaussian. Inc, Wallingford, Conn, USA, 2009.

[47] J. J. P. Stewart, "Optimization of parameters for semiempirical methods V: modification of NDDO approximations and application to 70 elements," *Journal of Molecular Modeling*, vol. 13, no. 12, pp. 1173–1213, 2007.

[48] E. Krieger, T. Darden, S. B. Nabuurs, A. Finkelstein, and G. Vriend, "Making optimal use of empirical energy functions: Force-field parameterization in crystal space," *Proteins: Structure, Function, and Genetics*, vol. 57, no. 4, pp. 678–683, 2004.

[49] F. Krieger, B. Fierz, O. Bieri, M. Drewello, and T. Kiefhaber, "Dynamics of unfolded polypeptide chains as model for the earliest steps in protein folding," *Journal of Molecular Biology*, vol. 332, no. 1, pp. 265–274, 2003.

[50] T. Darden, D. York, and L. Pedersen, "Particle mesh Ewald: an N·log(N) method for Ewald sums in large systems," *The Journal of Chemical Physics*, vol. 98, no. 12, pp. 10089–10092, 1993.

[51] M. Avbelj, H. Tahirovic, M. Debeljak et al., "High prevelance if thyroid peroxidase gene mutations in patients with thyroid dyshormonogenesis," *European Journal of Endocrinology*, vol. 156, no. 5, pp. 511–519, 2007.

[52] C. C. Lee, F. Harun, M. Y. Jalaludin, C. H. Heh, R. Othman, and S. Mat Junit, "A Novel, homozygous c.1502T>G (p.Val501Gly) mutation in the thyroid peroxidase gene in malaysian sisters

with congenital hypothyroidism and multinodular goiter," *International Journal of Endocrinology*, vol. 2013, Article ID 987186, 7 pages, 2013.

[53] N. Balmiki, B. Bankura, S. Guria et al., "Genetic analysis of thyroid peroxidase (TPO) gene in patients whose hypothyroidism was found in adulthood in West Bengal, India," *Endocrine Journal*, vol. 61, no. 3, pp. 289–296, 2014.

[54] F. Libert, J. Ruel, M. Ludgate et al., "Thyroperoxidase, an auto-antigen with a mosaic structure made of nuclear and mitochondrial gene modules.," *EMBO Journal*, vol. 6, no. 13, pp. 4193–4196, 1987.

[55] S. Kimura and M. Ikeda-Saito, "Human myeloperoxidase and thyroid peroxidase, two enzymes with separate and distinct physiological functions, are evolutionarily related members of the same gene family," *Proteins: Structure, Function, and Genetics*, vol. 3, no. 2, pp. 113–120, 1988.

[56] N. Yokoyama and A. Taurog, "Porcine thyroid peroxidase: Relationship between the native enzyme and an active, highly purified tryptic fragment," *Molecular Endocrinology*, vol. 2, no. 9, pp. 838–844, 1988.

[57] M. Godlewska, M. Góra, A. M. Buckle et al., "A redundant role of human thyroid peroxidase propeptide for cellular, enzymatic, and immunological activity," *Thyroid*, vol. 24, no. 2, pp. 371–382, 2014.

[58] V. Le Fourn, M. Ferrand, and J.-L. Franc, "Endoproteolytic cleavage of human thyroperoxidase: Role of the propeptide in the protein folding process," *The Journal of Biological Chemistry*, vol. 280, no. 6, pp. 4568–4577, 2005.

[59] H. Bikker, T. Vulsma, F. Baas, and J. J. M. de Vijlder, "Identification of five novel inactivating mutations in the human thyroid peroxidase gene by denaturing gradient gel electrophoresis," *Human Mutation*, vol. 6, no. 1, pp. 9–16, 1995.

[60] M. Huse and J. Kuriyan, "The conformational plasticity of protein kinases," *Cell*, vol. 109, no. 3, pp. 275–282, 2002.

[61] A. Krupa, G. Preethi, and N. Srinivasan, "Structural modes of stabilization of permissive phosphorylation sites in protein kinases: Distinct strategies in Ser/Thr and Tyr kinases," *Journal of Molecular Biology*, vol. 339, no. 5, pp. 1025–1039, 2004.

[62] A. E. Gomaa, N. M. Mohamed, B. A. Gaballah, and S. M. El Shabrawy, "Assessment of the role of thyroid peroxidase gene polymorphism as a cause of hypothyroidism in Zagazig university hospital patients," *Zagazig University Medical Journal*, vol. 23, no. 5, pp. 330–342, 2018.

[63] M. T. Islam, S. K. Sarkar, N. Sultana et al., "High resolution melting curve analysis targeting the HBB gene mutational hotspot offers a reliable screening approach for all common as well as most of the rare beta-globin gene mutations in Bangladesh," *BMC Genetics*, vol. 19, no. 1, p. 1, 2018.

[64] D. Altshuler, M. J. Daly, and E. S. Lander, "Genetic mapping in human disease," *Science*, vol. 322, no. 5903, pp. 881–888, 2008.

[65] D. Botstein and N. Risch, "Discovering genotypes underlying human phenotypes: past successes for mendelian disease, future approaches for complex disease," *Nature Genetics*, vol. 33, pp. 228–237, 2003.

[66] D. Eisenberg, R. Lüthy, and J. U. Bowie, "VERIFY3D: assessment of protein models with three-dimensional profiles," *Methods in Enzymology*, vol. 277, pp. 396–404, 1997.

[67] R. Prabhakar, P. E. M. Siegbahn, B. F. Minaev, and H. Ågren, "Spin transition during H2O2 formation in the oxidative half-reaction of copper amine oxidases," *The Journal of Physical Chemistry B*, vol. 108, no. 36, pp. 13882–13892, 2004.

[68] R. Prabhakar, P. E. M. Siegbahn, B. F. Minaev, and H. Ågren, "Activation of triplet dioxygen by glucose oxidase: Spin-orbit coupling in the superoxide ion," *The Journal of Physical Chemistry B*, vol. 106, no. 14, pp. 3742–3750, 2002.

[69] B. F. Minaev and V. A. Minaeva, "Spin-dependent binding of dioxygen to heme and charge-transfer mechanism of spin-orbit coupling enhancement," *Ukrainica Bioorganica Acta*, vol. 6, no. 2, pp. 56–64, 2008.

[70] O. P. Cherkasova, M. M. Nazarov, D. A. Sapozhnikov et al., "Vibrational spectra of corticosteroid hormones in the terahertz range," in *InLaser Applications in Life Sciences*, vol. 7376, p. 73760P, International Society for Optics and Photonics, 2010.

[71] V. A. Minaeva, B. F. Minaev, G. V. Baryshnikov et al., "Temperature effects in low-frequency Raman spectra of corticosteroid hormones," *Optics and Spectroscopy*, vol. 118, no. 2, pp. 214–223, 2015.

[72] K. Eberhardt, C. Stiebing, C. Matthäus, M. Schmitt, and J. Popp, "Advantages and limitations of Raman spectroscopy for molecular diagnostics: an update," *Expert Review of Molecular Diagnostics*, vol. 15, no. 6, pp. 773–787, 2015.

[73] C. A. Soto, L. P. Medeiros-Neto, L. dos Santos et al., "Infrared and confocal Raman spectroscopy to differentiate changes in the protein secondary structure in normal and abnormal thyroid tissues," *Journal of Raman Spectroscopy*, vol. 49, no. 7, pp. 1165–1173, 2018.

Hindawi
BioMed Research International
Volume 2019, Article ID 5920485, 14 pages
https://doi.org/10.1155/2019/5920485

Research Article

A Metabolomic Study on the Intervention of Traditional Chinese Medicine Qushi Huayu Decoction on Rat Model of Fatty Liver Induced by High-Fat Diet

Xiao-jun Gou,[1] **Shanshan Gao**,[2] **Liang Chen**,[3] **Qin Feng**,[4] **and Yi-yang Hu**[4]

[1]*Central Laboratory, Baoshan District Hospital of Integrated Traditional Chinese and Western Medicine of Shanghai, Shanghai University of Traditional Chinese Medicine, Shanghai 201999, China*
[2]*School of Pharmacy, Shaanxi University of Traditional Chinese Medicine, Yangxian, Shaanxi 712046, China*
[3]*Nantong Hospital Affiliated to Nanjing University of Chinese Medicine, Nantong, Jiangsu 226001, China*
[4]*Institute of Liver Disease, Shuguang Hospital, Shanghai University of Traditional Chinese Medicine, Shanghai 201203, China*

Correspondence should be addressed to Qin Feng; fengqin1227@163.com and Yi-yang Hu; yyhuliver@163.com

Received 25 October 2018; Accepted 10 January 2019; Published 7 February 2019

Guest Editor: Hossain U. Shekhar

Qushi Huayu Decoction (QHD), an important clinically proved herbal formula, has been reported to be effective in treating fatty liver induced by high-fat diet in rats. However, the mechanism of action has not been clarified at the metabolic level. In this study, a urinary metabolomic method based on gas chromatography-mass spectrometry (GC-MS) coupled with pattern recognition analysis was performed in three groups (control, model, and QHD group), to explore the effect of QHD on fatty liver and its mechanism of action. There was obvious separation between the model group and control group, and the QHD group showed a tendency of recovering to the control group in metabolic profiles. Twelve candidate biomarkers were identified and used to explore the possible mechanism. Then, a pathway analysis was performed using MetaboAnalyst 3.0 to illustrate the pathways of therapeutic action of QHD. QHD reversed the urinary metabolite abnormalities (tryptophan, uridine, and phenylalanine, etc.). Fatty liver might be prevented by QHD through regulating the dysfunctions of phenylalanine, tyrosine, and tryptophan biosynthesis, phenylalanine metabolism, and tryptophan metabolism. This work demonstrated that metabolomics might be helpful for understanding the mechanism of action of traditional Chinese medicine for future clinical evaluation.

1. Introduction

Nonalcoholic fatty liver disease (NAFLD) refers to the liver parenchymal cytoplasmic steatosis and fat storage as characteristics of the clinical pathological syndrome excluding alcohol and other determinants of liver damage [1]. With the improvement of living standards and lifestyle changes, the prevalence of diseases such as obesity, insulin resistance (IR), hyperlipidemia, diabetes, and metabolic syndrome contributes to the development of NAFLD. The increasing incidence of NAFLD has become a global medical and public health problem [2–4]. NAFLD can be developed from the original nonalcoholic fatty liver (NAFL) to nonalcoholic steatohepatitis (NASH), even to the later stage of liver fibrosis, liver cirrhosis, and advanced hepatocellular carcinoma in the absence of effective intervention [5]. At present, NAFLD has become the most common cause of chronic liver disease and hepatic enzyme abnormality in western developed countries such as Europe and the United States. Epidemiology shows that NAFLD involves an average of 10% to 24% of the world's population and the prevalence rate in obese people is up to 57% - 74%. About 50% of NAFLD patients can develop into nonalcoholic steatohepatitis after 4~13 years, and 40% of the patients develop into hepatic fibrosis. The incidence of NAFLD is significantly higher than that of hepatitis B, hepatitis C, and alcoholic liver disease, and it has become one of the most common diseases [6, 7]. In recent years, the prevalence of NAFLD in China and the Asia Pacific region has increased year by year, and the adult incidence in developed areas of China can reach 15% or

even higher [8]. The common risk factors of NAFLD are hypertriglyceridemia, obesity, and type II diabetes, and the pathophysiological process of NAFLD is extremely complex. Its exact cause and mechanism are not yet clear.

Lifestyle changes, such as weight loss, diet changes, and physical activity, can promote the treatment of NAFLD [9]; however, most people find it difficult to adhere to exercise [10]. In addition, although some pharmaceutical preparations have been approved for NAFLD, many drugs have potential side effects or only show efficacy for individual patients [11]. Therefore, researchers have become increasingly interested in finding natural products to treat NAFLD from diet and natural plants/herbs. Many natural products have been used to treat NAFLD due to their obvious liver protection, hypoglycemia, antihyperlipidemia effect, and negligible side effects [12].

QHD is an effective prescription for NAFLD treatment based on our long-term clinical practice. It is made up of five traditional Chinese medicines, including *Herba Artemisiae Capillaris, Rhizoma Polygoni Cuspidati, Herba Hyperici Japonici, Rhizoma Curcumae Longae, gardenia jasminoides ellis*. It has the functions of clearing heat, removing dampness and detoxifying, promoting blood circulation, and dispersing blood stasis. In nearly a decade, animal experiments have repeatedly confirmed that QHD has a significant preventive effect on fatty liver induced by high-fat diet alone and carbon tetrachloride (CCL_4) combined with a high-fat and low-protein diet in rats [13, 14]. Clinical studies have also shown that QHD can significantly improve the degree of fatty liver in patients with nonalcoholic steatohepatitis and effectively alleviate the main clinical symptoms of abdominal distention, flank pain, and other symptoms in patients with fatty liver and improve the efficacy of TCM syndromes. QHD has markedly reduced liver damage indicators, such as serum ALT, AST, TG, TC, and LDL-c levels in patients [15]. In the earlier period, our group investigated the mechanism of QHD in some aspects of the pathological mechanism of nonalcoholic fatty liver (NAFL), indicating that the mechanism of QHD in preventing and treating NAFL involves regulation of adenosine monophosphate-activated protein kinase (AMPK) activity, elevation of adiponectin, regulation of intestinal flora, reduction of free fatty acid (FFA) toxicity, etc. [16–19]. Traditional Chinese medicine (TCM) compound has the characteristics of multipathway and multitarget pharmacology, and the mechanism of action is very complex. These results suggested that QHD was a promising compound with good druggability. However, these studies are limited to the exploration of certain specific pathological aspects and elucidation of curative effect and mechanism of treatment of NAFLD is not sufficient for QHD.

Metabolomics aims to establish the metabolic profiles of low molecular weight endogenous metabolites in the biological system through modern analytical techniques [20]. Metabolomics is a branch of systems biology that focuses on the overall metabolite spectrum in various biological samples, such as urine, plasma, or tissues [21]. This research strategy is consistent with the overall and systematic nature of TCM [22]. Due to these advantages, more and more attention has been paid to the mechanism of TCM prescriptions revealed by metabonomics, such as Huangqin Decoction and Liuwei Dihuang Decoction [23, 24]. Some analytical tools have been used in metabolomic analysis, such as nuclear magnetic resonance spectroscopy (NMR), mass spectrometry (MS) and gas chromatography (GC/MS), liquid chromatography (LC/MS), and capillary electrophoresis (CE/MS). Among them, GC/MS provides sufficient separation of complex sample, high sensitivity and metabolite resolution, and easy access to NIST database, which has developed into a popular and useful analysis technology in metabolomic research [25]. Our previous serum and liver tissue metabolomic studies suggest that the effects of Qushi Huayu Decoction on fatty liver may involve regulation of beta-alanine metabolism, alanine, aspartate, and glutamate metabolism, glycine, serine, and threonine metabolism, pyruvate metabolism, and citrate cycle [26]. Owing to the limited time and the economic difficulty, we previously studied only the samples of serum and liver tissue and did not observe a time-dependent dynamic change in the metabolomic profile. Meanwhile, urine, as important biological samples, may be attractive for biomarker investigation to provide a new insight into the progression of fatty liver and the therapeutic basis of QHD. In addition, the urine sample is the end product of the body's metabolism. It is noninvasive and dynamic and can be used to observe changes in metabolic profiles during animal modeling. The results of urine metabolomics are also a complement to the results of serum and liver tissue metabolomic.

In this work, based on previous studies of serum and liver tissue metabolomics, we used a GC-MS-based urine metabolomic method combined with pattern recognition and pathway analysis to analyze their metabolic characteristics of control group, model group, and QHD group. In addition, we also introduced a typical metabolic pathway network to explain biochemical mechanisms, thus providing a multiobjective interpretation of the effect of QHD on NAFLD.

2. Materials and Methods

2.1. Chemicals. N,O-bis(trimethylsilyl)trifluoroacetamide (BSTFA+1%TMCS) and methoxyamine hydrochloride were obtained from TCI (Shanghai) Chemical Industry Development Co., Ltd. Myristic acid and urease were purchased from Sigma-Aldrich (St. Louis, MO, USA). Heptane, pyridine, and methanol are of analytical grade from Shanghai Aladdin Biochemical Technology Co., Ltd. Commercial kits for the determination of alanine aminotransferase (ALT), aspartate aminotransferase (AST), low density lipoprotein cholesterol (LDL), high density lipoprotein cholesterol (HDL), and triglyceride (TG) came from Nanjing Jiancheng Institute of Biotechnology (Nanjing, China).

2.2. Preparation of QHD. QHD was prepared as described in an earlier report [17]. The concentration for the final stock solution of QHD extract was adjusted to 0.93g/crude herb/mL, and the quality control of QHD was shown in the additional material files (available here).

2.3. Experimental Animals. The protocol was approved by the Animal Experiment Ethics Committee of Shanghai University of TCM, and the study was carried out under the

Guidelines for Animal Experimentation of Shanghai University of TCM (Shanghai, China). Thirty male Sprague-Dawley rats (weighing 170±20g) were commercially obtained from Shanghai Experimental Animal Center of Chinese Academy of Sciences (Shanghai, China), and the food materials for the animals were commercially obtained from Shanghai Laboratory Animal Center (Shanghai, China). All the animals were fed at a temperature ranging from 23°C to 24 23°C and humidity of 60% ± 10% in a 12/12-hour light-dark cycle. The rats were fed with certified standard chow and tap water ad libitum for 1 week acclimation.

2.4. Drug Treatment and Sample Collection. After 1 week of adaptation, 30 rats were randomly divided into the following three groups of 10 each: control group (feeding with normal diet for 8 weeks, and drinking tap water normally for the first 4 weeks, orally administered with saline daily on each of the last 4 weeks), model group [feeding with high-fat diet (10% lard+2% cholesterol + 88% normal diet) for 8 weeks, and drinking tap water normally for the first 4 weeks, orally administered with saline daily on each of the last 4 weeks], and QHD group [feeding with a high-fat diet for 8 weeks, drinking tap water normally for the first 4 weeks, orally administered with tap water ad libitum on each of the first 4 weeks, dosed orally with QHD 0.093gkg^{-1}day^{-1} on each of the last 4 weeks according to literature [14] with some modifications].

The samples of overnight (12h) urine from all the rats were collected in metabolism cages at 0 weeks before modeling, 4 weeks before QHD administration, 6 weeks during QHD administration, and 8 weeks after QHD administration throughout the experimental period and were immediately stored at −80°C after centrifugation at 3000rpm for 10min to remove the residues. All the rats were sacrificed by anesthesia with 2% sodium pentobarbital (3mLkg^{-1}). The serum samples were collected, centrifuged at 3000rpm for 10min, and stored at −80°C until analysis. The livers were immediately weighed and washed with cold normal saline. The samples from the right liver lobes were then fixed in 10% neutral formalin for histological analysis. The samples from the left liver lobes were immediately frozen at −80°C for subsequent analysis.

2.5. Analysis of Liver Function and Pathological Examination. Serum samples were used to measure the levels of triglycerides (TG), low-density lipoprotein cholesterol (LDL-c), high-density lipoprotein cholesterol (HDL-c), alanine aminotransferase (ALT), and aspartate aminotransferase (AST) by using ELISA Kit according to the manufacturer's instructions. The liver TG was also measured by using commercial kits as per the manufacturer's instructions. Liver tissue was fixed with formalin and embedded in paraffin, sectioned, and stained with hematoxylin and eosin (HE) and Oil-Red O, respectively, according to the standard protocol.

2.6. Urine Sample Preparation and Analysis. The analysis of urine samples was performed by using a published method [27] with some modifications, and detailed steps were shown in the additional material files.

2.7. GC/MS Analysis. Each 1μl aliquot of the analytes was injected into an Agilent 6890N GC/5975B inert MS detector (Agilent Technologies, Santa Clara, CA, USA). The separation was achieved on an HP-5MS capillary column (30m x 250μm internal diameter, 0.25μm film thickness, 5% phenyl methylpolysiloxane bonded and cross-linked; Agilent J&W Scientific, Folsom, CA, USA). The MS parameters used included the following: the injection and interface temperature were set at 260°C, and the ion source was adjusted to 200°C. The GC oven temperature was kept at 70°C for 2min, ramped at 5°Cmin^{-1} to 160°C, and finally held at 240°C at a rate of 10°C min^{-1} for 6 min. Helium was used as the carrier gas at a flow rate of 1ml/min. The electron energy was 70 eV, and detection was carried out in full scan mode (m/z 30-600) with a solvent delay of 5 min.

2.8. Data Processing. Unprocessed GC/MS raw files were converted to NetCDF format via DataBridge (PerkinElmer Inc, USA), and then the baseline correction, peak discrimination and alignment, and retention time correction were performed by the XCMS toolbox (https://xcmsonline.scripps.edu/) with default settings. The result table (TSV file) is exported to Microsoft Excel, and all data are standardized to spectral sum before multivariate analysis. Multivariate statistical analysis tools were used to analyze data by pattern recognition. The SIMCA-P11.5 software package (Umetrics AB, Umea, Sweden) was used for principal component analysis (PCA) and partial least squares discriminant analysis (PLS-DA). In addition, an unpaired Student t-test was used to assess significant differences in discriminant scores or concentrations of different metabolites obtained from PLS-DA modeling between the model group and the control group. The concentration of each metabolite was expressed as the ratio of its peak area value to that of the selected internal standard peak area of myristic acid.

2.9. Statistics. SPSS 21.0 statistical software package (SPSS, Chicago, USA) was used for quantitative analysis and expressed as mean ± standard deviation. Student-Newman-Kerr one-way analysis of variance was used to analyze the statistical differences among groups. The results of $P < 0.05$ were considered as statistically significant.

3. Result

3.1. Body Weight. As shown in Figure 1, there was no significant difference in initial body weight between the 3 groups. After 8 weeks, compared with the control group, the weight of the model group increased significantly ($p< 0.05$), while the weight of the QHD group decreased, and there was no significant difference compared with the model group.

3.2. TG Level in Liver. As shown in Figure 2(a), after 8 weeks on a high-fat diet, the rats in the model group exhibited increased TG levels compared to the rats in the control group ($P < 0.01$). After treatment with QHD, the level of TG was decreased compared to the rats in the model group ($P < 0.01$).

3.3. Serum Levels of ALT, AST, TG, LDL, and HDL. At the end of the experiment, the serum levels of ALT, AST, TG, and LDL

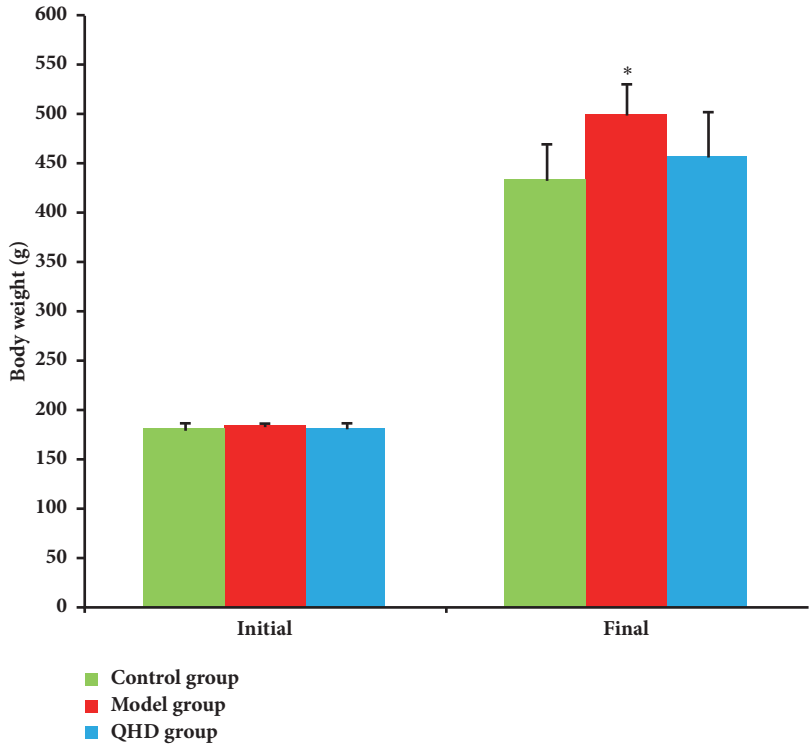

Figure 1: Body weight from animals of different groups, * $p<0.05$, compared with control group.

in the model group were significantly higher than those in the control group ($P < 0.01$). Compared with the model group, QHD significantly reduced ALT, AST, TG, and LDL ($P <0.05$ or $P <0.01$), respectively. There was no significant difference in serum HDL between QHD and model group [Figures 2(b), 2(c), and 2(d)].

3.4. Histopathological Changes of the Liver. Histopathological changes of liver were examined in H&E stained sections. Liver samples of model rats showed *degeneration of hepatocytes, abundant* fat deposition, inflammatory infiltration, prominent hepatocyte balloons, and a single large vacuole in the cytoplasm of hepatocytes. Histopathological features of fatty liver were observed in QHD group, but these symptoms were alleviated. No histopathological signs were found in the control group [Figures 3(a)–3(c)]. Oil red O staining of liver tissue showed that no red lipid droplets were seen in the normal group. Compared with the normal group, liver steatosis was obvious, lipid droplets were large, the central area of the lobule was darkly stained, and the marginal area was lightly stained in the model group. The above changes in the QHD group were obviously reduced [Figures 3(d)–3(f)]. These phenomena indicate that the rat fatty liver model induced by high fat diet was successful and the histopathological status was improved with the use of QHD.

3.5. Metabolomic Study

3.5.1. GC/MS Spectra of the Three Groups. A typical GC/MS total ion current (TIC) chromatogram of the urine samples from the control, model, and QHD groups was illustrated in Figures 4(a), 4(b), and 4(c), respectively. The visual inspection of the spectra revealed some obvious differences, but the complexity of GC/MS spectra prevented further comparison between classes. Thus, XCMS and Microsoft Excel software were used to pretreat the GC/MS spectra and obtained a three-dimensional matrix (RT–m/z pairs), 30 sample names (observations), and peak area percentage (variables). The resulting data set was subsequently analyzed to extract useful information by multivariate statistics including PCA and PLS-DA.

3.5.2. Analysis of Metabolic Profiles and Identification of Significantly Changed Metabolites. In this work, typical GC/MS TIC chromatograms of urine samples from the control, model, and QHD groups are shown in Figures 4(a), 4(b), and 4(c), respectively. Subtle changes can be found using pattern recognition methods such as PCA and PLS-DA. PCA and PLS-DA are two of the most popular pattern recognition methods for obtaining information about the classification and identification of metabolites. PCA is an unsupervised method used as the first step in the separation process to filter out noise and reduce the dimension of the observed data. PLS-DA is a monitoring method similar to PCA in principle for improving classification performance [28]. PCA displays the poor separation between the control group and the model group (Figure 5(a)).

To improve the classification of the model and control groups, a PLS-DA model was performed. As shown in Figure 5(b), the samples in the model and control groups were clearly separated; and the parameters of the modeling such as R^2X, R^2Y, and Q^2Y were 0.61, 0.97, and 0.78, respectively,

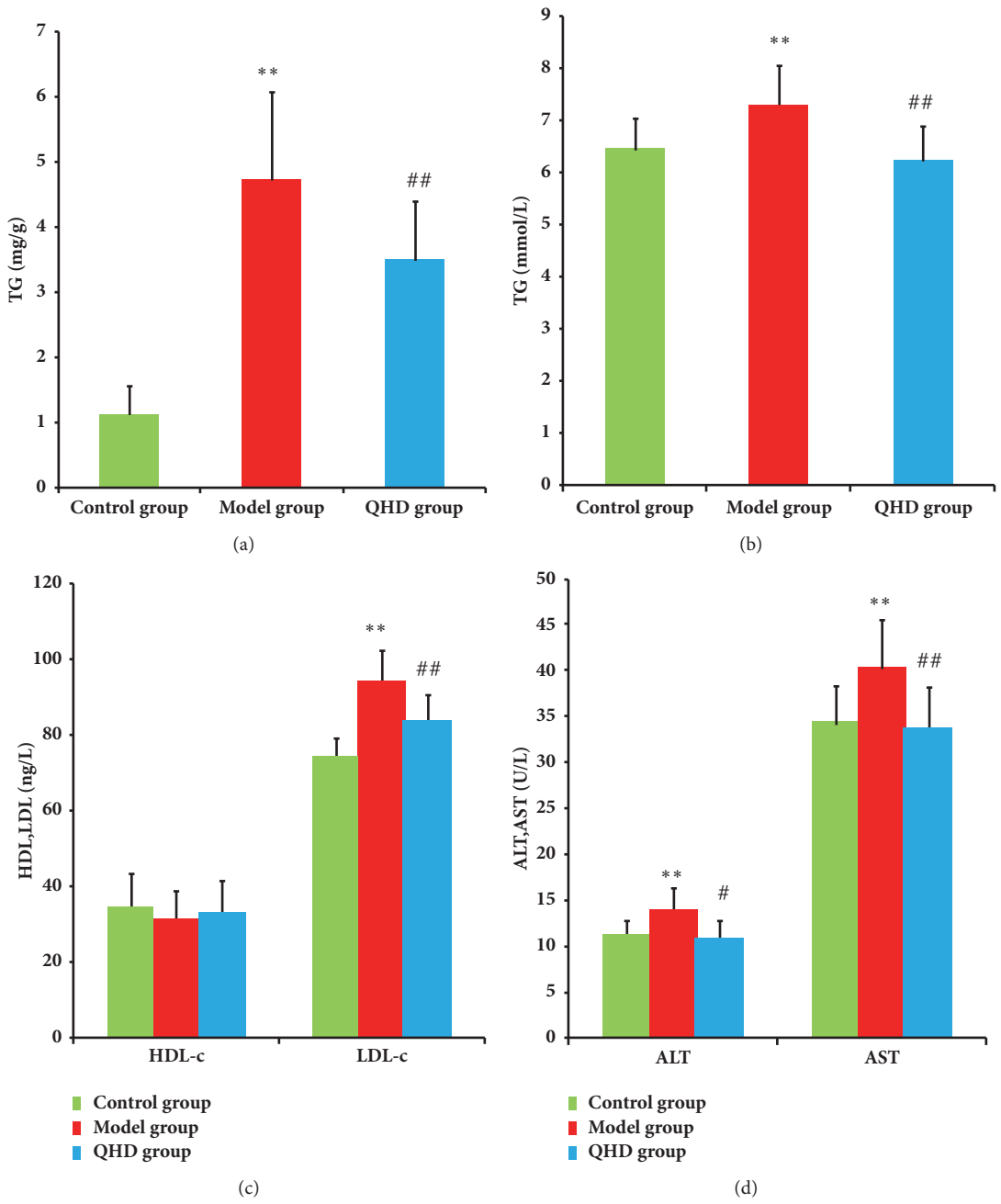

Figure 2: Hepatic levels of TG (a) and serum levels of TG (b), HDL and LDL (c), AST and ALT (d). $^{*}p$ <0.05, $^{**}p$ <0.01 compared with control group, $^{\#}p$<0.05, $^{\#\#}p$<0.01 compared with model group.

indicating that the metabolic profile of the rats in the model group was different from those in the control group. A permutation test was conducted to further validate the model [29]. After 200 permutations, the intercept values of R2 and Q2 are 0.48 and -0.38. The negative value of Q2 intercept indicates the robustness of the model, which shows a low risk of overfitting and reliability (Figure 6).

The PLS-DA loading plot (Figure 7) showed the variables that had contributed strongly to the separation of the groups, the significantly changed metabolites that were the furthest one from the origin in the loading plot. According to VIP (the variable importance in the projection)>1[30], 36 difference variables were found. Next, based on P value of Student t-test (p< 0.05), and matching value from the NIST library for more than 800 (out of 1000) endogenous metabolites, 12 significantly changed metabolites could be identified from the loading plot [31]. Among them, 4 were decreased in model rats, whereas the other 8 were upregulated. The results were summarized in Table 1.

3.5.3. The Influence of QHD on the Urinary Metabolic Profiles of High-Fat Diet Rats. To evaluate the influence of QHD

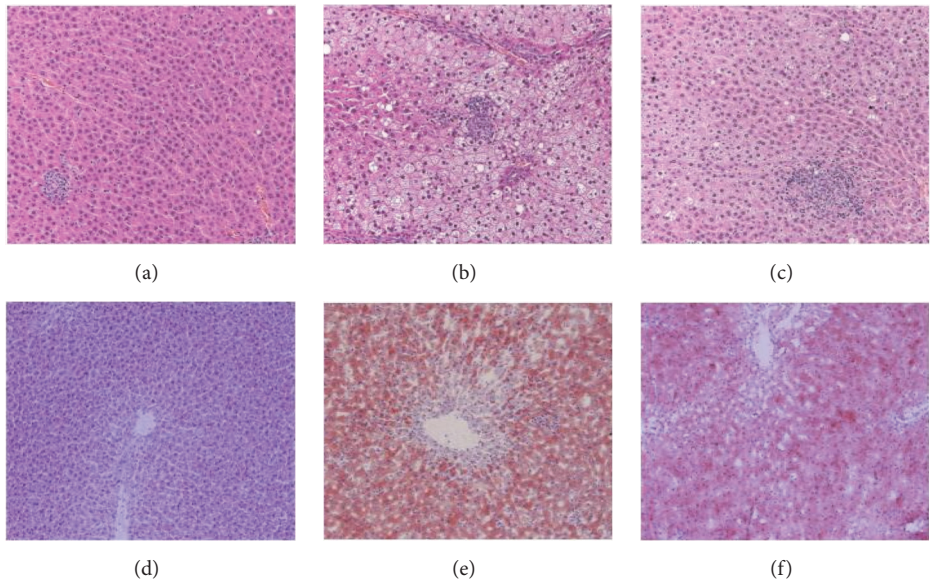

Figure 3: Liver sections showing steatosis and inflammation with H&E staining (×200) and Oil Red staining (×200). H&E staining from (a) control group, (b) model group, and (c) QHD group. Oil Red staining from (d) control group, (e) model group, and (f) QHD group.

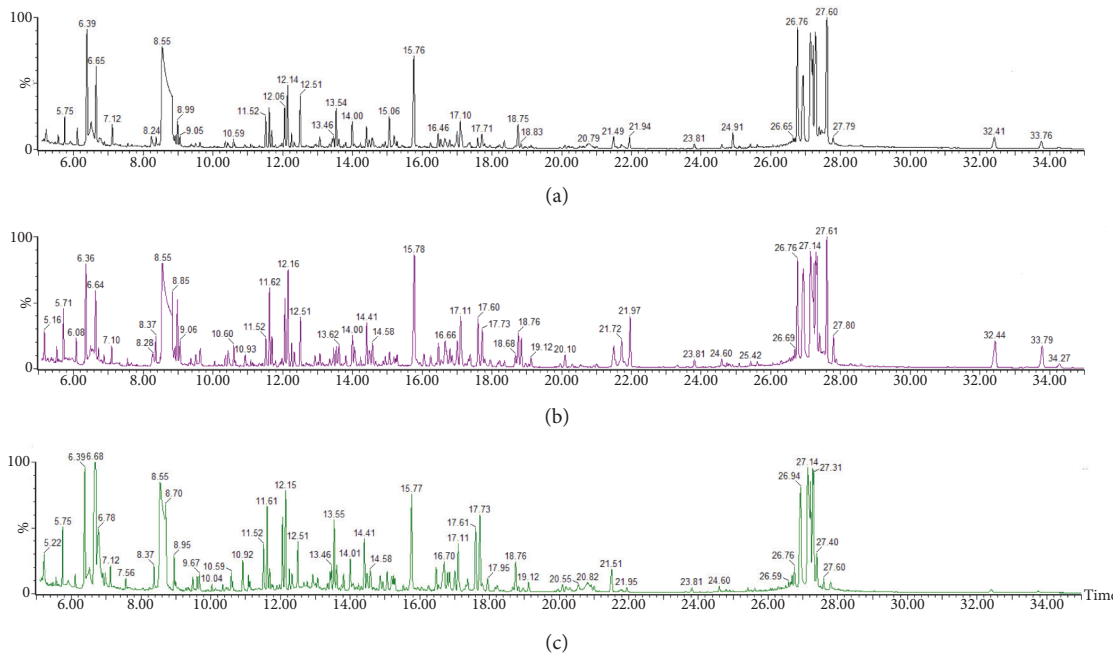

Figure 4: Typical GC/MS spectra of urine samples from (a) control group, (b) model group, and (c) QHD group.

on the urinary metabolic profiles of the high-fat diet rats, a three-dimensional PLS-DA scores plot was built to depict the general variation between the control and model groups with QHD intervention. The scores plot (Figure 8) showed clear separation of the model and control groups. The results indicated that the urinary metabolic pattern was significantly changed in the high-fat diet treated-model group. Also, the QHD treated-group located between the model and control groups, and it was much closer to the control group, implying that QHD did effectively prevent the progression of fatty liver and regulated the perturbed metabolism.

The mean level of the 12 metabolites showed a tendency to normal at different degrees after taking QHD (Table 1). Among these metabolites, tryptophan, uridine, and phenylalanine in the QHD-treated group were completely reversed to levels in the control group (Table 1). It was revealed that the concentrations of these metabolites, which were altered in the rats of model group, had the tendency to come back

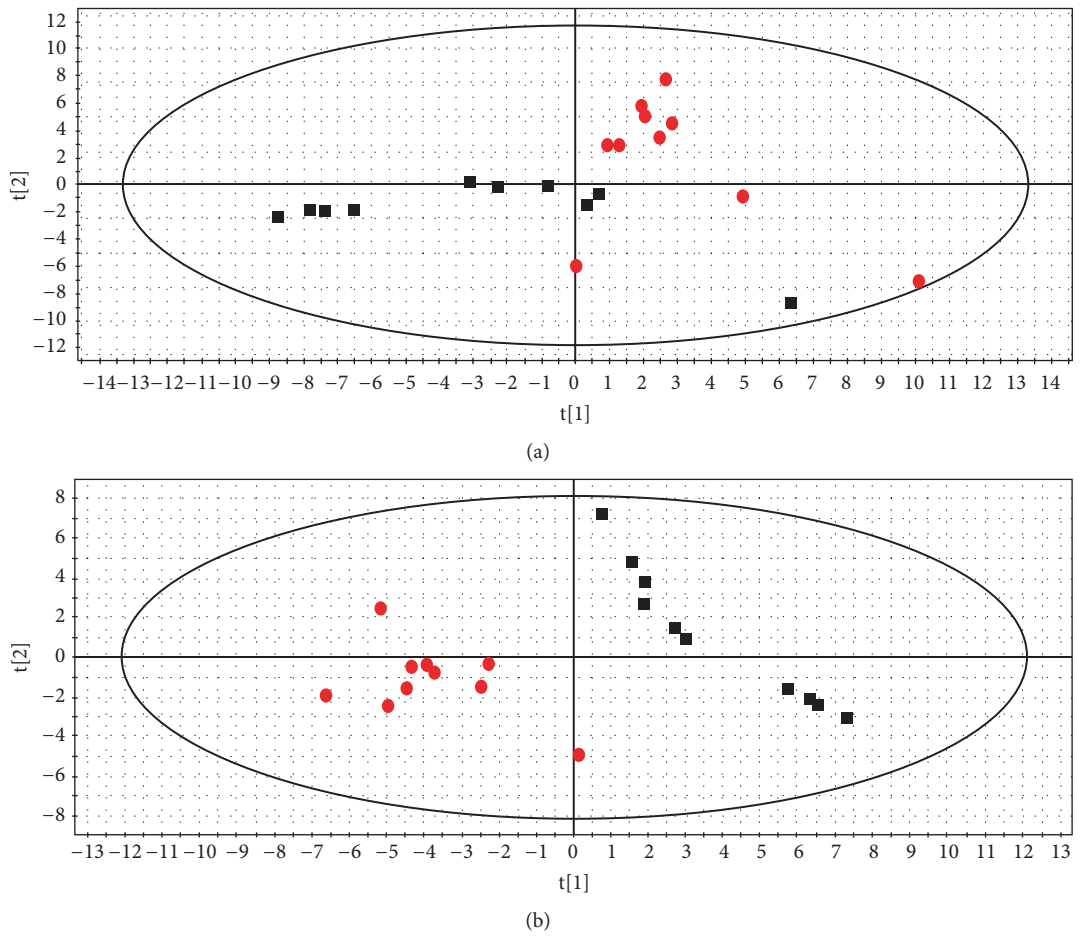

Figure 5: Score plot of control group (black square) and model group (red circle) from a PCA model (a) and a PLS-DA model (b).

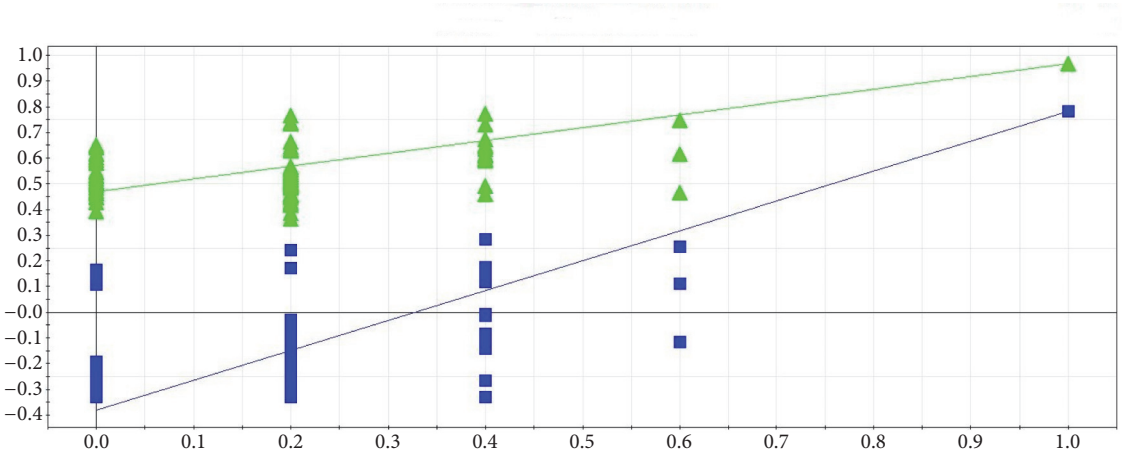

Figure 6: Two hundred permutations were performed, and the resulting R2 and Q2 values were plotted. Green triangle: R2; blue square: Q2. The green line represents the regression line for R2 and the blue line for Q2.

from the model group to the control group after taking QHD. Above results confirmed that the disturbed urine metabolites due to high-fat diet were regulated by QHD. The results of liver function tests, histological changes, and these change in urine metabolic pattern confirmed that QHD had obvious anti-liver fatty effect.

3.5.4. Time-Dependent Changes of Metabolic Profile. In this study, time-dependent changes of metabolic profile of urine samples from control group, model group, and QHD group rats were obtained at 0 weeks before modeling, 4 weeks before QHD administration, 6 weeks during QHD administration, and 8 weeks after QHD administration (Figure 9).

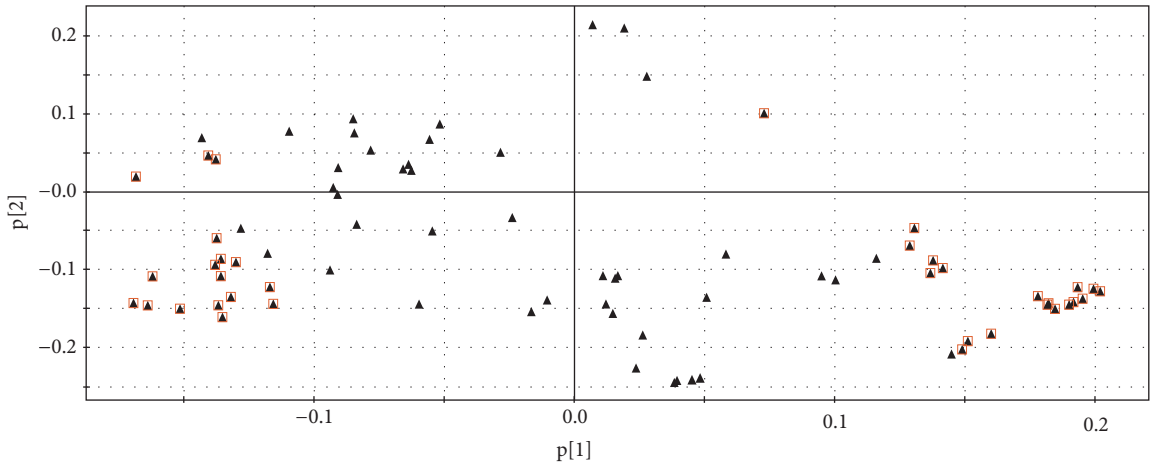

Figure 7: Loading plot from PLS-DA model classifying model obtained from control group and model group. Red square: difference variables.

Table 1: Significantly changed metabolites.

Metabolites	Model group[a]	QHD group[b]
Butyrate	↓ ∗∗	↑
Malic acid	↓ ∗∗	↑
Glycine	↓ ∗∗	↑
L-lactic acid	↑ ∗∗	↓
Indole	↑ ∗∗	↑
Tryptophan	↑ ∗	↓#
Glucose	↓ ∗	↑
Uridine	↑ ∗	↓#
Oleic acid	↓ ∗	↑
Phenylalanine	↑ ∗	↓#
Inositol	↑ ∗	↓
Benzoic acid	↑ ∗	↓

The up or down arrows represent the relatively increased or decreased levels of the metabolites in model group or QHD group, respectively. a: compared to the control group, b: compared to the model group. $**p < 0.01$, $*p < 0.05$, # $p < 0.05$.

In the PCA score plot, there was no significant change in the control group. The metabolic patterns of rats in the model group were significantly different at different time points, and there was a deviation trend from 0 weeks before modeling to 6 weeks after QHD administration, which showed a metabolic change induced by high-fat diet. In the QHD group, the metabolic pattern 4 weeks before QHD administration significantly deviated from the 0 week before modeling. Metabolic patterns at 6 and 8 weeks showed a reversal trend at 0 week before model state with the treatment of QHD. This result suggests that QHD has the potential to correct deviations caused by high-fat diets.

3.5.5. Metabolic Pathway Analysis of QHD on Rat Model of Fatty Liver Induced by High-Fat Diet. In order to identify the most relevant pathway, the threshold of the influence value of the pathway analysis by MetaboAnalyst 3.0 is set to 0.10 [32]. In this study, 12 potential biomarkers associated with group separation were entered into online system MetaboAnalyst. There are four significant pathways associated with rat model of fatty liver induced by high-fat diet. The top 4 metabolic pathways included (a) phenylalanine, tyrosine, and tryptophan biosynthesis, (b) phenylalanine metabolism, (c) glycine, serine, and threonine metabolism, and (d) tryptophan metabolism (Figure 10).

In this study, the metabolic changes related to fatty liver on the QHD treatment group were analyzed. Compared to the model group, three different metabolites were completely reversed to levels in the control group (Table 1). According to the MetPA analysis (Figure 11), phenylalanine, tyrosine, and tryptophan biosynthesis, phenylalanine metabolism, and tryptophan metabolism were significantly associated with effect of QHD on rat model of fatty liver induced by high-fat diet (Figure 11).

4. Discussion

The present study describes a urine metabolomic evaluation of rat model of fatty liver induced by high-fat diet and the treatment of QHD based on a GC-MS metabolomics approach combined with univariate and multivariate analyses. QHD markedly reduced liver tissue content TG apart from the lowering of serum levels of ALT, AST, and LDL. QHD significantly ameliorates the histological features of high-fat diet-treated rats. All these results suggested that intake of QHD may be useful in preventing and improving fatty liver induced by high-fat diet. Furthermore, metabolomics analysis indicated that QHD effectively regulates the perturbed metabolism by reversing changes of twelve small-molecule metabolites (especially three metabolites, tryptophan, uridine, and phenylalanine) (Table 1) and three metabolic pathways (phenylalanine, tyrosine, and tryptophan biosynthesis, phenylalanine metabolism, and tryptophan metabolism) (Figure 11).

Our findings showed that metabolic changes of QHD treatment on fatty liver are predominantly related to abnormal amino acid metabolism (phenylalanine, tyrosine, and tryptophan biosynthesis, phenylalanine metabolism, and

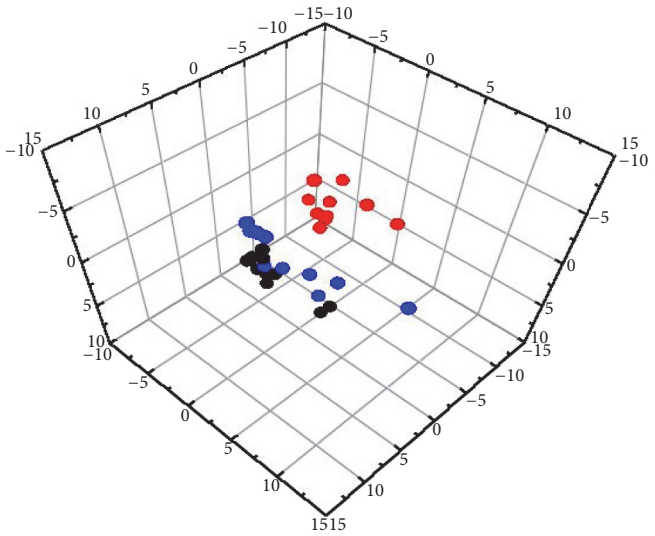

Figure 8: Score plot of 3D-PLS-DA model obtained from control group (black circle), model group (red circle), and QHD group (blue circle).

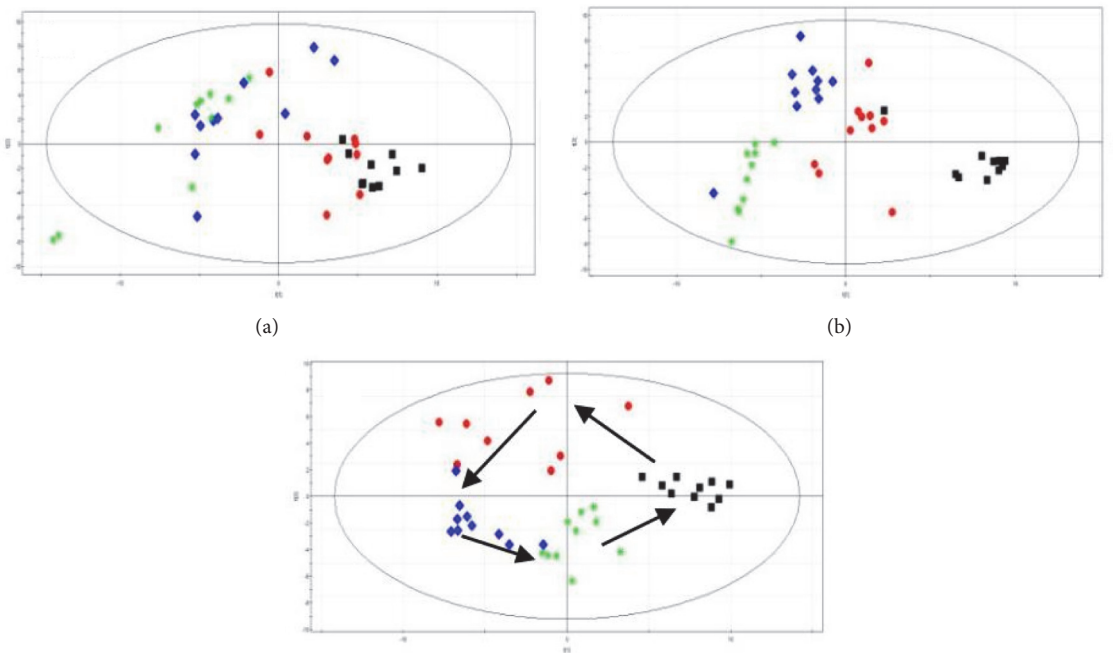

Figure 9: Score plot from PCA derived from the GC/MS profiles of urine samples obtained from (a) control group, (b) model group, and (c) QHD group. The plot shows the trajectories of metabolite patterns at different time points. Black square: 0 weeks before modeling, red circle: 4 weeks before QHD administration, blue diamond: 6 weeks during QHD administration, and green asterisk: 8 weeks after QHD administration.

tryptophan metabolism). In present work, the levels of amino acids (tryptophan, phenylalanine) were increased in model group compared with the normal control group. Most amino acids are synthesized and degraded in the liver; therefore, liver injury can lead to abnormal amino acid metabolism and release of amino acids from liver cells [33]. Tryptophan and phenylalanine are an aromatic amino acid, a metabolite of the intestinal flora that breaks down polyphenols and proteins in food [34]. Under the catalysis of phenylalanine deaminase, phenylalanine is converted to phenylpyruvic acid and ammonia through deamination. Phenylpyruvic acid is further converted to benzoic acid and phenylacetic acid through decarboxylation. Benzoic acid and phenylacetic acid eventually form succinic acid, which enters the tricarboxylic acid cycle [35]. Malic acid is an intermediate substance in the tricarboxylic acid cycle. In this study, the malic acid content of

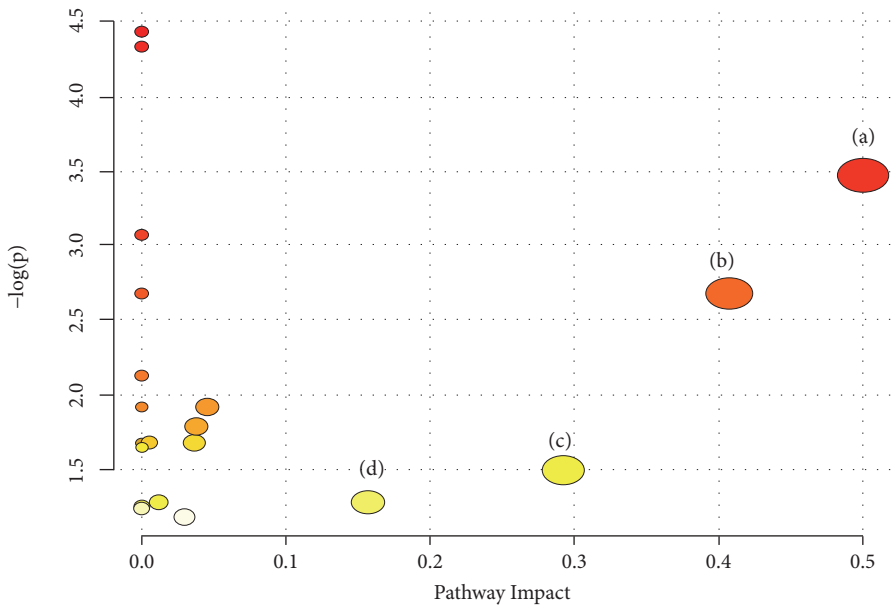

Figure 10: Summary of pathway associated with rat model of fatty liver induced by high-fat diet. (a) Phenylalanine, tyrosine, and tryptophan biosynthesis, (b) phenylalanine metabolism, (c) glycine, serine, and threonine metabolism, and (d) tryptophan metabolism.

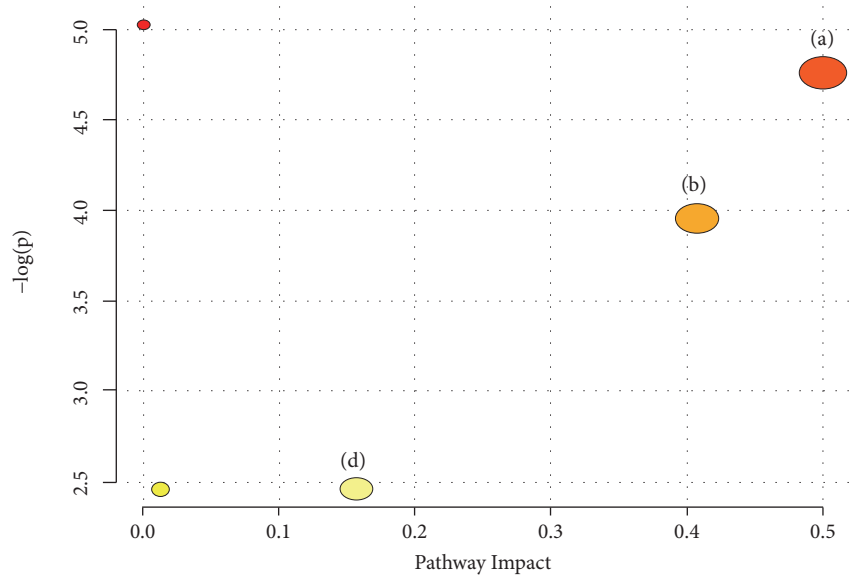

Figure 11: Summary of pathway associated with effect of QHD on rat model of fatty liver induced by high-fat diet. (a) Phenylalanine, tyrosine, and tryptophan biosynthesis, (b) phenylalanine metabolism, and (d) tryptophan metabolism.

the model group was decreased, indicating suppressed TCA cycle, and TCA cycle was disturbed by high-fat diet. In this study, tryptophan and phenylalanine were increased in model group. The reason for the analysis may be that after the liver is damaged, the tricarboxylic acid cycle in the liver is inhibited, and the inactivation and scavenging ability of the aromatic amino acid is decreased, resulting in a significant increase in the concentration of aromatic amino acids in the urine [36].

Therefore, the level of amino acid in urine of model group was higher than that of normal control group. QHD treatment could successfully reverse the raise of the above 2 amino acids, indicating that amino acid metabolism might be connected with the therapeutic mechanism of QHD.

The alteration in levels of glycine in fatty liver rats was observed in our study. Glycine is one of the substances in the synthesis of GSH. GSH is an antioxidant molecule produced by several tissues in response to oxidative stress and increased production of reactive oxygen species (ROS) [37]. Oxidative stress is one of the mechanisms leading to liver injury, characterized by mitochondrial dysfunction, oxidative damage, and ROS production [38]. Glycine has the potential to act as a hepatospecific antioxidant to reduce oxidant and cytokine

production by Kupffer cells and promote hepatic fatty acid oxidation [39]. Increasing glutathione biosynthesis by glycine supplementation to the diet of SF rats may protect the liver from oxidative stress and IR [40]. Therefore, supplemental glycine may be protective in NAFLD [39]. In the present study, glycine was significantly decreased in model group compared with the control group, which suggests that high-fat diet can cause the dysfunction of amino acid metabolism. QHD intervention of high-fat diet treated rats showed a tendency of bringing the level of glycine. Based on these findings, it is likely that QHD produced a major metabolic effects on amino acid.

Among these metabolites, butyrate and oleic acid were significantly changed in our study. Butyrate belongs to a volatile short chain fatty acid (SCFA) that is an endogenous substance of the human body, which comes from the fermentation of undigested food by the colonic microbiota. SCFA is an energy source of intestinal microorganisms and host intestinal epithelial cells, which can promote cell growth, reduce the pH value of the colon environment, and lower the growth of harmful bacteria. Supplemental SCFA can improve glucose and lipid metabolism disorders associated with obesity and may become a new therapeutic strategy for obesity-related diseases [41]. The content of oleic acid in model group was lower than that in normal control group, indicating that the synthesis of free fatty acids (FFA) increased in liver cells of rat. In the case of FFA accumulation in the liver, when lipids cannot be stored in the situation of high-fat diet or abnormal adipose tissue function, excess lipids directly enter into the liver and accumulate in the liver, causing liver inflammation and NAFLD [42]. In this paper, butyrate and oleic acid were significantly decreased in model group compared with the control group, while increase of them was shown in QHD group. These results suggested that high-fat diet affects fatty acids metabolism and QHD has a significant antihepatic fat effect by regulating abnormal fatty acid metabolism.

In this work, the decreased levels of malic acid and glucose and increased level of L-lactic acid were presented in the model group compared with the control group. The finding is mostly associated with disordered energy metabolism. Lactic acid is an end product of glycolysis, which is traditionally indicative of adverse consequence [43]. The increase of lactic acid content of urine in the model rats indicated that aerobic metabolism in vivo was inhibited due to the cause of modeling, thus promoting glycolysis, which was the manifestation of liver damage [44]. After the intervention of QHD, the dysfunction of lactate synthesis and secretion caused by modeling was obviously adjusted, and the metabolic network returned to normal range. Malic acid is the intermediate in the tricarboxylic acid cycle. The decreased level of malic acid in the model group indicates that the tricarboxylic acid cycle is inhibited and the energy metabolism in mitochondria is affected [44]. On the other hand, the inhibition of TCA cycle was alleviated by QHD, accompanied by an increase in malic acid level. Glucose was decreased in model group, which indicates the increase of energy demand and may be related to the observed alterations in the levels of metabolites participating in Kreb's cycle [45]. However, QHD intervention of high-fat diet treated rats showed a tendency of bringing the level of glucose and did not return to the level of the normal group, which was lower than that of the normal group; it is speculated that the mechanism of action QHD treatment of fatty liver is related to abnormalities in glucose metabolism

Uridine is a pyrimidine nucleoside composed of pyrimidine and ribose. The balance of uridine in the body is mainly regulated by uridine phosphorylase, and uridine can prevent fatty liver caused by some drugs. Fat metabolism in the liver can be modulated by modulating uridine phosphorylase or exogenous uridine supplementation to alter the uridine content in the body [46]. Uridine can cause insulin resistance, resulting in the failure of glucose to be used in time, resulting in high blood sugar and diabetes in severe cases. Excessive glucose enters the liver and undergoes a series of metabolisms to form triglycerides (TG), and too much TG accumulates in the liver, forming fatty liver [47]. In this study, the uridine content of urine in the model rats was significantly higher than that of the normal control group. After QHD treatment, the increased level of uridine was downregulated, suggesting that QHD may improve the pathological state of fatty liver model rats by regulating the metabolism of purine nucleotides.

Inositol is a kind of "biotin" that participates in metabolic activities in the body and has various functions such as immunization, prevention, and treatment of certain diseases [48]. Inositol plays an important role in the structural basis of eukaryotic second messengers (phosphatidylinositol, inositol phosphate, phosphoric acid, etc.) [49]. Therefore, inositol regulates intracellular calcium concentration, insulin signaling, and fatty acid oxidation [49]. The content of inositol in the model group was significantly increased, suggesting that high-fat diet feeding may cause insulin signal transduction dysfunction and fatty acid metabolism disorder in rats. After QHD treatment, the inositol content of QDH group was significantly reduced, indicating that QHD can regulate insulin signaling and fatty acid metabolism.

5. Conclusions

In this study, serum biochemistry, histopathology, and GC/MS-based on metabolomic analysis confirmed the anti-hepatic fat effect of QHD. In addition, 12 significantly disrupted biomarkers in rat urine among groups were identified as involved in phenylalanine, tyrosine, and tryptophan biosynthesis, phenylalanine metabolism, glycine, serine, and threonine metabolism, and tryptophan metabolism. These potential biomarkers and their corresponding pathways may help to further understand the mechanism of QHD in treating liver fat. Our study also showed that the established urine metabolomics method could provide a promising method for exploring the complex mechanism of Chinese herbal prescriptions.

Data Availability

The data used to support the findings of this study are included within the Supplementary Materials.

Disclosure

Permanent address for Qin Feng and Yi-yang Hu is Institute of Liver Disease, Shuguang Hospital, Shanghai University of Traditional Chinese Medicine, 258 Zhangheng Road, Pudong District, Shanghai 201203, China.

Conflicts of Interest

The authors declare that they have no conflicts of interest.

Authors' Contributions

Xiao-jun Gou, Shanshan Gao, and Liang Chen participated in the study design, carried out the experiments, analyzed the data, and wrote this report. Qin Feng and Yi-yang Hu reviewed the manuscript. All authors read and approved the final manuscript. Xiao-jun Gou, Shanshan Gao, and Liang Chen contributed equally to this work and should be considered co-first authors. Qin Feng and Yi-yang Hu contributed equally to this work and should be considered co-corresponding authors.

Acknowledgments

This study was financially supported by the National Natural Science Foundation of China (No. 81473475), the National Science and Technology Major Project "Key New Drug Creation and Manufacturing Program", China (no. 2018ZX09201001-001-002), Shanghai Science and Technology Commission Science and Technology Innovation Action Plan Project (No. 18401933100), and Nantong City Thirteenth Five Science and Education Strong Health Project.

Supplementary Materials

2.2. Preparation of QHD. The quality control of QHD. Our current study provides a new HPLC-based method for quality control of Qushi Huayu Decoction. The representative chemical fingerprint combined with simultaneous determination of 3 target components (polygoni, rhein, jasminoidin) offered a powerful and rational way to guarantee the quality of this herb. The results showed that extraction with water or ethanol yielded more stable components. The present study may serve as an important reference to establish the quality control method for the extracts and preparations of Qushi Huayu Decoction preparations. *2.6. Urine Sample Preparation and Analysis.* Two hundred microliters of urine added with 30 units of urease was incubated at 37°C for 15min to decompose and remove the excess urea present in it. Then, 800μl methanol and 10μl myristic acid (1mgmL^{-1}) used as internal standard were added to it. The solution was vigorously extracted for 1min and was centrifuged at 13,000xg, 4°C for 10min. The supernatant (200μl) was transferred to a gas chromatography (GC) vial and then evaporated to dryness under nitrogen at room temperature. Methoxyamine (50μl) in pyridine (15mg/ml) was added to each GC vial. The solution was then vigorously vortexed for 1min, after the methoxyation reaction at 30°C for 1.5h at room temperature. The samples were subsequently trimethylsilylated at 70°C for 1h using N-Methyl-N-(trimethylsilyl) trifluoroacetamide:trimethylchlorosilane (100:1, v/v, 50 μl). Finally, 40μl heptane was added to the GC vial, and the solution was vigorously vortexed again for 1min before the GC/mass spectroscopy (MS) analysis. *(Supplementary Materials)*

References

[1] K. Mehta, D. H. van Thiel, N. Shah, and S. Mobarhan, "Nonalcoholic fatty liver disease: pathogenesis and the role of antioxidants," *Nutrition Reviews*, vol. 60, no. 9, pp. 289–293, 2010.

[2] C. D. Williams, J. Stengel, M. I. Asike et al., "Prevalence of nonalcoholic fatty liver disease and nonalcoholic steatohepatitis among a largely middle-aged population utilizing ultrasound and liver biopsy: a prospective study," *Gastroenterology*, vol. 140, no. 1, pp. 124–131, 2011.

[3] D. Gu, K. Reynolds, X. Wu et al., "Prevalence of the metabolic syndrome and overweight among adults in China," *The Lancet*, vol. 365, no. 9468, pp. 1398–1405, 2005.

[4] Z. M. Younossi, M. Stepanova, M. Afendy et al., "Changes in the prevalence of the most common causes of chronic liver diseases in the United States from 1988 to 2008," *Clinical Gastroenterology and Hepatology*, vol. 9, no. 6, pp. 524–530, 2011.

[5] K. L. Kopec and D. Burns, "Nonalcoholic fatty liver disease: a review of the spectrum of disease, diagnosis, and therapy," *Nutrition in Clinical Practice*, vol. 26, no. 5, pp. 565–576, 2011.

[6] G. Bedogni, L. Miglioli, F. Masutti, C. Tiribelli, G. Marchesini, and S. Bellentani, "Prevalence of and risk factors for nonalcoholic fatty liver disease: the dionysos nutrition and liver study," *Hepatology*, vol. 42, no. 1, pp. 44–52, 2005.

[7] M. Ekstedt, L. E. Franzén, U. L. Mathiesen et al., "Long-term follow-up of patients with NAFLD and elevated liver enzymes," *Hepatology*, vol. 44, no. 4, pp. 865–873, 2006.

[8] J.-G. Fan and G. C. Farrell, "Epidemiology of non-alcoholic fatty liver disease in China," *Journal of Hepatology*, vol. 50, no. 1, pp. 204–210, 2009.

[9] N. Chalasani, Z. Younossi, and J. E. Lavine, "The diagnosis and management of non-alcoholic fatty liver disease: practice guideline by the American Gastroenterological Association, American Association for the Study of Liver Diseases, and American College of Gastroenterology," *Gastroenterology*, vol. 142, no. 7, pp. 1592–1609, 2012.

[10] J. E. Donnelly, S. N. Blair, J. M. Jakicic, M. M. Manore, J. W. Rankin, and B. K. Smith, "Appropriate physical activity intervention strategies for weight loss and prevention of weight regain for adults," *Medicine & Science in Sports & Exercise*, vol. 41, no. 2, pp. 459–471, 2009.

[11] E. A. Klein, I. M. Thompson Jr., and C. M. Tangen, "VitaminE and the risk of prostate cancer: the selenium and vitaminE cancer prevention, trial (SELECT)," *JAMA-Journal of theAmerican Medical Association*, vol. 306, no. 14, pp. 1549–1556, 2011.

[12] J.-Y. Xu, L. Zhang, Z.-P. Li, and G. Ji, "Natural products on nonalcoholic fatty liver disease," *Current Drug Targets*, vol. 16, no. 12, pp. 1347–1355, 2015.

[13] H. Zhang, Q. Feng, Y. Y. Hu et al., "Prevention and Treatment of "Qushi Huayu Decoction" on Fatty Liver of Rats induced by Carbon Tetrachloride Along with High -Fat and Low -Protein

Diet," *Shanghai Journal of Traditional Chinese Medicine*, vol. 40, no. 3, pp. 52–55, 2006 (Chinese).

[14] S. S. Li, Q. Feng, Y. Y. Hu et al., "Effect of Qushi Huayu Decoction on High-fat Diet Induced Hepatic Lipid Deposition in Rats," *Chinese Journal of Integrated Traditional and Western Medicine*, vol. 29, no. 12, pp. 1096–1099, 2009.

[15] S. S. Li, Q. Feng, D. D. Zhu et al., "Clinical Observation on Qushi Huayu Decoction for 82 Cases of Non -Alholic Steatohepatitis with Phlegm-Stasis Accumulation Syndrome," *Chinese Archives of Traditional Chinese Medicine*, vol. 31, no. 8, pp. 1764–1766, 2013.

[16] S. S. Li, Q. Feng, Y. Y. Hu et al., "The role of adiponectin and adiponectin receptor 2 in the pathology of fatty liver," *Chinese Journal of Hepatology*, vol. 17, no. 11, pp. 812–816, 2009.

[17] Q. Feng, X.-J. Gou, S. X. Meng et al., "Qushi Huayu Decoction inhibits hepatic lipid accumulation by activating AMP - activated protein kinase in vivo and in vitro," *Evidence-Based Complementary and Alternative Medicine*, vol. 2013, Article ID 184358, 14 pages, 2013.

[18] X. Yin, J. Peng, L. Zhao et al., "Structural changes of gut microbiota in a rat non-alcoholic fatty liver disease model treated with a Chinese herbal formula," *Systematic and Applied Microbiology*, vol. 36, no. 3, pp. 188–196, 2013.

[19] Q. Feng, Y. Cheng, Y.-Y. Hu, H. Zhang, J.-H. Peng, and N. Zhang, "Qushi Huayu Decoction inhibits CTSB protein expression and gene expression in HepG 2 cells induced by free fatty acid," *Chinese Journal of Integrative Medicine*, vol. 16, no. 6, pp. 518–524, 2010.

[20] S. Naz, M. Vallejo, A. García, and C. Barbas, "Method validation strategies involved in non-targeted metabolomics," *Journal of Chromatography A*, vol. 1353, pp. 99–105, 2014.

[21] D. Feng, Z. Xia, J. Zhou et al., "Metabolomics reveals the effect of Xuefu Zhuyu Decoction on plasma metabolism in rats with acute traumatic brain injury," *Oncotarget*, vol. 8, no. 55, pp. 94692–94710, 2017.

[22] X. Song, J. Wang, P. Wang, N. Tian, M. Yang, and L. Kong, "^{1}H NMR-based metabolomics approach to evaluate the effect of Xue-Fu-Zhu-Yu decoction on hyperlipidemia rats induced by high-fat diet," *Journal of Pharmaceutical and Biomedical Analysis*, vol. 78-79, pp. 202–210, 2013.

[23] D. Cui, X. Wang, J. Chen et al., "Quantitative Evaluation of the Compatibility Effects of Huangqin Decoction on the Treatment of Irinotecan-Induced Gastrointestinal Toxicity Using Untargeted Metabolomics," *Frontiers in Pharmacology*, vol. 8, p. 211, 2017.

[24] P. Wang, H. Sun, H. Lv et al., "Thyroxine and reserpine-induced changes in metabolic profiles of rat urine and the therapeutic effect of Liu Wei Di Huang Wan detected by UPLC-HDMS," *Journal of Pharmaceutical and Biomedical Analysis*, vol. 53, no. 3, pp. 631–645, 2010.

[25] K. K. Pasikanti, P. C. Ho, and E. C. Y. Chan, "Gas chromatography/mass spectrometry in metabolic profiling of biological fluids," *Journal of Chromatography B*, vol. 871, no. 2, pp. 202–211, 2008.

[26] X-J. Gou, Q. Feng, L. L. Fan et al., "Serum and Liver Tissue Metabonomic Study on Fatty Liver in Rats Induced by High-Fat Diet and Intervention Effects of Traditional Chinese Medicine Qushi Huayu Decoction," *Evidence-Based Complementary and Alternative Medicine*, vol. 2017, Article ID 6242697, 12 pages, 2017.

[27] Q. Zhong, G. Wang, Y. Du et al., "GC/MS analysis of the rat urine for Metabolomic research," *Journal of Chromatography B*, vol. 854, no. 1-2, pp. 20–25, 2007.

[28] X. Liu, S. Zhang, X. Lu, S. Zheng, F. Li, and Z. Xiong, "Metabonomic study on the anti-osteoporosis effect of Rhizoma Drynariae and its action mechanism using ultra-performance liquid chromatography-tandem mass spectrometry," *Journal of Ethnopharmacology*, vol. 139, no. 1, pp. 311–317, 2012.

[29] S. E. Singletary, C. Allred, P. Ashley et al., "Revision of the American Joint Committee on cancer staging system for breast cancer," *Journal of Clinical Oncology*, vol. 20, no. 17, pp. 3628–3636, 2002.

[30] J. Chen, W. Wang, S. Lv et al., "Metabonomics study of liver cancer based on ultra performance liquid chromatography coupled to mass spectrometry with HILIC and RPLC separations," *Analytica Chimica Acta*, vol. 650, no. 1, pp. 3–9, 2009.

[31] S.-A. Fancy, O. Beckonert, G. Darbon et al., "Gas chromatography/flame ionisation detection mass spectrometry for the detection of endogenous urine metabolites for metabonomic studies and its use as a complementary tool to nuclear magnetic resonance spectroscopy," *Rapid Communications in Mass Spectrometry*, vol. 20, no. 15, pp. 2271–2280, 2006.

[32] Y. Zhu, Z. Guo, L. Zhang et al., "System-wide assembly of pathways and modules hierarchically reveal metabolic mechanism of cerebral ischemia," *Scientific Reports*, vol. 5, no. 1, Article ID 17068, 2015.

[33] S. Dong, Z.-Y. Zhan, H.-Y. Cao et al., "Urinary metabolomics analysis identifies key biomarkers of different stages of nonalcoholic fatty liver disease," *World Journal of Gastroenterology*, vol. 23, no. 15, pp. 2771–2784, 2017.

[34] A. R. Rechner, M. A. Smith, G. G. Kuhnle et al., "Colonic metabolism of dietary polyphenols: influence of structure on microbial fermentation products," *Free Radical Biololgy & Medicine*, vol. 36, no. 2, pp. 212–225, 2004.

[35] W. Shi, L. R. Liu, and R. X. Su, "Study on the metabolic pathway of bacterial aromatic amino acids in coastal Zhejiang," *Water Conservancy and Fishery*, vol. 27, no. 2, pp. 22-23, 2007.

[36] Y. Chun and F. Yu, "Changes and Analysis of Serum Free Aminogram in Non-Alcoholic Fatty Liver Disease (NAFLD) Rats," *Journal of Nanjing Normal University(Natural Science Edition)*, vol. 39, no. 1, pp. 91–94, 2016.

[37] M. Gaggini, F. Carli, C. Rosso et al., "Altered amino acid concentrations in NAFLD: Impact of obesity and insulin resistance," *Hepatology*, vol. 67, no. 1, pp. 145–158, 2018.

[38] C. Koliaki, J. Szendroedi, K. Kaul et al., "Adaptation of Hepatic Mitochondrial Function in Humans with Non-Alcoholic Fatty Liver Is Lost in Steatohepatitis," *Cell Metabolism*, vol. 21, no. 5, pp. 739–746, 2015.

[39] M. F. McCarty, "Full-spectrum antioxidant therapy featuring astaxanth in coupled with lipoprivic strategies and salsalate for management of non-alcoholic fatty liver disease," *Medical Hypotheses*, vol. 77, no. 4, pp. 550–556, 2011.

[40] M. El-Hafidi, M. Franco, A. R. Ramírez et al., "Glycine Increases Insulin Sensitivity and Glutathione Biosynthesis and Protects against Oxidative Stress in a Model of Sucrose-Induced Insulin Resistance," *Oxidative Medicine and Cellular Longevity*, vol. 2018, Article ID 2101562, 12 pages, 2018.

[41] Q. Liu, C. Cheng, X. Xin et al., "Effects of short chain fatty acids on metabolism of glucose and lipid in obese mice induced by high fat diet," *Chinese Journal of Hepatology*, vol. 23, no. 7, pp. 591–595, 2018.

[42] T. Eslamparast, S. Eghtesad, H. Poustchi, and A. Hekmatdoost, "Recent advances in dietary supplementation, in treating non-alcoholic fatty liver disease," *World Journal of Hepatology*, vol. 7, no. 2, pp. 204–212, 2015.

[43] B. Venkatesh, T. J. Morgan, and J. Cohen, "Interstitium: The next diagnostic and therapeutic platform in critical illness," *Critical Care Medicine*, vol. 38, no. 10, pp. S630–S636, 2010.

[44] A. M. Bello-Ramírez and A. A. Nava-Ocampo, "A QSAR analysis of toxicity of Aconitum alkaloids," *Fundamental & Clinical Pharmacology*, vol. 18, no. 6, pp. 699–704, 2004.

[45] A. Zira, S. Kostidis, S. Theocharis et al., " ^{1}H NMR-based metabonomics approach in a rat model of acute liver injury and regeneration induced by CCl_4 administration," *Toxicology*, vol. 303, pp. 115–124, 2013.

[46] G. Pizzorno, D. Cao, J. J. Leffert, R. L. Russell, D. Zhang, and R. E. Handschumacher, "Homeostatic control of uridine and the role of uridine phosphorylase: a biological and clinical update," *Biochimica et Biophysica Acta (BBA) - Molecular Basis of Disease*, vol. 1587, no. 2-3, pp. 133–144, 2002.

[47] S. Y. Park, J. Ryu, and W. Lee, "O-GlcNAc modification on IRS-1 and Akt2 by PUGNAc inhibits their phosphorylation and induces insulin resistance in rat primary adipocytes," *Experimental & Molecular Medicine*, vol. 37, no. 3, pp. 220–229, 2005.

[48] P. G. Haydon, "Glia: listening and talking to the synapse," *Nature Reviews Neuroscience*, vol. 2, no. 3, pp. 185–193, 2001.

[49] G. Di Paolo and P. De Camilli, "Phosphoinositides in cell regulation and membrane dynamics," *Nature*, vol. 443, no. 7112, pp. 651–657, 2006.

Hindawi
BioMed Research International
Volume 2019, Article ID 5049746, 7 pages
https://doi.org/10.1155/2019/5049746

Research Article

Evaluation of Pathological Association between Stroke-Related QTL and Salt-Induced Renal Injury in Stroke-Prone Spontaneously Hypertensive Rat

Mohammad Farhadur Reza,[1] Davis Ngarashi,[1] Masamichi Koike,[2] Masaki Misumi,[2] Hiroki Ohara ,[1] and Toru Nabika [1]

[1]*Department of Functional Pathology, Shimane University Faculty of Medicine, Izumo, Japan*
[2]*Department of Oncology, Shimane University Faculty of Medicine, Izumo, Japan*

Correspondence should be addressed to Hiroki Ohara; oharah@med.shimane-u.ac.jp

Received 17 October 2018; Accepted 28 December 2018; Published 16 January 2019

Guest Editor: Hossain U. Shekhar

The stroke-prone spontaneously hypertensive rat (SHRSP) suffers from severe hypertension and hypertensive organ damage such as cerebral stroke and kidney injury under salt-loading. By a quantitative trait locus (QTL) analysis between SHRSP and SHR (the stroke-resistant parental strain of SHRSP), two major QTLs for stroke susceptibility were identified on chromosomes 1 and 18 of SHRSP, which were confirmed in congenic strains constructed between SHRSP and SHR. As the progression of renal dysfunction was suggested to be one of the key factors inducing stroke in SHRSP, we examined effects of the stroke-related QTLs on kidney injury using two congenic strains harboring either of SHRSP-derived fragments of chromosomes 1 and 18 in the SHR genome. The congenic strains were challenged with 1% NaCl solution for 4 weeks; measurement of systolic blood pressure and urinary isoprostane level (a marker for oxidative stress) and evaluation of renal injury by quantification of genetic marker expression and histological examination were performed. We found that the congenic rats with SHRSP-derived fragment of chromosome 18 showed more severe renal damage with higher expression of *Col1α-1* (a genetic marker for renal fibrosis) and higher urinary isoprostane level. In contrast, the fragment of chromosome 1 from SHRSP did not give such effects on SHR. Blood pressure was not greater in either of the congenic strains when compared with SHR. We concluded that the QTL region on chromosome 18 might deteriorate salt-induced renal injury in SHR through a blood pressure-independent mechanism.

1. Introduction

The stroke-prone spontaneously hypertensive rat (SHRSP) has been characterized as a good genetic model for severe hypertension and hypertensive organ damage such as cerebral hemorrhage [1–4]. It was therefore suggested that investigation of genetic mechanisms of stroke susceptibility in SHRSP provided us with important clues to understand genetic susceptibility to stroke in humans, which would be useful in its prevention and therapeutics [5]. In this context, several genetic studies were performed and identified quantitative trait locus (QTL) responsible for stroke occurrence [6–8]. We also identified two major QTLs for stroke on chromosomes (chr) 1 and 18 in SHRSP and confirmed their effects in reciprocal congenic strains constructed between SHR and SHRSP [9]; in brief, the congenic strains having the SHRSP-derived QTL fragments of chr_1 or 18 on SHR background showed a shorter stroke-latency when compared with SHR [9]. Of interest, these congenic strains did not show significant difference in blood pressure when compared with SHR, indicating that the greater susceptibility to stroke in these strains was blood pressure independent [9].

On the other hand, it was suggested that SHRSP suffered from severe renal damage under salt-loading when compared with SHR [3, 10, 11]. Further, several groups identified QTLs for salt-induced renal damage on chr_1 of rats, which were the vicinity of the QTL for stroke [6, 12]. If susceptibility to renal injury is influenced by the QTLs for stroke on chr_1 and/or

18, it may be useful as a clue to identify the genes responsible for stroke, and to understand the functions of those genes.

In this context, we compared salt-induced renal injury among two congenic strains and the parental strain (i.e., SHR) in this study to examine whether the QTLs on chr_1 and 18 affected renal injury. In addition, possible relevance between renal injury and the stroke susceptibility was discussed.

2. Materials and Methods

2.1. Animal Procedure. Two congenic strains for the QTLs on chr_1 and 18 [SHR.SHRSP-(*D1Rat93-D1Rat269*)/Izm and SHR.SHRSP-(*D18Rat73-D18Rat11*)/Izm, respectively] were employed in this study (abbreviated as Rp1.0 and Rp18.0, respectively). In Rp1.0 and 18.0, a chromosomal fragment of chr_1 and 18 of SHRSP/Izm was introgressed, respectively, into SHR/Izm [9]. SHR/Izm was used as the control strain. Six male rats at 12 weeks of age of each strain were used in the experiments and all rats were fed stroke permissive Japanese diet. SHR/Izm were provided by the Disease Model Cooperative Research Association (Kyoto, Japan).

After the measurement of blood pressure (BP) and body weight (BW) at 12 weeks of age, salt-loading was then started by feeding them with 1% salt water. BP and BW were monitored every week during 4 weeks of the experimental period. Urine samples were collected for 24h in metabolic cages every 2 weeks. Urine samples were centrifuged at 2000 rpm for 10 min at 4°C and the supernatants were stored at -20°C until further biochemical analysis. BP measurement was done using the tail-cuff method (BP-98A; Softron Corp., Tokyo, Japan). Each rat was acclimatized at 37°C for 10 min before BP measurement. Five consecutive readings were recorded and averaged to represent BP of an individual rat.

At the end of the experiment, each rat was deeply anesthetized in isoflurane inhalation-chamber (2% with 300~400ml/min flow rate) and perfused with ice-cold 0.9% saline solution for organ collection. The left kidney was stored in 10% formalin for histological analysis and the right kidney was dissected, frozen in liquid nitrogen, and kept at -80°C for RNA extraction. The study protocol was approved by the local ethical committee of animal research in Shimane University.

2.2. Biochemical Measurements. Urinary 15-isoprostane-F2t (IsoP) excretion level was measured to estimate oxidative stress [13] using an ELISA kit (JaICA, Nikken SEIL Co., Ltd.). Urinary protein level was determined in 24h urine samples as well with the protein assay BCA kit (Wako Pure Chemical Industries Ltd., Japan) [14]. The measurements were performed according to the manufacturer's protocol.

2.3. Renal Histopathology. For histological evaluation of renal damage, haematoxylin-eosin (HE) and Azan staining were performed on histological sections of left kidney. On HE-stained sections, glomeruli were categorized into three groups according to the severity of glomerulosclerosis (Figures 2(a)–2(c)). About 300 glomeruli were examined on each rat (about 1800 glomeruli were examined on 6 rats from each strain) and a ratio of partially + completely sclerotic and intact glomeruli was compared among the strains using $\chi 2$ test. The same results were obtained when we employed only completely sclerotic glomeruli instead of partially + completely sclerotic glomeruli (data not shown). On Azan staining, area of fibrotic regions (regions stained blue on Azan staining, see Figures 2(d) and 2(e)) was measured on digital images of the section using NIH Image J (ver1.8.0). A relative fibrotic area (%) was calculated as fibrotic area/total area x 100. Relative fibrotic area was compared among the strains using Student's t-test with Bonferroni's correction.

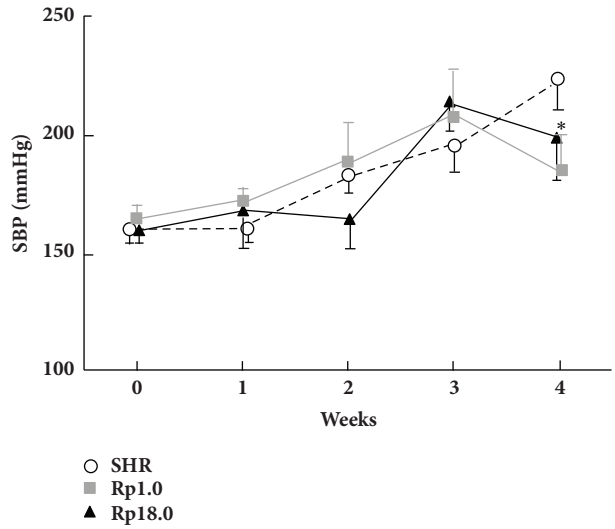

Figure 1: Effect of salt-loading on blood pressure. Six rats of each strain were used. *P <0.001 *vs* control SHR (Student's t-test), which was significant after Bonferroni's correction. Data are presented as mean ± SD.

2.4. Gene Expression. Gene expression of *Collα-1*, *Tgf- β*, *α-Sma* (markers for fibrosis), and *Kim-1*(a marker for tubular injury) was determined in the kidney by quantitative RT-PCR as described previously [15, 16]. The primers used are as follows: *α-Sma*: GAGATCTCACCGACTACCTCATGA (forward), TCATTTTCAAAGTCCAGAGCGACA (reverse), *Tgf- β*: ATCCATGACATGAACCGACCCT (forward), GCCGTACACAGCAGTTCTTCTC (reverse), *Collα -1*: ACATGTTCAGCTTTGTGGACCTC (forward), TCAGGTTTCCACGTCTCACCA (reverse), *Kim-1*: GGAGCAGCGGTCGATACAACATA (forward), TCTCCACTCGGCAACAATACAGAC (reverse). The PCR condition was as follows: 1 cycle of 95°C for 30s, followed by 40 cycles of 95°C for 30s and 60°C for 30s (Step One Plus Real Time PCR System, Thermo Fisher Scientific, Waltham, MA). Relative amount of mRNA was calculated against β–actin as a control.

2.5. Statistical Analysis. All the data are presented as mean ± SD. Statistical significance was tested either by $\chi 2$ test or by Student's t-test. In case of multiple comparisons, significant levels were adjusted by Bonferroni's correction. Difference was thought to be significant when $p<0.05$ (comparison between 2 groups) or $p<0.017$ (comparison among 3 groups).

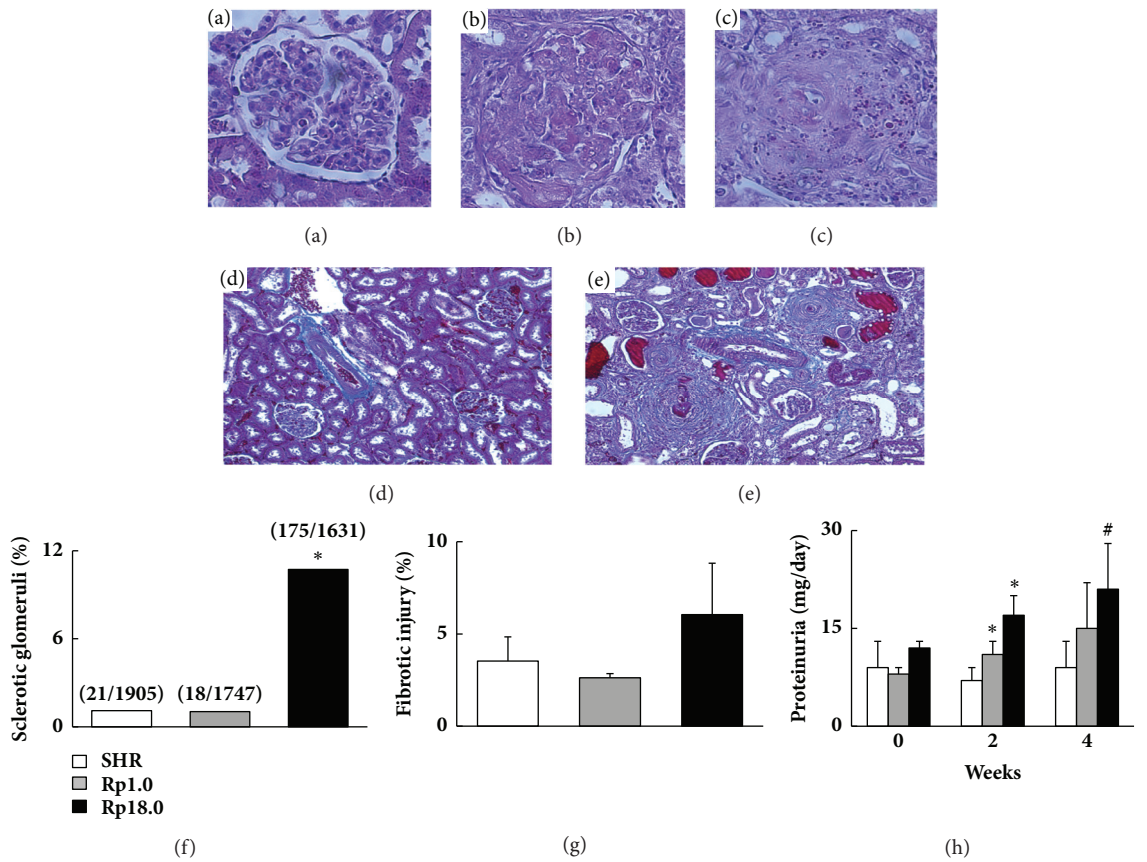

FIGURE 2: Comparison of severity of renal damages among the three strains. (a–c) Typical morphology of glomerulus with no (a), partially (b), and completely (c) sclerotic change, respectively. Photos were taken at 20X. (d, e) Typical microscopic appearance from SHR (d) and Rp18.0 (e) by Azan staining after 4 weeks of salt-loading. Photos were taken at 10X. (f-g) Prevalence of sclerotic glomeruli (f) and relative fibrotic area (g) were compared among the three strains. *Significantly different from both SHR and Rp1.0 after Bonferroni's correction (by the $\chi 2$ test). (h) Urinary protein excretion for 24h at 0, 2, and 4 weeks of salt-loading (n=6). *p <0.001 and #p<0.01 *vs* control SHR by Student's t-test, which were significant after Bonferroni's correction. Data are presented as mean ± SD.

3. Results

3.1. Blood Pressure under Salt-Loading. Baseline BP at 12 weeks of age was not significantly different among the strains (Figure 1). During salt-loading, BP increased gradually in all the three strains. At 4 weeks of salt-loading, BP of Rp1.0 was significantly lower than that of SHR.

3.2. Renal Injury Induced by Salt-Loading. Histopathological assessment of glomerulosclerosis showed that the number of sclerotic glomeruli was significantly greater in Rp18.0 when compared with Rp1.0 and SHR (Figure 2(f)). In accordance with it, fibrotic area tended to be increased in Rp18.0 though it did not reach a significant level (Figure 2(g)). Urinary protein level did not differ among the three strains before salt-loading as indicated (Figure 2(h)). During salt-loading, however, urinary protein excretion was increased in the two congenic strains whereas no significant increase was observed in SHR (Figure 2(h)).

3.3. Evaluation of Gene Expression in the Kidney under Salt-Loading. We evaluated expression of genes that are biomarkers of renal fibrosis and tubular damage [17–19]. As shown in Figure 3, *Col1α-1* expression was significantly greater (p=0.003) and *Tgf- β* expression tended to be greater (p=0.049) in Rp18.0 when compared with SHR (under Bonferroni's correction). The expression of both genes was significantly different between the two congenic strains (p=0.002 and 0.012 for *Col1α-1* and *Tgf- β*, respectively). No significant difference was observed in *α-Sma* or in *Kim-1* expression among the three strains.

Correlation of the gene expressions and severity of renal fibrosis and glomerulosclerosis were examined in Figure 4. The results indicated that while *Col1α-1* and *Tgf- β* expressions were correlated significantly with glomerulosclerosis and renal fibrosis, expressions of the other genes were not.

3.4. Salt-Loading Induced Oxidative Stress. It was pointed out that oxidative stress plays a key role in salt-induced renal damage [20]. We therefore measured urinary isoprostane, a sensitive marker of oxidative stress *in vivo*. At the baseline, isoprostane did not significantly differ among the strains (Figure 5). During salt-loading, isoprostane was increased in all the three strains and in contrast to the baseline

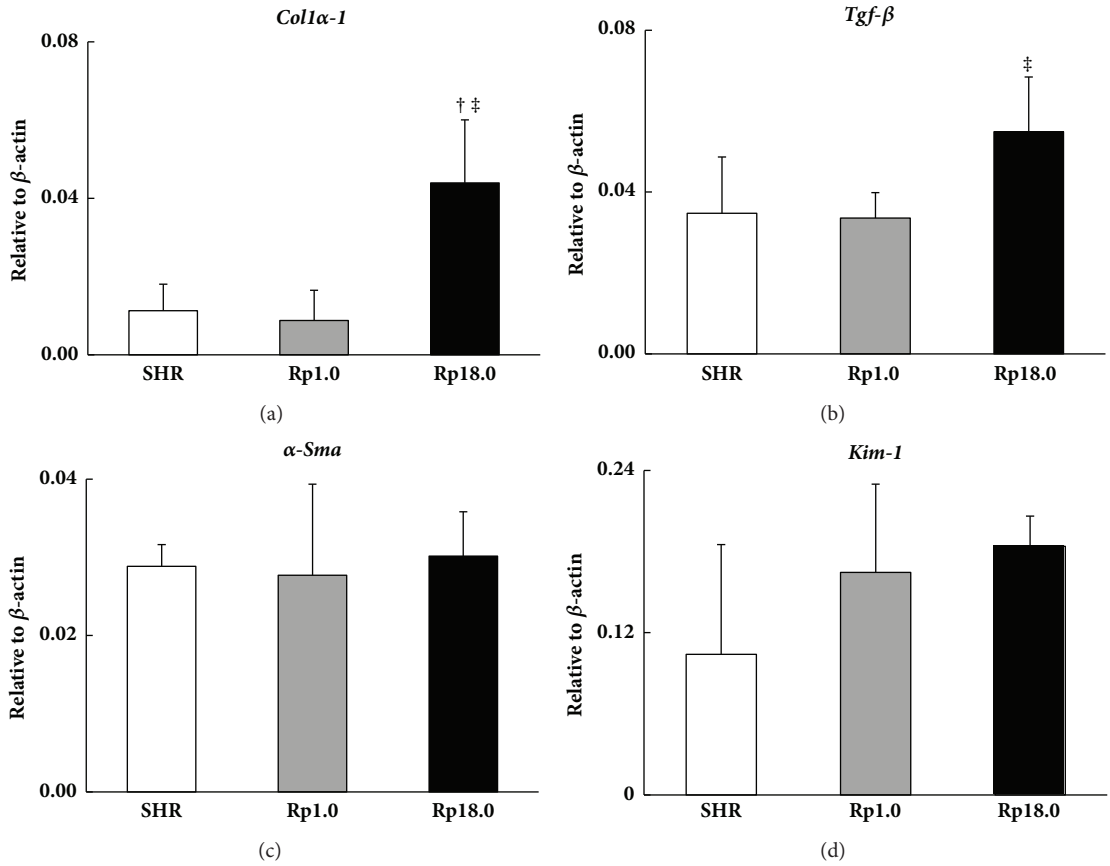

Figure 3: Expression of genetic markers for renal damage. (a–d) Gene expression of *Col1α-1* (a), *Tgf- β* (b), *α-Sma* (c), and *Kim-1*(d), respectively, in the kidney after 4 weeks of salt-loading (n=5 in each group). Gene expression was represented as relative amount against *β*–actin mRNA. †, ‡: significantly different from SHR (†) and Rp1.0 (‡), respectively, after Bonferroni's correction. Data are presented as mean ± SD.

status, Rp18.0 showed significantly greater level of urinary isoprostane when compared with SHR after 4 weeks of salt-loading. No significant difference was observed between SHR and Rp1.0.

4. Discussion

In this study, we found that the congenic strain Rp18.0 was more susceptible to salt-induced renal damage than was the other congenic strain Rp1.0. It seems that the susceptibility was independent of BP as no significant difference of BP was observed between the two congenic strains. Since the previous study pointed out that the effect of chr18 QTL on stroke was BP independent [9], it is attractive to hypothesize that the same gene(s) in the QTL region contributed to both renal damage and stroke in Rp18.0. In this regard, it is of interest that several reports indicated that vasculature in SHRSP was more vulnerable to hypertensive insult [2, 3, 11].

Several different interpretations are possible for the relation between cerebral stroke and hypertensive renal damage; the renal damage may causally relate to cerebral stroke, or may just be a bystander (in another word, risk genes for stroke may have pleiotropic effects on the kidney). We can even assume another gene (or genes) for renal damage located in the same QTL region. When causal roles of renal damage are considered, a putative mechanism is acceleration of hypertension due to renal damage. However, as shown in Figure 1, BP did not become higher in Rp18.0 during salt-loading. Further, despite the fact that the difference was statistically significant, the prevalence of glomerulosclerosis and the relative area of renal fibrosis were still modest even in Rp18.0 (around 10 and 5%, respectively, see Figures 2(f) and 2(g)). This observation suggested that renal injury observed in Rp18.0 was not likely to have direct causal relationship with greater incidence of cerebral stroke in this strain.

Another hypothesis is that the QTL on chr_18 affected both stroke and renal damage as parallel events. Salt intake inhibits the release of renin from the juxtaglomerular apparatus that results in the depletion of angiotensin II (AngII) level. In contrast, some studies showed that salt stimulated the intrarenal local renin-angiotensin system (RAS) that might contribute to the regulation of renal NADPH oxidase activity [20]. NADPH oxidases facilitate the generation of reactive oxygen species (ROS) in mesangial cells in glomeruli [21] and epithelial cells in thick ascending limbs [22] which might deteriorate glomerulosclerosis and renal fibrosis [23]. As the local RAS was identified in the brain as well [24],

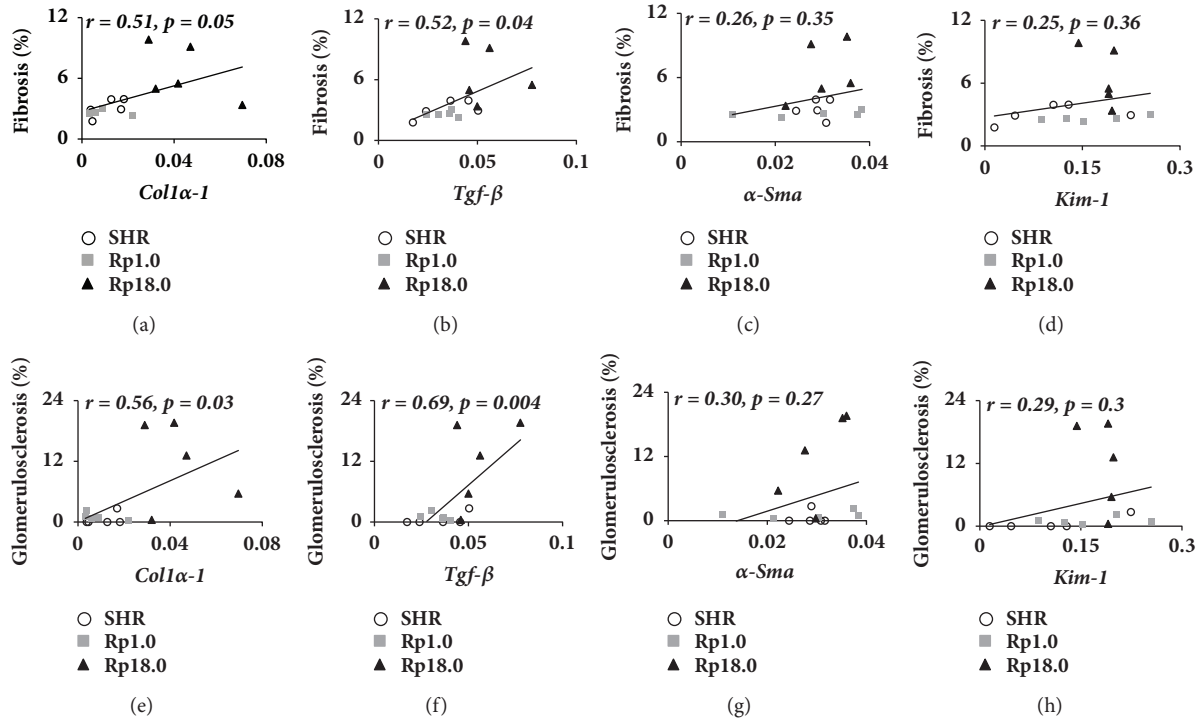

Figure 4: Correlation of mRNA expression with fibrosis and glomerulosclerosis. (a–d) Correlation between fibrotic area (%) and *Col1α-1* (a), *Tgf- β* (b), *α-Sma* (c), and *Kim-1* (d) expression. (e–h) Correlation between the prevalence of glomerulosclerosis (%) and the genetic marker expressions. Pearson's r is indicated with p values (n=5 in each group).

overproduction of ROS through activation of the local RAS might contribute simultaneously to stroke [25]. In this study, a greater level isoprostane was indeed shown in Rp18.0 only under the salt-loaded status. This suggested that a higher level of oxidative stress was actually induced under salt-loading in this strain (see Figure 5).

Several studies were done to investigate molecular mechanisms of how oxidative stress influenced renal injury and stroke; in the kidney, oxidative stress (mostly generated in renal mesangial cells) was shown to activate the protein kinase C (PKC) and the mitogen-activated protein kinases (MAPK), which then promoted the translocation of transcription factors such as NF-κB and AP-1 into the nucleus that eventually facilitated expression of the gene of extra cellular matrix proteins [26]. On the other hand, in the brain, oxidative stress was shown to lead activation of the extracellular signal-regulated kinases 1/2 and the N-methyl-D-aspartate receptor that facilitated Ca^{2+} influx. It then activated the cytosolic phospholipase $A_{2\alpha}$ ($PLA_{2\alpha}$) through MAPK and PKC activation [27]. The cytosolic $PLA_{2\alpha}$ enhanced production of arachidonic acid and conjugated dienic hydroperoxides that was decomposed into aldehydes, e.g., 4-hydroxynonenal which was toxic to neurons [28].

Future studies should focus on pathophysiological significance of increased oxidative stress in Rp18.0 and identify the responsible gene (or genes) for this phenomenon in the chr18 QTL region.

We had discrepancy among the expression of marker genes in the kidney; while *Col1α-1* and *Tgf- β* expression was significantly greater or tended to be greater in Rp18.0, *α-Sma* and *Kim-1* did not show a difference between Rp18.0

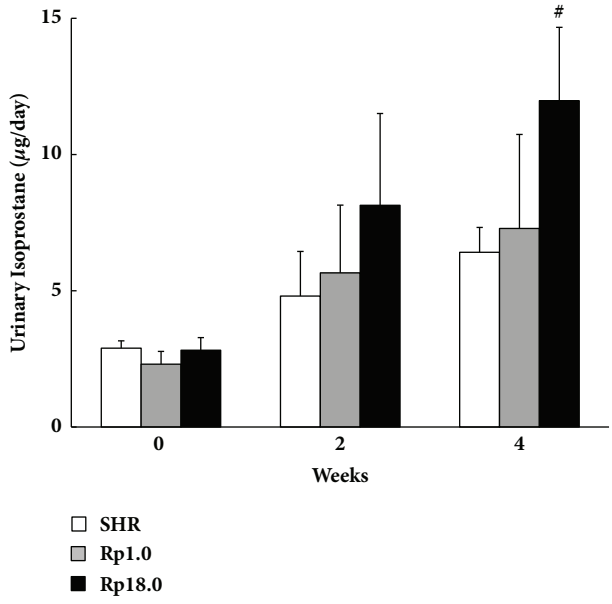

Figure 5: Urinary isoprostane level under salt-loading. Isoprostane was quantified in 24h urine collected after 0, 2, and 4 weeks of salt-loading (n=6 in each group). $^{\#}p<0.01$ *vs* control SHR by Student's t-test, which was significant after Bonferroni's correction. Data are presented as mean ± SD.

and the other two strains (see Figure 3). When correlation between the mRNA expression and renal fibrotic area/glomerulosclerosis was examined, we found that *α-Sma* showed no significant correlation with renal fibrotic area or with glomerulosclerosis while *Col1α-1* and *Tgf- β* did in the present study (see Figure 4). One possible reason for this discrepancy was that the expression was examined at one point, i.e., after 4 weeks of salt-loading. *α-Sma*, despite that it is a marker for fibrosis, might not be active at this point. In the meantime, *Kim-1* is known to be a marker for tubular injury. Therefore, tubular injury might not be a major player in the pathology of renal damage in the congenic strains studied here.

Although some classical parameters for renal damage, i.e., histological changes quantified by microscopic observation and urinary protein excretion, supported more advanced renal injury in Rp18.0, it may be useful to add other marker genes to obtain further support; the Bcl-3 and the urinary lipocalin-type prostaglandin D synthase were recently found to be sensitive markers for renal damage in several different diseases [29, 30], and urinary cystatin C is another established marker for renal function [31].

5. Conclusion

We showed that Rp18.0 suffered from more advanced renal injury under salt-loading when compared with SHR. As Rp18.0 was shown to be more susceptible to cerebral stroke in the previous study [9], this observation raised a possibility that the gene(s) in the QTL on chr_18 might induce both cerebral stroke and renal injury. We further showed that oxidative stress was significantly greater in Rp18.0, implying that oxidative stress played a pivotal role in the pathological changes observed in this congenic strain. The mechanisms of how increased oxidative stress promoted cerebral and renal injury observed in Rp18.0 is to be elucidated in a future study.

Data Availability

The data and materials supporting the conclusions of this article are included within the article.

Ethical Approval

Ethical concerns and experimental protocols were approved by the local committee of animal research in Shimane University.

Conflicts of Interest

The authors declare that there are no conflicts of interest regarding the publication of this paper.

Authors' Contributions

Toru Nabika was responsible for conceptualization, funding acquisition, project administration, supervision, and resources. Mohammad Farhadur Reza, Davis Ngarashi, Hiroki Ohara, Masamichi Koike, and Masaki Misumi were responsible for data curation and formal analysis. Mohammad Farhadur Reza, Hiroki Ohara, and Masamichi Koike were responsible for investigation. Mohammad Farhadur Reza, Hiroki Ohara, Masamichi Koike, and Masaki Misumi were responsible for methodology. Toru Nabika and Masamichi Koike were responsible for visualization. Toru Nabika and Mohammad Farhadur Reza were responsible for validation, writing of original draft, review, and editing of the manuscript.

Acknowledgments

We express our cordial thanks to Satoko Mishima for her technical assistance. This work was partly supported by JSPS KAKENHI 26293086.

References

[1] N. Ishikawa, Y. Harada, R. Maruyama, J. Masuda, and T. Nabika, "Genetic effects of blood pressure quantitative trait loci on hypertension-related organ damage: Evaluation using multiple congenic strains," *Hypertension Research*, vol. 31, no. 9, pp. 1773–1779, 2008.

[2] B. Gigante, S. Rubattu, R. Stanzione et al., "Contribution of genetic factors to renal lesions in the stroke-prone spontaneously hypertensive rat," *Hypertension*, vol. 42, no. 4, pp. 702–706, 2003.

[3] K. A. Griffin, P. C. Churchill, M. Picken, R. C. Webb, T. W. Kurtz, and A. K. Bidani, "Differential salt-sensitivity in the pathogenesis of renal damage in SHR and stroke prone SHR," *American Journal of Hypertension*, vol. 7061, pp. 311–320, 2018.

[4] K. Okamoto, "Establishment of the strokeprone spontaneously hypertensive rat (SHR)," *Circ Res Suppl*, vol. 1, pp. 143–153, 1972, http://ci.nii.ac.jp/naid/10026616354/en/.

[5] T. Nabika, Z. Cui, and J. Masuda, "The stroke-prone spontaneously hypertensive rat: how good is it as a model for cerebrovascular diseases?" *Cellular and Molecular Neurobiology*, vol. 24, no. 5, pp. 639–646, 2004, http://www.ncbi.nlm.nih.gov/entrez/query.fcgi?cmd=Retrieve&db=PubMed&dopt=Citation&list_uids=15485135.

[6] S. Rubattu, M. Volpe, R. Kreutz, U. Ganten, D. Ganten, and K. Lindpaintner, "Chromosomal mapping of quantitative trait loci contributing to stroke in a rat model of complex human disease," *Nature Genetics*, vol. 13, no. 4, pp. 429–434, 1996.

[7] S. Rubattu, N. Hubner, U. Ganten et al., "Reciprocal congenic lines for a major stroke QTL on rat chromosome 1," *Physiological Genomics*, vol. 27, no. 2, pp. 108–113, 2006.

[8] B. Jeffs, J. S. Clark, N. H. Anderson et al., "Sensitivity to cerebral ischaemic insult in a rat model of stroke is determined by a single genetic locus," *Nature Genetics*, vol. 16, no. 4, pp. 364–367, 1997.

[9] T.-A. Gandolgor, H. Ohara, Z.-H. Cui et al., "Two genomic regions of chromosomes 1 and 18 explain most of the stroke susceptibility under salt loading in stroke-prone spontaneously hypertensive Rat/Izm," *Hypertension*, vol. 62, no. 1, pp. 55–61, 2013.

[10] M. Volpe, M. J. F. Camargo, F. B. Mueller et al., "Relation of plasma renin to end organ damage and to protection of K feeding in stroke-prone hypertensive rats," *Hypertension*, vol. 15, no. 3, pp. 318–326, 1990.

[11] P. C. Churchill, M. C. Churchill, K. A. Griffin et al., "Increased genetic susceptibility to renal damage in the stroke-prone spontaneously hypertensive rat," *Kidney International*, vol. 61, no. 5, pp. 1794–1800, 2002.

[12] E. St Lezin, W. Liu, JM. Wang, N. Wang, V. Kren, D. Krenova et al., "Genetic isolation of a chromosome 1 region affecting blood pressure in the spontaneously hypertensive rat," *Hypertension*, vol. 30, pp. 854–859, 1997, http://www.ncbi.nlm.nih.gov/entrez/query.fcgi?cmd=Retrieve&db=PubMed&dopt=Citation&list_uids=9336384.

[13] K. Yuki and K. Tsubota, "Increased Urinary 8-Hydroxy-2′-deoxyguanosine (8-OHdG)/Creatinine Level is Associated with the Progression of Normal-Tension Glaucoma," *Current Eye Research*, vol. 38, no. 9, pp. 983–988, 2013.

[14] H. M. Zahid, M. Z. Ferdaus, H. Ohara, M. Isomura, and T. Nabika, "Effect of p22phox depletion on sympathetic regulation of blood pressure in SHRSP: evaluation in a new congenic strain," *Scientific Reports*, vol. 6, no. 1, pp. 4–11, 2016.

[15] M. Z. Ferdaus, B. Xiao, H. Ohara et al., "Identification of Stim1 as a Candidate Gene for Exaggerated Sympathetic Response to Stress in the Stroke-Prone Spontaneously Hypertensive Rat," *PLoS ONE*, vol. 9, no. 4, pp. 1–8, 2014.

[16] K. Niiya, H. Ohara, M. Isono et al., "Further dissection of QTLs for salt-induced stroke and identification of candidate genes in the stroke-prone spontaneously hypertensive rat," *Scientific Reports*, vol. 8, no. 1, 2018.

[17] M. Nagase, H. Matsui, S. Shibata, T. Gotoda, and T. Fujita, "Salt-Induced Nephropathy in Obese Spontaneously Hypertensive Rats Via Paradoxical Activation of the Mineralocorticoid Receptor," *Hypertension*, vol. 50, no. 5, pp. 877–883, 2007.

[18] H. C. M. Yu, L. M. Burrell, M. J. Black et al., "Salt Induces Myocardial and Renal Fibrosis in Normotensive and Hypertensive Rats," *Circulation*, vol. 98, no. 23, pp. 2621–2628, 1998.

[19] K. Hosohata, D. Yoshioka, A. Tanaka, H. Ando, and A. Fujimura, "Early urinary biomarkers for renal tubular damage in spontaneously hypertensive rats on a high salt intake," *Hypertension Research*, vol. 39, no. 1, pp. 19–26, 2016.

[20] C. Kitiyakara, T. Chabrashvili, and Y. Chen, "Salt intake, oxidative stress, and renal expression of NADPH oxidase and superoxide dismutase," *Journal of the American Society of Nephrology*, vol. 14, no. 11, pp. 2775–2782, 2003.

[21] E. A. Jaimes, J. M. Galceran, and L. Raij, "Angiotensin II induces superoxide anion production by mesangial cells," *Kidney International*, vol. 54, no. 3, pp. 775–784, 1998.

[22] N. Li, F. Yi, J. L. Spurrier, C. A. Bobrowitz, and A. Zou, "Production of superoxide through NADH oxidase in thick ascending limb of Henle's loop in rat kidney," *American Journal of Physiology-Renal Physiology*, vol. 282, no. 6, pp. F1111–F1119, 2002.

[23] H. J. Kim, T. Sato, B. Rodriguez-Iturbe, and N. D. Vaziri, "Role of Intrarenal Angiotensin System Activation, Oxidative Stress, Inflammation, and Impaired Nuclear Factor-Erythroid-2-Related Factor 2 Activity in the Progression of Focal Glomerulosclerosis," *The Journal of Pharmacology and Experimental Therapeutics*, vol. 337, no. 3, pp. 583–590, 2011.

[24] M. Paul, A. P. Mehr, and R. Kreutz, "Physiology of local renin-angiotensin systems," *Physiological Reviews*, vol. 86, no. 3, pp. 747–803, 2006.

[25] T. M. de Queiroz, M. M. Monteiro, and V. A. Braga, "Angiotensin-II-derived reactive oxygen species on baroreflex sensitivity during hypertension: new perspectives," *Frontiers in Physiology*, vol. 4, pp. 1–6, 2013.

[26] N. Kashihara, Y. Haruna, V. K. Kondeti, and Y. S. Kanwar, "Oxidative stress in diabetic nephropathy," *Current Medicinal Chemistry*, vol. 17, no. 34, pp. 4256–4269, 2010.

[27] P. B. Shelat, M. Chalimoniuk, J.-H. Wang et al., "Amyloid beta peptide and NMDA induce ROS from NADPH oxidase and AA release from cytosolic phospholipase A2 in cortical neurons," *Journal of Neurochemistry*, vol. 106, no. 1, pp. 45–55, 2008.

[28] E. McCracken, V. Valeriani, C. Simpson, T. Jover, J. McCulloch, and D. Dewar, "The Lipid Peroxidation By-product 4-Hydroxynonenal is Toxic to Axons and Oligodendrocytes," *Journal of Cerebral Blood Flow & Metabolism*, vol. 20, no. 11, pp. 1529–1536, 2000.

[29] R. Chen, L. Wang, S. Liu et al., "Bcl-3 is a novel biomarker of renal fibrosis in chronic kidney disease," *Oncotarget*, vol. 8, no. 57, pp. 97206–97216, 2017.

[30] H. Nakayama, H. Echizen, T. Gomi et al., "Urinary lipocalin-type prostaglandin D synthase: A potential marker for early gentamicin-induced renal damage?" *Therapeutic Drug Monitoring LWW*, vol. 31, no. 1, pp. 126–130, 2009.

[31] A. Onopiuk, A. Tokarzewicz, and E. Gorodkiewicz, "Cystatin C. A kidney function biomarker," *Advances in Clinical Chemistry*, vol. 68, pp. 57–69, 2015.

Hindawi
BioMed Research International
Volume 2019, Article ID 1602539, 8 pages
https://doi.org/10.1155/2019/1602539

Review Article

Unveiling the Role of DNA Methylation in Kidney Transplantation: Novel Perspectives toward Biomarker Identification

Antonella Agodi,[1] **Martina Barchitta**,[1] **Andrea Maugeri**,[1] **Guido Basile**,[2] **Matilde Zamboni**,[3] **Giulia Bernardini**,[3] **Daniela Corona**,[3] **and Massimiliano Veroux**[1]

[1]*Department of Medical and Surgical Sciences and Advanced Technologies "GF Ingrassia", University of Catania, Via S. Sofia, 87, 95123 Catania, Italy*
[2]*Department of General Surgery and Medical-Surgical Specialties, University of Catania, Via Plebiscito, 628, 95124 Catania, Italy*
[3]*Vascular Surgery Unit, University Hospital of Catania, Via Santa Sofia 87, 95123 Catania, Italy*

Correspondence should be addressed to Massimiliano Veroux; veroux@unict.it

Received 6 November 2018; Accepted 30 December 2018; Published 15 January 2019

Guest Editor: Kaiissar Mannoor

The burden of chronic kidney disease is dramatically rising, making it a major public health concern worldwide. Kidney transplantation is now the best treatment for patients with end-stage renal disease. Although kidney transplantation may improve survival and quality of life, its long-term results are hampered by immune- and/or non-immune-mediated complications. Thus, the identification of transplanted patients with a higher risk of posttransplant complications has become a big challenge for public health. However, current biomarkers of posttransplant complications have a poor predictive value, rising the need to explore novel approaches for the management of transplant patient. In this review we summarize the emerging literature about DNA methylation in kidney transplant complications, in order to highlight its perspectives toward biomarker identification. In the forthcoming future the monitoring of DNA methylation in kidney transplant patients could become a plausible strategy toward the prevention and/or treatment of kidney transplant complications.

1. Introduction

The burden of chronic kidney disease (CKD), in terms of human suffering and economic costs, is dramatically rising, making it a major public health concern worldwide [1]. The management of end-stage renal disease (ESRD) patients requires life-saving dialysis or kidney transplantation. Patients receiving renal replacement therapy are appraised at more than 1.4 million worldwide, with an estimated ≈8% increasing incidence each year [2]. The main reasons of this raise are ageing of populations and the consequent increasing incidence of type 2 diabetes mellitus and hypertension, which are the key risk factors for CKD [3].

Kidney transplantation currently remains the best replacement therapy for patients with irreversible ESRD [4], since it is associated with improved survival and quality of life compared to hemodialysis [5], but either immune- or non-immune-mediated complications significantly contribute to the higher morbidity of transplant patients [5]. While short-term kidney graft survival after transplantation has continuously improved over recent years [5], current evidence reports less marked improvements in long-term outcomes [6–10]. Several factors may affect transplant outcomes, including donor age, alloimmune response, ischemia-reperfusion injury, interstitial fibrosis of the allograft, recipient comorbidity, degree of human leukocyte antigen mismatch and polymorphisms in immunologic and nonimmunologic genes [11–14]. More recently, a particular consideration has been given to genomic and epigenomic differences between the donor and the recipient, which encompass 3.5 to 10 million genetic variants and substantial epigenetic variations related to ethnicity, environment, and lifestyles [15–17]. Blood-based biomarkers have been widely proposed as potential predictive and diagnostic biomarkers,

allowing the early identification of patients at high risk of transplant rejection and other adverse outcomes. The study of epigenetic mechanisms—including DNA methylation, histone modification, and noncoding RNA—is getting a lot of interest in this field of research, as reported by previous reviews [18–20].

In this review we provide an overview on how DNA methylation affects development and progression of CKD and we summarize the emerging literature about DNA methylation in kidney transplant complications. Finally, we discuss the perspectives and the clinical usefulness of DNA methylation changes as biomarkers of kidney transplant complications.

2. Epigenetics

Epigenetic mechanisms regulate gene expression without altering the DNA sequence. These molecular processes characterize the epigenome, which is dynamic in response to environmental stressors, modifiable during cell differentiation, and heritable in daughter cells [21]. There are several epigenetic mechanisms, which have been extensively reviewed by Portela and Esteller [22], affecting chromatin condensation, thereby regulating gene expression [23]: histone modifications (e.g., methylation or acetylation), noncoding RNA (e.g., siRNAs, lncRNAs, miRNAs), and DNA methylation [24].

The first lines of evidence on the role of epigenetics have been pointed out by cancer research, with several studies and meta-analyses demonstrating that epigenetic mechanisms regulate tumour suppressor genes silencing, activation of oncogenes, and increased chromosomal instability [25–29]. DNA methylation almost exclusively occurs within CpG islands—short sequences in gene promoters and regulatory regions that typically contain about 5-10 CpG dinucleotides per 100 bp [30]. In mammals, DNA methylation process is mediated by the activity of three DNA methyltransferases (DNMT1, DNMT3a, and DNMT3b).

3. DNA Methylation and Chronic Kidney Disease

Aberrant DNA methylation has been also described in other chronic diseases, such as cardiovascular disease, neurodegenerative diseases, diabetes and its complications, obesity, and CKD [31–38]. The latter has been recently associated with changes in the DNA methylation profile by *in vivo* and epidemiological studies [39]. Evidence from animal models indicated that *in utero* restriction of calories, proteins, and oxygen was linked to reduced nephron number, hypertension, and microalbuminuria. The influence of the intrauterine environment on the foetal epigenetic programming might explain foetal origin of adult diseases [40–42]. Beyond developmental programming, metabolic changes might also affect CKD development and long-term health. For instance, epidemiologic studies showed that the hyperglycaemia-related risk of diabetic kidney disease persisted even when metabolic control was restored. The discovery of the long-lasting effect of hyperglycaemia was the breakthrough for the development of the "metabolic memory" theory, particularly in the context of diabetic nephropathy [43, 44]. Consistently, the comparison between saliva samples of diabetic patients with or without end-stage kidney disease identified 187 genes that were differentially methylated, out of which 39 were involved in kidney development or diabetic nephropathy [45].

Recently, Smyth and colleagues compared DNA methylation of 485,577 CpG sites in blood samples between 255 CKD patients and 152 healthy controls [46]. Interestingly, they found aberrant DNA methylation of genes with known biological function in CKD (i.e., CUX1, ELMO1, FKBP5, INHBA-AS1, PTPRN2, and PRKAG2 genes). The relationship between PRKAG2 and CKD has also been confirmed by a meta-analysis of genomewide association data [47]. In addition, the Chronic Renal Insufficiency genomewide study compared the DNA methylation profiles of blood samples among patients classified by different glomerular filtration rates. The authors identified several differentially methylated regions in genes that were associated with kidney functions, including those involved in the epithelial to mesenchymal transition pathway (i.e., NPHP4, IQSEC1, and TCF3) [48].

Several lines of evidence also suggested the role of DNA methylation in kidney fibrosis progression. Stenvinkel and colleagues analysed DNA methylation of blood samples in CKD patients to evaluate the association between renal function, surrogate markers of inflammation, and aberrant DNA methylation. The authors concluded that stable CKD patients with no evidence of inflammation had comparable DNA methylation levels with age- and sex-matched controls, while end-stage kidney disease patients with higher inflammation exhibited DNA hypermethylation [49].

4. DNA Methylation in Kidney Transplantation

The identification of subgroups of transplant patients at higher risk of posttransplant complications has become a big challenge for public health, since it might improve long-term outcomes. However, until now, biomarkers of posttransplant complications have poor predictive value, rising the need to explore novel approaches for the management of transplant patient [20]. The dynamism of the epigenome and the long-lasting effect in response to environmental stimuli make the epigenetic mechanisms a suitable field of research for either biomarker discovery or the development of novel therapeutic strategies [18]. Overall, it has been acknowledged that epigenetic mechanisms play a crucial role in the multiple biological events involved in posttransplant complications, such as alloimmune response, ischemia/reperfusion (I/R) injury, and kidney graft fibrosis [18, 50]. It is also worth mentioning that both the recipient and the donor continuously undergo dynamic epigenetics modifications, even before transplantation [51, 52]. Meht and colleagues first described the usefulness of epigenetic modifications as rejection biomarkers [53]. The authors compared the methylation status of the promoters of DAPK and CALCA genes in urinary DNA from deceased or living donor kidney transplant recipients after 48 hours from the transplantation, and 65 healthy controls. CALCA hypermethylation was more frequently reported in kidney transplant recipients compared with healthy controls

and, in addition, CALCA methylation was more frequent in kidney transplant recipients from deceased than from living donors. Interestingly, there was a nonsignificant trend toward CALCA hypermethylation in patients with biopsy-proven acute tubular necrosis, when compared with acute rejection and delayed or immediate graft function [53].

4.1. DNA Methylation and Alloimmune Response. Epigenetic mechanisms might also affect the immune response of the recipient, which is a crucial driver of the alloresponse to the graft [54–57]. Although the use of immunosuppressive drugs improved the short-term kidney graft survival and decreased the incidence of acute graft rejection, the latter still remains accountable for one-tenth of graft loss [5]. The activation of immune cells relies on integrated pathways that in turn are tightly regulated by transcription factors and chromatin remodelers [58]. As extensively reviewed by Mas and colleagues [19], the regulation of gene transcription by epigenetic mechanisms might determine cell plasticity and the strength of posttransplant immune responses.

The major histocompatibility complex (MHC) encodes glycoproteins, which present antigens to the immune system, and its expression is fundamental to alloantigen recognition. Both in physiological (i.e., gametes and embryonic cells) and in pathological (i.e., neoplastic cells) conditions, the downregulation of MHC expression confers a degree of protection from the immune system [59]. In acute rejection there is an increase in MHC II glycoproteins within the allograft and recently it has been demonstrated that DNA methylation and histone modifications affected MHC class I and II expression [60]. DNA methylation also modulates T-cell activation through the production of interleukin-2 (IL-2). In fact, the IL-2 promoter is methylated in inactive T cells, while DNA demethylation allows upregulation of IL-2 following simultaneous T-cell receptor and costimulatory signalling [61]. Most of immune cells involved in allograft rejection are influenced by epigenetic factors. Hence, the investigation of DNA methylation profiles of immune cells before and after kidney transplantation might help the discovery of novel potential biomarkers for the clinical management of patients. For instance, epigenetic mechanisms might affect transcription factors, cytokines, and other molecules that are essential to control the transcriptional profiles and functions of memory T-cell [62]. Steinfelder and colleagues demonstrated that demethylation of the CCR6 gene, which encodes for a chemokine receptor in memory CD4+ T cells, enabled the migration toward the renal proximal tubular epithelial cells [63]. Several studies also demonstrated that epigenetic mechanisms modulated the cytolytic activity of natural killer (NK) cells, which are important in promoting rejection or tolerance [64], by regulating the expression of several NK cell receptors (i.e., KIR, NCRs, and NKG2D) and cytotoxic molecules (i.e., GRZ and PRF) [65, 66]. Others reported the complex epigenetic regulatory systems that modulated the differentiation of hematopoietic stem cells into antibody-producing B cells and antibody production [67–70]. However, most of studies focused on Foxp3, which encodes the transcription factor Scurfin. Foxp3 regulates development and function of CD25+CD4+ regulatory T (T_R) cells [71], which in turn maintain immunological self-tolerance and reduce many immune responses [72, 73]. These cells are mainly produced in the thymus as a functionally mature T-cell subpopulation specialized for immune suppression. In line with other genes, methylation of CpG sites within the Foxp3 gene leads to gene silencing whereas complete demethylation is necessary for stable and continuous Foxp3 expression [19]. Interestingly, subpopulations of T_R cells differ in the methylation of the T_R-specific demethylated region within the Foxp3 gene [74]: while T_R-specific demethylated region is methylated in naive CD4+ CD25− T cells, activated CD4+ T cells, and TGF-β–induced adaptive T_R cells, they are demethylated in natural T_R cells [74]. The main role of Foxp3+ natural T_R cells is to suppress several effectors of inflammation, such as T helper (T_H) 1, T_H2, and T_H17 cells [72, 73]. As comprehensively reviewed by Wilson and colleagues, there are also several lines of evidence demonstrating that chromatin conformation and DNA methylation at lineage restricted cytokine, transcription factor genes, and their regulatory elements in T_H cells both reflect and affect their development and functions [75].

4.2. DNA Methylation and Ischemia-Reperfusion Injury. Several studies proposed that ischemia-reperfusion injury might cause DNA methylation changes in the donor organ. During the ischemic period—in several clinical settings including kidney transplantation—tissues are deprived of oxygen and nutrients required to maintain physiological metabolism and energy homeostasis [76]. In kidney transplantation, the ischemia-reperfusion injury causes a series of pathological responses ranging from inflammation and fibrosis to cell and organ graft injury [76–78]. Pratt and colleagues were the first to propose that modifications of methylated CpG sites may occur as a result of prolonged ischemia-reperfusion injury in kidney transplantation [79], which is in turn associated with chronic nephropathy posttransplantation. In a rodent model of kidney transplantation, they demonstrated that prolonged cold ischemia in rat kidneys caused demethylation of a specific CpG site within the IFN-γ response element resident in the promoter region of complement component 3 (C3) gene [79]. Loss of transcriptional repression of this gene contributes to provide a plausible explanation for the accentuated immunologic injury, which often follows protracted ischemia of the allograft.

4.3. DNA Methylation and Kidney Graft Fibrosis. Progressive interstitial fibrosis is the crucial final pathway in renal destruction in either native or transplanted kidneys. Its pathogenesis is complex and comprises both immune- and non-immune-mediated mechanisms, culminating in interstitial fibrosis, tubular atrophy, and progressive loss of graft function. Similar to wound repair, fibrosis is triggered by an injury and characterized by the deposition of extracellular matrix through activated fibroblasts but conversely it can progress even after the injury has disappeared [80]. Fibrogenesis is the result of complex interactions among the different involved cell types which is coordinated by an extensive network of growth factors and signalling pathways [81].

Mechanisms that contribute to the maintenance of the profibrotic environment have not been well elucidated, but there is emerging evidence for the effects of epigenetics on gene expression and kidney fibrogenesis. Several lines of evidence demonstrated the role of DNA methylation in an abnormal wound healing process that resulted in fibrogenesis in CKD [48, 82]. However, few preclinical studies reported that DNA methylation might activate the fibrogenesis process in the kidney [83], suggesting a possible role for oxidative stress and inflammatory cytokines [84]. A genomewide methylation study of tubule epithelial cells identified ≈5000 differentially methylated CpG sites between CKD and control patients [82]. Interestingly, functional annotation analysis revealed that most of these regions were within or near developmental and profibrotic genes and that their methylation level correlated with the expression of many profibrotic genes [85]. In addition, a genomewide methylation study of fibroblasts identified 12 genes that were hypermethylated in fibrotic but not in nonfibrotic kidney biopsies [86]. Among these genes, hypermethylation of RASAL1—encoding an inhibitor of the Ras oncoprotein—was investigated further, since its silencing led to fibroblast activation by increased Ras-GTP activity. Notably, in vivo studies demonstrated that kidney fibrosis is ameliorated in DNMT1+/− mice [86], suggesting that RASAL1 hypermethylation was mediated by DNMT1. To uncover the molecular mechanisms that characterized kidney allografts, Bontha and colleagues applied an integrative multiomics approach in biopsies collected 24 months after transplantation. The authors reported hypomethylation of CpG sites within genes involved in activation of CD8+ and CD4+ T cells and MHC genes, and hypermethylation of genes related to metabolic functions, integrity, and structure of kidney [80].

4.4. DNA Methylation and Other Long-Term Complications after Kidney Transplantation. Aberrant DNA methylation is also studied for predicting long-term complications after kidney transplantation. For instance, transplant recipients are more likely to develop cutaneous squamous cell carcinoma (cSCC) [87, 88], for which immunosuppressive treatment seems to be a significant risk factor. Interestingly, Sherston and colleagues investigated methylation of T_R-specific demethylated region within the Foxp3 gene as a marker for cSCC in kidney transplant recipients [89]. The authors followed 58 survivors of a cohort of long-term kidney transplant patients, with and without skin cancer [89]. They found a significant increase in the proportion of demethylated CD4+FOXP3+ cells in patients who had previously developed cSCC. Although these results highlighted the methylation of T_R-specific demethylated region as a potential biomarker for cSCC posttransplantation [89], the use of peripheral blood mononuclear cells instead of sorted T_R cells may represent a limitation of the study. More recently, Peters and colleagues aimed to determine differentially methylated regions in T cells and their role in the development of cSCC in transplant patients [90]. Before transplantation, they compared DNA methylation of T cells between 27 recipients who developed a *de novo* cSCC and 27 who did not manifest cSCC. The authors found different methylation status in regulatory genomic and bivalent enhancer regions that coded for a zinc-finger protein (i.e., ZNF577) and a protein involved in T-cell migration (i.e., FLOT1), respectively [90]. While the DNA methylation status remained relatively stable in the majority of regions, it significantly changed in 9 differentially methylated regions after transplantation [90], and this could have a long-lasting effect on posttransplant cSCC development.

Recently, the effects of epigenetic mechanisms in cellular and molecular pathways involved in the pathogenesis of cardiorenal syndromes have been proposed [91]. CKD is associated with accumulation of uremic toxins and enhanced oxidative stress, which in turn might affect epigenetic signatures, including DNA methylation. Interestingly, it has been demonstrated that global hypermethylation is independently associated with cardiovascular mortality in patients with CKD [49]. Hypertension is one of the most common complications in kidney transplant recipients, increasing the risk of graft loss and other cardiovascular diseases. In these patients, treatment with angiotensin II (Ang II) blockers for preventing or treating hypertension is closely associated with improved survival. An *in vivo* study demonstrated that DNA methylation modulated the recipient vascular Ang II receptor (AT1R) gene expression, which in turn increased the vascular contractility in response to Ang II [92]. Another complication in kidney transplant recipients is the new-onset diabetes after transplantation (NODAT), which increases the risk of cardiovascular disease, infections, graft loss, and mortality [93, 94]. A recent genomewide DNA methylation analysis of adipose tissue found no significant difference in global DNA methylation between NODAT patients and healthy controls. However, patients who developed NODAT exhibited aberrant DNA methylation in ≈ 900 regions that were involved in insulin resistance, type 2 diabetes, and inflammation. These findings suggested that changes in DNA methylation of adipose tissue might increase infiltration of immune cells with consequent insulin resistance and inflammation, in patients who finally developed NODAT [95].

5. Conclusions

Uncovering the clinical potential of DNA methylation in CKD and complications after kidney transplantation is one of the main challenges toward the management of kidney transplant recipients. While aberrant DNA methylation has been plenty described in CKD by *in vivo* and epidemiological studies, further research is needed to discover novel potential biomarkers for kidney transplant rejection and complications. Our review highlights the fact that research behind the role of DNA methylation in kidney transplantation has so far exclusively been in the area of basic research, using *in vitro* or *in vivo* candidate-gene studies. Few studies provided evidence that epigenetic modifications might affect the individual risk to develop posttransplant complications. Biomarker validation also offers the possibility of identifying novel therapeutic targets. In fact, epigenetic drugs—especially DNA methylating or demethylating agents—are becoming available in oncology, and their potential to maintain functions and

integrity of the transplanted organ should be investigated. Furthermore, combined with routine clinical tests, the identification of biomarkers will contribute to an improvement of the patient management. Accordingly, further translational studies should be encouraged to transfer the abovementioned knowledge to the clinic. In the forthcoming future the monitoring of DNA methylation in kidney transplant patients could become a plausible strategy toward the prevention and/or treatment of kidney transplant complications in the clinical setting and could be useful for identifying those patients who are at higher risk of developing a cardiovascular complication after transplantation, which is the leading cause of death in kidney transplant recipients.

Conflicts of Interest

The authors declare that they have no conflicts of interest.

Acknowledgments

This work was partially supported by the Department of Medical and Surgical Sciences and Advanced Technologies "GF Ingrassia", University of Catania, Italy (Piano Triennale di Sviluppo delle Attività di Ricerca Scientifica del Dipartimento 2016–18).

References

[1] D. E. Weiner, "Public Health Consequences of Chronic Kidney Disease," *Clinical Pharmacology & Therapeutics*, vol. 86, no. 5, pp. 566–569, 2009.

[2] A. Schieppati and G. Remuzzi, "Chronic renal diseases as a public health problem: Epidemiology, social, and economic implications," *Kidney International Supplements*, vol. 68, no. 98, pp. S7–S10, 2005.

[3] S. Moeller, S. Gioberge, and G. Brown, "ESRD patients in 2001: Global overview of patients, treatment modalities and development trends," *Nephrology Dialysis Transplantation*, vol. 17, no. 12, pp. 2071–2076, 2002.

[4] D. J. Lo, B. Kaplan, and A. D. Kirk, "Biomarkers for kidney transplant rejection," *Nature Reviews Nephrology*, vol. 10, no. 4, pp. 215–225, 2014.

[5] A. J. Matas, J. M. Smith, M. A. Skeans et al. et al., "OPTN/SRTR 2012 annual data report: Kidney," *American Journal of Transplantation*, vol. 14, 1, pp. 11–44, 2014.

[6] M. Veroux, D. Corona, and P. Veroux, "Kidney transplantation: Future challenges," *Minerva Chirurgica*, vol. 64, no. 1, pp. 75–100, 2009.

[7] J. Pascual, M. J. Pérez-Sáez, M. Mir, and M. Crespo, "Chronic renal allograft injury: Early detection, accurate diagnosis and management," *Transplantation Reviews*, vol. 26, no. 4, pp. 280–290, 2012.

[8] J. M. Campistol, I. N. Boletis, J. Dantal et al. et al., "Chronic allograft nephropathy–a clinical syndrome: early detection and the potential role of proliferation signal inhibitors," *Clinical Transplantation*, vol. 23, no. 6, pp. 769–777, 2009.

[9] B. J. Nankivell and D. R. Kuypers, "Diagnosis and prevention of chronic kidney allograft loss," *The Lancet*, vol. 378, no. 9800, pp. 1428–1437, 2011.

[10] S. A. Lodhi, K. E. Lamb, and H. Meier-Kriesche, "Improving Long-Term Outcomes for Transplant Patients: Making the Case for Long-Term Disease-Specific and Multidisciplinary Research," *American Journal of Transplantation*, vol. 11, no. 10, pp. 2264-2265, 2011.

[11] M. Veroux, G. Grosso, D. Corona et al., "Age is an important predictor of kidney transplantation outcome," *Nephrology Dialysis Transplantation*, vol. 27, no. 4, pp. 1663–1671, 2012.

[12] A. E. Courtney, P. T. McNamee, and A. P. Maxwell, "The evolution of renal transplantation in clinical practice: for better, for worse?" *QJM: An International Journal of Medicine*, vol. 101, no. 12, pp. 967–978, 2008.

[13] J. Moore, A. J. McKnight, M. J. Simmonds et al. et al., "Association of caveolin-1 gene polymorphism with kidney transplant fibrosis and allograft failure," *JAMA2010*, vol. 303, pp. 1282–1287, 2010.

[14] A. Thakkinstian, S. Dmitrienko, M. Gerbase-DeLima et al. et al., "Association between cytokine gene polymorphisms and outcomes in renal transplantation: A meta-analysis of individual patient data," *Nephrology Dialysis Transplantation*, vol. 23, no. 9, pp. 3017–3023, 2008.

[15] G. R. Abecasis, D. Altshuler, A. Auton et al., "A map of human genome variation from population-scale sequencing," *Nature*, vol. 467, pp. 1061–1073, 2010.

[16] O. Carja, J. L. MacIsaac, S. M. Mah et al., "Worldwide patterns of human epigenetic variation," *Nature Ecology & Evolution*, vol. 1, no. 10, pp. 1577–1583, 2017.

[17] A. Agodi, M. Barchitta, A. Quattrocchi et al., "Low fruit consumption and folate deficiency are associated with LINE-1 hypomethylation in women of a cancer-free population," *Genes & Nutrition*, vol. 10, article 480, 2015.

[18] J. A. McCaughan, A. J. McKnight, A. E. Courtney, and A. P. Maxwell, "Epigenetics: Time to translate into transplantation," *Transplantation Journal*, vol. 94, no. 1, pp. 1–7, 2012.

[19] V. R. Mas, T. H. Le, and D. G. Maluf, "Epigenetics in kidney transplantation: Current evidence, predictions, and future research directions," *Transplantation*, vol. 100, no. 1, pp. 23–38, 2016.

[20] F. S. Peters, O. C. Manintveld, M. G. Betjes, C. C. Baan, and K. Boer, "Clinical potential of DNA methylation in organ transplantation," *The Journal of Heart and Lung Transplantation*, vol. 35, no. 7, pp. 843–850, 2016.

[21] S. S. Hammoud, B. R. Cairns, and D. A. Jones, "Epigenetic regulation of colon cancer and intestinal stem cells," *Current Opinion in Cell Biology*, vol. 25, no. 2, pp. 177–183, 2013.

[22] A. Portela and M. Esteller, "Epigenetic modifications and human disease," *Nature Biotechnology*, vol. 28, no. 10, pp. 1057–1068, 2010.

[23] J. Baird, C. Jacob, M. Barker et al., "Developmental origins of health and disease: A lifecourse approach to the prevention of non-communicable diseases," *Healthcare*, vol. 5, no. 1, p. 14, 2017.

[24] A. D. Goldberg, C. D. Allis, and E. Bernstein, "Epigenetics: A landscape takes shape," *Cell*, vol. 128, no. 4, pp. 635–638, 2007.

[25] M. Barchitta, A. Quattrocchi, A. Maugeri, M. Vinciguerra, and A. Agodi, "LINE-1 hypomethylation in blood and tissue samples as an epigenetic marker for cancer risk: A systematic review and meta-analysis," *PLoS ONE*, vol. 9, no. 10, Article ID e109478, 2014.

[26] A. Agodi, M. Barchitta, A. Quattrocchi, A. Maugeri, M. Vinciguerra, and R. A. Calogero, "DAPK1 Promoter Methylation and Cervical Cancer Risk: A Systematic Review and a Meta-Analysis," *PLoS ONE*, vol. 10, article e0135078, 2015.

[27] M. Barchitta, A. Quattrocchi, A. Maugeri et al., "LINE-1 hypermethylation in white blood cell DNA is associated with high-grade cervical intraepithelial neoplasia," *BMC Cancer*, vol. 17, article 601, 2017.

[28] A. Eden, F. Gaudet, A. Waghmare, and R. Jaenisch, "Chromosomal instability and tumors promoted by DNA hypomethylation," *Science*, vol. 300, article 455, 2003.

[29] V. Phé, O. Cussenot, and M. Rouprêt, "Methylated genes as potential biomarkers in prostate cancer," *BJU International*, vol. 105, no. 10, pp. 1364–1370, 2010.

[30] G. Auclair and M. Weber, "Mechanisms of DNA methylation and demethylation in mammals," *Biochimie*, vol. 94, no. 11, pp. 2202–2211, 2012.

[31] C. Y. Wang, S. S. Shie, I. C. Hsieh, M. L. Tsai, and M. S. Wen, "FTO modulates circadian rhythms and inhibits the CLOCK-BMAL1-induced transcription," *Biochemical and Biophysical Research Communications*, vol. 464, no. 3, pp. 826–832, 2015.

[32] R. S. Dwivedi, J. G. Herman, T. A. McCaffrey, and D. S. Raj, "Beyond genetics: Epigenetic code in chronic kidney disease," *Kidney International*, vol. 79, no. 1, pp. 23–32, 2011.

[33] E. Agardh, A. Lundstig, A. Perfilyev et al., "Genome-wide analysis of DNA methylation in subjects with type 1 diabetes identifies epigenetic modifications associated with proliferative diabetic retinopathy," *BMC Medicine*, vol. 13, article 182, no. 1, 2015.

[34] A. Baccarelli, M. Rienstra, and E. J. Benjamin, "Cardiovascular epigenetics: Basic concepts and results from animal and human studies," *Circulation: Cardiovascular Genetics*, vol. 3, no. 6, pp. 567–573, 2010.

[35] C. G. Bell, A. E. Teschendorff, V. K. Rakyan, A. P. Maxwell, S. Beck, and D. A. Savage, "Genome-wide DNA methylation analysis for diabetic nephropathy in type 1 diabetes mellitus," *BMC Medical Genomics*, vol. 3, article 33, 2010.

[36] D. Cui and X. Xu, "DNA methyltransferases, DNA methylation, and age-associated cognitive function," *International Journal of Molecular Sciences*, vol. 19, article 1315, no. 5, p. 1315, 2018.

[37] A. Maugeri, M. G. Mazzone, F. Giuliano et al., "Curcumin Modulates DNA Methyltransferase Functions in a Cellular Model of Diabetic Retinopathy," *Oxidative Medicine and Cellular Longevity*, vol. 2018, Article ID 5407482, 12 pages, 2018.

[38] A. Maugeri, M. Barchitta, M. Mazzone, F. Giuliano, G. Basile, and A. Agodi, "Resveratrol modulates SIRT1 and DNMT functions and restores LINE-1 methylation levels in ARPE-19 cells under oxidative stress and inflammation," *International Journal of Molecular Sciences*, vol. 19, no. 7, p. 2118, 2018.

[39] Y. Ko and K. Susztak, "Epigenomics: The science of no-longer-junk DNA. why study it in chronic kidney disease?" *Seminars in Nephrology*, vol. 33, no. 4, pp. 354–362, 2013.

[40] Y. Seki, L. Williams, P. M. Vuguin, and M. J. Charron, "Minireview: Epigenetic programming of diabetes and obesity: Animal models," *Endocrinology*, vol. 153, no. 3, pp. 1031–1038, 2012.

[41] M. J. Warner and S. E. Ozanne, "Mechanisms involved in the developmental programming of adulthood disease," *Biochemical Journal*, vol. 427, no. 3, pp. 333–347, 2010.

[42] G. C. Burdge and K. A. Lillycrop, "Nutrition, epigenetics, and developmental plasticity: Implications for understanding human disease," *Annual Review of Nutrition*, vol. 30, no. 1, pp. 315–339, 2010.

[43] M. A. Reddy and R. Natarajan, "Epigenetics in diabetic kidney disease," *Journal of the American Society of Nephrology*, vol. 22, no. 12, pp. 2182–2185, 2011.

[44] M. A. Reddy, J. T. Park, and R. Natarajan, "Epigenetic modifications and diabetic nephropathy," *Kidney Research and Clinical Practice*, vol. 31, no. 3, pp. 139–150, 2012.

[45] C. Sapienza, J. Lee, J. Powell et al., "DNA methylation profling identifes epigenetic differences between diabetes patients with ESRD and diabetes patients without nephropathy," *Epigenetics*, vol. 6, no. 1, pp. 20–28, 2011.

[46] L. J. Smyth, G. J. McKay, A. P. Maxwell, and A. J. McKnight, "DNA hypermethylation and DNA hypomethylation is present at different loci in chronic kidney disease," *Epigenetics*, vol. 9, no. 3, pp. 366–376, 2014.

[47] A. Köttgen, C. Pattaro, C. A. Böger et al. et al., "New loci associated with kidney function and chronic kidney disease," *Nature Genetics*, vol. 42, no. 5, pp. 376–384, 2010.

[48] M. R. Wing, J. M. Devaney, M. M. Joffe et al., "DNA methylation profile associated with rapid decline in kidney function: Findings from the CRIC Study," *Nephrology Dialysis Transplantation*, vol. 29, no. 4, pp. 864–872, 2014.

[49] P. Stenvinkel, M. Karimi, S. Johansson et al. et al., "Impact of inflammation on epigenetic DNA methylation - a novel risk factor for cardiovascular disease?" *Journal of Internal Medicine*, vol. 261, no. 5, pp. 488–499, 2007.

[50] Y. Obata, Y. Furusawa, and K. Hase, "Epigenetic modifications of the immune system in health and disease," *Immunology & Cell Biology*, vol. 93, no. 3, pp. 226–232, 2015.

[51] S. A. LaMere, H. K. Komori, and D. R. Salomon, "New opportunities for organ transplantation research: Epigenetics is likely to be an important determinant of the host immune response," *Epigenomics*, vol. 5, no. 3, pp. 243–246, 2013.

[52] M. D. Parker, P. A. Chambers, J. P. Lodge, and J. R. Pratt, "Ischemia- reperfusion injury and its influence on the epigenetic modification of the donor kidney genome," *Transplantation*, vol. 86, no. 12, pp. 1818–1823, 2008.

[53] T. Mehta, M. Hoque, R. Ugarte et al., "Quantitative detection of promoter hypermethylation as a biomarker of acute kidney injury during transplantation," *Transplantation Proceedings*, vol. 38, no. 10, pp. 3420–3426, 2006.

[54] N. Ohkura, Y. Kitagawa, and S. Sakaguchi, "Development and maintenance of regulatory T cells," *Immunity*, vol. 38, no. 3, pp. 414–423, 2013.

[55] D. Kumbala and R. Zhang, "Essential concept of transplant immunology for clinical practice," *World Journal of Transplantation*, vol. 3, no. 4, pp. 113–118, 2013.

[56] B. Youngblood, J. S. Hale, and R. Ahmed, "T-cell memory differentiation: Insights from transcriptional signatures and epigenetics," *The Journal of Immunology*, vol. 139, no. 3, pp. 277–284, 2013.

[57] J. Barbi, D. Pardoll, and F. Pan, "Treg functional stability and its responsiveness to the microenvironment," *Immunological Reviews*, vol. 259, no. 1, pp. 115–139, 2014.

[58] M. K. Atianand and K. A. Fitzgerald, "Long non-coding RNAs and control of gene expression in the immune system," *Trends in Molecular Medicine*, vol. 20, no. 11, pp. 623–631, 2014.

[59] P. J. Van Den Elsen, T. M. Holling, N. Van Der Stoep, and J. M. Boss, "DNA methylation and expression of major histocompatibility complex class I and class II transactivator genes in human developmental tumor cells and in T cell malignancies," *Clinical Immunology*, vol. 109, no. 1, pp. 46–52, 2003.

[60] M. Barrett, A. D. Milton, J. Barrett et al., "Needle biopsy evaluation of class II major histocompatibility complex antigen

expression for the differential diagnosis of cyclosporine nephrotoxicity from kidney graft rejection," *Transplantation*, vol. 44, no. 2, pp. 223–227, 1987.

[61] D. R. Fitzpatrick and C. B. Wilson, "Methylation and demethylation in the regulation of genes, cells, and responses in the immune system," *Clinical Immunology*, vol. 109, no. 1, pp. 37–45, 2003.

[62] N.-P. Weng, Y. Araki, and K. Subedi, "The molecular basis of the memory T cell response: Differential gene expression and its epigenetic regulation," *Nature Reviews Immunology*, vol. 12, no. 4, pp. 306–315, 2012.

[63] S. Steinfelder, S. Floess, D. Engelbert et al. et al., "Epigenetic modification of the human CCR6 gene is associated with stable CCR6 expression in T cells," *Blood*, vol. 117, no. 10, pp. 2839–2846, 2011.

[64] J. Villard, "The role of natural killer cells in human solid organ and tissue transplantation," *Journal of Innate Immunity*, vol. 3, no. 4, pp. 395–402, 2011.

[65] H. Ogbomo, M. Michaelis, J. Kreuter, H. W. Doerr, and J. Cinatl, "Histone deacetylase inhibitors suppress natural killer cell cytolytic activity," *FEBS Letters*, vol. 581, no. 7, pp. 1317–1322, 2007.

[66] G. Li, M. Yu, C. M. Weyand, and J. J. Goronzy, "Epigenetic regulation of killer immunoglobulin-like receptor expression in T cells," *Blood*, vol. 114, no. 16, pp. 3422–3430, 2009.

[67] J. Ramírez, K. Lukin, and J. Hagman, "From hematopoietic progenitors to B cells: Mechanisms of lineage restriction and commitment," *Current Opinion in Immunology*, vol. 22, no. 2, pp. 177–184, 2010.

[68] B. Barneda-Zahonero, L. Roman-Gonzalez, O. Collazo, T. Mahmoudi, and M. Parra, "Epigenetic Regulation of B Lymphocyte Differentiation, Transdifferentiation, and Reprogramming," *Comparative and Functional Genomics*, vol. 2012, Article ID 564381, 10 pages, 2012.

[69] M. Parra, "Epigenetic events during B lymphocyte development," *Epigenetics*, vol. 4, no. 7, pp. 462–468, 2009.

[70] J. Rodríguez-Ubreva, L. Ciudad, D. Gómez-Cabrero et al., "Pre-B cell to macrophage transdifferentiation without significant promoter DNA methylation changes," *Nucleic Acids Research*, vol. 40, no. 5, pp. 1954–1968, 2012.

[71] G. Lal and J. S. Bromberg, "Epigenetic mechanisms of regulation of Foxp3 expression," *Blood*, vol. 114, no. 18, pp. 3727–3735, 2009.

[72] P. Sagoo, G. Lombardi, and R. I. Lechler, "Relevance of regulatory T cell promotion of donor-specific tolerance in solid organ transplantation," *Frontiers in Immunology*, vol. 3, article 184, 2012.

[73] H. Fan, P. Cao, D. S. Game, F. Dazzi, Z. Liu, and S. Jiang, "Regulatory T cell therapy for the induction of clinical organ transplantation tolerance," *Seminars in Immunology*, vol. 23, no. 6, pp. 453–461, 2011.

[74] O. Bestard, L. Cuñetti, J. M. Cruzado et al. et al., "Intragraft regulatory T cells in protocol biopsies retain Foxp3 demethylation and are protective biomarkers for kidney graft outcome," *American Journal of Transplantation*, vol. 11, no. 10, pp. 2162–2172, 2011.

[75] C. B. Wilson, E. Rowell, and M. Sekimata, "Epigenetic control of T-helper-cell differentiation," *Nature Reviews Immunology*, vol. 9, no. 2, pp. 91–105, 2009.

[76] J. Menke, D. Sollinger, B. Schamberger, U. Heemann, and J. Lutz, "The effect of ischemia/reperfusion on the kidney graft," *Current Opinion in Organ Transplantation*, vol. 19, no. 4, pp. 395–400, 2014.

[77] P. Cravedi and P. S. Heeger, "Complement as a multifaceted modulator of kidney transplant injury," *The Journal of Clinical Investigation*, vol. 124, no. 6, pp. 2348–2354, 2014.

[78] C. Ponticelli, "Ischaemia-reperfusion injury: A major protagonist in kidney transplantation," *Nephrology Dialysis Transplantation*, vol. 29, no. 6, pp. 1134–1140, 2014.

[79] J. R. Pratt, M. D. Parker, L. J. Affleck et al., "Ischemic epigenetics and the transplanted kidney," *Transplantation Proceedings*, vol. 38, no. 10, pp. 3344–3346, 2006.

[80] S. V. Bontha, D. G. Maluf, K. J. Archer et al., "Effects of DNA methylation on progression to interstitial fibrosis and tubular atrophy in renal allograft biopsies: A multi-omics approach," *American Journal of Transplantation*, vol. 17, no. 12, pp. 3060–3075, 2017.

[81] X. Li and S. Zhuang, "Recent advances in renal interstitial fibrosis and tubular atrophy after kidney transplantation," *Fibrogenesis Tissue Repair*, vol. 7, article 15, no. 1, 2014.

[82] Y.-A. Ko, D. Mohtat, M. Suzuki et al. et al., "Cytosine methylation changes in enhancer regions of core pro-fibrotic genes characterize kidney fibrosis development," *Genome Biology*, vol. 14, article R108, 2013.

[83] E. M. Zeisberg and M. Zeisberg, "The role of promoter hypermethylation in fibroblast activation and fibrogenesis," *The Journal of Pathology*, vol. 229, no. 2, pp. 264–273, 2013.

[84] I. Fonseca, H. Reguengo, M. Almeida et al., "Oxidative stress in kidney transplantation: Malondialdehyde is an early predictive marker of graft dysfunction," *Transplantation*, vol. 97, no. 10, pp. 1058–1065, 2014.

[85] K. I. Woroniecka, A. S. D. Park, D. Mohtat, D. B. Thomas, J. M. Pullman, and K. Susztak, "Transcriptome analysis of human diabetic kidney disease," *Diabetes*, vol. 60, no. 9, pp. 2354–2369, 2011.

[86] W. Bechtel, S. McGoohan, E. M. Zeisberg et al., "Methylation determines fibroblast activation and fibrogenesis in the kidney," *Nature Medicine*, vol. 16, no. 5, pp. 544–550, 2010.

[87] C. M. Vajdic, S. P. McDonald, M. R. E. McCredie et al., "Cancer incidence before and after kidney transplantation," *Journal of the American Medical Association*, vol. 296, no. 23, pp. 2823–2831, 2006.

[88] P. Piselli, D. Serraino, G. P. Segoloni et al., "Risk of de novo cancers after transplantation: Results from a cohort of 7217 kidney transplant recipients, Italy 1997–2009," *European Journal of Cancer*, vol. 49, no. 2, pp. 336–344, 2013.

[89] S. N. Sherston, K. Vogt, S. Schlickeiser, B. Sawitzki, P. N. Harden, and K. J. Wood, "Demethylation of the TSDR is a marker of squamous cell carcinoma in transplant recipients," *American Journal of Transplantation*, vol. 14, no. 11, pp. 2617–2622, 2014.

[90] F. S. Peters, A. M. Peeters, P. R. Mandaviya et al., "Differentially methylated regions in T cells identify kidney transplant patients at risk for de novo skin cancer," *Clinical Epigenetics*, vol. 10, article 81, 2018.

[91] G. M. Virzì, A. Clementi, A. Brocca, M. de Cal, and C. Ronco, "Epigenetics: A potential key mechanism involved in the pathogenesis of cardiorenal syndromes," *Journal of Nephrology*, vol. 31, no. 3, pp. 333–341, 2018.

[92] Y. Zhao, Q. Zhu, S. Sun et al., "Renal transplantation increases angiotensin II receptor-mediated vascular contractility associated with changes of epigenetic mechanisms," *International Journal of Molecular Medicine*, vol. 41, pp. 2375–2388, 2018.

[93] F. G. Cosio, T. E. Pesavento, K. Osei, M. L. Henry, and R. M. Ferguson, "Post-transplant diabetes mellitus: Increasing

incidence in renal allograft recipients transplanted in recent years," *Kidney International*, vol. 59, no. 2, pp. 732–737, 2001.

[94] M. Veroux, T. Tallarita, D. Corona et al., "Conversion to sirolimus therapy in kidney transplant recipients with new onset diabetes mellitus after transplantation," *Clinical and Developmental Immunology*, vol. 2013, Article ID 496974, 7 pages, 2013.

[95] S. Baheti, P. Singh, Y. Zhang et al., "Adipose tissue DNA methylome changes in development of new-onset diabetes after kidney transplantation," *Epigenomics*, vol. 9, no. 11, pp. 1423–1435, 2017.

Hindawi
BioMed Research International
Volume 2019, Article ID 3460902, 11 pages
https://doi.org/10.1155/2019/3460902

Research Article

Age-Specific Cut-off Values of Amino Acids and Acylcarnitines for Diagnosis of Inborn Errors of Metabolism Using Liquid Chromatography Tandem Mass Spectrometry

Suprovath Kumar Sarker[1,2] **Md Tarikul Islam**[1] **Aparna Biswas**[1] **Golam Sarower Bhuyan**[3] **Rosy Sultana**[1,4] **Nusrat Sultana**[1,5] **Shagoofa Rakhshanda**[1] **Mst. Noorjahan Begum**[1,2] **Asifuzzaman Rahat**[3] **Sharmina Yeasmin**[6] **Mowshori Khanam**[7] **Asim Kumar Saha**[8] **Farjana Akther Noor**[1,9] **Abu A. Sajib**[2] **Abul B. M. M. K. Islam**[2] **Syeda Kashfi Qadri**[10] **Mohammod Shahidullah**[11] **Mohammad Abdul Mannan**[11] **A. K. M. Muraduzzaman**[12] **Tahmina Shirin**[12] **Sheikh Maksudur Rahman**[13] **Syed Saleheen Qadri**[1] **Narayan Saha**[14] **Sharif Akhteruzzaman**[2] **Firdausi Qadri**[1,3,15] **and Kaiissar Mannoor**[1,3]

[1] *Laboratory of Genetics and Genomics, Institute for Developing Science and Health Initiatives, Mohakhali, Dhaka 1212, Bangladesh*
[2] *Department of Genetic Engineering & Biotechnology, University of Dhaka, Dhaka 1000, Bangladesh*
[3] *Infectious Diseases Laboratory, Institute for Developing Science and Health Initiatives, Mohakhali, Dhaka 1212, Bangladesh*
[4] *Bangladesh University of Health Sciences, Bangladesh*
[5] *Department of Virology, Dhaka Medical College, Dhaka 1000, Bangladesh*
[6] *Department of Gynecology & Obstetrics, Bangladesh Institute of Health Sciences General Hospital, 125/1, Darus Salam, Mirpur-1, Dhaka 1216, Bangladesh*
[7] *Ain Shams General Hospital and Diagnostic Centre Pvt. Ltd., Vhushir Mill, Sign Board, Gazipur, Bangladesh*
[8] *Narsingdi Sadar Hospital, Raipur, Narsingdi, Bangladesh*
[9] *Department of Biochemistry and Molecular Biology, University of Dhaka, Bangladesh*
[10] *Department of Paediatric Medicine, KK Women's and Children's Hospital, Singapore*
[11] *Department of Neonatology, Bangabandhu Sheikh Mujib Medical University, Shahbag, Dhaka, Bangladesh*
[12] *Department of Virology, Institute of Epidemiology, Disease Control and Research, Mohakhali, Dhaka, Bangladesh*
[13] *Research and Development, Incepta chemicals Ltd., Barabaria, Saturia, Dhankora, Dhaka 1810, Bangladesh*
[14] *Pediatric Neurology, National Institute of Neurosciences & Hospital, Dhaka 1207, Bangladesh*
[15] *Department of Enteric and Respiratory Infectious Diseases, Infectious Diseases Division, International Centre for Diarrhoeal Disease Research, Bangladesh, Mohakhali, Dhaka, Bangladesh*

Correspondence should be addressed to Kaiissar Mannoor; kaiissar@ideshi.org

Received 11 July 2018; Revised 28 November 2018; Accepted 12 December 2018; Published 6 January 2019

Academic Editor: Abdelaziz M. Thabet

Liquid Chromatography tandem mass spectrometry (LC-MS/MS) is used for the diagnosis of more than 30 inborn errors of metabolisms (IEMs). Accurate and reliable diagnosis of IEMs by quantifying amino acids (AAs) and acylcarnitines (ACs) using LC-MS/MS systems depend on the establishment of age-specific cut-offs of the analytes. This study aimed to (1) determine the age-specific cut-off values of AAs and ACs in Bangladesh and (2) validate the LC-MS/MS method for diagnosis of the patients with IEMs. A total of 570 enrolled healthy participants were divided into 3 age groups, namely, (1) newborns (1-7 days), (2) 8 days–7 years, and (3) 8–17 years, to establish the age-specific cut-offs for AAs and ACs. Also, 273 suspected patients with IEMs were enrolled to

evaluate the reliability of the established cut-off values. Quantitation of AAs and ACs was performed on an automated LC-MS/MS system using dried blood spot (DBS) cards. Then the specimens of the enrolled clinically suspected patients were analyzed by the established method. Nine patients came out as screening positive for different IEMs, including two borderline positive cases of medium-chain acyl-CoA dehydrogenase deficiency (MCAD). A second-tier test for confirmation of the screening positive cases was conducted by urinary metabolic profiling using gas chromatography- mass spectrometry (GC-MS). Out of 9 cases that came out as screening positive by LC-MS/MS, seven cases were confirmed by urinary GC-MS analysis including 3 cases with phenylketonuria, 1 with citrullinemia type II, 1 with methylmalonic acidemia, 1 with isovaleric acidemia and 1 with carnitine uptake defect. Two borderline positive cases with MCAD were found negative by urinary GC-MS analysis. In conclusion, along with establishment of a validated LC-MS/MS method for quantitation of AAs and ACs from the DBS cards, the study also demonstrates the presence of predominantly available IEMs in Bangladesh.

1. Introduction

Inborn errors of metabolism (IEMs) are a group of phenotypically and genotypically heterogeneous metabolic disorders caused by mutations in the genes that encode enzymes of the metabolic pathways [1]. Deficiency or altered activities of the necessary enzymes or proteins in the intermediary metabolic pathways leads to a wide spectrum of diseases with clinical heterogeneity [2, 3]. Although, individually these disorders are rare, collectively they are numerous and the prevalence rate varies between 1 in 800 and 1 in 2500 live births [1, 4–6]. Moreover, there is population-wise variation of incidence of IEMs and it is assumed that 6-8% of world population can be affected by these disorders.

Till date, about 1000 IEMs disorders have been identified [7]. However, the clinical manifestations of these disorders are often nonspecific and sometimes the signs and symptoms of an individual IEM overlap with other IEMs and even non-IEMs diseases, such as septicemia [2, 8, 9]. Remarkably, one-third of the IEMs are characterized by involvement of the nervous system [10] and the repercussions of neurometabolic changes, particularly to neurological development during the early years of life make it imperative to detect and treat them at the earliest to prevent forthcoming disaster. The quality of life of the affected individuals can be improved by early diagnosis followed by immediate treatment initiation, provided that treatments are available. Also, preventive measures can be taken through genetic counseling [10]. Many IEMs including aminoacidopathies, organic acidemias, and fatty acid oxidation (FAO) disorders can be treated by simple diet therapy or other easy interventions [11, 12]. Unfortunately, diagnosis of individual IEMs are burdensome and practically impossible, because there is no single test available to diagnose these disorders.

Currently, liquid chromatography-tandem mass spectrometry (LC-MS/MS)-based high throughput technologies are being widely used which permits simultaneous quantification of several metabolites such as amino acids and acylcarnitines from a very small amount of biological specimen. However, age-specific reference ranges of cut-off values for each analyte must be established first for each population by individual laboratories prior to screening/diagnosis of the patients [13–16], because the cut-offs are highly influenced by various factors such as genetic background, geographical location of a population, diet and age [13, 17, 18]. At present, newborns are being screened or diagnosed for more than 30 IEMs using LC-MS/MS through newborn screening programs in the majority of the developed countries, and certain developing countries across the globe [1, 10, 19–22]. Unfortunately, newborn screening facilities do not exist in Bangladesh. As a result, biological specimens from individuals with suspected IEMs are being sent to other countries for screening purposes. However, the approach to analyze specimens in other countries is unaffordable for most Bangladeshis, and above all, the results are interpreted by comparing the data with the cut-off values derived from the people of other geographical location and genetic background.

In this study, we validated the method of LC-MS/MS-based quantification of amino acids and acylcarnitines with the target to establish reference values of the metabolites for three different age groups of our population. Finally, we screened clinical specimens and investigated whether the established reference values of amino acids and acylcarnitines could be used to identify the IEMs, especially aminoacidopathies, organic acidemias, and FAO disorders, among the clinically suspected patients with IEMs in Bangladesh. Our study is expected to motivate Bangladeshi health policy-makers to initiate a nationwide newborn screening program without further delay to contribute towards fulfilling the SDG goal 3 in time.

2. Methods and Materials

2.1. Ethical Approval and Study Population. The study protocol was reviewed and approved by the National Ethics Review Committee (NERC) of Bangladesh Medical Research Council (BMRC), Dhaka, Bangladesh (BMRC/NREC/2013-2016/990). Prior to the collection of blood specimens, written consent was obtained from the parents of the patients with IEMs and healthy participants. For the establishment of cut-off values of amino acids and acylcarnitines, a total of 570 healthy participants without any disease were enrolled in the study. The healthy participants were divided into 3 groups according to age, namely, group A (N= 120, aged 1-7 days), group B (N= 243, aged 8 days-7 years), and group C (N= 207, aged 8-17 years). Additionally, 273 patients (158 males and 115 females) with clinical manifestations suggestive of IEMs were also enrolled. The median age of the patients with suspected IEMs was 2.16 years (range: 0.03-17 years). Inclusion criteria for participation in the study were lethargy, irritation, poor feeding, tachypnea, seizures, persistent vomiting, toe-walking, unexplained developmental delay, abnormal movement, language retardation, history of death of previous sibling due to unexplained cause, positive family

history with metabolic disorders, and parental consanguinity. In addition, these patients were also subjected to investigation for the signs, metabolic acidosis with an increase in anion gap, persistent or recurrent hypoglycemia, hypotonia, hyperammonemia, splenomegaly, abnormal imaging and electrophysiologic findings, which are suggestive of metabolic disorders [6, 8, 10, 23]. However, the patients with aforementioned symptoms who had history of perinatal brain injury, infection of central nervous system, or chromosomal abnormalities were excluded from the study [10, 23]. Based on the inclusion criteria, the patients with suspected IEMs were referred by the pediatric clinicians from (1) National Institute of Neurosciences & Hospital, Bangladesh, (2) Bangabandhu Sheikh Mujib Medical University, Bangladesh, and (3) Dhaka Shishu Hospital, Bangladesh. All the patients were examined by expert clinicians before enrollment in the study. Before enrollment of the participants, written informed consent was taken from the parents or legal guardians.

2.2. Specimen Collection and Storage. The whole blood specimens of newborns were collected by heel prick method and ~75 μL of blood was spotted on Whatman™ 903 Generic Multipart filter paper (GE Healthcare, Westborough, MA, USA) to prepare a DBS (Dried blood spot) card for LC-MS/MS analysis. Approximately, 80% specimens were collected between 24 hours and 72 hours after birth and 20% specimens were collected between day 4 and day 7 after birth. The whole blood specimens for older children were collected after 4-hour fasting using standard venipuncture method and a DBS card was prepared by spotting ~75 μL blood on Whatman™ 903 filter paper. In addition, 5 mL fasting urine specimens were also collected for urinary metabolic screening tests including ferric chloride test, 2,4-Dinitrophenylhydrazine test, Cyanide nitroprusside test, and tests for urine reducing sugar and ketone bodies. The DBS cards were dried for 4 hours at room temperature and stored at -70°C in plastic ziplock bags with desiccants until analysis was done. After urinary metabolic screening tests, the leftover urine specimens (~ 2 mL) were stored at -70°C for second-tier tests such as metabolic profiling using gas chromatography-mass spectrometry (GC-MS).

2.3. Specimen Preparation and LC-MS/MS Analysis. A NeoMass AAAC kit (Labsystems Diagnostics Oy, Finland) was used for quantitation of amino acids and acylcarnitines from the DBS cards. A vial of lyophilized isotope-labeled internal standards (IS) containing $^{2}H_{4}$-Alanine (Ala IS), $^{2}H_{4}$-^{13}C-Arginine (Arg IS), $^{2}H_{2}$- Citrulline (Cit IS), $^{2}H_{3}$- Leucine (Leu IS), $^{13}C_{6}$-$^{15}N_{2}$- Lysine (Lys IS), $^{2}H_{3}$- Methionine (Met IS), $^{2}H_{6}$-Ornithine (Orn IS), $^{13}C_{6}$- Phenylalanine (Phe IS), $^{2}H_{5}$-Proline (Pro IS), $^{13}C_{3}$-Serine (Ser IS), $^{13}C_{6}$- Tyrosine (Tyr IS), and $^{2}H_{8}$- Valine (Val IS), $^{2}H_{9}$- free carnitine (C0 IS), $^{2}H_{3}$- Acetylcarnitine (C2 IS), $^{2}H_{3}$- Propionylcarnitine (C3 IS), $^{2}H_{3}$- Butyrylcarnitine (C4 IS), $^{2}H_{9}$- Isovalerylcarnitine (C5 IS), $^{2}H_{3}$- Glutarylcarnitine (C5DC IS), $^{2}H_{3}$- Hexanoylcarnitine (C6 IS), $^{2}H_{3}$- Octanoylcarnitine (C8 IS), $^{2}H_{3}$- Decanoylcarnitine (C10 IS), $^{2}H_{3}$- Lauroylcarnitine (C12 IS), $^{2}H_{9}^{-}$ Myristoylcarnitine (C14 IS), $^{2}H_{3}$- Palmitoylcarnitine (C16 IS), and $^{2}H_{3}$- Stearoylcarnitin (C18 IS) was reconstituted by adding 1 mL of extraction solution which was provided with the NeoMass kit. Daily working extraction solution was prepared by diluting the reconstituted internal standards with 1:100 (v/v) extraction solution.

For analysis of amino acids and acylcarnitines from the stored specimens, the DBS cards were brought to room temperature (+18 to +25°C) prior to extraction and a 3.2 mm disk (equivalent to ~3.1 μL whole blood) was punched out using an automated Wallac Delfia DBS puncher (Perkin-Elmer Life Sciences, Inc., USA) into a well of polystyrene U-bottomed 96-well microplate provided with the kit. After addition of 100 μL daily working extraction solution to each well of microplate, the plate was covered with adhesive film and incubated for 20 minutes at room temperature in a microplate shaker with shaking speed of 650 rpm. After incubation, 70 μL supernatant was transferred into a V-bottomed microplate and covered with aluminum foil to reduce the evaporation. The plate was placed in the autosampler of LC-MS/MS system and 5 μL supernatant was injected into the LC-MS/MS system for analysis.

2.4. Instrumentation and LC-MS/MS Analysis. Shimadzu LCMS-8050 liquid chromatograph mass spectrometer (Shimadzu Corporation, Japan) equipped with binary pump, autosampler and electrospray ionization (ESI) source was used for the analysis. The specimens were injected into the LC-MS/MS system through ESI source for atmospheric pressure ionization and specimen analysis was performed using flow injection analysis-electrospray ionization-tandem mass spectrometry (FIA-ESI-MS/MS) method.

2.5. Data Acquisition and Data Processing. The solvent delivery pump of LC-MS/MS system was programed for delivery of mobile phase (provided with the kit) at a constant flow rate of 150 μL/min and the data acquisition was done in positive ion multiple reaction monitoring (MRM) mode. The ionization source parameters of LC-MS/MS were interface voltage 4.5 kV, interface temperature 250°C, dissolution line temperature 250°C, heat block temperature 400°C, nebulizing gas flow 3.0 L/min, and drying gas flow 15.0 L/min. Argon was used as a collision gas at pressure of 230 kPa. A Lab Solution (version 5.82 SP1, Shimadzu Corporation, Japan) software was used for data acquisition and the concentration of each analyte was calculated using a Neonatal Solution software (version 2.20, Shimadzu Corporation, Japan). The total run time for each specimen was 1.5 min and the data were acquired for 0.9 min. The MRM parameters for analysis of amino acids and acylcarnitines have been shown in Supplementary Table S1 (Supplementary File 1). Three levels of quality control (QC) specimens (low, medium, and high) were provided with the NeoMass AAAC kit to ensure the accuracy of the test results. These QC specimens were extracted and analyzed parallel with the specimens of healthy controls and patients to monitor the reliability of the data generated from the LC-MS/MS analysis.

2.6. Validation of the Method. Validation of the method and performance of the Shimadzu LCMS 8050 (Shimadzu

Corporation, Kyoto, Japan) were done using three levels of control specimens (low, medium, and high) provided with the NeoMass AAAC kit (Labsystems Diagnostics Oy, Vantaa, Finland). Extraction of the analytes was done using aforementioned extraction method for the DBS cards and performance of the method was evaluated in terms of intra-assay and inter-assay accuracy and precision, linearity, limit of detection (LOD) or functional sensitivity, limit of quantitation (LOQ), and recovery. The method validation analysis was done for Ala, Arg, Cit, Leu, Lys, Met, Orn, Phe, Pro, Ser, Tyr, Val, C0, C2, C3, C4, C5, C6, C8, C10, C12, C14, C16, and C18.

2.7. GC-MS Analysis for Urinary Metabolic Profiling. For the second-tier test, urine specimens (~ 2 mL) of the patients who were screening positive by LC-MS/MS analysis were sent to NeoCare Diagnostics Pvt. Ltd., Mumbai, India, for urinary metabolic screening test using GC-MS.

2.8. Data Acquisition Statistical Analysis. GraphPad Prism 7 software (GraphPad Software, Inc., USA) and IBM SPSS Statistics (Version 20) were used for statistical analysis. Percentiles, mean values, standard deviations (SD), coefficients of variation (CV) and relative errors (RE %) were calculated using standard statistical formulas.

3. Results

3.1. Validation of LC-MS/MS Method for Quantitation of Amino Acids and Acylcarnitines. Intra-assay and inter-assay variability of the method for each analyte were done by analyzing three levels of control specimens in 15 different replicates over a period of 5 days according to the CLSI EP5-A2; Evaluation of Precision Performance of Quantitative Measurement Methods; Approved Guideline—Second Edition [24]. Supplementary Table S2 (Supplementary File 1) shows that the average range of intra-assay percentage of coefficient of variation (%CV) of 11 amino acids (Ala, Arg, Cit, Leu, Lys, Met, Orn, Phe, Pro, Ser, and Val) was within 20% of the target value which was within the acceptable limit [25, 26]. However, the intra-assay %CV for Tyr was 23.15%. The average range of %CV for free carnitine (C0) and acylcarnitines (C0, C2, C3, C4, C5, C8, C10, C12, C14, C16, and C18) was also within 20% of the target value, except for C6 (36.47%) which may have been due to very low concentrations of the analyte in the low level DBS controls which were supplied with the kit (0.13 μmol/L). The accuracy of the method was determined as percentage of relative error (RE%). In case of intra-assay accuracy, the average ranges of RE% of amino acids and acylcarnitines were -19.85 to +9.33% and -6.46 to +6.93%, respectively, which were within the acceptable ranges (Supplementary File 1: Supplementary Table S2) [26]. The average ranges of inter-assay %CV were 1.32%–11.60% and 1.16–14.14% for amino acids and acylcarnitines, respectively. The ranges of average inter-assay RE% were -19.31 to +3.55 % and -6.61 to +8.36% for amino acids and carnitine-acylcarnitines, respectively. These data indicated that the inter-assay accuracy and precision were within acceptable limits (Supplementary File 1: Supplementary Table S3) [25, 26]. The ranges of average recovery rates for amino acids and carnitine-acylcarnitines were 80.68–103.54% and 93.37–108.35%, respectively (Supplementary File 1: Supplementary Table S4) and they were within acceptable limits [26]. Linearity of the method for quantitation of each analyte was evaluated following CLSI EP06; Evaluation of the Linearity of Quantitative Measurement Procedures: A Statistical Approach; Approved Guideline [27]. As shown in Supplementary Table S4 (Supplementary File 1), the coefficient of determination (R^2 > 0.99) along with slope and y-intersect indicated that the method was linear for all concentration levels (low, mid, and high) of each analyte. LOD and LOQ for all analytes were also calculated following CLSI EP17; Evaluation of Detection Capability for Clinical Laboratory Measurement Procedures; Approved Guideline, and the results have been demonstrated in Supplementary File 1 (Supplementary Table S4) [28]. Together, the data generated for method validation study indicated that this method was suitable for quantitation of amino acids and acylcarnitines from the DBS specimens [25, 26].

3.2. Determination of Cut-off Values of Amino Acids, Acylcarnitines, and Marker Ratios. In this study, we calculated the cut-off values using percentile distribution of metabolites in healthy subjects according to CLSI C28-A2; How to Define and Determine Reference Intervals in the Clinical Laboratory; Approved Guideline—Second Edition [29]. The blood concentrations of metabolites (12 amino acids, free carnitine and 23 acylcarnitine species) and the ratios of metabolites (12 amino acid ratios and 18 ratios for acylcarnitines) were determined using LC-MS/MS and 2.5^{th}, 50^{th} (median), and 97.5^{th} percentiles were calculated for three groups of healthy population (Supplementary File 1: Supplementary Table S5). For each analyte of the healthy populations, the upper limit cut-offs were set at above the 97.5^{th} percentiles, whereas the lower limit cut-offs were set at below the 2.5^{th} percentiles. Table 1 presents the cut-off values for the analytes and marker ratios for screening of aminoacidopathies, organic acidemias, and FAO disorders. For screening of specific IEMs, we had also taken consideration of clinical manifestations of the patients, previous family histories, unexplained deaths of siblings, and consanguinity of the parents, etc.

3.3. Results of DBS Specimens from Clinically Suspected Patients Using LC-MS/MS. Among 273 clinically suspected patients with IEMs, 9 patients came out as screening positive for 6 different IEMs by LC-MS/MS analysis of DBS cards. Among these 9 patients, there were 3 cases of phenylketonuria (PKU); 1 case for each of citrullinemia type II (CIT-II), methylmalonic acidemia (MMA), isovaleric acidemia (IVA), and carnitine uptake defect (CUD); and 2 cases of medium-chain acyl-CoA dehydrogenase deficiency (MCAD).

Two female patients were found to be screening positive for PKU at the age of about 1 year and the only male patient was screening positive at the age of 10 years. Major clinical complications of these PKU patients were developmental delays, lethargy, and seizures (Table 2).

Table 1: The cut-off values of the analytes and marker ratios for screening of IEMs.

Suspected disease	Analytes/Marker ratios	Cut-offs Group A (μmol/L)	Cut-offs Group B (μmol/L)	Cut-offs Group C (μmol/L)
PKU	↑ Phe	> 85.45	> 88.12	> 82.08
	↑ Phe/tyr	> 3.47	> 5.11	> 8.03
BHD	↑ Phe/tyr	> 3.47	> 5.11	> 8.03
CIT	↑ Cit	> 17.17	> 35.91	> 39.74
	↑ Cit/Phe	> 0.42	> 0.75	> 0.80
TYR	↑ Tyr	> 199.96	> 128.12	> 136.63
	↑ Tyr/Phe	> 5.90	> 2.50	> 2.56
MSUD	↑ Val	> 188.83	> 187.45	> 210.34
	↑ Xle	> 200.85	> 201.74	> 220.69
	↑ Val/Phe	> 5.37	> 3.35	> 4.05
	↑ Xle/Ala	> 1.37	> 1.44	> 1.23
	↑ Xle/Phe	> 5.62	> 3.37	> 4.14
ARG	↑ Arg	> 21.39	> 74.98	> 95.36
	↑ Arg/Orn	> 0.26	> 1.00	> 1.04
OTC	↓ Cit	< 4.68	< 11.51	< 13.67
	↑ Orn	> 112.77	> 145.61	> 148.49
HCY	↑ Met	> 42.38	> 40.65	> 42.17
	↑ Met/Phe	> 0.74	> 0.77	> 0.78
MMA	↑ C3	> 6.88	> 2.69	> 2.70
	↑ C3/C2	> 0.19	> 0.15	> 0.14
IVA	↑ C5	> 0.55	> 0.26	> 0.29
	↑ C5/C3	> 0.42	> 0.16	> 0.19
GA-II	↑ C4	> 0.63	> 0.33	> 0.38
	↑ C8	> 0.14	> 0.14	> 0.30
	↑ C14	> 0.51	> 0.27	> 0.13
	↑ C16	> 7.23	> 2.47	> 2.20
	↑ C12	> 0.23	> 0.14	> 0.15
GA-I	↑ C5DC	> 0.29	> 0.17	> 0.20
CUD	↓ C0	< 15.60	< 12.34	< 13.38
	↓ C2	< 6.88	< 8.71	< 9.05
CPT-I	↑ C0	> 73.73	> 69.76	> 75.67
	↑ C0/(C16+C18)	> 21.67	> 43.54	> 56.08
	↓ C16	< 0.88	< 0.61	< 0.55
SCAD	↑ C4	> 0.63	> 0.33	> 0.38
	↑ C4/C2	> 0.03	> 0.02	> 0.02
MCAD	↑ C6	> 0.09	> 0.09	> 0.12
	↑ C8	> 0.14	> 0.14	> 0.30
	↑ C10	> 0.18	> 0.23	> 0.58
	↑ C10:1	> 0.11	> 0.16	> 0.21
	↑ C10:2	> 0.02	> 0.08	> 0.08
	↑ C8/C10	> 1.67	> 4.43	> 2.45
	↑ C8/C2	> 0.01	> 0.01	> 0.02
VLCAD	↑ C14:1	> 0.34	> 0.16	> 0.26
	↑ C14:1/C16	> 0.09	> 0.16	> 0.22
	↑ C14	> 0.51	> 0.27	> 0.13
CPT-II	↑ C16	> 7.23	> 2.47	> 2.20
CACT	↑ C18	> 1.69	> 0.91	> 0.88
	↑ C18:1	> 1.98	> 1.57	> 1.67

Table 1: Continued.

Suspected disease	Analytes/Marker ratios	Cut-offs Group A (μmol/L)	Cut-offs Group B (μmol/L)	Cut-offs Group C (μmol/L)
TFP	↑ C18OH	> 0.05	> 0.01	> 0.01
	↑ C18:1OH	> 0.03	> 0.02	> 0.02

PKU, phenylketonuria; BHD, BH4 deficiency; CIT, citrullinemia; TYR, tyrosinemia; MSUD, maple syrup urine disease; ARG, argininemia; OTC, ornithine transcarbamylase deficiency; HCY, homocystinuria; MMA, methylmalonic acidemia; IVA, isovaleric acidemia; GA-II, glutaric acidemia type II (multiple acyl-CoA dehydrogenase deficiency); GA-I, glutaric acidemia type I; CUD, carnitine uptake defect; CPT-I, carnitine palmitoyltransferase I deficiency; SCAD, short-chain acyl-CoA dehydrogenase deficiency; MCAD, medium-chain acyl-CoA dehydrogenase deficiency; VLCAD, very long-chain acyl-CoA dehydrogenase deficiency; CPT-II, carnitine palmitoyltransferase II deficiency; CACT, carnitine-acylcarnitine translocase deficiency; TFP, trifunctional protein deficiency.

The male patient was positive for citrullinemia type II (CIT-II) upon screening at the age of 10 years and his major clinical complications included irritability, restlessness, and excessive crying followed by unconsciousness (Table 2).

A one-year-old boy with developmental delay, seizure, and low muscle tone was found to be screening positive for methylmalonic acidemia (MMA). A male patient who came out as screening positive for isovaleric acidemia (IVA) was diagnosed at the age of 1.9 years. He was hospitalized multiple times with clinical manifestations like acute respiratory infections and acute watery diarrhea. He had developmental delay and elevated level of plasma ammonia.

One male patient who was screening positive for carnitine uptake deficiency (CUD) was diagnosed at the age of 2 years had clinical complications including lethargy, restlessness, poor feeding, seizure, vomiting, abnormal movement, developmental delay, speech problems, and inability of walking. Two patients, a boy and a girl who were screening positive for medium-chain acyl-CoA dehydrogenase deficiency (MCAD), were siblings. The boy was 10 years of age, whereas the girl was aged 8.5 years at the time of screening. Common clinical complications of these patients were restlessness, irritability, abnormal behavior, speech problem, and mental retardation. The blood concentrations of C6, C8, C10, C10:1, and C8/C10 ratio of both the male and the female MCAD patients were slightly higher than the reference cut-off values, while the concentration of C10:2 and the C8/C10 ratio were within the reference cut-off values in case of both male and female patients (Table 2).

3.4. GC-MS-Based Second-Tier Test for Analysis of Urine Specimens from the LC-MS/MS-Based Screening Positive IEMs Cases. As mentioned earlier, nine patients came out as screening positive by LC-MS/MS analysis. Next, urine specimens from all these 9 patients were subjected to a second-tier test using GC-MS. The urinary metabolic profiling of 3 screening positive patients with PKU revealed elevated levels of 4-hydroxyphenylacetic acid, phenyllactic acid, 4-hydroxyphenyllactic acid, 2 hydroxyphenylacetic acid and mandelic acid. Elevated levels of these organic acids are suggestive of PKU caused by the deficiency of phenylalanine hydroxylase enzyme (Supplementary File 1: Supplementary Table S6).

In case of CIT-II screening positive patient, urinary metabolite profiling using GC-MS revealed an elevated level of citrulline, which is suggestive of citrullinemia (Supplementary File 1: Supplementary Table S6). GC-MS analysis of urine specimens from screening positive patient with MMA showed an elevated level of urinary excretion of methylmalonic acid, suggesting confirmatory diagnosis of the screening positive MMA case (Supplementary File 1: Supplementary Table S6). The second-tier test using GC-MS analysis of urine specimen from IVA screening positive case revealed that IVA specific metabolites such as isovalerylglycine and 3-OH-isovalerate were elevated (Supplementary File 1: Supplementary Table S6).

The urine metabolic profiling of screening positive patient with CUD revealed elevated levels of urinary excretions of 3-hydroxy butyric acid (3HB), adipic acid, and p-Cresol. An elevated level of adipic acid along with a highly elevated level of 3HB is suggestive of carnitine uptake deficiency (Supplementary File 1: Supplementary Table S6).

For the MCAD screening positive patients which had LC-MS/MS-derived borderline positive values above the cut-off, urinary metabolic profiling by GC-MS revealed that the levels of all the analytes tested were within the range of the cut-off, which confirms that these patients were not true cases of MCAD, i.e., false positive (Supplementary File 1: Supplementary Table S6).

4. Discussion

The number, intricacy, and diverse clinical spectrum of IEMs present a daunting diagnostic challenge to the physicians. However, in order to reduce morbidity and mortality, or other severe repercussions like irreversible neurological damage to the patients with IEMs, early diagnosis and institution of appropriate therapy are very critical. The use of LC-MS/MS during the past decades has led to a remarkable increase in screening of IEMs. Many countries have established newborn screening (NBS) tests using LC-MS/MS which analyzes metabolites from dried blood spots (DBSs) to detect the IEM-associated disorders, particularly the treatable one [30–32]. Although NBS is not in practice in Bangladesh, the government health policymakers have initiated official processes to start nationwide NBS program for management of IEMs. Under the circumstances, establishment of local cut-offs for IEMs-associated metabolites is timely. This is the first study on screening of IEMs using LC-MS/MS in Bangladesh, where the cut-off values of individual amino acids and acylcarnitines were established by analyzing the

Table 2: Abnormal blood concentrations of metabolites and marker ratios together with clinical manifestations of the patients with suspected IEMs, as screened by LC-MS/MS.

Name of disorders	Total no. of positive cases (frequency among detected cases)	Case ID	Age at diagnosis	Metabolites or marker ratios	Concentrations of metabolites (μmol/L) or marker ratios	Cut-offs (μmol/L)	Major clinical complications
PKU	3 (33.3%)	Case 1	1.1 years	Phe	180.12	> 88.12	Lethargy, irritation, seizure and developmental delay
				Phe/tyr	5.97	> 5.11	
		Case 2	1.0 year	Phe	282.45	> 88.12	
				Phe/tyr	6.30	> 5.11	
		Case 3	10.0 years	Phe	1170.32	> 82.08	
				Phe/tyr	46.58	> 8.03	
CIT-II	1 (11.1%)	Case 4	10.0 years	Cit	1494.66	> 39.74	Irritability, restlessness and excessive crying followed by unconsciousness
				Cit/Phe	26.68	> 0.80	
MMA	1 (11.1%)	Case 5	1.0 year	C3	5.39	> 2.69	Developmental delay, seizure and low muscle tone
				C3/C2	0.29	> 0.15	
IVA	1 (11.1%)	Case 6	1.9 years	C5	13.80	> 0.26	Recurrent infection and developmental delay
				C5/C3	25.07	> 0.16	
CUD	1 (11.1%)	Case 7	2.0 years	C0	6.13	< 12.34	Lethargy, restless, poor feeding, seizure, vomiting, developmental delay, speech problem and inability of walking
				C2	6.47	< 8.71	
MCAD	2 (22.2%)	Case 8	10.0 years	C6	0.62	> 0.12	Restlessness, irritability, abnormal behavior, speech problem and mental retardation
				C8	1.90	> 0.30	
				C10	2.90	> 0.58	
				C10:1	1.14	> 0.21	
				C10:2	0.04	> 0.08	
				C8/C10	0.65	> 2.45	
				C8/C2	0.16	> 0.02	
		Case 9	8.5 years	C6	0.23	> 0.12	
				C8	1.15	> 0.30	
				C10	1.88	> 0.58	
				C10:1	0.66	> 0.21	
				C10:2	0.03	> 0.08	
				C8/C10	0.61	> 2.45	
				C8/C2	0.09	> 0.02	

PKU, phenylketonuria; CIT-II, citrullinemia type II; MMA, methylmalonic acidemia; IVA, isovaleric acidemia; CUD, carnitine uptake defect; and MCAD, medium-chain acyl-CoA dehydrogenase deficiency.

DBS specimens of healthy subjects and the patients with suspected IEMs were screened using the established cut-off values.

LC-MS/MS has been widely adopted for IEMs screening as it offers simultaneous and robust multiple disease screening using a single analytical high throughput technique [33]. Moreover, LC-MS/MS-based screening of IEMs provide the advantages of rapidity and convenience in sample collection and the stable isotopic internal standards used for quantification in this method increases the specificity and sensitivity of the test. In addition, it is possible to detect a number of common to very rare diseases inexpensively. To reduce the cost, usually a large number of specimens are analyzed in a single run.

Most aminoacidopathies, organic acidemias, and FAO disorders can be diagnosed using LC-MS/MS with 99% sensitivity and 99.995% specificity [1, 34–36] but it requires establishment of rigorous reference cut-off limits to detect the IEM-related disorders. Reliable cut-offs would help to minimize the false positive or false negative cases [14, 16, 37]. Through a worldwide collaborative project, the cut-off values for screening of IEMs were determined using 25-30 million healthy newborns, where 10742 cases were diagnosed with IEMs [38]. However, the cut-off limits of metabolites depend on different factors, such as analysis method, instrument platform, genetic background or ethnicity of a particular population [14, 39]. Since an NBS program does not yet exist in Bangladesh, the patients are hospitalized or they visit the physicians with clinical manifestations of IEMs during postneonatal period when irreversible damage has already occurred. Also, due to perplexing clinical presentation of IEMs signs and symptoms and lack of proper screening facilities, specimens are being sent to other countries where the results are interpreted by comparing the data with the cut-off values set for other geographical location and ethnic backgrounds. This study is an initiative to overcome those issues, as here, we have demonstrated the establishment of cut-off values for different amino acids and acylcarnitines for 3 different age groups. Sex-dependent variations of blood amino acids and acylcarnitines concentrations are very rare and this is why we generated only age-specific data considering age-specific variations of blood metabolites in healthy population are frequently reported [7, 17, 18, 40]. Moreover, the cut-off limits for screening of some amino acids and acylcarnitines are very close to normal reference intervals [18]. In the present study, all 7 patients who had been detected with IEMs were older than one year and we could successfully diagnose these patients using the established cut-off values for group B (8 days-7 years) and group C (8-17 years), which further emphasizes the necessity of age-specific cut-off ranges of different analytes.

In the study, among 273 patients with clinical signs and symptoms of IEMs, 7 (2.6%) came out as screening positive when DBS specimens were analyzed using LC-MS/MS. Different research groups across the world reported different frequencies of IEMs; e.g., Han and coworkers confirmed 1135 (6.2%) cases with IEMs among 18303 suspected inherited metabolic diseases in China [2], while Al Riyami S *et al.* reported a rate of 10.8% IEMs from Oman [41]. Furthermore, frequencies of 0.29%, 0.92% and 6% IEMs cases were reported from Korea, Turkey and Egypt, respectively. Our results are not directly comparable with other published survey data because the prevalence rates of IEMs vary due to geographical location, ethnicity, instrumentation platform, diagnostic strategies and time span of the surveillance in a particular population [13]. However, despite the difference in criteria for selection of IEMs-suspected patients and diagnostic approach, the results of our study are comparable with the published data from India, the neighboring country of Bangladesh, where IEM frequency has been reported to be as high as 3.2% (113 cases among 3550 suspected patients) [10]. Although the results of our study, which were generated in a time span of two years, do not reflect the true prevalence of IEMs in Bangladesh, it clearly demonstrates that IEMs are not uncommon in this country and thus the authorities in health sector and policymakers should be notified of the importance of screening of IEMs. In addition, consanguineous marriage, which is a common practice in Muslim countries like Bangladesh, is a major factor behind high rates of IEMs [42, 43]. We found that about 43% of our confirmed IEM cases came with consanguineous family history and the findings are consistent with others reports published across the globe.

Among 7 patients who had been detected with IEMs using the established cut-off ranges in this study, 3 had PKU (aminoacidopathies) and 1 patient for each of isovaleric acidemia and methylmalonic acidemia (organic academia), carnitine uptake deficiency and citrullinemia (urea cycle disorder). Our study identified aminoacidopathies with higher frequencies than other types of IEMs, and a similar pattern was also reported from two other neighboring countries, namely China and India, with PKU as the most prevalent IEM [10, 44]. All these 7 patients could possess a satisfactory quality of life provided that they would have undergone NBS and started receiving treatment earlier, because the IEM disorders they were suffering from were preventable. Thus, the effort to thwart disease progression and severity, and to provide diagnosed children with a tolerable living standard is only conceivable with the initiation and application of a nationwide screening program for IEMs in the first few days of life, followed by quick and specific treatment and care. Moreover, the benefits of such a program includes societal, ethical, and economic aspects, as the present health expenditures on handicapped people in Bangladesh are huge and beyond affordable limit for most people. Furthermore, the LC-MS/MS technology has been cost-effective for NBS in many developed countries as well as in developing countries [45–47]. Bangladesh's health policymakers must therefore consider LC-MS/MS technology for IEMs screening, at least for the most common disorders.

For the diagnosis of IEMs, the interpretation of LC-MS/MS results may be inconvenient or arguable if there is debate about the appropriateness of the reference ranges. In our study there were two false positive MCAD cases who had borderline positive concentrations of C6 acylcarnitines on LC-MS/MS analysis and these cases came out as negative when urinary GC-MS analysis was done. The reason for such false positive cases might be due to relatively low number of

sample size for determination of cut-offs and this might be seen as the shortfall of the study. Analysis of more samples in the future is expected to generate more reliable cut-offs. In addition to screening, the second-tier tests need to be performed by experienced biochemical and genetic experts. Usually, various biochemical test, GC-MS, HPLC, enzymatic assay and molecular analysis can be used as a second-tier or confirmatory test. However, none of these tests offers the conveniences of LC-MS/MS which is why LC-MS/MS has been widely granted and used in NBS program all across the globe.

Finally, apart from establishing cut-off values for various amino acids and acylcarnitines for Bangladeshi population and screening for metabolic disorders in Bangladesh, the current study also aimed to gain practical experience in using the technology and evaluating the overall efficiency of the method in a Bangladeshi setting. We hope this experience would assist other researchers or government authorities in installing and establishing the new technology for screening of IEMs through NBS program.

In conclusion, LC-MS/MS techniques may play a vital role in screening and diagnosis of IEMs in newborns and this may be helpful in facilitating timely therapy of treatable IEMs. Furthermore, diagnosis of the relatively prevalent metabolic disorders among Bangladeshi population, along with their clinical features and ages of onsets, may provide physicians with a deeper understanding of these conditions, which would allow for early diagnosis and better treatment. Lastly, given the high birth rate and economical condition in countries like Bangladesh, introducing NBS for these disorders would be a considerable but worthwhile challenge.

Data Availability

All relevant data generated or analyzed during this study are included in this article and supporting information file.

Conflicts of Interest

The authors declare that they have no conflicts of interest.

Acknowledgments

This study was supported by Institute for Developing Science and Health Initiatives (ideSHi) and a grant (CP-4029) from the Higher Education Quality Enhancement Project of the University Grant Commission (UGC) of Bangladesh. We thank the clinicians and staff of the National Institute of Neurosciences & Hospital, Bangladesh, Bangabandhu Sheikh Mujib Medical University, Bangladesh, and Dhaka Shishu Hospital, Bangladesh, for their assistance in recording clinical informations and collecting blood and urine specimens.

Supplementary Materials

Supplementary Table S1: Data acquisition parameters of MRM method for analysis of amino acids and acylcarnitines. Supplementary Table S2: Intra-assay precision and accuracy analysis of LC-MS/MS method for amino acids and acylcarnitines using low, medium and high control specimens. Supplementary Table S3: Inter-assay precision and accuracy analysis of LC-MS/MS method for amino acids, free carnitine, and acylcarnitines using low, medium, and high control specimens. Supplementary Table S4: Linearity, limit of detection (LOD), limit of quantitation (LOQ), and recovery analysis of LC-MS/MS method for amino acids and acylcarnitines using low, medium, and high control specimens. Supplementary Table S5: Percentile distribution of amino acids, acylcarnitines, and related ratios in different age groups of healthy participants. Supplementary Table S6: GC-MS-based urinary metabolic profiling for confirmatory diagnosis of the screening positive patients with IEMs. *(Supplementary Materials)*

References

[1] C. M. Mak, H.-C. H. Lee, A. Y.-W. Chan, and C.-W. Lam, "Inborn errors of metabolism and expanded newborn screening: Review and update," *Critical Reviews in Clinical Laboratory Sciences*, vol. 50, no. 6, pp. 142–162, 2013.

[2] L. Han, F. Han, J. Ye et al., "Spectrum analysis of common inherited metabolic diseases in Chinese patients screened and diagnosed by tandem mass spectrometry," *Journal of Clinical Laboratory Analysis*, vol. 29, no. 2, pp. 162–168, 2015.

[3] J. Golbahar, E. A. Al-Jishi, D. D. Altayab, E. Carreon, M. Bakhiet, and H. Alkhayyat, "Selective newborn screening of inborn errors of amino acids, organic acids and fatty acids metabolism in the Kingdom of Bahrain," *Molecular Genetics and Metabolism*, vol. 110, no. 1-2, pp. 98–101, 2013.

[4] D. A. Applegarth, J. R. Toone, and R. B. Lowry, "Incidence of inborn errors of metabolism in British Columbia, 1969-1996.," *Pediatrics*, vol. 105, no. 1, p. e10, 2000.

[5] S. Sanderson, A. Green, M. A. Preece, and H. Burton, "The incidence of inherited metabolic disorders in the West Midlands, UK," *Archives of Disease in Childhood*, vol. 91, no. 11, pp. 896–899, 2006.

[6] Z. M. Yunus, S. A. Rahman, Y. S. Choy, W. T. Keng, and L. H. Ngu, "Pilot study of newborn screening of inborn error of metabolism using tandem mass spectrometry in Malaysia: Outcome and challenges," *Journal of Pediatric Endocrinology and Metabolism*, vol. 29, no. 9, pp. 1031–1039, 2016.

[7] N. Céspedes, A. Valencia, C. A. Echeverry et al., "Reference values of amino acids, acylcarnitines and succinylacetone by tandem mass spectrometry for use in newborn screening in southwest Colombia," *Colombia Médica*, vol. 48, no. 3, pp. 112–118, 2017.

[8] R. M. Shawky, H. S. Abd-Elkhalek, and S. E. Elakhdar, "Selective screening in neonates suspected to have inborn errors of metabolism," *Egyptian Journal of Medical Human Genetics*, vol. 16, no. 2, pp. 165–171, 2015.

[9] S. Sharma, P. Kumar, R. Agarwal, M. Kabra, A. K. Deorari, and V. K. Paul, "Approach to inborn errors of metabolism presenting in the neonate," *The Indian Journal of Pediatrics*, vol. 75, no. 3, pp. 271–276, 2008.

[10] D. Nagaraja, S. N. Mamatha, T. De, and R. Christopher, "Screening for inborn errors of metabolism using automated electrospray tandem mass spectrometry: Study in high-risk Indian population," *Clinical Biochemistry*, vol. 43, no. 6, pp. 581–588, 2010.

[11] N. Blau, J. T. Clarke, G. F. Hoffmann, and J. Leonard, *Physician's Guide to the Treatment and Follow-Up of Metabolic Diseases*, Springer, 2006.

[12] J. V. Leonard, "Komrower lecture: Treatment of inborn errors of metabolism: A review," *Journal of Inherited Metabolic Disease*, vol. 29, no. 2-3, pp. 275–278, 2006.

[13] E. Dogan, S. Uysal, Y. Ozturk, N. Arslan, and C. Coker, "Selective screening for inborn errors of metabolism: A report of six years experience," *Iranian Journal of Pediatrics*, vol. 27, no. 5, 2017.

[14] C. Yang, N. Wei, M. Li et al., "Diagnosis and therapeutic monitoring of inborn errors of metabolism in 100,077 newborns from Jining city in China," *BMC Pediatrics*, vol. 18, no. 1, Article ID 110, 2018.

[15] S. R. Rose, R. S. Brown, A. A. o. Pediatrics, and A. T. Association, "Update of newborn screening and therapy for congenital hypothyroidism," *Pediatrics*, vol. 117, no. 6, pp. 2290–2303, 2016.

[16] CLSI, *Newborn Screening by Tandem Mass Spectrometry*, CLSI, Wayne, Pa, USA, 2nd edition, 2017.

[17] N. Lepage, N. Mcdonald, L. Dallaire, and M. Lambert, "Age-specific distribution of plasma amino acid concentrations in a healthy pediatric population," *Clinical Chemistry*, vol. 43, no. 12, pp. 2397–2402, 1997.

[18] C. T. Cavedon, P. Bourdoux, K. Mertens et al., "Age-related variations in acylcarnitine and free carnitine concentrations measured by tandem mass spectrometry," *Clinical Chemistry*, vol. 51, no. 4, pp. 745–752, 2005.

[19] R. Ziadeh, E. P. Hoffman, D. N. Finegold et al., "Medium chain Acyl-CoA dehydrogenase deficiency in pennsylvania: neonatal screening shows highincidence and unexpected mutation frequencies," *Pediatric Research*, vol. 37, no. 5, pp. 675–678, 1995.

[20] Y. Shigematsu, S. Hirano, I. Hata et al., "Newborn mass screening and selective screening using electrospray tandem mass spectrometry in Japan," *Journal of Chromatography B*, vol. 776, no. 1, pp. 39–48, 2002.

[21] A. Schulze, M. Lindner, D. Kohlmüller, K. Olgemöller, E. Mayatepek, and G. F. Hoffmann, "Expanded newborn screening for inborn errors of metabolism by electrospray ionization-tandem mass spectrometry: Results, outcome, and implications," *Pediatrics*, vol. 111, no. 6 I, pp. 1399–1406, 2003.

[22] G. J. C. Borrajo, "Newborn screening in Latin America at the beginning of the 21st century," *Journal of Inherited Metabolic Disease*, vol. 30, no. 4, pp. 466–481, 2007.

[23] X. Huang, L. Yang, F. Tong, R. Yang, and Z. Zhao, "Screening for inborn errors of metabolism in high-risk children: A 3-year pilot study in Zhejiang Province, China," *BMC Pediatrics*, vol. 12, no. 1, Article ID 18, 2012.

[24] D. W. Tholen, A. Kallner, J. W. Kennedy, J. S. Krouwer, and K. Meier, "Evaluation of precision performance of quantitative measurement methods; approved guideline," in *Evaluation*, vol. 24, 2nd edition, 2004.

[25] J. S. Lim, E. S. Tan, C. M. John et al., "Inborn error of metabolism (IEM) screening in Singapore by electrospray ionization-tandem mass spectrometry (ESI/MS/MS): An 8year journey from pilot to current program," *Molecular Genetics and Metabolism*, vol. 113, no. 1, pp. 53–61, 2014.

[26] Health UDo, "Services H. bioanalytical method validation, guidance for industry," http://www.fda/gov/cder/guidance/4252fnl/htm.

[27] D. W. Tholen, M. Kroll, J. R. Astles, A. L. Caffo, T. Happe, J. Krouwer et al., *Evaluation of the liNearity of Quantitative Measurement Procedures: A Statistical Approach; Approved Guideline*, CLSI, 2003.

[28] J. F. Pierson-Perry, J. E. Vaks, and A. P. Durham, *Evaluation of Detection Capability for Clinical Laboratory Measurement Procedures; Approved Guideline*, CLSI, 2012.

[29] E. A. Sasse, "How to define and determine reference intervals in the clinical laboratory," *Approved Guidelines*, 2000.

[30] A. E. Garrod and H. Harris, *Inborn Errors of Metabolism*, 1909.

[31] M. Welsh, B. Ramsey, F. Accurso et al., "The metabolic and molecular basis of inherited disease," in *Scriver*, pp. 5121–5189, 2001.

[32] D. S. Millington, N. Kodo, D. L. Norwood, and C. R. Roe, "Tandem mass spectrometry: A new method for acylcarnitine profiling with potential for neonatal screening for inborn errors of metabolism," *Journal of Inherited Metabolic Disease*, vol. 13, no. 3, pp. 321–324, 1990.

[33] B. Wilcken, V. Wiley, J. Hammond, and K. Carpenter, "Screening newborns for inborn errors of metabolism by tandem mass spectrometry," *The New England Journal of Medicine*, vol. 348, no. 23, pp. 2304–2312, 2003.

[34] H.-R. Yoon, "Screening newborns for metabolic disorders based on targeted metabolomics using tandem mass spectrometry," *Annals of Pediatric Endocrinology & Metabolism*, vol. 20, no. 3, pp. 119–124, 2015.

[35] R. J. Pollitt, A. Green, C. J. McCabe et al., "Neonatal screening for inborn errors of metabolism: cost, yield and outcome," *Health Technology Assessment*, vol. 1, no. 7, pp. 1–202, 1997.

[36] M. S. Rashed, Z. Rahbeeni, and P. T. Ozand, "Application of electrospray tandem mass spectrometry to neonatal screening," *Seminars in Perinatology*, vol. 23, no. 2, pp. 183–193, 1999.

[37] C. Stockdale, *Inborn Errors of Metabolism: From Neonatal Screening to Metabolic Pathways*, SAGE Publications Sage, London, UK, 2015.

[38] D. M. McHugh, C. A. Cameron, J. E. Abdenur, M. Abdulrahman, O. Adair, S. A. Al Nuaimi et al., "Clinical validation of cutoff target ranges in newborn screening of metabolic disorders by tandem mass spectrometry: a worldwide collaborative project," *Genetics in Medicine*, vol. 13, no. 11, p. 230, 2011.

[39] G. L. Hoffman, *Newborn Screening by Tandem Mass Spectrometry: Approved Guideline*, Clinical and Laboratory Standards Institute, 2010.

[40] A. F. Cruz, T. M. Barbosa, T. É. Adelino, W. P. Lima, M. O. Mendes, and E. R. Valadares, "Amino acid reference intervals by high performance liquid chromatography in plasma sample of Brazilian children," *Jornal Brasileiro de Patologia e Medicina Laboratorial*, vol. 52, no. 2, pp. 70–77, 2016.

[41] S. Al Riyami, M. Al Maney, S. N. Joshi, and R. Bayoumi, "Detection of inborn errors of metabolism using tandem mass spectrometry among high-risk Omani patients," *Oman Medical Journal*, vol. 27, no. 6, pp. 482–485, 2012.

[42] I. Khneisser, S. Adib, S. Assaad, A. Megarbane, and P. E. Karam, "Cost-benefit analysis: Newborn screening for inborn errors of metabolism in Lebanon," *Journal of Medical Screening*, vol. 22, no. 4, pp. 182–186, 2015.

[43] G. O. Tadmouri, P. Nair, T. Obeid, M. T. Al Ali, N. Al Khaja, and H. A. Hamamy, "Consanguinity and reproductive health among Arabs," *Reproductive Health*, vol. 6, no. 1, article no. 17, 2009.

[44] L. S. Han, J. Ye, W. J. Qiu, X. L. Gao, Y. Wang, and X. F. Gu, "Selective screening for inborn errors of metabolism on clinical patients using tandem mass spectrometry in China: A four-year report," *Journal of Inherited Metabolic Disease*, vol. 30, no. 4, pp. 507–514, 2007.

[45] R. Norman, M. Haas, M. Chaplin, P. Joy, and B. Wilcken, "Economic evaluation of tandem mass spectrometry newborn screening in Australiaz," *Pediatrics*, vol. 123, no. 2, pp. 451–457, 2009.

[46] L. Feuchtbaum and G. Cunningham, "Economic evaluation of tandem mass spectrometry screening in California," *Pediatrics*, vol. 117, no. 5, pp. S280–S286, 2006.

[47] L. E. Cipriano, C. A. Rupar, and G. S. Zaric, "The cost-effectiveness of expanding newborn screening for up to 21 inherited metabolic disorders using tandem mass spectrometry: Results from a decision-analytic model," *Value in Health*, vol. 10, no. 2, pp. 83–97, 2007.

Hindawi
BioMed Research International
Volume 2018, Article ID 6359174, 7 pages
https://doi.org/10.1155/2018/6359174

Review Article

RNF213 Variant Diversity Predisposes Distinct Populations to Dissimilar Cerebrovascular Diseases

Jing Lin and Wenli Sheng

Department of Neurology, First Affiliated Hospital, Sun Yat-sen University, Guanghzou, China

Correspondence should be addressed to Wenli Sheng; shengwl@mail.sysu.edu.cn

Received 30 October 2018; Accepted 2 December 2018; Published 20 December 2018

Guest Editor: Sajib Chakraborty

In recent years, the ring finger protein 213 gene (RNF213) has gradually attracted attention, mainly because it has been found that RNF213 c.14429 G>A is associated with moyamoya disease (MMD) in East Asian populations. Recent studies have revealed that RFN213 is not only associated with MMD but is also connected with intracranial major artery stenosis/occlusion (ICASO) and intracranial aneurysm (IA). However, only the relationship between RNF213 c.14429 G>A and ICASO has been confirmed, and whether RNF213 has other mutations related to ICASO remains unclear. RNF213 and IA are currently only confirmed to be correlated in French-Canadian Population and no correlation has been found in the Japanese population. This review summarizes the advances in the associations between RNF213 and different cerebrovascular diseases and highlights that variant diversity of RNF213 may predispose distinct populations to dissimilar cerebrovascular diseases.

1. Introduction

The *RNF213* gene is located on chromosome 17 and encodes a ring finger protein of 5207 amino acids. This gene has two important functional domains: a RING finger domain and an AAA+ATPase domain [1]. In recent years, RNF213 has attracted attention mainly because studies have found that RNF213 is a susceptibility gene for moyamoya disease (MMD) in East Asian populations, especially in Japanese populations [2]. Further studies have revealed that RNF213 is also connected with intracranial major artery stenosis/occlusion (ICASO) in Asian populations [3]. Zhou et al. found that different mutations of RNF213 are correlated with intracranial aneurysm (IA) in French-Canadian Population [4]. In translational medicine, partial angiogenesis was observed after knocking down *rnf213* gene in zebrafish, similar to angiogenesis in MMD [5]. However, mice with *Rnf213* gene knockout and mice with mutations corresponding to the human *RNF213* c.14429 G>A point mutation do not present phenotypes mimicking those of MMD [6, 7]. More interestingly, the overexpression of p.R4810K in human umbilical vein endothelial cells (HUVECs) inhibits angiogenesis [8], which contradicts the phenotype of moyamoya vessels partly due to angiogenesis. This review elaborates on the advances of the associations between RNF213 and different cerebrovascular diseases. RNF213 p.R4859K and RNF213 p.R4810K are amino acid variants of the same locus (rs112735431), with p.R4859K based on an in silico predicted open reading frame and p.R4810K based on the open reading frame verified by cDNA cloning. Similarly, RNF213 c.14429 G>A and RNF213 c.14576 G>A correspond to the same single nucleotide variation. RNF213 p.R4810K and RNF213 c.14429 G>A are used consistently in this review.

2. RNF213 and MMD

2.1. Genetic Factors Involved in MMD, Especially RNF213. MMD is a rare cerebrovascular disease and is one of the main causes of stroke in children. It is primarily characterized by the progressive stenosis of the internal carotid artery and an abnormal vascular network at the base of the brain [9]. Thickening of the tunica intima and thinning of the media is the main pathological feature of MMD [10], but the pathogenesis of MMD remains unclear. Some MMD patients present autosomal dominant inheritance, and MMD is more common in Asians than in Europeans, suggesting that genetic

factors may be involved in the pathogenesis of MMD. It has been found that multiple loci are associated with MMD: 3p24-p26, 6q25, 8q23, and 17q25 [11–14]. Kamada et al. found that *RNF213* at 17q25 is a new susceptibility gene in East Asian MMD patients. The polymorphism c.14429 G>A of this gene is present in 95% of familial MMD and in 79% of sporadic MMD patients [2]. This suggests that genetic factors are involved in the pathogenesis of MMD, especially RNF213.

2.2. Clinical Studies

2.2.1. RNF213 p.R4810K and Distinct Populations. There is a significant racial difference in the correlation between RNF213 p.R4810K and MMD. This mutation is found in 90.1% of Japanese MMD patients, in 78.9% of Korean MMD patients, and in 23.1% of Chinese MMD patients. Normal populations also have this variation, which is found in 2.5% of Japanese, 2.7% of Korean, and 0.9% of Chinese populations [5]. Compared with Japanese and Korean patients, the rate of this mutation in Chinese Han MMD patients is lower [15]. The incidence of MMD in Europeans is about 1/10 of that found in Japanese [16], and RNF213 p.R4810K was not identified in Europeans [5], which may be one of the reasons for the low incidence of MMD in Europeans. In a study of RNF213 p.R4810K and MMD patients with different descent living in the similar environment, p.R4810K was found in 56% of Asian descent MMD patients and not found in non-Asian descent MMD patients [17]. Our previous meta-study found that p.R4810K is associated with MMD, and compared with China, the association was more prominent in Japan and Korea. Additionally, p.A4399T was not associated with Asian MMD patients, and p.A5021V was only related to Chinese Han MMD patients [18]. This suggests that RNF213 p.R4810K involved in the pathogenesis of MMD is ethnically diverse.

2.2.2. RNF213 R4810K Homozygote/Heterozygote and MMD. It has been found that the dose effect of RNF213 is correlated to the presence of MMD. Miyatake et al. found that the homozygous mutation of RNF213 p.R4810K was only present in patients with MMD and was not found in normal populations, and homozygous mutants showed earlier disease onset and more severe conditions than did heterozygous mutants [19]. However, later studies have confirmed that RNF213 p.R4810K homozygous mutations also exist in normal people [20], and twins with the same genetic background can present different phenotypes [5]. This suggests that the MMD phenotype cannot be explained solely by gene dose effects.

2.3. Basic Research

2.3.1. HUVECs E2488Q Mutants Corresponding to p.R4810K Inhibit Angiogenesis. RNF213 has two important functional domains: the RING finger domain and the AAA+ATPase domain. The AAA+ATPase domain has two AAA+ modules. The first module is essential for assembling RNF213 oligomers, whereas the second module contributes to disassemble RNF213 oligomers. The oligomeric state is initiated by ATP binding to the Walker A motif in the first AAA+ module and the Walker B motif in the second AAA+ module can hydrolyze ATP to disassemble oligomers [1]. Kobayashi et al. found that the point mutation in the Walker B motif of the first AAA+ module of RNF213 (E2488Q) similar to the RNF213 p.R4810K mutation decreases ATPase activity and stabilizes oligomers, thereby inhibiting angiogenesis. However, the deletion mutation of the first AAA+ module of RNF213 (RNF213 delAAA) does not inhibit angiogenesis, similar to the wild type. The Walker B motif point mutation (E2488Q) of the AAA+ module can maintain oligomers, and the AAA+ module deletion mutation (RNF213 delAAA) cannot maintain the oligomeric state [8]. This suggests that the RNF213 p.R4810K mutant inhibits ATP hydrolysis to maintain the oligomeric state, thereby inhibiting angiogenesis.

2.3.2. Mouse Rnf213 Knockout or p.R4828K Mutant Does Not Completely Mimic the Phenotype of MMD. Clinical studies suggest that RNF213 is associated with MMD. Since there is no suitable animal model for MMD, many studies have attempted to establish MMD models based on *RNF213* gene knockout or point mutations. Sonobe et al. used the cre-lox system to knockout exon 32 of mouse *Rnf213*, but the resulting mice did not show intracranial artery stenosis and smog-like vascular phenotypes. They also did not show phenotypes mimicking those related to MMD even when superimposed with hypoxic environmental factors (by occluding the carotid artery); however, the common carotid artery showed transient intimal and medial thinning [6]. Kanoke et al. used the cre-lox system to generate the mouse Rnf213 p.R4828K point mutation (corresponding to the human p.R4810K point mutation), which does not show phenotypes mimicking those related to MMD even when superimposed with hypoxia [7]. In addition, Kanoke et al. gave *Rnf213* exon 32 knockout mice a strong dose of immunoadjuvant, which did not mimic the phenotype of MMD [21]. Ito et al. found that the *Rnf213* exon 32 knockout mice showed significantly enhanced angiogenesis after long-term ischemia [22]. Studies on a variety of mice specifically overexpressing RNF213 p.R4757K (corresponding to the human p.R4810K locus) revealed that a hypoxic environment promoted angiogenesis, but angiogenesis in mice in which endothelial cells overexpressed RNF213 p.R4757K was significantly inhibited [8]. This suggests that *Rnf213* gene knockout promotes angiogenesis, but p.R4810K point mutation inhibits angiogenesis. After transient occlusion of the middle cerebral artery in rats, Sato-Maeda et al. found a significant increase in RNF213 expression in the ischemic penumbra, which showed association with apoptotic neurons [23]. This group later briefly clamped the rat common carotid artery to cause general cerebral ischemia and found that neuronal apoptosis in hippocampal CA1 region was associated with elevated *Rnf213* mRNA [24], suggesting that RNF213 mediates apoptosis of hypoxic-ischemic neurons.

2.3.3. Zebrafish rnf213 Knockdown or Knockout Partly Mimics the Phenotype of MMD. The entire cerebral blood vessels of

zebrafish can be clearly observed after inhibiting the formation of melanin. Therefore, Liu et al. used zebrafish as an animal model and found that knockdown of *rnf213* expression by morpholino could promote angiogenesis and partially mimic smog-like blood vessels [5]. However, the phenotypes produced through morpholino-mediated knockdown of *rnf213* expression in zebrafish may have been affected by off-target effects, and recent studies have found that morpholinos have a high probability of off-target effects [25, 26]. Therefore, we knocked out zebrafish *rnf213* via a transcription activator-like effector nuclease and found significant angiogenesis of the intersegmental blood vessels and cerebral blood vessels and small blood vessel stenosis in the F0 generation [27]. By similarly knocking out RNF213, the zebrafish model can partially mimic the MMD phenotype, but mouse models failed to mimic the MMD phenotype, even if the mice were superimposed with hypoxia or immunoadjuvant, suggesting that RNF213 may play different roles in MMD in different species.

3. RNF213 and ICASO

Recent studies found that RNF213 p.R4810K is not only related to MMD but is also related to non-MMD ICASO. Miyawaki et al. found that the RNF213 p.R4810K point mutation was present in 9 of 41 ICASO patients [3]. To confirm this finding, Miyawaki et al. conducted an expanded sample size study and found the RNF213 p.R4810K point mutation in 20/84 ICASO patients [28]. Bang et al. found that 176/352 ICASO patients had RNF213 p.R4810K point mutations [29]. Shinya et al. found that RNF213 p.R4810K is associated with anterior circulation ICASO and is not associated with posterior circulation ICASO or extracranial carotid atherosclerosis [30]. Yeung et al. found a significant association between RNF213 p.R4810K and the ICASO phenotype in CADASIL (cerebral autosomal dominant arteriopathy with subcortical infarcts and leukoencephalopathy) patients [31]. Liao et al. conducted a meta-analysis, summarizing 11 studies of p.R4810K and ICASO (including 1778 ICASO patients and 3140 normal controls) and found that p.R4810K was significantly associated with ICASO (OR 13.89, 95% CI 8.01–24.09, and $p < 0.0001$) [32]. The above studies suggest that RNF213 p.R4810K is correlated with ICASO. However, studies on the correlation between RNF213 and ICASO have only reported one locus of p.R4810K, and correlations between RNF213 other variant and ICASO have not been found up to now.

4. RNF213 and IA

It has been found that French-Canadian population has a higher incidence of IA, and IA patients are often found in families, especially large families. Zhou et al. found that two RNF213 point mutations (p.R2438C and p.A2826T) were associated with intracranial aneurysms in French-Canadian Population, both of which are located in the AAA+ATPase domain, and ATPase activity was increased in IA patients. It is thus speculated that RNF213 p.R2438C and RNF213 p.A2826T cause an increase in ATPase activity to promote angiogenesis and participate in the formation of IA [4]. However, Miyawaki et al. found that RNF213 p.R4810K was not significantly associated with IA patients of Japanese descent, but no other site mutations were examined [3, 28]. This suggests that different mutation sites may be involved in the pathogenesis of IA.

5. RNF213 Variant Diversity Is Associated with Different Phenotypes

Various *RNF213* genetic mutations related to cerebrovascular disease have been reported (Table 1). These mutations are predominantly missense mutations, and most of the point mutation sites are located at the C-terminus (Figure 1). Mutations in different sites of RNF213 may have different effects on blood vessels. The RNF213 p.R4810K mutation may be the main cause of MMD intracranial artery stenosis [3, 33]. It has been found that the RNF213 p.A4399T mutation is more related to the MMD bleeding phenotype, while RNF213 p.R4810K is more related to the MMD ischemic phenotype [15]. Two reported mutation sites in the AAA+ATPase domain (c.7312 C>T and c.8476 G>A) are related to IA [4], and four reported mutation sites in the RING finger domain (c. 11990 G>A, c.12020 C>G, c.12037 G>A, and c.12055 C>T) are all related to MMD [15, 17, 34]. This suggests that the AAA+ATPase domain may be more related to IA, and the RING finger domain may be more relevant to MMD. In addition to point mutations, it has been found that four frameshift mutations in *RNF213* are also associated with cerebrovascular disease, with c.1214_1216delGAG and c.11415delC associated with aneurysms [4] and c.1587_1589delCGC and c.12343_12345delAAA associated with MMD [17]. Frameshift mutations often cause loss function of the entire protein, but the three reported frameshift mutations of *RNF213* (c.1214_1216delGAG, c.1587_1589delCGC, c.12343_12345delAAA) all cause the missing of 3bp, which may have little effect on the whole protein function. The c.11415delC frameshift mutation only deletes 1bp and is located in front of the RING finger domain, which may result in loss of the RING finger domain function.

6. Conclusion

There are significant racial differences in the correlations of *RNF213* with MMD and IA. The correlation between RNF213 p.R4810K and MMD is reported in Asian populations but not identified in Europeans and non-Asian descent Americans. Similarly, the correlation between RNF213 and IA was confirmed only in French-Canadian Population, and no correlation was found in the Japanese population. Different site mutations in RNF213 may be involved in different cerebrovascular diseases. Current ICASO studies report that only RNF213 p.R4810K is associated with ICASO, and other mutation sites have not been reported. In addition to RNF213 p.R4810K, many RNF213 sites have been reported to be associated with MMD, and RNF213 p.R4810K is more related to MMD patients in East Asia. In terms of RNF213 sites associated with IA, only two mutations (p.R2438C and

Table 1: RNF213 variants diversity in cerebrovascular diseases (Italic represents variant associated with hemorrhagic type MMD; bold represents variant related to ischemic type MMD).

Diseases	Nucleotide	Amino acid	Reference
MMD	c.1407G>T	p.Q469H	Schilter (2017) Am J Med Genet A 173, 2557
	c.1549G>A	p.G517R	Shoemaker (2015) G3 (Bethesda) 6, 41
	c.1587_1589delCGC		Cecchi (2014) Stroke 45, 3200
	c.2986G>A	p.E996K	Akagawa (2018) Hum Genome Var 5, 17060
	c.4421C>T	p.S1474F	Shoemaker (2015) G3 (Bethesda) 6, 41
	c.4865C>T	p.A1622V	Lee (2015) J Neurol Sci 353, 161
	c.5180C>T	p.T1727M	Zhang (2017) J Neurosurg 126, 1106
	c.10997T>C	p.M3666T	Shoemaker (2015) G3 (Bethesda) 6, 41
	c.11671A>G	p.M3891V	Kamada (2011) J Hum Genet 56, 34
	c.11797G>A	p.V3933M	Lee (2015) J Neurol Sci 353, 161
	c.11884A>G	p.N3962D	Liu (2011) PLoS One 6, e22542
	c.11945A>G	p.K3982R	Shoemaker (2015) G3 (Bethesda) 6, 41
	c.11990G>A	p.C3997Y	Cecchi (2014) Stroke 45, 3200
	c.12020C>G	p.P4007R	Wu (2012) PLoS One 7, e48179
	c.12037G>A	p.D4013N	Cecchi (2014) Stroke 45: 3200
	c.12055C>T	p.R4019C	Kobayashi (2016) PLoS One 11: e0164759
	c.12124G>A	p.E4042K	Kobayashi (2016) PLoS One 11, e0164759
	c.12173A>C	p.H4058P	Akagawa (2018) Hum Genome Var 5, 17060
	c.12185G>A	p.R4062Q	Moteki (2015) J Am Heart Assoc 4: e001862
	c.12226A>G	p.I4076V	Cecchi (2014) Stroke 45, 3200
	c.12343_12345delAAA		Cecchi (2014) Stroke 45, 3200
	c.12353C>T	p.S4118F	Harel (2015) Am J Med Genet A 167, 2742
	c.12391C>T	p.R4131C	Lee (2015) J Neurol Sci 353, 161
	c.12437T>C	p.V4146A	Kobayashi (2016) PLoS One 11, e0164759
	c.12478A>C	p.K4160Q	Zhang (2017) J Neurosurg 126, 1106
	c.12554A>C	p.K4185T	Smith (2014) Int J Stroke 9, E26
	c.12711C>G	p.D4237E	Cecchi (2014) Stroke 45, 3200
	c.13100A>T	p.Q4367L	Wu (2012) PLoS One 7, e48179
	c.13195G>A	*p.A4399T*	*Wu (2012) PLoS One 7, e48179*
	c.13699G>A	p.V4567M	Kamada (2011) J Hum Genet 56, 34
	c.13756A>C	p.T4586P	Wu (2012) PLoS One 7, e48179
	c.13822C>T	p.P4608S	Liu (2011) PLoS One 6, e22542
	c.13891C>G	p.L4631V	Wu (2012) PLoS One 7, e48179
	c.14030G>T	p.W4677L	Schilter (2017) Am J Med Genet A 173, 2557
	c.14195A>C	p.K4732T	Cecchi (2014) Stroke 45, 3200
	c.14248G>A	p.E4750K	Moteki (2015) J Am Heart Assoc 4, e001862
	c.14293G>A	p.V4765M	Kamada (2011) J Hum Genet 56, 34
	c.14428A>G	p.R4810G	Shoemaker (2015) G3 (Bethesda) 6, 41
	c.14429G>A	**p.R4810K**	**Kamada (2011) J Hum Genet 56, 34**
	c.14587G>A	p.D4863N	Liu (2011) PLoS One 6, e22542
	c.14780G>A	p.R4927Q	Moteki (2015) J Am Heart Assoc 4, e001862
	c.14850G>C	p.E4950D	Liao (2017) Environ Health Prev Med 22: 75
	c.15062C>T	p.A5021V	Liu (2011) PLoS One 6, e22542
	c.15408G>A	p.M5136I	Wu (2012) PLoS One 7, e48179
	c.15480C>G	p.D5160E	Liu (2011) PLoS One 6, e22542
	c.15487G>A	p.V5163I	Cecchi (2014) Stroke 45, 3200
	c.15527A>G	p.E5176G	Liu (2011) PLoS One 6, e22542
IA	c.1214_1216delGAG		Zhou (2016) Am J Hum Genet 99, 1072
	c.1699A>G	p.M567V	Zhou (2016) Am J Hum Genet 99, 1072
	c.2017C>T	p.R673W	Zhou (2016) Am J Hum Genet 99, 1072
	c.3674A>G	p.D1225G	Zhou (2016) Am J Hum Genet 99, 1072

Table 1: Continued.

Diseases	Nucleotide	Amino acid	Reference
	c.7312C>T	p.R2438C	Zhou (2016) Am J Hum Genet 99, 1072
	c.8476G>A	p.A2826T	Zhou (2016) Am J Hum Genet 99, 1072
	c.9562G>A	p.V3188M	Zhou (2016) Am J Hum Genet 99, 1072
	c.9709C>A	p.Q3237K	Zhou (2016) Am J Hum Genet 99, 1072
	c.11415delC		Zhou (2016) Am J Hum Genet 99, 1072
	c.12496G>A	p.D4166N	Zhou (2016) Am J Hum Genet 99, 1072
	c.12854G>A	p.S4285N	Zhou (2016) Am J Hum Genet 99, 1072
	c.13074G>A	p.K4358=	Zhou (2016) Am J Hum Genet 99, 1072
	c.13577T>C	p.I4526T	Zhou (2016) Am J Hum Genet 99, 1072
	c.15275G>A	p.R5092Q	Zhou (2016) Am J Hum Genet 99, 1072
ICASO	c.14429G>A	p.R4810K	Miyawaki (2012) Stroke 43, 3371 Miyawaki (2013) Stroke 44, 2894

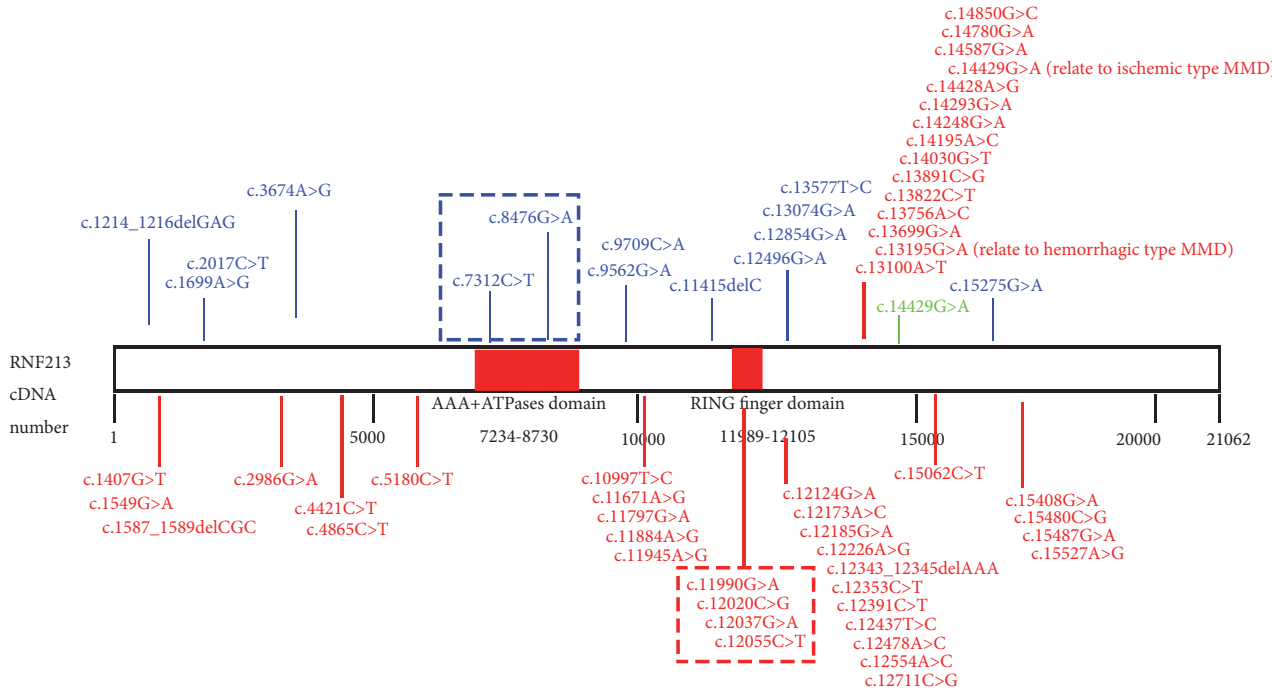

Figure 1: **RNF213 Nucleotide Variants Found In MMD, IA, and ICASO.** Variants associated with MMD are marked in red; variants associated with IA are marked in blue; variants associated with ICASO are marked in green; red box represent variants in RING finger domain related to MMD; blue box represent variants in AAA+ATPases domain related to IA. Two special variants (c.13195G>A and c.14429G>A) are associated with different type MMD, respectively.

p.A2826T) have been reported. Different mutation sites of RNF213 are associated with different cerebrovascular diseases, possibly because different mutations affect different functional domains of RNF213. Therefore, RNF213 variant diversity predisposes distinct populations to dissimilar cerebrovascular diseases. Unfortunately, mice with *Rnf213* knockout or point mutations similar to those of humans do not fully mimic the MMD phenotype. Environmental aspects may also be important factors in MMD pathogenesis. More studies are required to confirm the correlation of RNF213 with various cerebrovascular diseases, thus providing a new target for the prevention and treatment of cerebrovascular diseases.

Conflicts of Interest

The authors declare that there are no conflicts of interest regarding the publication of this paper.

References

[1] D. Morito, K. Nishikawa, J. Hoseki et al., "Moyamoya disease-associated protein mysterin/RNF213 is a novel AAA+ ATPase, which dynamically changes its oligomeric state," *Scientific Reports*, vol. 4, p. 4442, 2014.

[2] F. Kamada, Y. Aoki, A. Narisawa et al., "A genome-wide association study identifies RNF213 as the first Moyamoya

disease gene," *Journal of Human Genetics*, vol. 56, no. 1, pp. 34–40, 2011.

[3] S. Miyawaki, H. Imai, S. Takayanagi, A. Mukasa, H. Nakatomi, and N. Saito, "Identification of a genetic variant common to moyamoya disease and intracranial major artery stenosis/occlusion," *Stroke*, vol. 43, no. 12, pp. 3371–3374, 2012.

[4] S. Zhou, A. Ambalavanan, D. Rochefort et al., "RNF213 Is Associated with Intracranial Aneurysms in the French-Canadian Population," *American Journal of Human Genetics*, vol. 99, no. 5, pp. 1072–1085, 2016.

[5] W. Liu, D. Morito, S. Takashima et al., "Identification of RNF213 as a Susceptibility Gene for Moyamoya Disease and Its Possible Role in Vascular Development," *PLoS ONE*, vol. 6, no. 7, p. e22542, 2011.

[6] S. Sonobe, M. Fujimura, K. Niizuma et al., "Temporal profile of the vascular anatomy evaluated by 9.4-T magnetic resonance angiography and histopathological analysis in mice lacking RNF213: A susceptibility gene for moyamoya disease," *Brain Research*, vol. 1552, pp. 64–71, 2014.

[7] A. Kanoke, M. Fujimura, K. Niizuma et al., "Temporal profile of the vascular anatomy evaluated by 9.4-tesla magnetic resonance angiography and histological analysis in mice with the R4859K mutation of RNF213, the susceptibility gene for moyamoya disease," *Brain Research*, vol. 1624, pp. 497–505, 2015.

[8] H. Kobayashi, Y. Matsuda, T. Hitomi et al., "Biochemical and Functional Characterization of RNF213 (Mysterin) R4810K, a Susceptibility Mutation of Moyamoya Disease, in Angiogenesis In Vitro and In Vivo," *Journal of the American Heart Association*, vol. 4, no. 7, 2015.

[9] J. Suzuki and A. Takaku, "Cerebrovascular "Moyamoya" Disease. Disease Showing Abnormal Net-Like Vessels in Base of Brain," *JAMA Neurology*, vol. 20, no. 3, pp. 288–299, 1969.

[10] K. Oka, M. Yamashita, S. Sadoshima, and K. Tanaka, "Cerebral haemorrhage in Moyamoya disease at autopsy," *Virchows Archiv A: Pathological Anatomy and Histology*, vol. 392, no. 3, pp. 247–261, 1981.

[11] H. Ikeda, T. Sasaki, T. Yoshimoto, M. Fukui, and T. Arinami, "Mapping of a familial moyamoya disease gene to chromosome 3p24.2-p26," *American Journal of Human Genetics*, vol. 64, no. 2, pp. 533–537, 1999.

[12] T. K. Inoue, K. Ikezaki, T. Sasazuki, T. Matsushima, and M. Fukui, "Linkage analysis of moyamoya disease on chromosome 6," *Journal of Child Neurology*, vol. 15, no. 3, pp. 179–182, 2000.

[13] K. Sakurai, Y. Horiuchi, H. Ikeda et al., "A novel susceptibility locus for moyamoya disease on chromosome 8q23," *Journal of Human Genetics*, vol. 49, no. 5, pp. 278–281, 2004.

[14] T. Yamauchi, M. Tada, K. Houkin et al., "Linkage of familial moyamoya disease (spontaneous occlusion of the circle of Willis) to chromosome 17q25," *Stroke*, vol. 31, pp. 930–935, 2000.

[15] Z. Wu, H. Jiang, L. Zhang et al., "Molecular Analysis of RNF213 Gene for Moyamoya Disease in the Chinese Han Population," *PLoS ONE*, vol. 7, no. 10, p. e48179, 2012.

[16] Y. Yonekawa, N. Ogata, Y. Kaku, E. Taub, and H.-G. Imhof, "Moyamoya disease in Europe, past and present status," *Clinical Neurology and Neurosurgery*, vol. 99, no. 2, pp. S58–S60, 1997.

[17] A. C. Cecchi, D. Guo, Z. Ren et al., "RNF213 rare variants in an ethnically diverse population with moyamoya disease," *Stroke*, vol. 45, no. 11, pp. 3200–3207, 2014.

[18] X.-S. Sun, J. Wen, J.-X. Li et al., "The association between the ring finger protein 213 (RNF213) polymorphisms and moyamoya disease susceptibility: a meta-analysis based on case–control studies," *Molecular Genetics and Genomics*, vol. 291, no. 3, pp. 1193–1203, 2016.

[19] S. Miyatake, N. Miyake, H. Touho et al., "Homozygous c.14576G>A variant of RNF213 predicts early-onset and severe form of moyamoya disease," *Neurology*, vol. 78, no. 11, pp. 803–810, 2012.

[20] A. Koizumi, H. Kobayashi, W. Liu et al., "P.R4810K, a polymorphism of RNF213, the susceptibility gene for moyamoya disease, is associated with blood pressure," *Environmental Health and Preventive Medicine*, vol. 18, no. 2, pp. 121–129, 2013.

[21] A. Kanoke, M. Fujimura, K. Niizuma et al., "Temporal profile of magnetic resonance angiography and decreased ratio of regulatory T cells after immunological adjuvant administration to mice lacking RNF213, a susceptibility gene for moyamoya disease," *Brain Research*, vol. 1642, pp. 1–9, 2016.

[22] A. Ito, M. Fujimura, K. Niizuma et al., "Enhanced post-ischemic angiogenesis in mice lacking RNF213; A susceptibility gene for moyamoya disease," *Brain Research*, vol. 1594, pp. 310–320, 2015.

[23] M. Sato-Maeda, M. Fujimura, A. Kanoke, Y. Morita-Fujimura, K. Niizuma, and T. Tominaga, "Transient middle cerebral artery occlusion in mice induces neuronal expression of RNF213, a susceptibility gene for moyamoya disease," *Brain Research*, vol. 1630, pp. 50–55, 2016.

[24] M. Sato-Maeda, M. Fujimura, S. Rashad et al., "Transient Global Cerebral Ischemia Induces RNF213, a Moyamoya Disease Susceptibility Gene, in Vulnerable Neurons of the Rat Hippocampus CA1 Subregion and Ischemic Cortex," *Journal of Stroke and Cerebrovascular Diseases*, vol. 26, no. 9, pp. 1904–1911, 2017.

[25] J. S. Eisen and J. C. Smith, "Controlling morpholino experiments: Don't stop making antisense," *Development*, vol. 135, no. 10, pp. 1735–1743, 2008.

[26] M. Blum, E. M. De Robertis, J. B. Wallingford, and C. Niehrs, "Morpholinos: Antisense and Sensibility," *Developmental Cell*, vol. 35, no. 2, pp. 145–149, 2015.

[27] J. Wen, X. Sun, H. Chen et al., "Mutation of rnf213a by TALEN causes abnormal angiogenesis and circulation defects in zebrafish," *Brain Research*, vol. 1644, pp. 70–78, 2016.

[28] S. Miyawaki, H. Imai, M. Shimizu et al., "Genetic variant RNF213 c.14576G>A in various phenotypes of intracranial major artery stenosis/occlusion," *Stroke*, vol. 44, no. 10, pp. 2894–2897, 2013.

[29] O. Y. Bang, J. Chung, J. Cha et al., "A Polymorphism in RNF213 Is a Susceptibility Gene for Intracranial Atherosclerosis," *PLoS ONE*, vol. 11, no. 6, p. e0156607, 2016.

[30] Y. Shinya, S. Miyawaki, H. Imai et al., "Genetic Analysis of Ring Finger Protein 213 (RNF213) c.14576G>A in Intracranial Atherosclerosis of the Anterior and Posterior Circulations," *Journal of Stroke and Cerebrovascular Diseases*, vol. 26, no. 11, pp. 2638–2644, 2017.

[31] W. T. E. Yeung, I. Mizuta, A. Watanabe-Hosomi et al., "RNF213-related susceptibility of Japanese CADASIL patients to intracranial arterial stenosis," *Journal of Human Genetics*, vol. 63, no. 5, pp. 687–690, 2018.

[32] X. Liao, J. Deng, W. Dai, T. Zhang, and J. Yan, "Rare variants of RNF213 and moyamoya/non-moyamoya intracranial artery stenosis/occlusion disease risk: A meta-analysis and systematic review," *Environmental Health and Preventive Medicine*, vol. 22, no. 1, 2017.

[33] O. Y. Bang, S. Ryoo, S. J. Kim et al., "Adult Moyamoya Disease: A Burden of Intracranial Stenosis in East Asians?" *PLoS ONE*, vol. 10, no. 6, p. e0130663, 2015.

[34] H. Kobayashi, M. Brozman, K. Kyselová et al., "RNF213 Rare Variants in Slovakian and Czech Moyamoya Disease Patients," *PLoS ONE*, vol. 11, no. 10, p. e0164759, 2016.

Hindawi
BioMed Research International
Volume 2018, Article ID 4678362, 9 pages
https://doi.org/10.1155/2018/4678362

Research Article

Cutaneous Malignancy due to Arsenicosis in Bangladesh: 12-Year Study in Tertiary Level Hospital

Md. Iqbal Mahmud Choudhury,[1] **Nilufar Shabnam**,[2] **Tazin Ahsan**,[3] **S. M. Abu Ahsan**,[4] **Md. Saiful Kabir**,[5] **Rashed Md. Khan**,[6] **Md. Abdal Miah**,[7] **Mohd. Kamal Uddin**,[8] **and Md. Aminur Rashid Liton**[9]

[1]*Assistant Professor, Plastic Surgery Unit, Bangabandhu Sheikh Mujib Medical University (BSMMU), Dhaka, Bangladesh*
[2]*Assistant Professor, Department of Surgery, BIRDEM Hospital and Ibrahim Medical College, Dhaka, Bangladesh*
[3]*Honorary Medical Officer, Department of Surgery, Bangabandhu Sheikh Mujib Medical University (BSMMU), Dhaka, Bangladesh*
[4]*Associate Professor and Head of the Department of Surgery, Ad-din Sakina Medical College, Jessore, Bangladesh*
[5]*Professor and Head of Department of Dermatology and Venereology, National Medical College and Hospital, Dhaka, Bangladesh*
[6]*Professor and Head of the Department of Dermatology & VD, Dhaka Medical College Hospital, Dhaka, Bangladesh*
[7]*Assistant Professor, Department of Dermatology and Venereology, Centre for Medical Education, Dhaka, Bangladesh*
[8]*Senior Consultant, Department of Dermatology, 250 bedded General Hospital, Gopalganj, Bangladesh*
[9]*Assistant Professor, Department of Dermatology and Venereology, Holy Family Red Crescent Medical College and Hospital, Dhaka, Bangladesh*

Correspondence should be addressed to Md. Iqbal Mahmud Choudhury; drimcrony@gmail.com

Received 28 October 2018; Accepted 3 December 2018; Published 16 December 2018

Guest Editor: Sajib Chakraborty

Bangladesh is grappling with the largest mass poisoning of a population in the world due to contamination of drinking water with naturally occurring inorganic arsenic. It is estimated that 75 million people of 59 (out of 64) districts are at risk of drinking contaminated water with arsenic above 50μg/L. Long term exposure to arsenic causes cancers, including skin, lung, and bladder. This is a randomized prospective study to see the prevalence of skin cancer from arsenic affected area of Bangladesh, as well as their variation by geographical area, age, gender, location on the body, and socioeconomic conditions, in outpatient department of plastic surgery unit of Bangabandhu Sheikh Mujib Medical University (BSMMU). A total of 960 patients with skin cancers comprised of 528 males and 432 females were selected for the study from January 2004 to December 2015. In this 12-year study, we found squamous cell carcinoma, basal cell carcinoma, melanoma, and Merkel cell carcinoma to be associated with the ingestion of arsenic contaminated ground water. This is a reflection of a small part of the total national scenario of devastating result of arsenic mediated cancer in terms of skin malignancy. This study will help the future researchers who are contemplating to work on arsenic induced health problem.

1. Introduction

Arsenic contamination of ground water in Bangladesh is reported to be the worst problem in the world in terms of affected population [1, 2]. Survey data from 2000 to 2010 have demonstrated that an estimated 35 to 77 million Bangladeshi people, especially in rural area, have been chronically exposed to arsenic through drinking water and daily food [3–5]. Before 1970s, people in this country used surface water for drinking and daily activities. The surface water was pathogen laden and as a result they suffered from several types of diarrheal diseases in epidemic manner. To solve this problem, since 1970s, the government and other international organizations introduced shallow tube wells. The people got the apparent benefit but the hidden problem was discovered years later. The water from shallow tube wells (depth of 10-70m) contains arsenic in toxic level, which causes a lot of hazards to the human body. But ground water from deep

tube wells (depths >150m) is safe and contains arsenic in less concentration [5, 6].

According to WHO guidelines, water containing arsenic over 10μg/L is said to be contaminated but in Bangladesh, this bench mark rises to 50μg/L [7–12]. Natural Drinking Water Quality Survey report used an estimated population of 164 million to estimate that 22 million and 5.6 million people are drinking water with arsenic concentrations >50μg/L and >200μg/L, respectively [13]. This can lead to massive chronic poisoning—called **arsenicosis**—causing neoplastic and nonneoplastic health problems in local population. This can occur at genetic and epigenetic level [14]. The arsenic biotransformation process which involves methylation changes is thought to play a key role for malignant transformation. Arsenic can damage DNA through oxidative stress by generation of toxic species such as reactive oxygen species (ROS) [10, 15–17]. According to the United States Environmental Protection Agency, the risk of developing skin cancer in association with daily consumption of around 1.0 liters of arsenic contaminated water at 50μg/L concentration has been estimated to be 1 in 1000 to 2 in 1000[18]. Basal cell carcinoma (BCC) and squamous cell carcinoma (SCC) are the most common nonmelanotic cutaneous malignancy in patients with long term exposure to arsenic. Merkel's Cell Carcinoma (MCC), which is uncommon, and melanoma have been documented at low frequency [19–22].

In 1983, Krishna Chandra Shah identified arsenic induced skin lesions in India and by 1987, he detected several arsenic induced skin lesions in patients who came from neighboring Bangladesh. In 1993, the Public Health Engineering Department of Bangladesh officially declared the confirmation of arsenic contamination in Nawabganj district [23–25]. In 1998, British Geological Survey (BGS) collected water samples from 41 arsenic affected districts [26] and 35% of water sample were found to have arsenic contamination above 50μg/L. The recent statistic on arsenic contamination indicates that 59 out of 64 districts of Bangladesh have been affected [27]. Approximately 85% area of Bangladesh has arsenic contaminated ground water and around 75 million people are at risk of arsenic ingestion from the tube-wells water [1]. Apart from the national survey there have been a number of thana and village surveys in many districts. The districts where most upazillas and villages have a large number of contaminated wells (up to 100%) are termed as **worst affected** districts. Those districts are Chandpur (90%), Munshiganj (83%), Gopalganj (79%), Brahmanbaria (70%), Jhenaidah (69%), Madaripur (69%), Noakhali (69%), Satkhira (67%), Comilla (65%), Shariatpur (65%), Lakshmipur (64%), Pabna (62%), Meherpur (60%), Bagerhat (60%), and Natore (58%). The **least affected** districts are the ones where none of the samples exceed the Bangladesh limit. They are Thakurgaon, Panchagarh, Nilphamari, Lalmonirhat, Patuakhali, Barguna, Barisal, Chuadanga, Jessore, Feni, Khulna, Magura, Narail, Rajbari, and Pirojpur [28]. In about half of the measurements, the arsenic concentration in tube-well water was about 50μg/L [29, 30], which reached above 150-300μg/L in some districts or parts of some districts along the border of West Bengal, India [21, 31].

The occurrence of arsenic diseases depends on the ingestion of arsenic compounds and their excretion from the body. It has been reported that 40% to 60% arsenic can be retained by the human body [32, 33]. The daily consumption of arsenic contaminated water is very high in Bangladesh, especially in villages. The villagers are more involved in manual labour and for the hard-work they consume more water (more than 5 liters per day), especially in the summer [1]. They retain arsenic not only by drinking water but by all of their food chains and cooked food which is contaminated by arsenic. We have almost no data to state exactly when the problem with arsenic poisoning started in Bangladesh, but it may be assumed that the consumption of arsenic contaminated water since 1970 is the beginning of the problem.

2. Materials and Methods

We performed a prospective study. Study period was from January 2004 to December 2015. The cases were selected random-wise from outpatient department (plastic surgery) of Bangabandhu Sheikh Mujib Medical University (BSMMU), Dhaka, Bangladesh. All the patients were referred from the department of dermatology of BSMMU, different medical colleges, and private chambers of dermatologists in Bangladesh with histopathology reports of incisional biopsy (**incisional biopsy** is a surgical procedure to remove a piece of tissue from a lesion or mass. The tissue is then tested by the histopathologists to find out what it is). All the lesions were larger than 2.5cm in diameter and required plastic surgical maneuver, that is, wide excision and reconstruction by skin graft or flap coverage. We then sent the excisional biopsy (**excisional biopsy** is a surgical procedure in which whole lesion or mass is removed then tested to find out what it is) specimen for histopathology after marking its different borders with different suture materials (Prolene, Vicryl, and Silk) to delineate the exact area of the body from where we have removed it. We used a container containing 10% formalin to transport the specimen to the department of histopathology. The main target of this histopathology was to see the deep surface and marginal clearance of this excised specimen. The histopathologists did immunohistochemistry (**immunohistochemistry** refers to the process of detecting the antigens in the cells of tissue section by exploiting the principle of antibodies binding specifically to the antigens in the biological tissue) for Merkel Cell Tumour and Melanoma. The histopathologists did the diagnosis of the cancer by world-wide standard methods.

Within these 12 years, 1403 patients were found with cutaneous malignancy among which 1156 cases were related to arsenic exposure. 960 cases fulfilled the selection criteria (which are listed below) and 196 patients who had multiple lesions due to arsenicosis were not included in the study.

2.1. Selection Criteria

(i) Those who have one of the dichotomous physician-diagnosed skin lesions [34],

Melanosis, Keratosis, Hyperkeratosis, and Leucomelanosis

Table 1: Demographic analysis of patients.

	Male	Female	Total
Number of Patients (%)	528(55)	432(45)	960 (100)
P value	χ^2 p = 0.22	χ^2 p = 0.09	χ^2 p = 0.13
Age (Mean and SD)	49.1 & 12.11	46.6 & 13.3	47.8 & 12.76
Age (Median)	64	69	67
Age Range	20-90	18-95	18-95
Family history of cutaneous malignancy due to arsenicosis	268 (27.92)	252 (26.25)	520 (54.17)

(**Melanosis** is termed as a diffuse or spotted lesion characterized by dark pigmentation on the face, neck, limbs and trunk. **Keratosis** is defined as any diffuse or spotted lesion characterized by hard and roughened skin elevations observed on the hands and feet. **Hyperkeratosis** is defined as extensively thickened keratosis observed on the hands and/or feet that are easily visible from a distance. **Leucomelanosis** is defined as depigmentation characterized by black and white spots present anywhere in the body)

(ii) History of ingestion of water from tube-wells for at least 10 years in arsenic prevalent districts marked by the government of Bangladesh

(iii) Patients with single malignant lesion with histopathology report of incisional biopsy

Statistical analysis was performed using SPSS 16.0 software. Normally distributed continuous variables were expressed and categorical variables were expressed as numbers and percentages. Mann-Whitney U test used in comparison with the continuous variables and chi-square test was used in comparison with categorical variables. The level of statistical significance was considered as <0.05.

Ethical approval was taken from Institutional Review Board (IRB), BSMMU. The declaration of Helsinki was followed. All the patients were involved in the study after taking informed written consent. All the information was collected using a questionnaire by face to face interview.

3. Results

A sample of 960 patients from January 2004 to December 2015 presenting with cutaneous malignancy (single lesion) from different arsenic contaminated districts of Bangladesh. There were 528 (55%) male and 432 (45%) female. The mean age of patients was 47.8±12.76 years (male 49.1±12.11 and female 46.6±13.3). About 520 patients have family history of malignancy due to arsenicosis (Table 1).

Cancers were very less below the age of 24. Higher prevalence (28.99%) of patients was noted in 40-49 years age group which was found to be statistically significant (P <0.05). BCC was found in 563 (58.65%) cases, SCC in 384 (40%), melanoma in 11 (1.15%), and MCC in 2 (0.21%) cases. There was no statistically significant difference between male and female population. Melanomas were found in above 40 years of age and more in male (0.73%) population. Two MCC cases were found in the female population (Table 2).

In Table 3, face (10.31%) was least affected area where limbs (34.27%) were most. There was a statistically significant (P <0.05) difference between male and female patients. 270 (28.13%) lesions were found on the scalp and 262 (27.29%) were in the trunk. About 78.56% (754) patients came from low education level, whereas 3.64% (35) in high education level, which was found to be statistically significant (P <0.05). Melanomas were more among the lower educational group where MCCs were found in the educated group (Table 4).

In Tables 5(a) and 5(b), highest (n=67, 6.98%) number of patients came from Chandpur (90% affected area) and all types of cancer (BCC, SCC, Melanoma, and MCC) are found in this area. The lowest number of patient (n=11, 1.15%) came from Pirojpur and Patuakhali (P <0.05). About 66.55% (N=637) patient came from worst affected districts with 35.22% (N=338) BCC, 29.83% (N=286) SCC, 1.14% (N=11) melanoma, and 0.21% (N=2) MCC. But from the least affected areas only 33.65% (N=323) came with 23.44% (N=225) BCC and 10.21% (N=95) SCC. No melanoma or MCC was found in the least affected districts.

4. Discussion

Arsenic (As) is a metalloid. It is widely distributed in nature [35]. Arsenic compounds can be found in organic (when combined with carbon and hydrogen) and inorganic form (when combined with oxygen, chlorine, and sulfur among other elements) [36]. In Environment, arsenic can be found with an oxidation state +3 (Arsenite or, As [III]), or, +5 (Arsenate or As [V]), exhibiting different grades of toxicity [37]. An increased level of inorganic arsenic in drinking water is the major cause of arsenic toxicity [36, 38]. For this reason, IARC (International Agency for Research on Cancer) declared that arsenic is a human carcinogen (class I) and recommended threshold for arsenic concentration of drinking water ≤10μg/L [39–41]. Smith AD et al. also showed arsenic levels as low as 2 μg/L may be cancerous [42].

It is now widely believed that high arsenic levels in ground water in Bangladesh have natural geological source which may be due to abstraction of quaternary confined and semi-confined alluvial or deltaic aquifers. This is also inferred that arsenic is occurring in the alluvial sediments; the ultimate origin is perhaps in the out crops of hard rocks higher up the Ganga catchment [43]. A large number of chemical and biological reactions, namely, oxidation, reduction, adsorption, precipitation, methylation, and volatilization, participate in the cycling of the toxic element in ground water [35]. It is

Table 2: Analysis of malignant lesions on the basis of age group and sex.

Age group	Squamous Cell Carcinoma SCC				Basal Cell Carcinoma BCC				Melanoma				Merkel Cell Carcinoma MCC				Total	
	Male		Female		Male		Female		Male		Female		Male		Female			
	N	%	N	%	N	%	N	%	N	%	N	%	N	%	N	%	N	%
20-29	12	1.25	9	1.15	13	1.35	9	0.94	-	-	-	-	-	-	-	-	43	4.48
30-39	31	3.23	27	2.81	58	6.04	29	3.02	-	-	-	-	-	-	1	0.10	146	15.21
40-49	65	6.77	46	4.79	85	8.85	79	8.23	1	0.10	2	0.21	-	-	-	-	259	26.98
50-59	51	5.31	49	5.10	81	8.44	73	7.60	4	0.42	-	0	-	-	1	0.10	278	28.99
>60	54	5.63	40	4.17	71	7.40	65	6.77	2	0.21	2	0.21	-	-	-	-	234	23.38
Total	213	22.19	171	18.02	308	32.08	255	26.56	7	0.73	4	0.42	-	-	2	0.21	960	100

Table 3: Age and sex variation according to the location of lesion.

Age Group (yrs)	Face				Scalp				Limbs				Trunk			
	Male		Female		Male		Female		Male		Female		Male		Female	
	N	%	N	%	N	%	N	%	N	%	N	%	N	%	N	%
20-29	4	0.42	2	0.21	5	0.52	4	0.42	11	1.15	5	0.52	5	0.52	7	0.73
30-39	13	1.35	7	0.73	17	1.77	13	1.35	35	3.65	17	1.77	24	2.50	20	2.08
40-49	14	1.46	8	0.83	57	5.93	26	2.71	53	5.52	40	4.17	27	2.81	53	5.53
50-59	8	0.83	11	1.15	52	5.42	32	3.33	39	4.06	51	5.31	37	3.85	29	3.02
>60	11	1.15	21	2.19	41	4.27	23	2.40	48	4.99	30	3.13	27	2.81	33	3.44
Total	50	5.21	49	5.11	172	17.91	98	10.21	186	19.37	143	14.9	120	12.49	142	14.8

Table 4: Analysis of patients according to education level.

Patient	None-primary				Secondary-College				Graduation or, further			
	Male		Female		Male		Female		Male		Female	
	N	%	N	%	N	%	N	%	N	%	N	%
SCC	173	18.02	136	14.17	38	3.96	30	3.13	4	0.42	3	0.31
BCC	237	24.69	198	20.63	57	5.94	45	4.69	14	1.46	12	1.25
Melanoma	6	0.63	4	0.42	-	-	-	-	1	0.10	-	-
MCC	-	-	-	-	-	-	1	0.10	-	-	1	0.10
Total	416	43.34	338	35.22	95	9.90	76	7.92	19	1.98	16	1.66

also manmade causes; i.e., the use of fertilizers, pesticides, insecticides, waste disposal, and arsenic treated wooden poles for power grids was blamed for the contamination [28]. That underground water system flows into shallow tube wells used by many. The water pulled to the surface from the wells is often contaminated with high levels of arsenic- causing problems in food chain [44].

Arsenic toxicity is close dependent and particularly on the amount of ingestion of arsenic compounds and their excretion from the body through urine, stool, skin, hair, nail, and breath. It has been reported that 40%-60% arsenic is retained in human body and passes slowly out through skin and nail [33]. Both arsenite and arsenate accumulate in dermis and epidermis, epidermal stem cells, have been proposed as a potential target for arsenic induced carcinogenesis [31, 45, 46]. Arsenic also has the potential to induce malignant transformation of human keratinocyte [47]. The carcinogenic mechanism in the cell includes the following: (a) biotransformation, methylation can activate the toxic and carcinogenic potential of arsenic [48, 49]; (b) arsenic induced oxidative stress, such as reactive oxygen species (ROS) leading to genomic alteration [50–53]; (C) epigenetic changes, DNA methylation, histone modification, and micro-RNAg [54, 55]. Moreover, malnutrition which is basically due to poverty of this region has a great effect on immunosuppression, causing arsenic induced malignancy [26]

In this 12 years study, we found 960 patients with cutaneous malignancy where the mean age was 47.8 years and showed male predominance. Basal Cell Carcinoma (BCC) was 58.65% (N=563) and Squamous Cell Carcinoma (SCC) was 40% (N= 384) of the study population. Ghosh SK et al. did a field study from July to August 2013, on arsenic contaminated area of West Bengal, India, where the mean age was 52.2 years, 37.5% BCC and 41.7% SCC. This result is nearly identical to our study probably due to similar geographical location, genetic constitution of the people, and mode of contamination of ground water in both the regions [56]. A similar study conducted in India supported our finding of male predominance. This could be explained by the observation that males of the rural areas of this region are more engaged in manual labour (day labourer, farmer, rickshaw puller, etc.) and consume more water per day than the females [57]. About 54.17% (N=520) patient had positive family history of cutaneous malignancy due to arsenicosis. This fact maybe attributed to the use of water (drinking, cooking, and other purposes) obtained from the same tube well by all the members of a family. Majority of the people of rural area of Bangladesh live in poverty, and they have to use only one common tube well for many families [58].

We found 1.15% (N-11) melanoma patients in our study, highest in 50-59-year age group. Melanoma is a relatively rare finding in other studies of the world. All the melanoma were located in the lower limbs, especially on sole and toe nail, found mainly in Chandpur, Gopalganj, Madaripur, and Sariatpur where the arsenic concentration is >50μg/L, sometimes even up to 500μg/L in some villages [29]. A study conducted in Iowa, IA, USA, suggested a potential link between elevated arsenic levels and melanoma, found mostly in patients aged >40 years. They suggested that arsenic's affinity for sulfhydryl group of keratin causes accumulation where scleroprotein is abundant, e.g., finger nails and toe nails. It is found when average arsenic concentration was 21μg/L [19, 59–61].

In our series, we found 0.21% (N- 02) Merkel Cell Carcinoma (MCC) in the temporal region (sun exposed area)

Table 5

(a) History of arsenic associated malignancy in the worst affected districts

	Name and % of affected area	Basal Cell Carcinoma (BCC)				Squamous Cell Carcinoma (SCC)				Melanoma				Merkel Cell Carcinoma (MCC)				Total	
		Male		Female		Male		Female		Male		Female		Male		Female			
		N	%	N	%	N	%	N	%	N	%	N	%	N	%	N	%	N	%
WORST AFFECTED DISTRICTS	Chandpur (90%)	20	2.08	4	0.42	23	2.4	16	1.67	1	0.1	2	0.21	-	-	1	0.1	67	6.98
	Munshiganj (83%)	12	1.25	3	0.31	8	0.83	4	0.42	-	-	-	-	-	-	-	-	27	2.81
	Gopalganj (79%)	15	1.56	7	0.73	10	1.04	12	1.25	1	0.1	-	-	-	-	-	-	45	4.69
	Brahmanbaria (70%)	13	1.35	17	1.77	11	1.15	6	0.63	-	-	-	-	-	-	-	-	47	4.90
	Jhenaidah (69%)	16	1.67	10	1.04	3	0.31	1	0.10	-	-	-	-	-	-	-	-	30	3.13
	Madaripur (69%)	12	1.25	4	0.42	23	2.4	17	1.77	3	0.31	1	0.1	-	-	-	-	60	6.25
	Noakhali (69%)	13	1.35	11	1.15	6	0.63	8	0.83	-	-	-	-	-	-	1	0.1	39	4.06
	Satkhira (67%)	8	0.83	6	0.63	5	0.52	4	0.42	-	-	-	-	-	-	-	-	23	2.40
	Comilla (65%)	17	1.77	10	1.04	13	1.35	11	1.15	-	-	-	-	-	-	-	-	51	5.31
	Faridpur (65%)	4	0.42	5	0.52	9	0.94	5	0.52	-	-	-	-	-	-	-	-	23	2.40
	Shariatpur (65%)	14	1.46	11	1.15	14	1.46	3	0.31	2	0.21	1	0.1	-	-	-	-	45	4.69
	Lakshmipur (64%)	12	1.25	13	1.35	9	0.94	6	0.63	-	-	-	-	-	-	-	-	40	4.17
	Pabna (62%)	18	1.88	7	0.73	6	0.63	7	0.73	-	-	-	-	-	-	-	-	38	3.96
	Meherpur (60%)	6	0.63	5	0.52	11	1.15	7	0.73	-	-	-	-	-	-	-	-	29	3.02
	Bagerhat (60%)	12	1.25	6	0.63	10	1.04	12	1.25	-	-	-	-	-	-	-	-	40	4.17
	Natore (58%)	14	1.46	13	1.35	6	0.63	-	-	-	-	-	-	-	-	-	-	33	3.44
	Total	206	21.46	132	13.76	167	17.42	119	12.41	7	0.72	4	0.41	-	-	2	0.2	637	66.35

(b) History of arsenic associated malignancy in the least affected districts

		BCC				SCC				Melanoma				MCC				Total	
		Male		Female		Male		Female		Male		Female		Male		Female			
		N	%	N	%	N	%	N	%	N	%	N	%	N	%	N	%	N	%
LEAST AFFECTED DISTRICTS	Thakurgaon	6	0.63	11	1.15	3	0.31	-	-	-	-	-	-	-	-	-	-	20	2.08
	Panchagarh	5	0.52	9	0.94	4	0.42	1	0.10	-	-	-	-	-	-	-	-	19	1.98
	Nilphamari	13	1.35	6	0.63	4	0.42	8	0.83	-	-	-	-	-	-	-	-	31	3.23
	Lalmonirhat	6	0.63	10	1.04	2	0.21	4	0.42	-	-	-	-	-	-	-	-	22	2.29
	Patuakhali	7	0.73	3	0.31	1	0.10	-	-	-	-	-	-	-	-	-	-	11	1.15
	Barguna	2	0.21	9	0.94	1	0.10	4	0.42	-	-	-	-	-	-	-	-	16	1.67
	Barisal	6	0.63	10	1.04	-	-	3	0.31	-	-	-	-	-	-	-	-	19	1.98
	Chuadanga	7	0.73	9	0.94	3	0.31	1	0.10	-	-	-	-	-	-	-	-	20	2.08
	Jessore	10	1.04	9	0.94	-	-	5	0.52	-	-	-	-	-	-	-	-	24	2.50
	Feni	13	1.35	11	1.15	10	1.04	8	0.83	-	-	-	-	-	-	-	-	42	4.38
	Khulna	4	0.42	6	0.63	-	-	-	-	-	-	-	-	-	-	-	-	10	1.04
	Magura	9	0.94	13	1.35	3	0.31	2	0.21	-	-	-	-	-	-	-	-	27	2.81
	Narail	11	1.15	8	0.83	4	0.42	5	0.52	-	-	-	-	-	-	-	-	28	2.92
	Rajbari	2	0.21	6	0.63	9	0.94	6	0.63	-		-	-	-	-	-	-	23	2.40
	Pirojpur	1	0.10	3	0.31	2	0.21	5	0.52	-	-	-	-	-	-	-	-	11	1.15
	Total	102	10.64	123	12.83	46	4.79	52	5.41	-	-	-	-	-	-	-	-	323	33.65

of two female patients hailing from Chandpur and Noakhali, where contaminated water contain high concentration of arsenic (>300 μg/L). MCC is normally related to advanced age, sun exposure, and immunosuppression [62]. Ho SY et al. conducted a study in Taiwan and found three cases of MCC with history of ingestion of arsenic contaminated water more than 50 μg/L (3.5 liters daily for male and 2.0 liters for female) with average duration of 20 years [63].

We found limb to be the most affected region (34.27%, N = 329), followed by scalp (28.13%, N=270). Face is the least affected area (10.31%, N=99). But nonarsenic mediated cancer especially BCC affects the face [64]. Limbs, scalp, and trunk are more affected probably due to hair, which accumulate arsenic and cause malignant changes in the area [61].

More than three-fourth patients in our study (78.56%, N=754) had education up to primary level or below, which is supported by another study in Bangladesh, where 69% patients studied up to primary level or below [34]. People of this education level suffer more from arsenic mediated cancer due to lack of knowledge, minimum perception to counseling, low financial capability for treatment, fail to take part in mitigation program, superstition, and malnutrition. They are mostly manual labourers, consuming more than 5 liters of arsenic contaminated water per day [1]. Cancer risk associated with daily consumption of 1.0 liter of water with organic arsenic (50μg/L) has been estimated [18]. Malnutrition also plays a role in the pathogenesis of cancer by reducing the immunity [26].

5. Conclusion

Our study was aimed at presenting the prevalence of arsenic associated skin malignancy in patients coming to the plastic surgery outpatient department of BSMMU, a tertiary level hospital in Dhaka. This study shows only a small part of the national problem. Only the patients with detected cutaneous malignancy, large enough (more than 2.5cm in diameter) to require plastic surgical maneuver, were included, so a large number of patients with smaller lesions were beyond the scope of this study. The problem of arsenic exposure has started since the 1970s and a considerable amount of time has gone by since then, as a result a large number of people have become affected by arsenic associated skin malignancy. These patients only represent a portion of the total population. Many others with smaller sized lesions or precancerous lesions do not even present themselves at the proper place. The big number of skin malignancies of this small study population is very alarming and could be the tip of the ice-berg of the real problem. Future studies should be targeted at developing a nation-wide screening and management protocol in different levels of hospitals, both by the government and the nongovernment organizations. Drawing the attention of the concerned policymakers is really vital in this regard.

Data Availability

The data used to support the findings of this study are available from the corresponding author upon request.

Conflicts of Interest

The authors declare that there are no conflicts of interest regarding the publication of this paper.

References

[1] M. Saifuddin and M. M. Karim, "Groundwater Arsenic Contamination in Bangladesh: Causes, Effects and Remedation," in *Proceedings of the 1st IEB international conference and 7th annual paper meet, Chittagong*, 2001.

[2] S. A. Talukder, A. Chatterjee, J. Zheng et al., "Studies of Drinking Water Quality and Arsenic Calamity in Groundwater of Bangladesh," in *Studies of Drinking Water Quality and Arsenic Calamity in Groundwater of Bangladesh Proceedings of the International Conference on Arsenic Pollution of Groundwater in Bangladesh: Causes, Effects and Remedies*, Dhaka, Bangladesh, 1998.

[3] S. V. Flangan, R. B. Johnston, and Y. Zheng, "Arsenic in tube well in Bangladesh: health and economic impacts and implications for arsenic mitigation," *Bulletin of the World Health Organization*, 2012.

[4] New Nation Report, "Immediate Government Steps Needed, Millions Affected by Arsenic Contamination," *The New Nation, A daily newspaper of Bangladesh*, 1996.

[5] D. G. Kinninburgh and P. L. Smedley, Eds., *Arsenic contamination of groundwater in Bangladesh*, British Geological Survey, Keyworth, 2001.

[6] Multiple Indicator Cluster Survey (MICS), *New York: United Nations Children's Fund, Bangladesh & Bangladesh Bureau of statistics; 2010*, 2009, http://www.unicef.org/bangladesh/knowledgecentre_6292.htm.

[7] M. Argos, T. Kalra, B. L. Pierce et al., "A prospective study of arsenic exposure from drinking water and incidence of skin lesions in Bangladesh," *American Journal of Epidemiology*, vol. 174, no. 2, pp. 185–194, 2011.

[8] "WHO Guidelines for Drinking-Water Quality. Vol. 2," Health Criteria and Other Supporting Information.

[9] S. J. Ryker, "Mapping arsenic in groundwater," *Geotimes*, vol. 46, pp. 34–36, 2001.

[10] V. D. Martinez, E. A. Vucic, D. D. Becker-Santos et al., "Arsenic Exposure and the Induction of Human Cancers," *Journal of Toxicology*, vol. 2011, Article ID 431287, 13 pages, 2011.

[11] World Health Organisation (WHO), *WHO Guidelines for Drinking-Water Quality*, WHO, Geneva, Switzerland, 1993.

[12] B. K. Caldwell, W. T. Smith, and K. Lokuge, "Access to drinking-water and arsenicosis in Bangladesh," *Journal of Health, Population and Nutrition*, vol. 24, pp. 336–345, 2006.

[13] *Bangladesh national drinking water quality survey 2009*, Dhaka: United Nations Children's Fund, Bangladesh, 2011, http://www.unicef.org/bangladesh/knowledgecentre_6868.htm.

[14] G. Marshall, C. Ferreccio, Y. Yuan et al., "Fifty-Year study of lung and bladder cancer mortality in Chile related to arsenic in drinking water," *Journal of the National Cancer Institute*, vol. 99, no. 12, pp. 920–928, 2007.

[15] P. P. Simeonova and M. I. Luster, "Mechanisms of arsenic carcinogenicity: Genetic or epigenetic mechanisms?" *Journal of Environmental Pathology, Toxicology and Oncology*, vol. 19, no. 3, pp. 281–286, 2000.

[16] C.-J. Chen and C.-J. Wang, "Ecological correlation between arsenic level in well water and age-adjusted mortality from

malignant neoplasms," *Cancer Research*, vol. 50, no. 17, pp. 5470–5474, 1990.

[17] W. Cullen, B. McBride, and J. Reglinski, "The reaction of methylarsenicals with thiols: Some biological implications," *Journal of Inorganic Biochemistry*, vol. 21, no. 3, pp. 179–193, 1984.

[18] H. H. Wong and J. Wang, "Merkel cell carcinoma," *Archives of Pathology & Laboratory Medicine*, vol. 134, no. 11, pp. 1711–1716, 2010.

[19] W. Boonchai, A. Green, J. Ng, A. Dicker, and G. Chenevix-Trench, "Basal cell carcinoma in chronic arsenicism occurring in Queensland, Australia, after ingestion of an asthma medication," *Journal of the American Academy of Dermatology*, vol. 43, no. 4, pp. 664–669, 2000.

[20] H.-C. Lien, T.-F. Tsai, Yu Yun Lee, and C.-H. Hsiao, "Merkel cell carcinoma and chronic arsenicism," *Journal of the American Academy of Dermatology*, vol. 41, no. 4, pp. 641–643, 1999.

[21] S. S. Wong, K. C. Tan, and C. L. Goh, "Cutaneous manifestations of chronic arsenicism: Review of seventeen cases," *Journal of the American Academy of Dermatology*, vol. 38, no. 2 I, pp. 179–185, 1998.

[22] M. Rahman, "Arsenic and contamination of drinking water in Bangladesh: A public health perspective," *Journal of Health, Population and Nutrition*, vol. 20, pp. 193–197, 2002.

[23] K. C. Saha, "Chronic arsenical dermatoses from tube-well water in West Bengal during 1983-1987," *Indian Journal of Dermatology*, vol. 40, pp. 1–12, 1995.

[24] S. M. Ullah, "Arsenic contamination of ground water and irrigated soils of Bangladesh," in *Processing of the International Conference on Arsenic Pollution of Ground Water in Bangladesh: Causes, Effects, and Remedies*, Jadavpur University, Calcutta, Dhaka, 1998.

[25] A. H. Smith, E. O. Lingas, and M. Rahman, "Contamination of drinking-water by arsenic in Bangladesh: a public health emergency," *Bulletin of the World Health Organization*, vol. 78, no. 9, pp. 1093–1103, 2003.

[26] Daily Star Report, "An Urgent Call to Save a Nation," *The Daily Star, A national daily newspaper of Bangladesh*, 1999.

[27] "Arsenic, Banglapedia-National Encyclopedia of Bangladesh," http://en.banglapedia.org/index.php?title=Arsenic&oldid=378.

[28] M. G. Alam, G. Allinson, F. Stagnitti et al., "rsenic contamination in Bangladesh groundwater: a major environmental and social disaster," *International Journal of Environmental Health Research*, vol. 12, no. 3, pp. 235–253, 2002.

[29] *Country situation report: arsenic in drinking water in Bangladesh, 1996: a challenge in near future*, World Health Organization, Geneva, 1996.

[30] *Executive summary of the main report of Phase I, ground water and arsenic contamination in Bangladesh. British Geological Survey And Mott MacDonald (UK) for the Government of Bangladesh, Ministry of local Government, Rural Development and Cooperatives*, Department of Public Health Engineering, and Department of International Development (UK), 1999, http://www.damient-consul.co.jp/english/arenic/article/DFID-sum.html.

[31] T. J. Patterson and R. H. Rice, "Arsenite and insulin exhibit opposing effects on epidermal growth factor receptor and keratinocyte proliferative potential," *Toxicology and Applied Pharmacology*, vol. 221, no. 1, pp. 119–128, 2007.

[32] J. G. Farmer and L. R. Johnson, "Assessment of occupational exposure to inorganic arsenic based on urinary concentrations and speciation of arsenic.," *Occupational and Environmental Medicine*, vol. 47, no. 5, pp. 342–348, 1990.

[33] W. J. Seow, W.-C. Pan, M. L. Kile et al., "Arsenic reduction in drinking water and improvement in skin lesions: A follow-up study in Bangladesh," *Environmental Health Perspectives*, vol. 120, no. 12, pp. 1733–1738, 2012.

[34] M. S. Islam and F. Islam, "Arsenic Contamination in Groundwater in Bangladesh: An environmental and Social Disaster," in *IWA Water Wiki*, 2010, http://www.iwaterwiki.org/.

[35] Agency for Toxic Substances and Disease Registry (ATSDR), *Toxicological Profile for Arsenic*, U.S Department of Health and Human Services, Washington, DC, USA, 2007.

[36] M. Vahter, "Mechanisms of arsenic biotransformation," *Toxicology*, vol. 181-182, pp. 211–217, 2002.

[37] D. N. G. Mazumder, *Diagnosis and treatment of chronic arsenic poisoning*, United Nations Synthesis Report on Arsenic in Drinking Water, 2000.

[38] "Interantional Agency for Research on Cancer (IARC) Some drinking-water disinfectants and contaminants, including arsenic. Monographs on chloramines, chloral and chloral hydrate, dichloroacetic acid, trichloroacetic acid and 3-chloro-4-(dichloromethyl)-5-hydroxy-2(5H)-furanone," *IARC Monographs on the Evaluation of Carcinogenic Risks to Humans*, vol. 84, pp. 269–477, 2004.

[39] R. H. McCuen, "Guidelines for drinking-water quality," *Journal of the American Water Resources Association*, vol. 38, no. 3, p. 879, 2002.

[40] *U.S. Environmental Protection Agency (EPA) National Primary Drinking Water Regulation. Arsenic and Clarifications to compliance and New Source Contaminants Monitoring, in Final rule. Delay of effective date*, Federal Registry, 2001.

[41] A. H. Smith, C. Hopenhayn-Rich, M. N. Bates et al., "Cancer Risks from Arsenic in Drinking Water," *Environmental Health Perspectives*, vol. 97, p. 259, 1992.

[42] M. M. Karim, Y. Komori, and M. Alam, "Subsurface Arsenic Occurrence and Depth of Contamination in Bangladesh," *Journal of Environmental Chemistry*, vol. 7, no. 4, pp. 783–792, 1997.

[43] S. M. I. Huq, J. C. Joardar, S. Parvin, R. Correll, and R. Naidu, "Arsenic contamination in food-chain: Transfer of arsenic into food materials through groundwater irrigation," *Journal of Health, Population and Nutrition*, vol. 24, no. 3, pp. 305–316, 2006.

[44] S. Ouypornkochagorn and J. Feldmann, "Dermal uptake of arsenic through human skin depends strongly on its speciation," *Environmental Science & Technology*, vol. 44, no. 10, pp. 3972–3978, 2010.

[45] T. J. Patterson, T. V. Reznikova, M. A. Phillips, and R. H. Rice, "Arsenite maintains germinative state in cultured human epidermal cells," *Toxicology and Applied Pharmacology*, vol. 207, no. 1, pp. 69–77, 2005.

[46] S.-J. Wei, C. S. Trempus, R. E. Cannon, C. D. Bortner, and R. W. Tennant, "Identification of Dss1 as a 12-O-tetradecanoylphorbol-13-acetate-responsive gene expressed in keratinocyte progenitor cells, with possible involvement in early skin tumorigenesis," *The Journal of Biological Chemistry*, vol. 278, no. 3, pp. 1758–1768, 2003.

[47] M. Stýblo, Z. Drobná, I. Jaspers, S. Lin, and D. J. Thomas, "The role of biomethylation in toxicity and carcinogenicity of arsenic: A research update," *Environmental Health Perspectives*, vol. 110, no. 5, pp. 767–771, 2002.

[48] D. J. Thomas, M. Styblo, and S. Lin, "The cellular metabolism and systemic toxicity of arsenic," *Toxicology and Applied Pharmacology*, vol. 176, no. 2, pp. 127–144, 2001.

[49] M. Kessel, S. X. Liu, A. Xu, R. Santella, and T. K. Hei, "Arsenic induces oxidative DNA damage in mammalian cells," *Molecular and Cellular Biochemistry*, vol. 234-235, pp. 301–308, 2002.

[50] K. T. Kitchin, "Recent advances in arsenic carcinogenesis: modes of action, animal model systems, and methylated arsenic metabolites," *Toxicology and Applied Pharmacology*, vol. 172, no. 3, pp. 249–261, 2001.

[51] Y. An, Z. Gao, Z. Wang et al., "Immunohistochemical analysis of oxidative DNA damage in arsenic-related human skin samples from arsenic-contaminated area of China," *Cancer Letters*, vol. 214, no. 1, pp. 11–18, 2004.

[52] M. Matsui, C. Nishigori, S. Toyokuni et al., "The role of oxidative DNA damage in human arsenic carcinogenesis: Detection of 8-hydroxy-2'-deoxyguanosine in arsenic-related Bowen's disease," *Journal of Investigative Dermatology*, vol. 113, no. 1, pp. 26–31, 1999.

[53] X. Ren, C. M. Mchale, C. F. Skibola, A. H. Smith, M. T. Smith, and L. Zhang, "An emerging role for epigenetic dysregulation in arsenic toxicity and carcinogenesis," *Environmental Health Perspectives*, vol. 119, no. 1, pp. 11–19, 2011.

[54] J. F. Reichard and A. Puga, "Effects of arsenic exposure on DNA methylation and epigenetic gene regulation," *Epigenomics*, vol. 2, no. 1, pp. 87–104, 2010.

[55] S. K. Ghosh, D. Bandyopadhyay, S. K. Bandyopadhyay, and K. Debbarma, "Cutaneous malignant and premalignant conditions caused by chronic arsenicosis from contaminated ground water consumption: a profile of patients from eastern India.," *SKINmed Journal*, vol. 11, no. 4, pp. 211–216, 2013.

[56] D. N. Guha Mazumder, R. Haque, N. Ghosh et al., "Arsenic levels in drinking water and the prevalence of skin lesions in West Bengal, India," *International Journal of Epidemiology*, vol. 27, no. 5, pp. 871–877, 1998.

[57] H. Ahsan, Y. Chen, F. Parvez et al., "Arsenic exposure from drinking water and risk of premalignant skin lesions in Bangladesh: baseline results from the health effects of arsenic longitudinal study," *American Journal of Epidemiology*, vol. 163, no. 12, pp. 1138–1148, 2006.

[58] W. E. Morton and D. A. Dunnette, "Health effects of environmental arsenic," in *Arsenic in the environment, Part II : human health and ecosystem effects*, J. O. Nriagu, Ed., John Wiley & Sons, New York, 1994.

[59] C. Watanabe, T. Inaoka, T. Kadono et al., "Males in rural Bangladeshi communities are more susceptible to chronic arsenic poisoning than females: Analyses based on urinary arsenic," *Environmental Health Perspectives*, vol. 109, no. 12, pp. 1265–1270, 2001.

[60] L. E. B. Freeman, L. K. Dennis, C. F. Lynch, P. S. Thorne, and C. L. Just, "Toenail arsenic content and cutaneous melanoma in Iowa," *American Journal of Epidemiology*, vol. 160, no. 7, pp. 679–687, 2004.

[61] M. L. Heath, N. Jaimes, B. Lemos et al., "Clinical characteristics of Merkel cell carcinoma at diagnosis in 195 patients: the AEIOU features," *Journal of the American Academy of Dermatology*, vol. 58, no. 3, pp. 375–381, 2008.

[62] S.-Y. Ho, Y.-C. Tsai, M.-C. Lee, and H.-R. Guo, "Merkel cell carcinoma in patients with long-term ingestion of arsenic," *Journal of Occupational Health*, vol. 47, no. 2, pp. 188–192, 2005.

[63] L. Sartore, L. Lancerotto, M. Salmaso et al., "Facial basal cell carcinoma: Analysis of recurrence and follow-up strategies," *Oncology Reports*, vol. 26, no. 6, pp. 1423–1429, 2011.

[64] Y. Ö. Tiftikcioğlu, Ö. Karaaslan, H. M. Aksoy, B. Aksoy, and U. Koçer, "Basal cell carcinoma in Turkey," *The Journal of Dermatology*, vol. 33, no. 2, pp. 91–95, 2006.

Hindawi
BioMed Research International
Volume 2018, Article ID 1252897, 9 pages
https://doi.org/10.1155/2018/1252897

Research Article

Effect of Comorbidity on Lung Cancer Diagnosis Timing and Mortality: A Nationwide Population-Based Cohort Study in Taiwan

Shinechimeg Dima,[1] Kun-Huang Chen,[2,3] Kung-Jeng Wang,[2] Kung-Min Wang,[4] and Nai-Chia Teng [1,5]

[1]*School of Dentistry, College of Oral Medicine, Taipei Medical University, 250 Wu-Hsing Street, Taipei, Taiwan*
[2]*National Taiwan University of Science and Technology, Taipei, Taiwan*
[3]*Big Data Research Center, Asia University, Taichung, Taiwan*
[4]*Department of Surgery, Shin-Kong Wu Ho-Su Memorial Hospital, Shilin District, Taipei 111, Taiwan*
[5]*Department of Dentistry, Taipei Medical University Hospital, 250 Wu-Hsing Street, Taipei, Taiwan*

Correspondence should be addressed to Nai-Chia Teng; tengnaichia@hotmail.com

Received 14 June 2018; Accepted 4 October 2018; Published 4 November 2018

Guest Editor: Sajib Chakraborty

The effect of comorbidity on lung cancer patients' survival has been widely reported. The aim of this study was to investigate the effects of comorbidity on the establishment of the diagnosis of lung cancer and survival in lung cancer patients in Taiwan by using a nationwide population-based study design. This study collected various comorbidity patients and analyzed data regarding the lung cancer diagnosis and survival during a 16-year follow-up period (1995–2010). In total, 101,776 lung cancer patients were included, comprising 44,770 with and 57,006 without comorbidity. The Kaplan–Meier analyses were used to compare overall survival between lung cancer patients with and without comorbidity. In our cohort, chronic bronchitis patients who developed lung cancer had the lowest overall survival in one (45%), five (28.6%), and ten years (26.2%) since lung cancer diagnosis. Among lung cancer patients with nonpulmonary comorbidities, patients with hypertension had the lowest overall survival in one (47.9%), five (30.5%), and ten (28.2%) years since lung cancer diagnosis. In 2010, patients with and without comorbidity had 14.86 and 9.31 clinical visits, respectively. Lung cancer patients with preexisting comorbidity had higher frequency of physician visits. The presence of comorbid conditions was associated with early diagnosis of lung cancer.

1. Introduction

Lung cancer is the most commonly diagnosed cancer worldwide and places a considerable burden on public health [1, 2]. Lung cancer incidence and mortality exceed that of any other cancer globally, with 1.6 million cases (accounting for 12.7% of total cancer incidence) and 1.4 million deaths occurring in 2008 worldwide [3]. According to the 2011 Taiwan Cancer Registry annual report, lung cancer was the third most common diagnosed cancer accounting for 13% of all cancers among men and 10% among women in Taiwan [4]. Despite advances in treatment, lung cancer survival has remained relatively poor because most patients are diagnosed as having lung cancer at an advanced stage [5]. Specific comorbidities have been recognized as being highly prevalent in lung cancer patients, including chronic obstructive pulmonary disease (COPD), hypertension, cardiovascular disease, diabetes mellitus (DM), and other malignancies [6, 7], with a prevalence of 26.4%–81.2% [8].

Asthma, COPD, and tuberculosis (TB) are the most common pulmonary comorbidities. However, studies regarding the effects of these comorbidities on lung cancer survival have included small samples sizes and yielded conflicting results. In a cohort of 1155 patients, Tammemagi et al. [9] reported that 18 of 56 comorbidities, including asthma, COPD, TB, and pulmonary fibrosis, were associated with a reduced

lung cancer survival. In a cohort of 5406 patients, preexisting pulmonary diseases increased mortality risk in male patients with squamous cell carcinoma, whereas preexisting asthma reduced mortality in female patients with early-stage squamous cell carcinoma [10]. Kuo et al. [11] reported that compared with those without comorbidity, non-small-cell lung cancer (NSCLC) patients with concomitant active TB had a more favorable survival outcome, particularly those with squamous cell carcinoma. Furthermore, patients with bronchiectasis, a chronic inflammatory airway disease, have an increased risk of lung cancer compared with the general population [12]; however, studies regarding the effects of bronchiectasis and other pulmonary diseases on lung cancer survival are scarce.

Despite increasing recognition of the impact of comorbidities on the prognosis of cancer patients, challenges remain. Population-based cohort studies are preferable for a detailed evaluation of the association between comorbidity and lung cancer. This nationwide population-based study explored the effects of comorbidity on lung cancer diagnosis timing and survival in lung cancer patients in Taiwan.

2. Methods

2.1. Database. In this study, we obtained patient data from the National Health Insurance Research Database (NHIRD), derived from the National Health Insurance (NHI) program. The NHIRD contains all medical claims for inpatient and ambulatory care services, registry files of contracted medical facilities, board-certified specialists, other medical service providers, and prescriptions covered by the NHI program for 25.68 million enrollees in Taiwan. The NHIRD data is deidentified secondary data, released to the public for research purposes by the Taiwan National Health Research Institutes.

This study was approved by the institutional review board of Shin-Kong Wu Ho-Su Memorial Hospital, Taiwan (20140703R). The study was conducted in accordance with the regulations of National Health Research Institute of Taiwan. The NHIRD is protected by computer-processed personal data protection act and does not include any personal data of enrollees. Therefore, no informed consent was obtained during this study.

2.2. Study Patients and Design. We employed a retrospective cohort to investigate the effect of comorbidity on the establishment of the diagnosis of lung cancer and survival. The lung cancer patients included in this study were identified from the NHIRD by using the International Classification of Diseases, 9th Revision, Clinical Modification (ICD-9-CM) code 162. The study population comprised lung cancer patients with and without comorbidity, selected from complete NHI claims database in the period 1995–2010.

In total, 101,776 lung cancer patients were included, the comorbidity group comprised 44,770 patients who received a principal diagnosis of comorbidity (under ICD-9-CM) during ambulatory medical care visits between January 1, 1995, and December 31, 2010, at least 6 months before the lung cancer diagnosis. The index visit was defined as the first ambulatory visit, during which a principal diagnosis of comorbidity was made. To maximize case ascertainment, only patients with at least five ambulatory visits (including the index visit) and who received their principal diagnosis of comorbidity in this period were included in the comorbidity group. The noncomorbidity group comprised the remaining patients from the NHI claims database diagnosed as having lung cancer during 1995–2010; in total, 57,006 patients were included in the noncomorbidity group. Details were described in the Figure 1.

All ambulatory medical care records and inpatient records for each patient in both groups were tracked since their index visit for lung cancer. The date of the first principal diagnosis of lung cancer within the follow-up period was defined as the primary endpoint in cancer diagnosis timing analysis. The mortality data of the patients who died during the follow-up period was subsequently considered to determine the survival of lung cancer patients. Patients newly diagnosed as having lung cancer during 1995–2010 were followed up until death, loss to follow-up, or the study endpoint in 2010.

2.3. Comorbidities. The 15 most prevalent chronic conditions in Taiwan are hepatitis, cancer, diabetes, hyperlipidemia, gout and other crystal arthropathies, depression, eye disorders, nervous system disorders, hypertension, heart disease, cerebrovascular disease, respiratory disease, digestive disease, genitourinary disease, and joint disorder. We selected common chronic diseases which probably have association with lung cancer for evaluation. The following individual comorbidities were identified using ICD-9-CM codes for exploring their effects on lung cancer survival: cerebrovascular accident, coronary artery disease, diabetes mellitus (DM), disorders of adrenal gland, disorders of thyroid gland, duodenal ulcer, gastric ulcer, gastrojejunal ulcer, hyperlipidemia, hypertension, hypoparathyroidism, peptic ulcer, asthma, bronchiectasis, chronic bronchitis, emphysema, empyema, and pulmonary tuberculosis. The detailed information of ICD-9-CM codes used to identify comorbidities were described in Table 1.

2.4. Variables. The data on patients' gender, lung cancer diagnosis period, age at lung cancer diagnosis, geographical region, and residence urbanization level were retrieved from the NHIRD. On the basis of their age at lung cancer diagnosis, the patients were classified into five age groups: ≤39, 40–49, 50–59, 60–69, and ≥70 years. According to the cancer diagnosis period, the patients were classified into three groups: 1995–2000, 2000–2005, and 2006–2010. We then geographically divided Taiwan into northern, central, southern, eastern, and islands regions. On the basis of the population density, manufacturing industries, number of physicians per 1000 people, and availability of health care facilities, patients in each region were classified into three urbanization levels—from most (level 1) to least (level 5) urbanized. In addition, the 22 cities and counties of Taiwan were grouped into four regions: northern (Taipei, New Taipei,

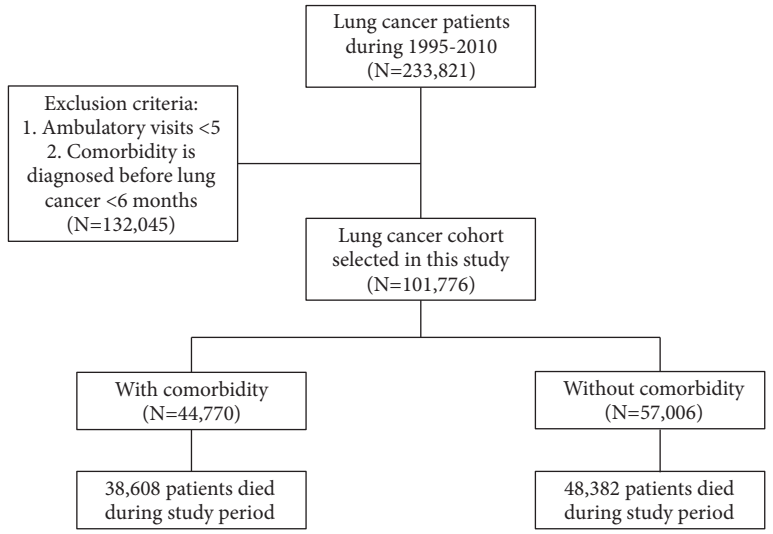

Figure 1: Flowchart of study population selection.

Table 1: ICD-9-CM codes used to identify comorbidity.

Pulmonary diseases	Diagnosis	ICD-9-CM
No	Cerebrovascular accident	430, 431, 432.X, 433.X, 434.X, 434.X, 435.X, 436, 437.X, 438.X
	Coronary artery disease	410.X, 411.X, 412, 413.X, 414.X
	Diabetes mellitus	250, 357.2, 362.X, 366.41
	Disorders of adrenal glands	255.X
	Disorders of thyroid gland	240.X-246.X
	Duodenal ulcer	532.X
	Gastric ulcer	531.X
	Gastrojejunal ulcer	534.X
	Hyperlipidemia	272.X
	Hypertension	362.11, 401.X–405.X, 437.2
	Hypoparathyroidism	252.X
	Peptic ulcer	533.X
Yes	Asthma	493.X
	Bronchiectasis	494.X, 496
	Chronic bronchitis	491.X
	Emphysema	492.X
	Empyema	510.X
	Pulmonary tuberculosis	011.X

Hsinchu, Keelung, and Taoyuan cities; Yilan and Miaoli counties), central (Taichung city; Changhua, Nantou, and Yunlin counties), southern (Chiayi, Tainan, and Kaohsiung cities; Chiayi, Pingtung, and Penghu counties), and eastern (Hualien, Taitung, Kinmen, and Lienchiang counties) Taiwan and islands.

2.5. Statistical Analysis. Frequency distributions on demographic characteristics of death subjects among comorbidity and noncomorbidity groups were compared by the chi-square test. A two-tailed p value of <0.05 was considered statistically significant. The Kaplan–Meier method was used to calculate cumulative curves of lung cancer in patients with different comorbidities. The overall survival of lung cancer patients with and without comorbidity was calculated using the Kaplan–Meier method, and the difference in overall survival was determined using the log-rank test. All statistical analyses were performed using SAS version 9.4 (IBM, USA). The survival curves and cumulative proportion curves were plotted using SPSS version 20.0 (IBM, USA).

3. Results

Of the 101,776 lung cancer patients enrolled in present study (mean age, 64.42 ± 13.22 years), 44% had comorbidities. Over the follow-up period, patients with comorbidity had

a higher frequency of clinical visits than did those without comorbidity (Figures 2(a) and 2(b)). The mean number of clinical visits of patients with comorbidity increased from 5.19 per person in 1996 to 14.86 in 2010. By contrast, patients without comorbidity had 6.53 mean clinical visits per person in 1996, gradually increasing to 9.31 in 2010. The increase in frequency of clinical visits was observed in patients of both genders.

Table 2 presents the distribution of demographic characteristics by comorbidity presence in lung cancer death subjects. Results showed each characteristic to be strongly associated with comorbidity presence. Males accounted for higher mortality in both groups than females. For the period of diagnosis, death subjects without comorbidity were predominantly diagnosed in higher proportion before 2005 than subjects with comorbidity. With regard to diagnostic age, subjects without comorbidity were higher than subjects with comorbidity in age groups younger than 69. Except in most urbanized areas (level 1), death subjects with comorbidity were likely to reside in less urbanized areas. With regard to geographic region, northern Taiwan accounted for significantly higher proportion of residence in death subjects of both groups, followed by southern and central regions.

Figure 3 illustrates the Kaplan–Meier survival curve of lung cancer patients with and without comorbidity over the 16-year follow-up period. Patients without comorbidity had significantly lower 16-year survival than did those with comorbidity ($p < 0.001$) (Figure 3(a)). Figure 3(b) presents the subgroup survival of comorbidity group by nature of comorbidity. The survival of lung cancer patients without pulmonary comorbidities was higher than that of those with pulmonary comorbidities (89%; $p < 0.001$).

Figure 3(c) presents the proportion and timing of lung cancer diagnosis with comorbidity. Figure 3(d) depicts the survival analysis of the lung cancer patients with different comorbidities ($p<0.001$). In our cohort, chronic bronchitis patients who developed lung cancer had the lowest overall survival in one (45%), five (28.6%), and ten years (26.2%) since lung cancer diagnosis. Among pulmonary comorbidities, lung cancer patients with asthma had the second lowest overall survival with 48.5%, 32.1%, and 29.3% overall survival in one, five, and ten years since lung cancer diagnosis, respectively. The highest overall survival was observed in empyema patients with 54.1%, 45.1%, and 44.7% overall survival in one, five, and ten years since lung cancer diagnosis, respectively. Lung cancer patients with TB had higher overall survival (48.8%, 36.1%, and 33.9% in 1, 5, and 10 years since cancer diagnosis) compared to patients with other pulmonary comorbidities. Among lung cancer patients with nonpulmonary comorbidities, patients with hypertension had the lowest overall survival in one (47.9%), five (30.5%), and ten (28.2%) years since lung cancer diagnosis.

4. Discussion

Our findings of 101,776 patients showed that lung cancer patients with comorbidity had significantly superior overall survival compared with those without comorbidity. The potential factors contributing to this finding are discussed as follows.

Lung cancer is the most prevalent cause of cancer death. A reason for low lung cancer survival rates is the lack of observable symptoms in the early stages. Lung cancer diagnosed on the basis of advanced-stage symptoms has limited treatment options. In Taiwan, data from 2004 to 2008 demonstrated that more than half of the lung cancer cases were diagnosed at advanced stages (e.g., stage IV) [13]. The odds of being diagnosed with advanced-stage lung cancer is lowered in the presence of comorbidity [14–18]. Comorbidity is associated with lung cancer diagnosis at an earlier stage, whereas the absence of comorbidity is associated with lung cancer diagnosis at a later stage [19]. In their population-based study in Taiwan [20], Wang et al. reported that early-stage lung cancer patients had more favorable survival rates; the 5-year survival rates were 60.7%, 36.3%, 13.3%, and 4.9% for stages I, II, III, and IV lung cancer, respectively. On the basis of data from the Taiwan Cancer Registry, Chang et al. [21] reported increased survival of patients with lung adenocarcinoma in Taiwan, which is also attributable to EGFR inhibitors having been approved for treating adenocarcinoma since 2003 (Gefitinib) and 2007 (Erlotinib). The chance of earlier cancer diagnosis is increased through seeking care for the symptoms of comorbidities or during regular monitoring of comorbidities, potentially assisting in the timely administration of adequate curative measures. With respect to health care utilization, our results showed increase in health-seeking behavior in lung cancer patients with comorbidity compared with those without comorbidity. Our findings are reasonable from a clinical perspective because patients with comorbidity are more likely to require frequent medical care and clinical visits than are healthier patients, resulting in closer monitoring and detection of cancer at early stages. This phenomenon previously explained as screening bias [7] or the surveillance effect was also seen in other cancers. Several studies have revealed the diagnosis of breast cancer [22, 23] and colon cancer [24] at early stages is associated with higher comorbidity scores. This pattern has most commonly been reported for screen-detected cancers (breast and colorectal), supporting the contention that a higher number of clinical visits may be related to a higher number of screenings, particularly where screening coverage rates are associated with health service funding, potentially encouraging the screening of patients with high comorbidity scores.

For detailed investigation on the impact of comorbidity on lung cancer, we performed proportion and timing of diagnosis and survival analysis of lung cancer in patients with nine comorbidities. The results indicated that lung cancer patients with pulmonary diseases had lower overall survival than did those with nonpulmonary diseases. These results corroborated the analysis that patients with respiratory tracts compromised by cancer cannot tolerate additional pulmonary comorbidities as well as those with tumor-free lungs. However, further survival analysis revealed that patients with asthma and chronic bronchitis had lower overall survival than did those with other pulmonary comorbidities. Although previous studies have reported the effects of asthma

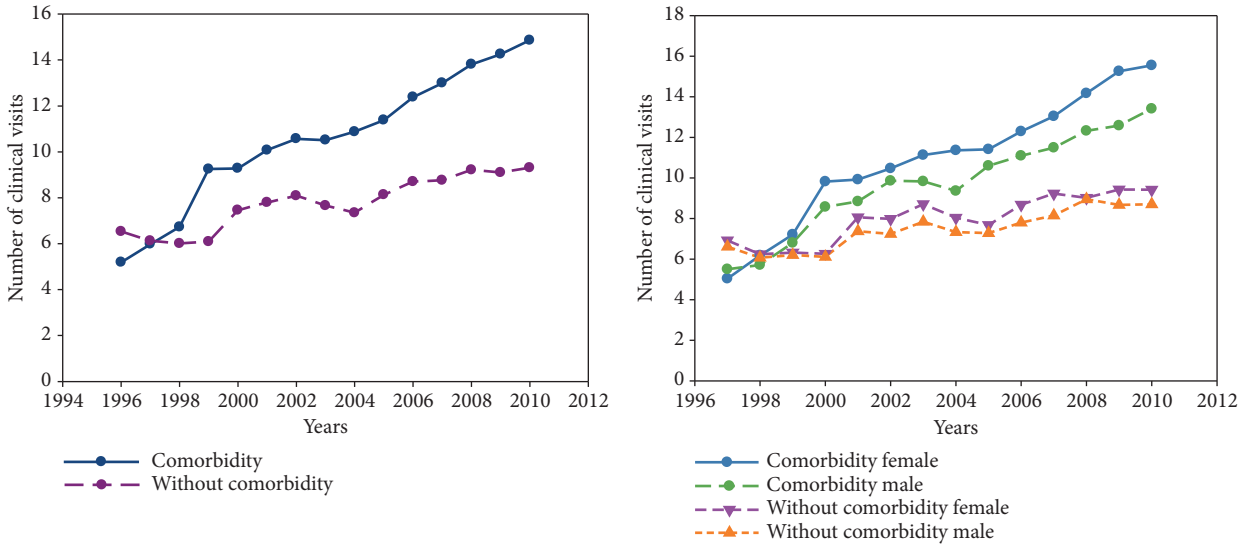

(a) The frequency of clinical visits among lung cancer patients with and without comorbidity (mean times per person/per year)

(b) The frequency of clinical visits among lung cancer patients by gender (mean times per person/per year)

Figure 2

Table 2: Characteristics of lung cancer death subjects between 1995 and 2010 (n =86,990).

Comorbidity Characteristics	With comorbidity (N=38,608)		Without comorbidity (N=48,382)		p-value
	No.	%[a]	No.	%[a]	
Gender					< 0.0001
Female	12,019	31.13%	13,924	28.78%	
Male	26,589	68.87%	34,458	71.22%	
Period of diagnosis (years)					0. 0018
1995-2000	7,204	18.66%	9,383	19.40%	
2001-2005	13,752	35.62%	17,412	35.99%	
2006-2010	17,652	45.72%	21,587	44.62%	
Diagnostic age (yrs)					< 0.0001
<=39	436	1.13%	1,552	3.21%	
40-49	1,537	3.98%	4,842	10.01%	
50-59	4,387	11.36%	9,225	19.07%	
60-69	8,835	22.88%	11,969	24.74%	
>=70	23,413	60.64%	20,794	42.98%	
Urbanization level					< 0.0001
1	12,742	33.00%	17,476	36.12%	
2	20,216	52.36%	25,304	52.30%	
3	3,607	9.34%	3,701	7.65%	
4	1,491	3.86%	1,456	3.01%	
5	552	1.43%	445	0.92%	
Geographic region					< 0.0001
Central	9,784	25.34%	10,581	21.87%	
Northern	17,398	45.06%	23,064	47.67%	
Eastern	903	2.34%	842	1.74%	
Southern	10,483	27.15%	13,837	28.60%	
Islands	40	0.10%	58	0.12%	

[a] May not total 100% due to rounding. [b] $(e^{\ln(RR)-1.96SE[\ln(RR)]}, e^{\ln(RR)+1.96SE[\ln(RR)]})$.

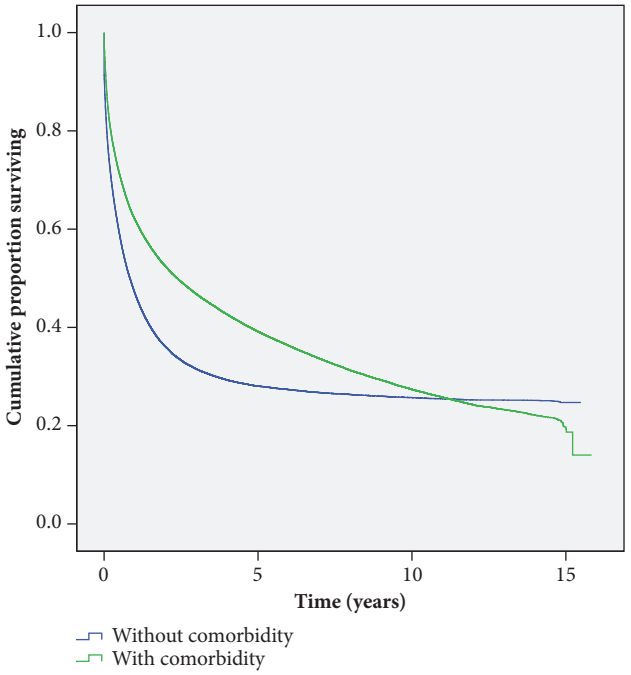

(a) Overall survival of lung cancer patients with and without comorbidity ($p<0.001$)

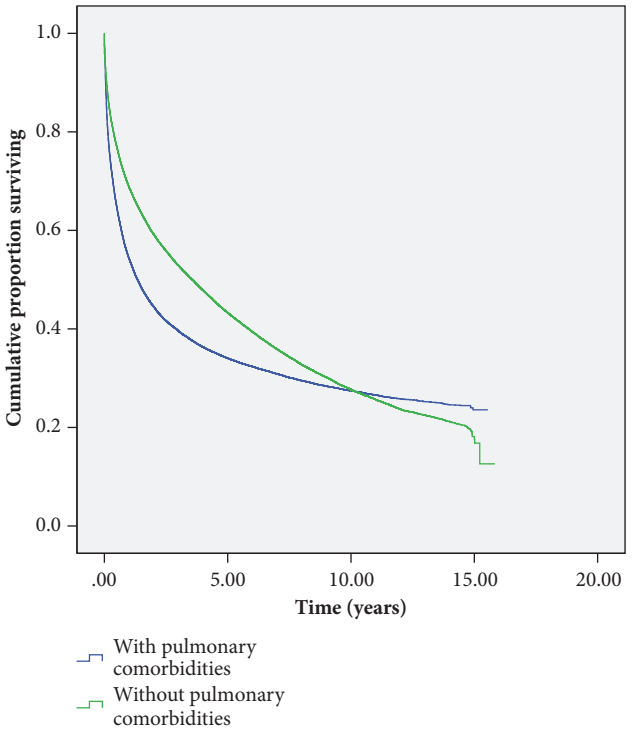

(b) Overall survival of lung cancer patients with and without pulmonary comorbidities ($p<0.001$)

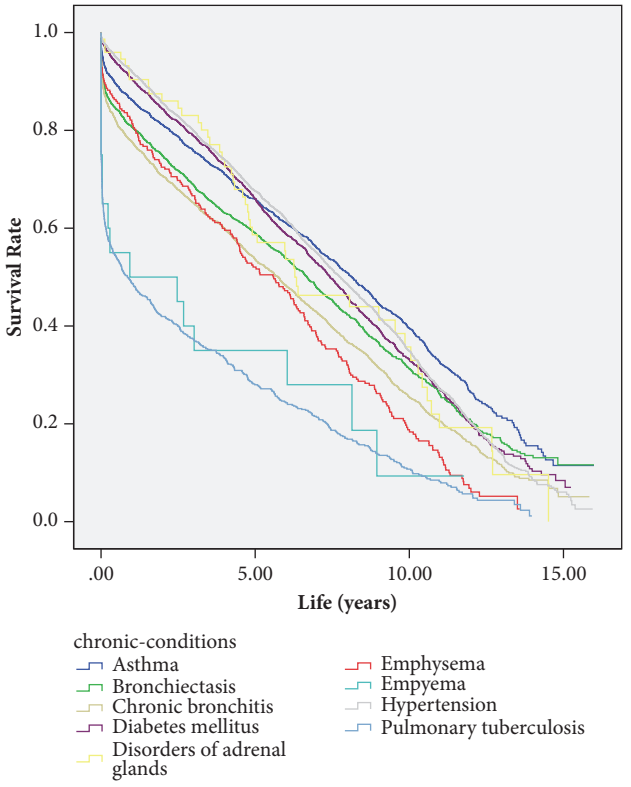

(c) Proportion of lung cancer diagnosis timing in subjects with different comorbidities ($p<0.001$)

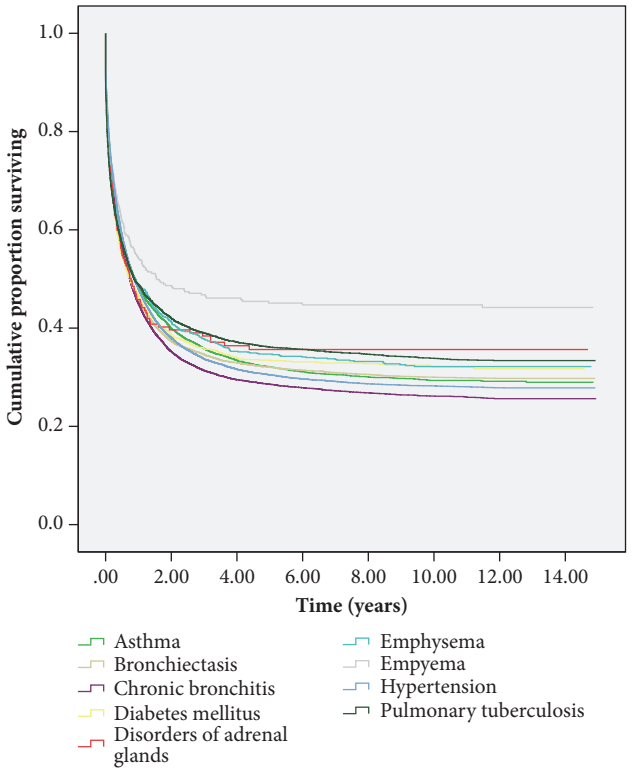

(d) Overall survival of lung cancer patients with different comorbidities ($p<0.001$)

Figure 3: Kaplan–Meier survival curve of lung cancer patients with and without comorbidity over the 16-year follow-up period.

and COPD on decreased survival in lung cancer, gender differences in the survival of patients with different lung cancer types and preexisting asthma or COPD were reported in Taiwan. A study that involved enrolling 5406 squamous cell carcinoma patients from Taiwan demonstrated a hazard ratio for mortality of 1.08 and 1.04 for participants with asthma and COPD, respectively. Furthermore, female stage I and II squamous cell carcinoma patients with preexisting asthma had a hazard ratio of 0.19, suggesting decreased mortality for these patients [10]. In another study including 13,399 patients with lung adenocarcinoma, the hazard ratios for male adenocarcinoma patients with asthma and COPD were 1.20 and 1.32, whereas for female patients they were 1.05 and 0.97, respectively. In particular, male patients with lung adenocarcinoma and preexisting pulmonary diseases exhibited an increased mortality risk, whereas female patients demonstrated no change in mortality risk [25]. Therefore, the burden of preexisting pulmonary comorbidities and their effects on survival of specific lung cancer types should be investigated further.

In addition, our analyses of lung cancer establishment of the diagnosis in comorbidity patients revealed that time period for lung cancer diagnosis in tuberculosis patients was shorter than those with asthma and COPD. Previous findings reported higher HRs for tuberculosis than for asthma and COPD [26]. The survival in those patients with coexisting TB and lung cancer remains inconclusive [11, 27]. We found lung cancer patients with preexisting TB had higher overall survival than those with other pulmonary comorbidities. In this study, the overall survival of lung cancer patients with preexisting adrenal glands disorder was 35.6% after ten years since cancer diagnosis. Currently, the data required for exploring the association between adrenal gland disorders and lung cancer are limited. The relevant literature indicates that approximately 30% of all small-cell lung cancer (SCLC) cases are associated with the hypersecretion of adrenocorticotrophic hormone (ACTH) [28]. Patients with SCLC associated with ectopic ACTH production exhibit low responses to chemotherapy and high rates of complication to therapy [29], which may shorten survival. The management of these patients is extremely complex. Future studies should focus on establishing the mortality risk of lung cancer in these patients. In this study, overall survival of lung cancer patients with bronchiectasis was 32% and 30% after five and ten years since cancer diagnosis, respectively. Only few studies have examined the association between lung cancer and noncystic fibrosis bronchiectasis, a representative chronic airway inflammatory disease. A cohort study in Taiwan reported that patients with bronchiectasis had a 2.36-fold higher risk of lung cancer than did the general population [12]. Kim et al. observed that the concomitant presence of bronchiectasis in advanced COPD patients was associated with lower risk of lung cancer [30]. This is a crucial area for future research, given the potential for learning more on reported protective effects of concomitant bronchiectasis on lung cancer diagnosis timing and survival.

In Taiwan, after the implementation of the NHI program in 1995, the number of diagnosed cancer cases increased, with lung cancer being one of 10 leading cancers [31]. Present study found geographic and urbanization variations in lung cancer mortality across Taiwan. In comparison to China, where rural areas with limited health care resources have higher cancer incidence and mortality [32], we found higher mortality among patients residing in urbanized areas of northern, central, and southern Taiwan compared with those in rural areas. Notably, the most high polluting industries, such as the petroleum, petrochemical, iron, steel, pig farming, and energy industries, are located in the areas of central [33] and southern [34] Taiwan. Moreover, a higher incidence of lung cancer has been reported in the endemic arseniasis areas of southwestern [35] and northeastern Taiwan [36, 37].

Following the promulgation of the Cancer Control Act in 2003, a 5-year national cancer control program was implemented in 2005 in Taiwan. Subsequently, the incidence of certain cancers, including cervical, stomach, and nasopharyngeal cancers [31], has reduced in Taiwan. This decline is attributable to the successful nationwide screening programs launched by the Taiwan government for cervical, oropharyngeal, colon and rectal cancers, and nationwide HBV vaccination. By contrast, no universal screening program has been implemented in Taiwan for lung cancer. Currently, lung cancer screening is included only as a part of the regular chest X-ray survey for pulmonary tuberculosis [38]. Therefore, the Taiwan government should consider promoting early diagnosis of potential high-risk individuals, for instance, implementing low-dose CT for high-risk patients with systemic diseases.

The major strengths of this study are the large number of included population-based cases and controls, high validity of the cancer diagnoses, and focus on health care services utilization. Nonetheless, the study has some limitations. First, we could not confirm early cancer diagnoses in patients with comorbidity based on their cancer stages because the NHIRD does not contain comprehensive data on cancer staging and treatment modalities in cancer patients; these data are recorded in the Taiwan Cancer Registry Database. Second, the period of 6 months before cancer diagnosis allowed for comorbidity diagnosis is insufficient for the monitoring of some chronic diseases; this may have limited the early cancer screening opportunities in some patients. Third, because of the inherent limitations of the NHIRD, information regarding the status of comorbid conditions was lacking.

In conclusion, different comorbid conditions will have unique effects and a given comorbidity can affect cancer care at multiple points in the cancer care decision making. We reported the significant outcome of lower mortality in lung cancer patients with comorbidity compared with those without comorbidity in 10 years after establishment of diagnosis. Patients with comorbidity required more frequent physician visits and greater opportunity to undergo screening which may assist in early cancer diagnosis. According to our findings, physicians should use caution regarding comorbidity in lung cancer patients, including regular monitoring of those with chronic conditions to facilitate early detection of lung cancer. The adverse consequences of comorbidity pose a major clinical challenge in the care of older cancer patients. Health services research that focuses on specific

comorbidities and their effects in a cancer patient's clinical treatment decisions can produce new insights into the optimal diagnosis, treatment, and long-term surveillance of cancer patients with comorbid disease.

Data Availability

The data used to support the findings of this study are available from the corresponding author upon request.

Conflicts of Interest

The authors declare no competing financial interests.

Authors' Contributions

Nai-Chia Teng and Kung-Min Wang designed the study, Shinechimeg Dima and Kun-Huang Chen analyzed the data and prepared tables and figures, Shinechimeg Dima drafted the manuscript, and Kung-Jeng Wang revised the manuscript. All authors reviewed the manuscript.

References

[1] Stewart, W. Bernard, P. Kleihues, and International Agency for Research on Cancer, *World cancer report*, vol. 57, IARC press Lyon, 2003.

[2] A. Jemal, F. Bray, M. M. Center, J. Ferlay, E. Ward, and D. Forman, "Global cancer statistics," *CA: A Cancer Journal for Clinicians*, vol. 61, no. 2, pp. 69–90, 2011.

[3] J. Ferlay, H. R. Shin, F. Bray, D. Forman, C. Mathers, and D. M. Parkin, "Estimates of worldwide burden of cancer in 2008: GLOBOCAN 2008," *International Journal of Cancer*, vol. 127, no. 12, pp. 2893–2917, 2010.

[4] Taiwan Cancer Registry, "Promoting Your Health," https://www.hpa.gov.tw.

[5] D. R. Youlden, S. M. Cramb, and P. D. Baade, "The international epidemiology of lung cancer: geographical distribution and secular trends," *Journal of Thoracic Oncology*, vol. 3, no. 8, pp. 819–831, 2008.

[6] A. López-Encuentra, "Comorbidity in operable lung cancer: A multicenter descriptive study on 2992 patients," *Lung Cancer*, vol. 35, no. 3, pp. 263–269, 2002.

[7] M. L. G. Janssen-Heijnen, R. M. Schipper, P. P. A. Razenberg, M. A. Crommelin, and J.-W. W. Coebergh, "Prevalence of comorbidity in lung cancer patients and its relationship with treatment: A population-based study," *Lung Cancer*, vol. 21, no. 2, pp. 105–113, 1998.

[8] M. Søgaard, R. W. Thomsen, K. S. Bossen, H. T. Sørensen, and M. Nørgaard, "The impact of comorbidity on cancer survival: A review," *Journal of Clinical Epidemiology*, vol. 5, no. 1, pp. 3–29, 2013.

[9] C. M. Tammemagi, C. Neslund-Dudas, M. Simoff, and P. Kvale, "Impact of comorbidity on lung cancer survival," *International Journal of Cancer*, vol. 103, no. 6, pp. 792–802, 2003.

[10] J.-Y. Huang, Z.-H. Jian, O. N. Nfor et al., "The Impact of Coexisting Asthma, Chronic Obstructive Pulmonary Disease and Tuberculosis on Survival in Patients with Lung Squamous Cell Carcinoma," *PLoS ONE*, vol. 10, no. 7, 2015.

[11] C.-H. Kuo, C.-Y. Lo, F.-T. Chung et al., "Concomitant active tuberculosis prolongs survival in non-small cell lung cancer: A study in a tuberculosis-endemic country," *PLoS ONE*, vol. 7, no. 3, 2012.

[12] W.-S. Chung, C.-L. Lin, W.-H. Hsu, and C.-H. Kao, "Increased risk of lung cancer among patients with bronchiectasis: A nationwide cohort study," *QJM: An International Journal of Medicine*, vol. 109, no. 1, Article ID hcu237, pp. 17–25, 2016.

[13] C.-J. Chiang, W.-C. Lo, Y.-W. Yang, S.-L. You, C.-J. Chen, and M.-S. Lai, "Incidence and survival of adult cancer patients in Taiwan, 2002–2012," *Journal of the Formosan Medical Association*, vol. 115, no. 12, pp. 1076–1088, 2016.

[14] M. Lüchtenborg, E. Jakobsen, M. Krasnik, K. M. Linklater, A. Mellemgaard, and H. Møller, "The effect of comorbidity on stage-specific survival in resected non-small cell lung cancer patients," *European Journal of Cancer*, vol. 48, no. 18, pp. 3386–3395, 2012.

[15] E. Pagano, C. Filippini, D. Di Cuonzo et al., "Factors affecting pattern of care and survival in a population-based cohort of non-small-cell lung cancer incident cases," *Cancer Epidemiology*, vol. 34, no. 4, pp. 483–489, 2010.

[16] B. H. Grønberg, S. Sundstrøm, S. Kaasa et al., "Influence of comorbidity on survival, toxicity and health-related quality of life in patients with advanced non-small-cell lung cancer receiving platinum-doublet chemotherapy," *European Journal of Cancer*, vol. 46, no. 12, pp. 2225–2234, 2010.

[17] S. O. Dalton, B. L. Frederiksen, E. Jacobsen et al., "Socioeconomic position, stage of lung cancer and time between referral and diagnosis in Denmark, 2001-2008," *British Journal of Cancer*, vol. 105, no. 7, pp. 1042–1048, 2011.

[18] S. Wang, M. L. Wong, N. Hamilton, J. B. Davoren, T. M. Jahan, and L. C. Walter, "Impact of age and comorbidity on non - Small-cell lung cancer treatment in older veterans," *Journal of Clinical Oncology*, vol. 30, no. 13, pp. 1447–1455, 2012.

[19] D. H. Ahn, N. Mehta, J. T. Yorio, Y. Xie, J. Yan, and D. E. Gerber, "Influence of medical comorbidities on the presentation and outcomes of stage I-III non-small-cell lung cancer," *Clinical Lung Cancer*, vol. 14, no. 6, pp. 644–650, 2013.

[20] B.-Y. Wang, J.-Y. Huang, C.-Y. Cheng, C.-H. Lin, J.-L. Ko, and Y.-P. Liaw, "Lung cancer and prognosis in taiwan: A population-based cancer registry," *Journal of Thoracic Oncology*, vol. 8, no. 9, pp. 1128–1135, 2013.

[21] J. S. Chang, L.-T. Chen, Y.-S. Shan et al., "Comprehensive Analysis of the Incidence and Survival Patterns of Lung Cancer by Histologies, Including Rare Subtypes, in the Era of Molecular Medicine and Targeted Therapy: A Nation-Wide Cancer Registry-Based Study From Taiwan," *Medicine*, vol. 94, no. 24, p. e969, 2015.

[22] P. A. Vaeth, W. A. Satariano, and D. R. Ragland, "Limiting Comorbid Conditions and Breast Cancer Stage at Diagnosis," *The Journals of Gerontology. Series A, Biological Sciences and Medical Sciences*, vol. 55, no. 10, pp. M593–M600, 2000.

[23] S. Yasmeen, G. Xing, C. Morris, R. T. Chlebowski, and P. S. Romano, "Comorbidities and mammography use interact to explain racial/ethnic disparities in breast cancer stage at diagnosis," *Cancer*, vol. 117, no. 14, pp. 3252–3261, 2011.

[24] C. P. Gross, M. S. Andersen, H. M. Krumholz, G. J. McAvay, D. Proctor, and M. E. Tinetti, "Relation between medicare screening reimbursement and stage at diagnosis for older patients with colon cancer," *The Journal of the American Medical Association*, vol. 296, no. 23, pp. 2815–2822, 2006.

[25] Z.-H. Jian, J.-Y. Huang, P.-C. Ko et al., "Impact of coexisting pulmonary diseases on survival of patients with lung adenocarcinoma: A STROBE-compliant article," *Medicine (United States)*, vol. 94, no. 4, 2015.

[26] Z.-H. Jian, C.-C. Lung, J.-Y. Huang et al., "The coexistence of common pulmonary diseases on the histologic type of lung cancer in both genders in Taiwan," *Medicine (United States)*, vol. 93, no. 27, article no. e127, 2014.

[27] Y. Zhou, Z. Cui, X. Zhou et al., "The presence of old pulmonary tuberculosis is an independent prognostic factor for squamous cell lung cancer survival," *Journal of Cardiothoracic Surgery*, vol. 8, no. 1, 2013.

[28] B. Mennecier, L. Moreau, B. Goichot, G. Pauli, and E. Quoix, "Paraneoplastic Cushing syndrome and small-cell lung cancer," *Revue de Pneumologie Clinique*, vol. 55, no. 2, pp. 77–80, 1999.

[29] F. A. Shepherd, J. Laskey, W. K. Evans, P. E. Goss, E. Johonsen, and F. Khamsi, "Cushing's syndrome associated with ectopic corticotropin production and small-cell lung cancer," *Journal of Clinical Oncology*, vol. 10, no. 1, pp. 21–27, 1992.

[30] Y. W. Kim, K.-N. Jin, E. Y. Heo, S. S. Park, H. S. Chung, and D. K. Kim, "The association between combined non-cystic fibrosis bronchiectasis and lung cancer in patients with chronic obstructive lung disease," *International Journal of Chronic Obstructive Pulmonary Disease*, vol. 10, pp. 873–879, 2015.

[31] C. J. Chiang, Y. C. Chen, and C. J. Chen, "Cancer trends in Taiwan," *Japanese Journal of Clinical Oncology*, vol. 40, no. 10, pp. 897–904, 2010.

[32] W. Chen, R. Zheng, P. D. Baade et al., "Cancer statistics in China, 2015," *CA: A Cancer Journal for Clinicians*, vol. 66, no. 2, pp. 115–132, 2016.

[33] Y.-M. Chen, W.-Y. Lin, and C.-C. Chan, "The impact of petrochemical industrialisation on life expectancy and per capita income in Taiwan: an 11-year longitudinal study," *BMC Public Health*, vol. 14, no. 1, article 247, 2014.

[34] H. K. Wang, C. H. Huang, K. S. Chen, Y. P. Peng, and C. H. Lai, "Measurement and source characteristics of carbonyl compounds in the atmosphere in Kaohsiung city, Taiwan," *Journal of Hazardous Materials*, vol. 179, no. 1-3, pp. 1115–1121, 2010.

[35] H.-Y. Chiou, Y.-M. Hsueh, K.-F. Liaw et al., "Incidence of internal cancers and ingested inorganic arsenic: a seven-year follow-up study in Taiwan," *Cancer Research*, vol. 55, no. 6, pp. 1296–1300, 1995.

[36] C.-L. Chen, H.-Y. Chiou, L.-I. Hsu, Y.-M. Hsueh, M.-M. Wu, and C.-J. Chen, "Ingested arsenic, characteristics of well water consumption and risk of different histological types of lung cancer in northeastern Taiwan," *Environmental Research*, vol. 110, no. 5, pp. 455–462, 2010.

[37] C.-L. Chen, L.-I. Hsu, H.-Y. Chiou et al., "Ingested arsenic, cigarette smoking, and lung cancer risk: A follow-up study in arseniasis-endemic areas in Taiwan," *Journal of the American Medical Association*, vol. 292, no. 24, pp. 2984–2990, 2004.

[38] C.-J. Chen, S.-L. You, L.-H. Lin, W.-L. Hsu, and Y.-W. Yang, "Cancer epidemiology and control in Taiwan: a brief review," *Japanese Journal of Clinical Oncology*, vol. 32, supplement, pp. S66–S81, 2002.

Hindawi
BioMed Research International
Volume 2018, Article ID 9836256, 14 pages
https://doi.org/10.1155/2018/9836256

Review Article

Onco-Multi-OMICS Approach: A New Frontier in Cancer Research

Sajib Chakraborty,[1] **Md. Ismail Hosen**,[1] **Musaddeque Ahmed**,[2] **and Hossain Uddin Shekhar**[1]

[1]*Department of Biochemistry and Molecular Biology, University of Dhaka, Dhaka 1000, Bangladesh*
[2]*Princess Margaret Cancer Centre/University Health Network, Toronto, Ontario, Canada*

Correspondence should be addressed to Sajib Chakraborty; sajib@du.ac.bd and Hossain Uddin Shekhar; hossainshekhar@du.ac.bd

Received 4 July 2018; Accepted 6 September 2018; Published 3 October 2018

Academic Editor: Luenda Charles

The acquisition of cancer hallmarks requires molecular alterations at multiple levels including genome, epigenome, transcriptome, proteome, and metabolome. In the past decade, numerous attempts have been made to untangle the molecular mechanisms of carcinogenesis involving single OMICS approaches such as scanning the genome for cancer-specific mutations and identifying altered epigenetic-landscapes within cancer cells or by exploring the differential expression of mRNA and protein through transcriptomics and proteomics techniques, respectively. While these single-level OMICS approaches have contributed towards the identification of cancer-specific mutations, epigenetic alterations, and molecular subtyping of tumors based on gene/protein-expression, they lack the resolving-power to establish the casual relationship between molecular signatures and the phenotypic manifestation of cancer hallmarks. In contrast, the multi-OMICS approaches involving the interrogation of the cancer cells/tissues in multiple dimensions have the potential to uncover the intricate molecular mechanism underlying different phenotypic manifestations of cancer hallmarks such as metastasis and angiogenesis. Moreover, multi-OMICS approaches can be used to dissect the cellular response to chemo- or immunotherapy as well as discover molecular candidates with diagnostic/prognostic value. In this review, we focused on the applications of different multi-OMICS approaches in the field of cancer research and discussed how these approaches are shaping the field of personalized oncomedicine. We have highlighted pioneering studies from "The Cancer Genome Atlas (TCGA)" consortium encompassing integrated OMICS analysis of over 11,000 tumors from 33 most prevalent forms of cancer. Accumulation of huge cancer-specific multi-OMICS data in repositories like TCGA provides a unique opportunity for the systems biology approach to tackle the complexity of cancer cells through the unification of experimental data and computational/mathematical models. In future, systems biology based approach is likely to predict the phenotypic changes of cancer cells upon chemo-/immunotherapy treatment. This review is sought to encourage investigators to bring these different approaches together for interrogating cancer at molecular, cellular, and systems levels.

1. Introduction to "OMICS" Technologies

"OMICS" technologies are characterized by high-throughput interfaces which facilitate the investigation of genome, epigenome, transcriptome, proteome, and metabolome in a global-unbiased manner. OMICS techniques are now being used to understand the intricate biological systems and uncover the molecular signatures underlying the complex cellular phenotypes [1, 2]. Different OMICS approaches were developed to untangle the complexity of biological systems at different dimensions (e.g., gene, RNA, and protein levels). Recent advancements of OMICS techniques have been proved to be the weapon of choice to dissect the aberrant cellular functions that lay in the heart of multifactorial diseases such as cancer [1].

1.1. Increase of Complexity from Genome to Proteome. The different OMICS levels—Genomics, Transcriptomics, and Proteomics—vary greatly in their complexity that is largely driven by the spatial- and/or temporal dynamics and chemical modifications (Figure 1). The flow of information from

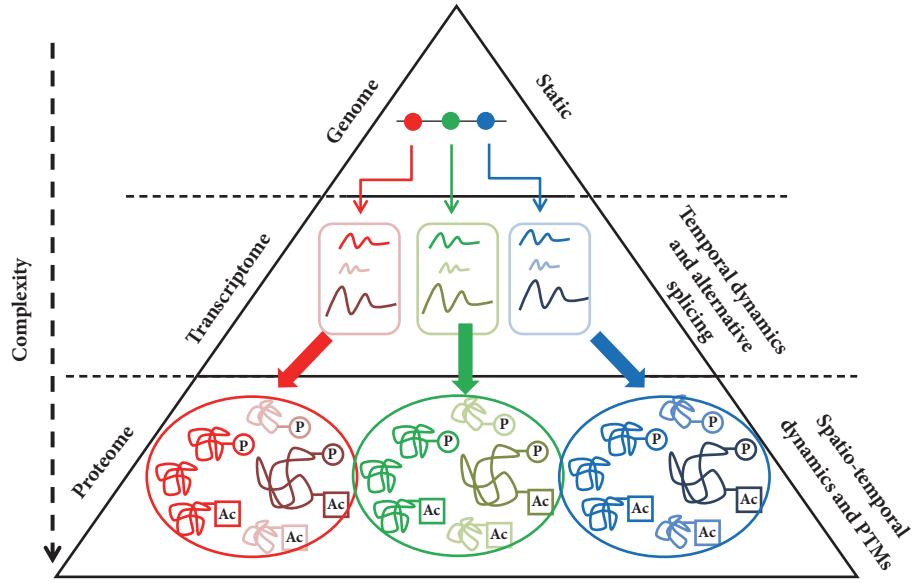

FIGURE 1: **Pyramid of complexity.** The pyramid represents the flow of information from genome (top) to transcriptome (middle), to proteome (bottom). The complexity increases from genome to proteome (indicated by down arrow). The complexity of transcriptome is largely mediated by temporal dynamics and alternative splicing. In contrast, spatiotemporal dynamics and posttranslational modifications (PTMs) are mainly responsible for high proteome complexity. Examples of PTMs include phosphorylation (P) and acetylation (Ac).

DNA to RNA and ultimately to protein is accompanied by an exponential increase in the complexity. The hereditary information stored in the genome in the form of 4 nucleotides remains largely static but temporal dynamics is introduced in the process of transcription by which genes are transcribed into RNAs. Orchestration of temporal regulation of gene expression depending on developmental, environmental, and extracellular cues via gene-regulatory networks makes the transcriptome a highly dynamic entity [3]. Alternative splicing in addition to temporal dynamics increases the complexity of transcriptome. mRNAs are engaged into even more complex information coding systems: translation process where mRNAs encode for proteins comprising 20 amino acids. After synthesis, proteins are typically folded into many possible conformations depending on the primary amino acid sequences and chemical modification of amino acid residues known as posttranslational modifications (PTMs). Proteins undergo a large number of PTMs (e.g., phosphorylation, acetylation, and glycosylation) that may directly affect their structure and functionality. Moreover, unlike mRNAs which are synthesized in nucleus and translated in cytoplasm, proteins have different subcellular localizations such as cell membrane, cytoplasm, and different membrane bound subcellular organelles—nucleus, mitochondria, endoplasmic reticulum, etc. Altogether these events confer huge complexity to the proteome. Two most important technologies—next-generation sequencing (NGS) and mass-spectrometry (LC-MS/MS)—have revolutionized the field of OMICS by deciphering the human genome, transcriptome, and proteome. Schematic diagram representing the typical workflow of NGS (left panel) and mass-spectrometry (right panel) experiments is shown in Figure 2.

1.2. Next-Generation Sequencing Based Approaches: Genomics, Epigenomics, and Transcriptomics. In recent years, the genomics-techniques are mostly dedicated to sequence the genome of an individual to understand the interindividual variations at both the germline and somatic levels. The eventual graduation of the sequencing technologies from the Sanger sequencing based approaches to the NGS-based massively parallel sequencing has enabled researchers to sequence the genome/exome of interest deeply enough to characterize the mutational landscapes of a given tissue. For example, in a large scale project known as "The Cancer Genome Atlas (TCGA)", the scientists employed the NGS coupled with downstream bioinformatics analysis to discover somatic mutational landscape across thousands of tumor samples representing major cancer types under the assumption that these genome-wide mutational studies would be pivotal in understanding complexity of different cancer [4, 5].

Epigenomics is defined by the genome-wide identifications of chemical modifications such as methylation and acetylation of DNA and/or DNA-binding histone proteins. Epigenetic-modifications of DNA and histones proteins serve as a major regulatory mechanism controlling gene expression and cellular phenotypes [6]. The epigenomics studies have played integral role in uncovering the disease-associated epigenetic markers. Epigenomics techniques that are widely used include chromatin immunoprecipitation (ChIP) assays coupled NGS commonly known as ChIP-Sequencing or ChIP-seq and methylation analysis through whole-genome bisulfite/array-based sequencing. ChIP-Seq has been developed as a powerful tool for the identification of DNA-binding sites for transcription factors (TFs) and

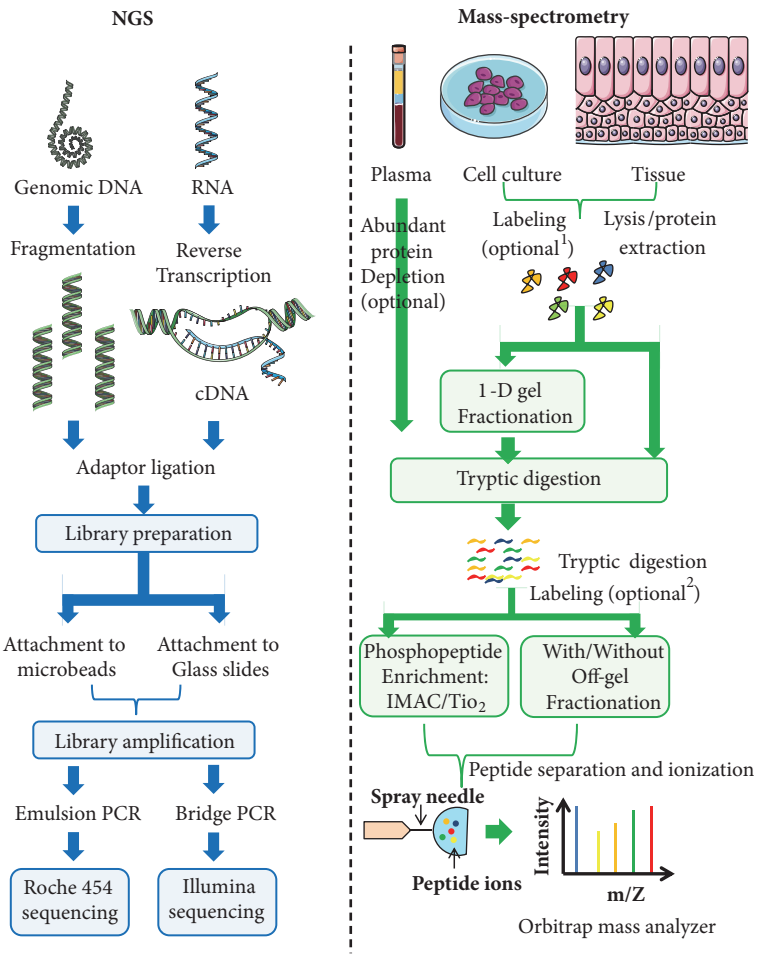

FIGURE 2: **Schematic diagram representing the basic steps of NGS and mass-spectrometry.** NGS (left) can be used for both genomic DNA and RNA-sequencing. Mass-spectrometry based proteomics (right) are typically used to identify and quantify large amount of proteins from cells, tissues, and body fluids. [1]Primary cells and tissues from patients can be mixed with labelled proteins, typically extracted from cell lines cultured in presence of stable isotopically labelled amino acids. This method is called Super-SILAC. Proteomics can also be done without any labelling steps. This method is known as label free-quantification (LFQ). [2]Peptides obtained after tryptic digestion can also be labelled chemically by methods known as "Tandem Mass Tag (TMT)" or "Isobaric tags for relative and absolute quantitation (iTRAQ)".

histone proteins in a genome-wide manner to construct high-resolution genome-wide maps of histone modification marks. ChIP-seq follows a straightforward protocol where DNA-bound proteins are typically immunoprecipitated by specific antibody followed by the extraction, purification, and sequencing of the bound DNA. In recent years application of ChIP-seq has enabled us to gain deep-insights into gene-regulatory events that are responsible for various diseases and biological pathways, such as cancer progression and development, respectively. By comparing these genome-wide profiles of histone modifications marks between cancer and normal tissues it has been possible to understand how epigenetic deregulation manifested in various cancers such as breast [7] and lung [8]. Apart from histone modifications, chemical modifications in certain DNA base can have dramatic epigenetic effects. For instance, chemical modification of Cytosine residue in the promoter DNA sequence of genes can modify their expression. By harnessing the power of NGS, it is now possible to analyze genome-wide methylome patterns at a single nucleotide resolution. Whole-genome bisulfite sequencing (WGBS) or Bisulfite sequencing (BS-Seq) in short is a powerful technology that can detect the methylated Cytosine bases in genomic DNA. In brief the method involves the treatment of genomic DNA with sodium bisulfite followed by sequencing to construct a genome-wide map of methylated Cytosine with single-base resolution. Apart from this, a relatively novel technique known as MBD-isolated Genome Sequencing (MiGS) has recently been used to analyze whole-genome methylation pattern [9]. This technique relies on the precipitation of methylated DNA by recombinant methyl-CpG binding domain of MBD2 protein followed by sequencing. A study by Vidal et al. investigated the genome-wide methylation analysis of 1112 primary tumors of various cancers types where the authors identified hypermethylated promoters and enhancers that regulate the expression of tumor-suppressor genes and concluded that changes in DNA methylation pattern tend to occur in the onset, progression, and dissemination of cancer [10].

Transcriptomics techniques are engaged in the detection of the presence and quantification of RNA transcripts especially mRNAs but can also be extended to other types of noncoding RNA transcripts such as long noncoding transcripts (LncRNAs) and microRNAs. Transcriptome in a particular cell includes all RNA molecules that are transcribed from the genome at a given time. In contrast to the genome, which is static in nature, the transcriptome is subjected to change depending on cellular, environment, extracellular, and developmental stimuli in temporal manner. Before the advent of NGS, microarray was used as the conventional laboratory technique to detect the changes in the mRNA levels within the cells at different stages in a high-throughput manner. Microarrays can typically be used to quantify the relative abundance of mRNAs for thousands of genes simultaneously. By this technique, it is possible to construct cellular or tissue gene expression profiles between normal and cancer states which may facilitate the identification of genes that exhibit differential expression between normal and cancer states.

Leveraged by the development of efficient NGS techniques, the cutting edge "Transcriptomics" technique—RNA-sequencing (RNA-seq)—can identify the presence as well as the abundance of RNA transcripts in an unbiased genome-wide manner (Figure 2). Unlike microarrays, RNA-seq technology does not rely upon the transcript-specific probes and thus can successfully perform the unbiased detection of novel transcripts. The other advantages that the RNA-seq offers over microarrays include broad dynamic range, increased specificity/sensitivity, and detection of low abundant transcripts. RNA-Seq analysis has shown that the mammalian transcriptional landscape is much more complex than was previously imagined before. Apart from diverse range of protein-coding RNAs and well established regulatory RNAs such as microRNAs, different types of noncoding RNAs (ncRNAs) are pervasively transcribed from the vast majority of noncoding regions of the genome including intergenic and intronic sequences [11]. The recent influx of huge RNA-seq data has revealed a differential gene expression pattern between various types of cancer tissues and their normal counterparts and thus harbors the potential to uncover the intricate molecular mechanisms to understand the progression of cancer [12]. The huge data repositories such TCGA offer the opportunity to reanalyze the OMICS data by a pan-cancer approach where different types of cancers can be compared and contrasted in terms of genomic and transcriptomic landscapes [13]. Li et al. comprehensively analyzed the gene expression profiles across 33 human cancer types from the TCGA database and identified up- and downregulated genes that exhibited remarkable consistency across different cancer [12]. Table 1 represents summary of the applications of different NGS-based OMICS techniques.

1.3. Mass-Spectrometry (LC-MS/MS) Based Techniques: Proteomics and Metabolomics. While transcriptomics is dedicated to the measurement of RNA transcripts, proteomics is specialized in the identification and quantification of the proteins that are present at a given time in biological samples. Unlike the transcriptomics, quantification of the proteome requires special strategies, since the identification and quantification of proteins in large scale are challenging due to the high complexity and dynamic range of the proteome. Transcriptomics platforms such as RNAseq-based approaches are designed to reveal the information at the transcriptome level that in turn shapes the proteome to carry out the functional cellular processes. Since most of the biological processes are controlled by proteins, it is important to reliably and accurately measure proteome alterations in aberrant cellular state such as in a cancer context to understand how cellular processes are carried out mechanistically. However, genome-wide proteomics data for cancer is exasperatingly limited. To tackle this problem as a part of TCGA a protein-expression dataset for a large number of tumor samples and cell lines has been generated using reverse-phase protein arrays (RPPAs) which is called The Cancer Proteome Atlas (TCPA)" [14]. TCPA utilized antibodies to detect and quantify nearly 200 proteins and phosphoproteins across large number of TCGA tumor samples. The major limitation of the antibody based methods is the nonspecificity of the antibodies and low-throughput. Advancements of the tandem mass-spectrometry (LC-MS/MS) techniques at the level of MS resolution, accurate quantitation, and data analysis has made it a solid platform for simultaneous identification and quantification of the proteome of a cell [15]. The aim of quantitative proteomics is to obtain reliable quantitative information about all the proteins that fall within the mass-spectrometric dynamic range. In recent years the advent of cutting edge high-resolution "Orbitrap" mass-spectrometer instruments coupled with powerful computational platforms such as MaxQuant [16] facilitated the genome-wide identification and quantification of nearly all expressed proteins (roughly 18,000 proteins) in human cells and tissues which paved the foundation for the construction of the first draft of the human proteome [17, 18]. The application of mass-spectrometry based proteomics techniques has recently been extended to investigate the proteome alteration in various human cancer tissues [19]. However, unlike genomics and transcriptomics, mass-spectrometry (LC-MS/MS) based deep-proteomics techniques are under development to be routinely applicable in clinical settings. Nevertheless the promise this technology holds to identify novel diagnostic and prognostic biomarkers for cancer is enormous. Applications of mass-spectrometry-based OMICS techniques are summarized in Table 1.

The application of mass-spectrometric techniques is not limited to proteins and peptides but rather can be extended to small molecules such as metabolites. While proteomics covers the analysis of proteins, metabolomics on the other hand is characterized by the quantifications of metabolites that are synthesized as products of cellular metabolic activities, such as amino acids, fatty acids, carbohydrates, and lipids. The levels of metabolites and/or ratios of certain metabolites can be altered in disease states and thus reflect aberrant metabolic functions in complex diseases such as cancer [1, 20]. Metabolomics, though a relatively new field of OMICS, powered by the mass-spectrometry (LC-MS/MS) technology is beginning to provide biological insights into the changes of diverse metabolic pathways and fluxes in diseases states [21]. However, there are certain challenges (such as unknown

Table 1: Different omics techniques and their applications.

Omics	Type	Principle	Throughput	Application
Genomics	Whole exome sequencing	NGS	high	Genome-wide mutational/ analysis
	Whole genome sequencing	NGS	high	Exome-wide mutational analysis
	Targeted gene/exome sequencing	Sanger-sequencing	Low	Mutational analysis in targeted gene/exon
Epigenomics	Methylomics	Whole-genome bisulfite sequencing	High	Genome-wide mapping of DNA methylation pattern
	ChIP-sequencing	Chromatin IP∗ and NGS	high	Genome-wide mapping of epigenetic marks
Transcriptomics	RNA-sequencing	NGS	High	Genome-wide differential gene expression analysis
	microarray	Hybridization	High	Differential gene expression analysis
Proteomics	RPPA	Antibody based	Low	Differential protein abundance analysis
	Deep-proteomics	Mass-spectrometry	high	Genome-wide differential protein expression analysis
Metabolomics	Deep-metabolomics	Mass-spectrometry	high	Differential metabolite expression analysis

metabolite identification, enormous diversity of metabolites and reproducibility) that must be overcome to materialize the full potential of mass-spectrometry-based metabolomics. The field of metabolomics is still emerging and embraces the potential to be highly effective in the discovery of biomarkers for cancer diagnosis and progression.

All the OMICS levels are important to decipher the complex phenotype of cells and organisms. Understanding the molecular basis of cellular phenotypes involving genes, RNA transcripts, proteins, and metabolites is particularly important because it not only gives an opportunity to predict the phenotypic alteration by examining the molecular signatures but also may serve as an unbiased platform to identify targets for therapeutic interventions. The next step towards the technological advances of OMICS fields would be to decrease sample processing/measurement time and increase reproducibility to firmly establish these techniques in clinical settings for diagnosis and prognosis of cancer.

2. Advantages of OMICS-Driven Studies in Cancer Context

Acquisition of cancer hallmarks allows the transition of a normal cell to malignancy. The hallmarks typically include complex phenotypic and molecular changes including uncontrolled and sustained proliferation, evading growth suppressors, resisting cell death, replicative immortality, angiogenesis, and metastasis [22]. Moreover mechanistic understanding of cancer progression though a series of experiments allowed us to get a glimpse of some other emerging hallmarks of cancer such as reprogramming of energy metabolism and evading immune destruction [22]. Attaining these hallmarks requires a series of alterations in the cellular machinery driven by molecular aberration in the genome, epigenome, transcriptome, proteome, and metabolome within cancer cells and/or tissues. For instance NGS of cancer cell genomes uncovered how activating mutations in certain proproliferative genes such as B-raf drives constitutive activation of mitogen-activated protein- (MAP-) kinase signalling which eventually manifests as uncontrolled proliferation of cells [23]. Molecular aberrations that drive the cancer are not restricted only to genomic mutational events but are extended into epigenome. For instance, silencing of certain tumor-suppressor genes can also be achieved through aberrant epigenetic mechanisms such as DNA methylation and histone modifications [24].

The hallmark—invasion and metastasis—requires the epithelial cells to undergo a transition towards mesenchymal phenotype thus enabling them to invade and migrate to distant sites for colonization. This complex phenotypic manifestation requires a complete gene-regulatory network that governs multiple genes/proteins to work in concert to achieve such dramatic changes. It has recently been shown that epithelial-mesenchymal transition (EMT) is indeed induced by certain transcription factors (TFs)—Snail, Slug, Twist, and Zeb1/2—coordinating the multistep process of invasion and metastasis [22, 25]. Transcriptomics techniques are suitable to uncover such TF-driven transcription regulatory networks that are assumed to be activated in a cancer context.

Although cell-fate decisions and phenotypic changes in cancer cells are initiated by transcriptional networks, these complex processes are executed by intracellular machineries composed of proteins. In this view, obtaining cancer hallmarks is essentially achieved by the alteration of the protein levels and/or PTMs (e.g., Phosphorylation status). For example, proproliferative signalling can be constitutively activated by upregulating the expression of the receptor proteins at the cancer cell surface [22] which can be detected

by proteomics-centric studies. Unbiased global proteomics studies conducted by Tyanova et al. generated proteomic profiles comprising 19 proteins that can be successfully used to distinguish between oestrogen receptor positive (luminal), Her2 positive, and triple negative breast tumors [26].

The manifestation of cancer hallmarks does not leave the cellular metabolism unaffected. In a counterintuitive way, cancer cells are able to reprogram glucose metabolism and subsequent energy production by restricting oxidative phosphorylation even in the presence of oxygen. This phenomenon is commonly known as Warburg effect [22, 27]. In recent times with the technological progression of mass-spectrometry instruments, we can now better understand the metabolic reprogramming of cancer in great detail. For example, recently it has been shown that certain tumors are comprised of two metabolically distinct subpopulations of cells: one subpopulation has been shown to be glucose dependent and employ metabolic reprogramming to produce lactate as presumed in classical "Warburg effect", whereas the second population channels the lactate from their neighbouring lactate producing cells as energy source for themselves [28].

All together it has now become apparent that to understand cancer progression, discover new therapeutic interventions, and develop novel cancer biomarkers we need to employ diverse OMICS strategies at multiple levels. While a single type of OMICS study can reveal a great deal of information at an unidirectional level (such as genomics can only reveal the mutational landscapes of cancer patients), the complexity of cancer-host interactions requires multi-dimensional approaches (such as genomics, epigenomics, transcriptomics, proteomics, and metabolomics) to portray the complete picture. Compared to single OMICS studies, multi-OMICS investigations have the potential to allow a deeper-understating of how the cancerous transformation is affecting the flow of information from one OMICS level to the next. Multi-OMICS approaches can bridge the link between cancerous genotype and the phenotypic characteristics.

3. Application of Multi-OMICS Approach: Success Stories So Far

Adaptation of cancer cells to a new cell-fate decision such as resisting apoptosis and phenotypic characteristics like metastatic invasion requires changes in the genome, epigenome, and gene expression profile that subsequently reshapes the proteome and metabolome to meet the challenges of altered cell-fate and phenotype. Integrating multi-OMICS profiles such as transcriptomics and proteomics offers the perfect strategy to unravel the information regarding differential abundance profile of mRNAs and proteins in varying conditions. In the following sections, we have discussed different integration approach of multi-OMICS data to understand the complexity of information processing systems in cancer cells.

3.1. Epigenomics versus Transcriptomics. The complexity of the mammalian cell is largely driven by the heritable genome constrained by epigenetic mechanism to regulate the expression of genes in different cellular contexts. This enables the cells to acquire the necessary functions for differentiation and proliferation. The epigenetic mechanisms are mediated through DNA/chromatin and histone protein modifications. In recent decades it has become apparent that the cancer epigenome harbors numerous alterations compared to their normal counterpart. For instance, genome-wide loss of methylation leading to aberrant unregulated expression of tissue specific and imprinted genes was observed to be associated with cancer [29, 30]. In line with this argument, studies have shown that hypomethylation in the promoter region of oncogenes, *RRAS, S100P*, and melanoma antigen family A1 (*MAGEA1*) activates their gene expression in gastric, pancreatic, and hepatocellular carcinoma, respectively [31]. In contrast to hypomethylation which was observed to manifest in global genome-wide manner, hypermethylation in different types of cancer occurs locally within specific segments of the genome. For instance promoter hypermethylation triggers the silencing of tumor-suppressor genes (TSGs), *BRCA1, CDKN2A*, and *MLH1*, thus making them unable to control cell cycle, apoptosis, and/or DNA repair [24, 32]. DNA-hypermethylation in CpG islands residing within promoter regions, known as CpG island methylator phenotype, has now turned out to be a tumor stratification strategy in many cancer types especially colorectal cancer [33]. Like the methylation pattern, many studies have now shown the association of altered histone modification profiles and cancer progression [30]. Aberrant epigenetic marks such as histone acetylation loss and altered H3K4, H3K9, and H3K27 methylation patterns are associated with various cancer types [30]. Since the manifestations of these epigenomic changes are essentially reflected in transcriptome level, integration of epigenomics and transcriptomics data have the potential to broaden our understanding of how molecular mechanisms initiate the acquisition of cancer hallmarks. Based on the casual relationship between methylation and gene expression it is generally accepted that hyper- and hypomethylation of promoter regions should essentially be reflected in decreased and increased expression of corresponding genes, respectively. Moreover histone methyl transferases gene, *EZH2*, was observed to be highly expressed in breast [34] and prostate cancer [35] implying bidirectional interactions between epigenome and transcriptome. Therefore in principle the reciprocal relationship between differential gene expression and epigenomic alterations can be investigated through the integration of ChIP-seq, methylomics, and RNA-seq data. Under this assumption a recent study conducted by Kelley et al. which integrated ChIP-seq and RNA-seq data obtained from patient-derived xenografts from head and neck squamous cell carcinoma (HNSCC) samples showed that H3K4me3 and H3K27ac histone marks are associated with tumor-specific transcriptional changes in their target genes including *EGFR, FGFR1, and FOXA1* [36]. Similarly another study by Bhasin et al. focused on the integration of genome-wide methylomics with publicly available RNA-seq data (obtained from TCGA) to characterize indolent and aggressive prostate cancer [37]. Here the

authors identified certain differentially methylated regions (DMRs) within the promoter (e.g., *CCDC8*) and gene-body (e.g., *HOXC4*) of certain genes which showed strong negative and positive correlations, respectively with gene expression. These findings point towards a more complex scenario that a simple on- and off-state of genes is associated with the absence or presence of methylation. Methylation in the gene-body can also have a positive and direct correlation with gene expression [37]. A hypothesis involving the alternative splicing regulation by DNA methylation has recently been put forward to explain the correlation between gene-body methylation and gene expression [38]. A meta-analysis involving methylomes and gene expressions from 672 matched cancer and healthy tissues obtained from TCGA showed that hypermethylation in certain genomic regions is not necessarily linked to a decrease in expression of the corresponding genes [39]. This finding points towards the fact that genes may exhibit an unchanged expression even if their promoter region is methylated. New emerging hypotheses such as promoter cross-talk through a shared enhancer [40] and switching of promoter and enhancer domains [41] are proposed to suggest novel association mechanisms between genomic imprinting and gene expression for Nctc1 and Tet1/Tet2 genes, respectively. Whether this discordant relationship between methylation and gene expression is achieved by gene-specific or global mechanisms controlling gene expression bypassing the methylation status in cancer remains to be elucidated. Whatever the mechanisms underlying the discordance between epigenome and transcriptome are, these fundamental features of cancer cells can only be solved by harnessing the power of multi-OMICS technology.

3.2. Transcriptomics versus Proteomics. Over the last decade several large scale multi-OMICS studies involving transcriptomics and proteomics in mammalian cells demonstrated that the translational rate is the major contributor for the variation in protein abundance [18, 42, 43]. Earlier studies involving mass-spectrometry and microarray/mRNA sequencing (mRNA-seq) for the quantification of protein and mRNA levels of several thousand genes demonstrated the absence of a strong correlation between mRNA and protein levels. Rather mRNA and proteins levels showed moderate to poor correlation (coefficient of correlation $R \leq 0.4$) [18, 42, 44]. This moderate correlation reflects that less than 40% variance on the protein levels is attributed to the mRNA levels. The remaining variance (>60%) is then essentially considered as the manifestation of differences in translational rate and protein degradation. In addition, using the information about degradation rates for mRNAs and proteins Schwanhäusser et al. estimated that transcription, mRNA degradation, translation, and protein degradation explains 34%, 6%, 55%, and 5% of protein abundance variation highlighting the role of translation as a dominant factor for regulating protein abundance [42, 44]. Schwanhäusser et al. showed that the translational rate can be considered as the most dominant factor governing the protein abundance. Although mRNA and protein levels may vary between cell types or tissues, the protein-to-mRNA ratio has been found to be highly conserved across twelve different human tissues for any given gene [18]. This conservation of the gene-specific protein-to-mRNA ratio showed the translational rate as an inherent and constant phenomenon for mRNA. Wilhelm et al. utilized this conserved protein-to-mRNA ratio for predicting the protein abundance for a gene in any given tissue from experimental mRNA abundance. Using the median protein-to-mRNA ratios per gene across twelve tissues, it was possible to predict protein levels from mRNA levels for every tissue. As a validation strategy they compared predicted protein abundance with experimental data to show strong correlation highlighting the role of translational rates defining the protein abundance [18]. However, it has not been investigated if the protein-to-mRNA ratios change or remain constant over time in highly evolving cells such as tumor cells. Therefore investigation of gene-specific protein-to-mRNA ratios in cancer cells in a temporal manner is necessary to uncover the dynamic interrelationship between transcriptome and proteome. The majority of the multi-OMICS studies directed towards deciphering the complex relation between transcriptome and proteome was performed in the context of steady state levels of proteins and mRNAs [17, 42, 44]. Studies of the transcriptome-proteome relationship under dynamic conditions are essential to understand how the information is propagated through these levels and ultimately contributes to the determination of cell-fate decisions. In order to dissect the individual roles of transcriptome and proteome in the context of dynamic cellular response, Jovanovic et al. showed that induction of novel cellular function in response to external stimuli is largely controlled by transcriptional alteration followed by proteome adaptations. In contrast the regulation of protein synthesis and degradation is mainly responsible for the maintenance of preexisting cellular functions [45]. However, with the cessation of the dynamic response, cells approach a new steady state. How cells maintain the newly acquired cellular function in a cancer context in the new steady state remains to be elucidated.

Transcriptome and proteome interrogations have been performed to decipher the aberrant molecular mechanisms in different cancer tissues such as oral squamous cell carcinoma [46], ovarian [47], breast [26, 48], colorectal [49], and lung [50] (Table 2). All these studies sought to investigate the tumor-specific transcriptome and proteome profiles to understand how the intricate molecular mechanisms drive the phenotypic changes in tumor cells. For instance, proteome profiling of breast tumors identified a set of 19 protein markers which could be used to stratify oestrogen receptor positive (luminal), Her2 positive, and triple negative breast tumors [26]. Out of the 19 markers analyzed, nine genes including MAPK3, MCM5, STMN1, and ENO1 exhibited concordant changes in protein and mRNA levels, rendering them as potential therapeutic targets of breast cancer [26]. Another study conducted by Li et al. analyzed genomics, transcriptomics, and proteomics of 33 samples, each comprising 11 non-small-cell lung carcinoma (NSCLC) tumor tissues, patient-matched tumor-free lung tissues, and patient-derived xenograft (PDX) [50]. By integrating the multi-OMICS data the authors argued that protein abundance is not a linear function of DNA copy number and mRNA abundance.

Table 2: Multiomics studies focusing on cancer.

PMID	Tumor type	Cohort	Samples no#	Genomics	Methylomics	Transcriptomics	Proteomics	Metabolomics
28878238	OSCC[1]	Taiwanese	T=38, N=38	+		+	+	
27372738	Ovarian	TCGA[2]	T=174	+	+	+	+	
27251275	Breast	TCGA[2]	T=105	+	+	+	+	
25043054	Colorectal	TCGA[2]	T=96	+	+	+	+	
26725330	Breast	N/A	T=40			+	+	
25429762	Lung	N/A	T=11, N=11	+		+	+	
28947419	Head/Neck Tumor	N/A	T=47			+		
26628371	Prostate	N/A	Unknown		+	+		
28225065	Cervical	N/A	T=52			+		+
26545398	Prostate	N/A	T=25, N=25			+		+
27406679	Breast and HCC[3]	N/A	N[3]=105			+		+
24316975	Breast	N/A	T=67, N=65		+	+	+	+
29898407	TGCT[4]	TCGA[2]	T=137	+	+	+	+	
29100075	Soft Tissue Sarcomas	TCGA[2]	T=206	+	+	+		
29622466	GIAC[5]	TCGA[2]	T=921	+	+	+		
29925010	ccRCC[6]	TCGA[2]	T=400	+	+	+		
26544944	Prostate	TCGA[2]	T=333	+	+	+		
24476821	UBC[7]	TCGA[2]	T=131	+	+	+		
26091043	Melanoma	TCGA[2]	T=331	+	+	+		
25079317	GA[8]	TCGA[2]	T=295	+	+	+		
28052061	OEC[9]	TCGA[2]	T=164	+	+	+		
24120142	Glioblastoma	TCGA[2]	T=500	+	+	+	+	
23634996	AML[10]	TCGA[2]	T=200	+	+	+		
25079552	LUAD[11]	TCGA[2]	T=230	+	+	+		

T: Tumor, [1]OSCC: Oral Squamous Cell Carcinoma, [2]TCGA: The Cancer Genome Atlas, N: Normal, [3]HCC: Hepatocellular Carcinoma, [4]TGCT: Testicular Germ Cell Tumors, [5]GIAC: Gastrointestinal Adenocarcinomas, [6]ccRCC: Clear Cell Renal Cell Carcinoma, [7]UBC: Urothelial Bladder Carcinoma, [8]GA: Gastric Adenocarcinoma, [9]OEC: Oesophageal Carcinoma, [10]AML: Acute Myeloid Leukemia, [11]LUAD: Lung Adenocarcinoma.

Therefore mRNA and DNA copy number alteration (CNA) cannot serve as a proxy and good predictor for protein abundance. Intriguingly, they claimed this discordance of mRNA and protein levels to be highly gene-specific and consistent in both primary and PDX tumors [50].

In summary the integration of transcriptomics and proteomics data has already revealed some fundamental features of mammalian cellular systems. Although this multi-OMICS strategy is already in use to decipher molecular intricacy and mechanistic views of cancer pathophysiology, there are some fundamental questions which remain unanswered till date. For example, it is now accepted that mRNA and protein levels are not correlated in mammalian systems [17, 18, 42]. Whether this poor/moderate correlation is increased (or decreased) in a cancer context is unknown. Similarly whether a constant protein-to-mRNA ratio for a given gene within epithelial cells of different tissues changes upon cancerous transformation remains unresolved. We need to tackle these fundamental questions to be able to harness the full potential of the integration of multi-OMICS studies.

3.3. Proteogenomics: Connecting Proteome to Genome. While genomics, epigenomics, and transcriptomics studies have proved to be pivotal in gaining substantial insights into the architecture of the genome as well as the dynamics of transcriptome, the functional capacity of the genome that determines the cellular phenotype depends on the mechanistic power of the proteins. Moreover proteins are regulated extensively by PTMs and their interactions to other partner-proteins which cannot be predicted from genomics or transcriptomics data. To link genotype to phenotype, the "Clinical Proteomic Tumour Analysis Consortium (CPTAC)" has performed proteomic profiling of TCGA tumor specimens and linked to genomics, epigenomics, and transcriptomic profiles for colorectal (CRC) [49], breast [48], and ovarian [47] cancers (Table 2). Modest correlation between mRNAs and proteins was found for colorectal (0.47), breast (0.39), and ovarian (0.45) cancer as hypothesized by earlier studies. While the impact of copy number alterations (CNAs) was prominent on mRNA levels, a strong effect of CNAs was absent in protein levels as evident by the higher CNA-mRNA than CNA-protein correlations in CRC. Interestingly, amplification of chromosomal region 20q was associated with significant global changes in both mRNA and protein levels that are encoded by genes residing in these regions. These findings that emerged from the multi-OMICS data integration underscore the potential impact of 20q amplification in CRC, which was previously unknown. Hepatocyte-nuclear factor 4 alpha

(HNF4A), Translocase of outer mitochondrial membrane (TOMM34), and SRC protooncogene, nonreceptor tyrosine kinase (SRC) proteins encoded by the 20q chromosomal region, were highly affected by the 20q amplification event and may play a vital role in attaining the cancer hallmark of sustained proliferation [49].

For breast cancer, when CNA-mRNA and CNA-protein pairs were analyzed for 478 oncogenes and TSGs, these cancer-related genes where found to be enriched in the subset that exhibited concordance on both CNA-mRNA and CNA-protein levels compared to the subset that only correlates on CNA-mRNA but not on CNA-protein levels [48]. This finding is of particular importance because it underscored that the tumor-promoting CNA events are more likely to have an effect on both the protein and mRNA levels. In contrast nontumorigenesis CNA events are more likely to lose their impact and may be neutralized on the protein level rather than on the mRNA level. In addition the proteogenomic approach has proved to be particularly effective in identifying possible druggable targets. Proteogenomic analysis of breast cancer tissues resulted in the identification of such candidate proteins,- CDK12, TLK2, PAK1, and RIPK2, that showed gene-amplification-driven proteogenomic patterns [48].

High-Grade Serous Ovarian Cancer (HGSC) is characterized by high CNAs leading to chromosomal instability (CIN) [47]. CNAs may have an impact on the abundance of mRNA/proteins in the same (cis-effect) and/or different (trans-effect) locus. In colorectal cancer CNA-driven trans-effects were observed on both mRNA and protein levels [49]. On the contrary, in ovarian cancer, trans-effect of CNAs on protein abundances was independent of change in mRNA levels. For instance, CNA on specific segments on Chromosome 2 was observed to have strong trans-effect on more than 200 proteins whereas such effects on mRNA levels were very small [47]. As a plausible mechanism to explain the trans-effect of CNA on protein levels without affecting the corresponding mRNA levels, the authors argued that cis-regulation of RNA-binding proteins or microRNAs that are associated with mRNA stability and translational process may be responsible for such trans-effect on protein levels. The proteins for which the abundance is modulated by CNAs mostly belong to cell invasion and migration indicating a possible role of CNA-driven proteogenomic events in attaining these hallmarks of cancer [47]. Next, correlation analysis between CIN and protein abundances led to the identification of two candidate proteins CHD4 and CHD5 that are normally associated with chromatin organization. Abundance variation of these proteins can potentially elicit CIN in ovarian cancer [47]. Under the assumption that PTMs such as phosphorylation may also play a crucial role in activating the signalling cascade to attain cancer hallmarks, proteomic and phosphoproteomic data was integrated with transcriptomic data for ovarian cancer. This integration approach was particularly helpful in the identification of the differentially regulated pathways, PDGFR-beta signalling pathway associated with angiogenesis and integrin-linked kinase pathways associated with cell mobility and invasion (Figure 3), that may serve as a predictor of patient survival. A recent study carried out by the TCGA consortium used integrated genomics, transcriptomic, epigenomics, and proteomics approaches to identify distinct molecular subtypes of the Testicular Germ Cell Tumors (TGCT) [51].

Overall the proteogenomic approach underscores the complementarities of proteomics/phosphoproteomics dataset to harmonize genomics/epigenomics and transcriptomics to gain deeper understanding into the molecular mechanisms that help malignant cell to attain cancer hallmarks. These studies also corroborated the previous notion that mRNA levels are not a good proxy for protein abundance and thus cannot be predicted only from mRNA data. Moreover CNAs driven changes in protein abundance may serve as reliable marker for cancer prognosis and treatment stratification. Taking account of all the insights gained from these three proteogenomic studies, it can be safely assumed that the integration of multi-OMICS data may have significant impact on the diagnosis, prognosis, and treatment-outcome of individual cancer patients in a personalized manner.

3.4. Transcriptomics versus Metabolomics. Unbiased metabolomic-profiling of cancer cell is becoming increasingly popular due to its potential to identify and quantify novel oncometabolites which may serve as biomarkers for different cancer types. Apart from obvious advantages in identifying novel cancer biomarkers, metabolomics may provide key-insights into the pathophysiology of cancer when merged with other OMICS data. In order to extract biologically meaningful insights from metabolomics data and contextualize the differential abundances of oncometabolites, multi-OMICS data integration is necessary. In the following examples, we have shown how metabolomics data integration to other OMICS can be used not only to advance our understanding into the molecular mechanism of cancer progression but also to predict the survival rates of cancer patients.

In a multi-OMICS integration study, Terunuma et al. showed that levels of the oncometabolite-2-hydroxyglutarate (2HG) were elevated in predominantly ER-negative subgroup of breast tumors and associated with poor clinical outcome. Moreover, integration of metabolomics with genome-wide methylomics data revealed that the subtype of breast tumors marked by elevated 2HG levels exhibited a hypermethylation phenotype [52]. Corroborating with this result, earlier studies also demonstrated the association between the elevated 2HG levels and DNA-hypermethylation and enhanced histone methylation causing epigenetic alterations in gliomas [53] and leukemias [54].

In another study, integration of publicly available transcriptomic and metabolomic datasets showed a strong enzyme-metabolite concordance in breast cancer and hepatocellular carcinoma tissues [55]. Both breast and hepatocellular cancer exhibited increased gene-metabolites associations in comparison to adjacent noncancerous tissues. The authors argued that alerted gene-regulatory networks in cancer context may force the changes in cancer-related metabolic pathways causing an abundance change in the metabolite levels [55]. Based on the multi-OMICS data integration, a prediction model, developed and validated against a large cohort of breast cancer patients, showed several cancer-related

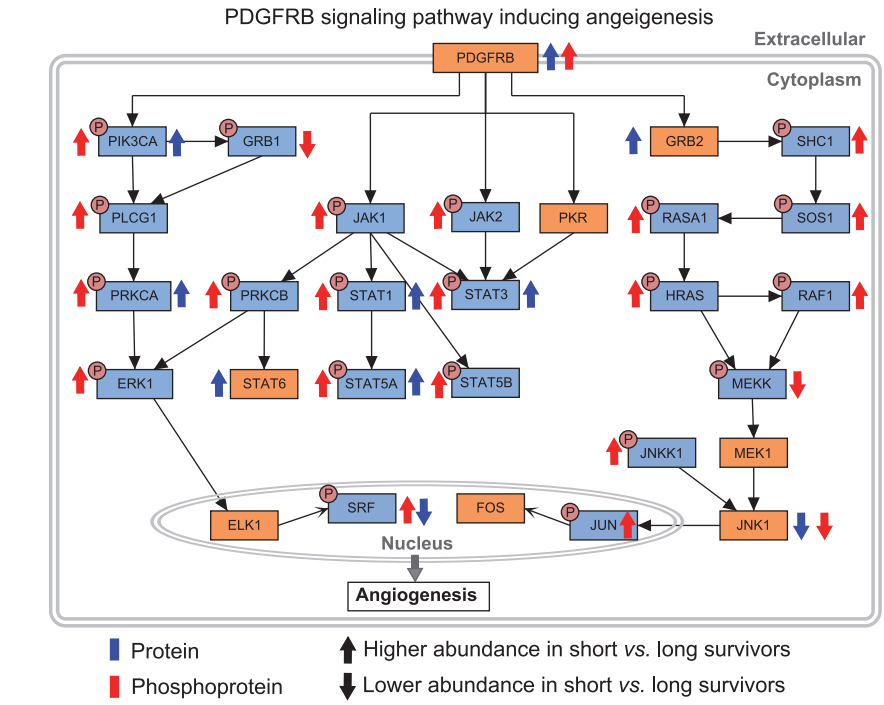

(a)

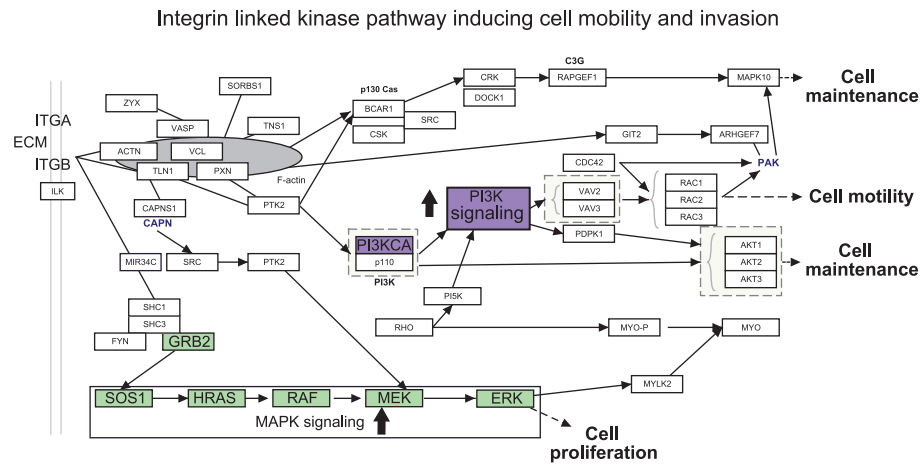

(b)

FIGURE 3: **Proteomics and phosphoproteomics driven identification of the aberrant regulation of signalling pathways leading to poor patient survival.** (a) Aberrant PDGFRB signalling pathway induces angiogenesis in patients and results in poor survival. Phosphorylated and unphosphorylated forms of proteins are indicated by blue and orange color. The directions of arrows indicate the regulation—up and down arrows indicate upregulation and downregulation, respectively. Colors of the arrows indicate the phosphoform or the total protein detected by (phospho)proteomics experiments. Blue and red arrows indicate phospho- and total protein, respectively. (b) Integrin-linked kinase pathway induces cell mobility and invasion, leading to poor patient survival. Two signalling pathways, MAPK (green) and PI3K (purple), are highlighted. Both these pathways were found to be upregulated in cancer patients with poor survival.

metabolites; namely, glucose, Glycine, serine, and acetate are significantly associated with patient survival [55]. A similar OMICS integration approach including metabolomics and transcriptomics was applied to identify potential diagnostic and prognostic cancer biomarkers for prostate [56] and cervical cancers [57]. Ren et al. identified the accumulation of certain metabolites such as S-adenosylhomoserine (SAH), 5-methylthioadensine (MTA), and S-adenosylmethionine (SAM) in prostate cancer compared to noncancerous tissues [56]. Elevated expression of Glycine N-methyltransferase (*GNMT*) evident from transcriptomics analysis was assumed to be responsible for the induction of SAH and was proposed as a tumor-susceptibility gene in prostate cancer [56]. On the other hand, Yang et al. identified five metabolites, bilirubin, LysoPC(17:0), n-oleoyl threonine, 12-hydroxydodecanoic acid, and tetracosahexaenoic acid, as

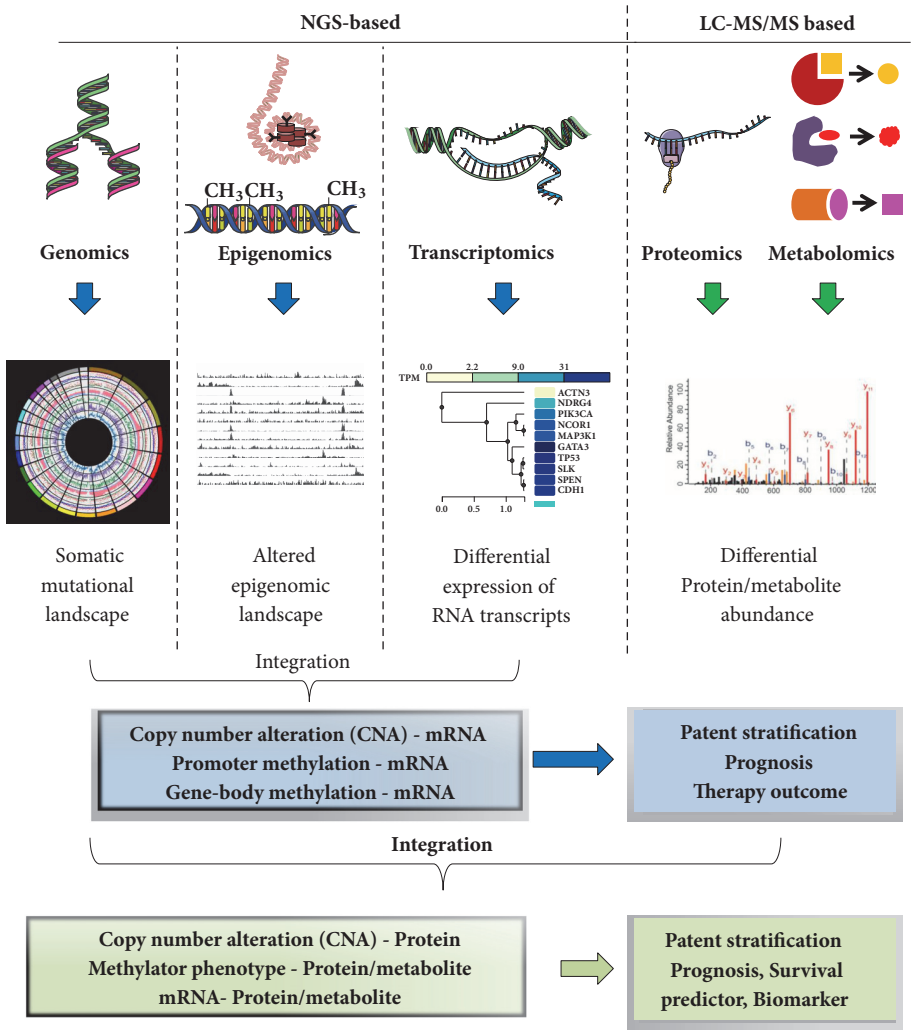

FIGURE 4: **Application of NGS and mass-spectrometry (LC-MS/MS) based OMICS techniques in cancer research.** Genomics, epigenomics, and transcriptomics are based on NGS techniques; whereas proteomics and metabolomics are driven by mass-spectrometric (LC-MS/MS) technique. The principal application of genomics, epigenomics, and transcriptomics is screening of genome-wide somatic mutations, identification of altered epigenomic landscape, and exploring differential RNA expression, respectively. The major application of proteomics/metabolomics is identification of differentially regulated proteins/phosphoproteins/metabolites. The integration of NGS-based techniques can identify the concordance or discordance between copy number alterations (CNAs), promoter/gene-body methylation, and RNA levels. Integration of NGS and LC-MS/MS based techniques may result in the correlation analysis between CNAs, promoter/gene-body methylation, and mRNA levels with protein/metabolite levels.

candidate biomarkers for cervical cancers [57]. Integration strategy leads to the reconstruction of an interconnected gene-metabolic network where seven biochemical pathways were used to identify five candidate metabolite biomarkers [57]. The metabolomics integration studies provided systems-level insights into altered metabolic networks that are tightly regulated with transcriptional network. These interconnected networks could potentially serve as a platform for the identification of novel therapeutic targets and biomarkers for cancer.

In the era of cutting-edge OMICS technologies, the multi-OMICS integration approaches have emerged as a powerful strategy to better understand the molecular basis of cancer and eventually to develop intervention strategies through the identification of robust patient stratification methods, biomarker for early cancer diagnosis/prognosis, and prediction of therapy-outcome. Figure 4 represents the different methods of multi-OMICS data integration and their subsequent application in cancer research.

4. TCGA as a Resource for Multi-OMICS Platform

With the goal of creating a publicly available comprehensive "atlas" of the molecular alterations in the cancer cells, The Cancer Genome Atlas (TCGA), so far, has performed integrative analysis of more than 30 human tumor types [13]. The TCGA Research Network is engaged in cataloguing aberrations in the DNA and chromatin of the cancer-genomes from

thousands of tumors by matching with the normal genomes and linking these aberrations to RNA and proteins levels. The main TCGA-strategy of multi-OMICS integration involves genomics, epigenomics, and transcriptomics which has been successfully implemented in the investigation of various cancer types including testicular germ cell tumors [51], soft tissue sarcomas [58], gastrointestinal adenocarcinomas [59], clear cell renal cell carcinoma [60], prostate [61], urothelial bladder carcinoma [62], gastric adenocarcinoma [63], oesophageal carcinoma [64], acute myeloid leukemia [65], melanoma [66], and lung adenocarcinoma [67] (Table 2). For colorectal [49], breast [48], and ovarian [48] cancer, mass-spectrometry-based proteomics data has been integrated into the existing strategy of OMICS integration as described earlier (see Table 2). For glioblastoma [68] RPPA based targeted proteomics was integrated to existing strategy of OMICS data integration.

The new TCGA-atlas called the "Pan-Cancer initiative" has been developed and is dedicated to comparing and contrasting among the genomic, epigenomic, and transcriptomic alterations found in numerous tumor types [13]. The pan-cancer analysis involving multi-OMICS data in combination with robust bioinformatics methods and statistical tools offers a unique platform to identify common molecular signatures for the stratification of patients with different cancer types and uncover shared molecular pathology of different cancer types for designing targeted therapies. With the genomics, epigenomics, and transcriptomics data from over 11,000 tumors representing 33 of the most prevalent forms of cancer, the Pan-Cancer Atlas presents the unique opportunity for comprehensive and integrated analysis to broaden our current understanding of how, where, and why a normal cell attains cancer hallmarks. Analysis of the enormous amount of cancer-specific data deposited in TCGA requires special bioinformatics methods and techniques to be able to extract biologically meaningful information. Various data analysis and visualization platforms have been developed to assist the rapid analysis of TCGA data. For instance, cBioPortal originally developed at Memorial Sloan Kettering Cancer Center provides opportunities like visualization, analysis, and download of large scale cancer genomics data sets [69].

5. Future of Multi-OMICS Studies: Emerging Era of Systems Biology

Recent advances in high-throughput NGS and mass-spectrometric techniques enabled a paradigm shift from studies involving discrete biochemical reactions and signalling pathways to large scale studies attempting to analyze the whole cellular system. With powerful computational tools one can identify the link between genomic aberrations with differentially expressed mRNAs, proteins, and metabolites that are associated with a cancer-driven cellular perturbation. Integration of multi-OMICS data provides a platform to link the genomic/epigenomic alterations to interconnected transcriptome, proteome, and metabolome networks, which underlie the cellular response to a perturbation. This vision provides an opportunity to better understand cellular response on the systems level but poses a challenge for systems biology driven modelling at the same time. The next phase of systems biology research will focus on models that can deal with thousands of mRNA, protein, and metabolite changes in a dynamic manner. Systems biology approach has the potential to develop effective strategies to administer personalized cancer therapy [70]. The aim of the systems biology approach is to develop predictive models that are refined and constrained by experimental validations. These predictive models will be particularly beneficial to select patients based on personalized multi-OMICS data and stratifying the patients to determine who are most likely to benefit from targeted therapies [71]. In summary systems biology models driven by multi-OMICS data may help to increase the onco-drug efficacy and overcome the chemo-/immunotherapy resistance phenotype of cancer cells rendering them vulnerable to targeted therapies and ultimately in improving the quality of life of patients.

Conflicts of Interest

The authors declare that there are no competing financial interests.

Acknowledgments

This work was supported by the Department of Biochemistry and Molecular Biology, University of Dhaka, Bangladesh.

References

[1] Y. Hasin, M. Seldin, and A. Lusis, "Multi-omics approaches to disease," *Genome Biology*, vol. 18, no. 1, 2017.

[2] C. Manzoni, D. A. Kia, J. Vandrovcova et al., "Genome, transcriptome and proteome: the rise of omics data and their integration in biomedical sciences," *Briefings in Bioinformatics*, vol. 19, no. 2, pp. 286–302, 2018.

[3] G. L. Hager, J. G. McNally, and T. Misteli, "Transcription Dynamics," *Molecular Cell*, vol. 35, no. 6, pp. 741–753, 2009.

[4] C. Kandoth, M. D. McLellan, F. Vandin et al., "Mutational landscape and significance across 12 major cancer types," *Nature*, vol. 502, no. 7471, pp. 333–339, 2013.

[5] M. S. Lawrence, P. Stojanov, and P. Polak, "Mutational heterogeneity in cancer and the search for new cancer-associated genes," *Nature*, vol. 499, pp. 214–218, 2013.

[6] A. Piunti and A. Shilatifard, "Epigenetic balance of gene expression by polycomb and compass families," *Science*, vol. 352, no. 6290, 2016.

[7] U. Raj, I. Aier, R. Semwal, and P. K. Varadwaj, "Identification of novel dysregulated key genes in Breast cancer through high throughput ChIP-Seq data analysis," *Scientific Reports*, vol. 7, no. 1, Article ID 3229, 2017.

[8] J. Li, T. Ching, S. Huang, and L. X. Garmire, "Using epigenomics data to predict gene expression in lung cancer," *BMC Bioinformatics*, vol. 16, 5, p. S10, 2015.

[9] D. Serre, B. H. Lee, and A. H. Ting, "MBD-isolated Genome Sequencing provides a high-throughput and comprehensive survey of DNA methylation in the human genome," *Nucleic Acids Research*, vol. 38, no. 2, pp. 391–399, 2010.

[10] E. Vidal, S. Sayols, S. Moran et al., "A DNA methylation map of human cancer at single base-pair resolution," *Oncogene*, vol. 36, no. 40, pp. 5648–5657, 2017.

[11] S. Djebali, C. A. Davis, and A. Merkel, "Landscape of transcription in human cells," *Nature*, vol. 489, pp. 101–108, 2012.

[12] M. Li, Q. Sun, and X. Wang, "Transcriptional landscape of human cancers," *Oncotarget* , vol. 8, no. 21, pp. 34534–34551, 2017.

[13] Cancer Genome Atlas Research N et al., "The Cancer Genome Atlas Pan-Cancer analysis project," *Nature Genetics*, vol. 45, no. 10, pp. 1113–1120, 2013.

[14] J. Li, Y. Lu, R. Akbani et al., "TCPA: A resource for cancer functional proteomics data," *Nature Methods*, vol. 10, no. 11, pp. 1046-1047, 2013.

[15] N. Iwamoto and T. Shimada, "Recent advances in mass spectrometry-based approaches for proteomics and biologics: Great contribution for developing therapeutic antibodies," *Pharmacology & Therapeutics*, vol. 185, pp. 147–154, 2017.

[16] J. Cox and M. Mann, "Maxquant enables high peptide identification rates, individualized ppb-range mass accuracies and proteome-wide protein quantification," *Nature Biotechnology*, vol. 26, no. 12, pp. 1367–1372, 2008.

[17] M.-S. Kim, S. M. Pinto, D. Getnet et al., "A draft map of the human proteome," *Nature*, vol. 509, no. 7502, pp. 575–581, 2014.

[18] M. Wilhelm, J. Schlegl, H. Hahne et al., "Mass-spectrometry-based draft of the human proteome," *Nature*, vol. 509, no. 7502, pp. 582–587, 2014.

[19] B. S. Shruthi, P. Vinodhkumar, and Selvamani, "Proteomics: A new perspective for cancer," *Advanced Biomedical Research*, vol. 5, no. 67, 2016.

[20] W. B. Dunn, D. I. Broadhurst, H. J. Atherton, R. Goodacre, and J. L. Griffin, "Systems level studies of mammalian metabolomes: the roles of mass spectrometry and nuclear magnetic resonance spectroscopy," *Chemical Society Reviews*, vol. 40, no. 1, pp. 387–426, 2011.

[21] G. A. Nagana Gowda and D. Djukovic, "Overview of mass spectrometry-based metabolomics: Opportunities and challenges," *Methods in Molecular Biology*, vol. 1198, pp. 3–12, 2014.

[22] D. Hanahan and R. A. Weinberg, "Hallmarks of cancer: the next generation," *Cell*, vol. 144, no. 5, pp. 646–674, 2011.

[23] M. A. Davies and Y. Samuels, "Analysis of the genome to personalize therapy for melanoma," *Oncogene*, vol. 29, no. 41, pp. 5545–5555, 2010.

[24] M. Berdasco and M. Esteller, "Aberrant epigenetic landscape in cancer: how cellular identity goes awry," *Developmental Cell*, vol. 19, no. 5, pp. 698–711, 2010.

[25] A. E. Karnoub and R. A. Weinberg, "Chemokine networks and breast cancer metastasis," *Breast Disease*, vol. 26, no. 1, pp. 75–85, 2006.

[26] S. Tyanova, R. Albrechtsen, P. Kronqvist, J. Cox, M. Mann, and T. Geiger, "Proteomic maps of breast cancer subtypes," *Nature Communications*, vol. 7, Article ID 10259, 2016.

[27] O. Warburg, "On respiratory impairment in cancer cells," *Science*, vol. 124, no. 3215, pp. 269-270, 1956.

[28] K. M. Kennedy and M. W. Dewhirst, "Tumor metabolism of lactate: The influence and therapeutic potential for MCT and CD147 regulation," *Future Oncology*, vol. 6, no. 1, pp. 127–148, 2010.

[29] M. R. Hassler and G. Egger, "Epigenomics of cancer - Emerging new concepts," *Biochimie*, vol. 94, no. 11, pp. 2219–2230, 2012.

[30] B. V. S. K. Chakravarthi, S. Nepal, and S. Varambally, "Genomic and epigenomic alterations in cancer," *The American Journal of Pathology*, vol. 186, no. 7, pp. 1724–1735, 2016.

[31] A. S. Wilson, B. E. Power, and P. L. Molloy, "DNA hypomethylation and human diseases," *Biochimica et Biophysica Acta*, vol. 1775, no. 1, pp. 138–162, 2007.

[32] S. Sharma, T. K. Kelly, and P. A. Jones, "Epigenetics in cancer," *Carcinogenesis*, vol. 31, no. 1, pp. 27–36, 2010.

[33] J. P. Issa, "CpG island methylator phenotype in cancer," *Nature Reviews Cancer*, vol. 4, no. 12, pp. 988–993, 2004.

[34] C. G. Kleer, Q. Cao, S. Varambally et al., "EZH2 is a marker of aggressive breast cancer and promotes neoplastic transformation of breast epithelial cells," *Proceedings of the National Acadamy of Sciences of the United States of America*, vol. 100, no. 20, pp. 11606–11611, 2003.

[35] S. Varambally, S. M. Dhanasekaran, M. Zhou et al., "The polycomb group protein EZH2 is involved in progression of prostate cancer," *Nature*, vol. 419, no. 6907, pp. 624–629, 2002.

[36] D. Z. Kelley, E. L. Flam, E. Izumchenko et al., "Integrated analysis of whole-genome ChIP-Seq and RNA-Seq data of primary head and neck tumor samples associates HPV integration sites with open chromatin marks," *Cancer Research*, vol. 77, no. 23, pp. 6538–6550, 2017.

[37] J. Bhasin, B. Lee, L. Matkin et al., "Methylome-wide Sequencing Detects DNA Hypermethylation Distinguishing Indolent from Aggressive Prostate Cancer," *Cell Reports*, vol. 13, no. 10, pp. 2135–2146, 2015.

[38] S. Shukla, E. Kavak, M. Gregory et al., "CTCF-promoted RNA polymerase II pausing links DNA methylation to splicing," *Nature*, vol. 479, no. 7371, pp. 74–79, 2011.

[39] M. Moarii, V. Boeva, J.-P. Vert, and F. Reyal, "Changes in correlation between promoter methylation and gene expression in cancer," *BMC Genomics*, vol. 16, no. 1, article no. 873, 2015.

[40] B. Eun, M. L. Sampley, A. L. Good, C. M. Gebert, and K. Pfeifer, "Promoter cross-talk via a shared enhancer explains paternally biased expression of Nctc1 at the Igf2/H19/Nctc1 imprinted locus," *Nucleic Acids Research*, vol. 41, no. 2, pp. 817–826, 2013.

[41] A. Sohni, M. Bartoccetti, R. Khoueiry et al., "Dynamic switching of active promoter and enhancer domains regulates Tet1 and Tet2 expression during cell state transitions between pluripotency and differentiation," *Molecular and Cellular Biology*, vol. 35, no. 6, pp. 1026–1042, 2015.

[42] B. Schwanhüusser, D. Busse, N. Li et al., "Global quantification of mammalian gene expression control," *Nature*, vol. 473, no. 7347, pp. 337–342, 2011.

[43] A. R. Kristensen, J. Gsponer, and L. J. Foster, "Protein synthesis rate is the predominant regulator of protein expression during differentiation," *Molecular Systems Biology*, vol. 9, p. 689, 2013.

[44] J. J. Li and M. D. Biggin, "Gene expression. Statistics requantitates the central dogma," *Science*, vol. 347, no. 6226, pp. 1066-1067, 2015.

[45] M. Jovanovic, M. S. Rooney, P. Mertins et al., "Immunogenetics. Dynamic profiling of the protein life cycle in response to pathogens," *Science*, vol. 347, no. 6226, Article ID 1259038, 2015.

[46] T. Chen, C. Lee, H. Liu et al., "APOBEC3A is an oral cancer prognostic biomarker in Taiwanese carriers of an APOBEC deletion polymorphism," *Nature Communications*, vol. 8, no. 1, 2017.

[47] H. Zhang, T. Liu, and Z. Zhang, "Integrated proteogenomic characterization of human high-grade serous ovarian cancer," *Cell*, vol. 166, no. 3, pp. 755–765, 2016.

[48] P. Mertins et al., "Proteogenomics connects somatic mutations to signalling in breast cancer," *Nature*, vol. 534, no. 7605, pp. 55–62, 2016.

[49] B. Zhang, J. Wang, and X. Wang, "Proteogenomic characterization of human colon and rectal cancer," *Nature*, vol. 513, no. 7518, pp. 382–387, 2014.

[50] L. Li, Y. Wei, C. To et al., "Integrated Omic analysis of lung cancer reveals metabolism proteome signatures with prognostic impact," *Nature Communications*, vol. 5, article no. 5469, 2014.

[51] H. Shen et al., "Integrated molecular characterization of testicular germ cell tumors," *Cell Reports*, vol. 23, no. 11, pp. 3392–3406, 2018.

[52] A. Terunuma et al., "MYC-driven accumulation of 2-hydroxyglutarate is associated with breast cancer prognosis," *The Journal of clinical investigation*, vol. 124, no. 1, pp. 398–412, 2014.

[53] S. Turcan, D. Rohle, A. Goenka et al., "IDH1 mutation is sufficient to establish the glioma hypermethylator phenotype," *Nature*, vol. 483, no. 7390, pp. 479–483, 2012.

[54] M. E. Figueroa et al., "Leukemic IDH1 and IDH2 mutations result in a hypermethylation phenotype, disrupt TET2 function, and impair hematopoietic differentiation," *Cancer Cell*, vol. 18, no. 6, pp. 553–567, 2010.

[55] N. Auslander et al., "A joint analysis of transcriptomic and metabolomic data uncovers enhanced enzyme-metabolite coupling in breast cancer," *Scientific Reports*, vol. 6, Article ID 29662, 2016.

[56] S. Ren et al., "Integration of metabolomics and transcriptomics reveals major metabolic pathways and potential biomarker involved in prostate cancer," *Molecular and cellular proteomics : MCP*, vol. 15, no. 1, pp. 154–163, 2016.

[57] K. Yang, B. Xia, W. Wang et al., "A comprehensive analysis of metabolomics and transcriptomics in cervical cancer," *Scientific Reports*, vol. 7, no. 1, Article ID 43353, 2017.

[58] Cancer Genome Atlas Research Network, "Comprehensive and integrated genomic characterization of adult soft tissue sarcomas," *Cell*, vol. 171, no. 4, Article ID e928, pp. 950–965, 2017.

[59] Y. Liu et al., "Comparative molecular analysis of gastrointestinal adenocarcinomas," *Cancer Cell*, vol. 33, no. 4, Article ID e728, pp. 721–735, 2018.

[60] C. J. Ricketts et al., "The cancer genome atlas comprehensive molecular characterization of renal cell carcinoma," *Cell Reports*, vol. 23, no. 12, p. 3698, 2018.

[61] Cancer Genome Atlas Research N, "The Molecular Taxonomy of Primary Prostate Cancer," *Cell*, vol. 163, no. 4, pp. 1011–1025, 2015.

[62] Cancer Genome Atlas Research N, "Comprehensive molecular characterization of urothelial bladder carcinoma," *Nature*, vol. 507, no. 7492, pp. 315–322, 2014.

[63] Cancer Genome Atlas Research N, "Comprehensive molecular characterization of gastric adenocarcinoma," *Nature*, vol. 513, no. 7517, pp. 202–209, 2014.

[64] Cancer Genome Atlas Research N et al., "Integrated genomic characterization of oesophageal carcinoma," *Nature*, vol. 541, no. 7636, pp. 169–175, 2017.

[65] Cancer Genome Atlas Research N et al., "Genomic and epigenomic landscapes of adult de novo acute myeloid leukemia," *The New England journal of medicine*, vol. 368, no. 22, pp. 2059–2074, 2013.

[66] Cancer Genome Atlas N, "Genomic Classification of Cutaneous Melanoma," *Cell*, vol. 161, no. 7, pp. 1681–1696, 2015.

[67] Cancer Genome Atlas Research N, "Comprehensive molecular profiling of lung adenocarcinoma," *Nature*, vol. 511, no. 7511, pp. 543–550, 2014.

[68] C. W. Brennan, R. G. Verhaak, A. McKenna et al., "The somatic genomic landscape of glioblastoma," *Cell*, vol. 155, pp. 462–477, 2013.

[69] E. Cerami, J. Gao, U. Dogrusoz et al., "The cBio cancer genomics portal: an open platform for exploring multidimensional cancer genomics data," *Cancer Discovery*, vol. 2, no. 5, pp. 401–404, 2012.

[70] H. M. J. Werner, G. B. Mills, and P. T. Ram, "Cancer systems biology: a peek into the future of patient care?" *Nature Reviews Clinical Oncology*, vol. 11, no. 3, pp. 167–176, 2014.

[71] D. Guhathakurta, N. A. Sheikh, T. C. Meagher, S. Letarte, and J. B. Trager, "Applications of systems biology in cancer immunotherapy: From target discovery to biomarkers of clinical outcome," *Expert Review of Clinical Pharmacology*, vol. 6, no. 4, pp. 387–401, 2013.

Hindawi
BioMed Research International
Volume 2018, Article ID 7532507, 13 pages
https://doi.org/10.1155/2018/7532507

Review Article

Complement System and Age-Related Macular Degeneration: Implications of Gene-Environment Interaction for Preventive and Personalized Medicine

Andrea Maugeri,[1] **Martina Barchitta**,[1] **Maria Grazia Mazzone**,[2] **Francesco Giuliano**,[2] **and Antonella Agodi**[1]

[1]*Department of Medical and Surgical Sciences and Advanced Technologies "GF Ingrassia", University of Catania, Via S. Sofia 87, 95123 Catania, Italy*
[2]*SIFI SpA, Research and Development Department, Via Ercole Patti 36, 95025 Catania, Italy*

Correspondence should be addressed to Antonella Agodi; agodia@unict.it

Received 18 May 2018; Accepted 18 July 2018; Published 26 August 2018

Academic Editor: Sajib Chakraborty

Age-related macular degeneration (AMD) is the most common cause of visual loss in developed countries, with a significant economic and social burden on public health. Although genome-wide and gene-candidate studies have been enabled to identify genetic variants in the complement system associated with AMD pathogenesis, the effect of gene-environment interaction is still under debate. In this review we provide an overview of the role of complement system and its genetic variants in AMD, summarizing the consequences of the interaction between genetic and environmental risk factors on AMD onset, progression, and therapeutic response. Finally, we discuss the perspectives of current evidence in the field of genomics driven personalized medicine and public health.

1. Introduction

Age-related macular degeneration (AMD), characterized by the progressive destruction of neurosensory retina at the macular area, is the most common cause of visual loss in developed countries, with a significant economic and social burden on public health [1]. The early stage of AMD leads to aberrant pigmentation of retinal pigment epithelium (RPE) and accumulation of extracellular material, called "drusen," underneath the RPE basement membrane. Drusen are small, yellowish, extracellular deposits of lipid, cellular debris and protein that may lead to impaired RPE function and disruption of the metabolic transport between RPE and choroid [2]. The advanced stages manifest as choroidal neovascularization (CNV) in the wet AMD, or geographic atrophy (GA) in the dry AMD [3]. Pathological features of AMD are caused by the interaction of oxidative stress, impaired RPE activity and function, increased apoptosis, and abnormal immune system activation [4, 5]. Smoking is the strongest modifiable risk factor for AMD, leading to oxidative stress, ischemia, hypoxia, and neovascularization [6]. Although both current and former smoking may increase AMD risk, a protective effect has been observed for time since smoking cessation [7]. Particularly, subjects who had stopped smoking for more than 20 years were not at risk of advanced stages of AMD [8, 9]. Other modifiable risk factors, such as obesity [10–13] and sunlight exposure [14, 15], are still under debate, since their role in AMD susceptibility may be related to an overall unhealthy lifestyle [16–18]. To date, the only factor that may be protective against AMD is a healthy diet, rich in omega-3 fatty acids, lutein, zeaxanthin, and antioxidants [19–22]. Consistently, the Age-Related Eye Disease Study 2 (AREDS2) formulation (i.e., a combination of zinc, b-carotene, and vitamins C, and E) has been shown to reduce the risk of progression to advanced AMD [23]. While AREDS formulation represents the only available treatment for dry AMD, intravitreal injections of antivascular endothelial growth factor (VEGF) agents (i.e., ranibizumab, bevacizumab, and aflibercept) may improve visual acuity in patients with wet AMD [24–29].

In addition to the effect of modifiable factors, genetic variants confer about 60% of the attributable risk [30], with at least 34 genomic loci implicated in AMD pathogenesis [31]. Genetic risk factors associated with AMD susceptibility include polymorphisms in complement factor H (*CFH*) [32], age-related maculopathy susceptibility 2 (*ARMS2*) [33], apolipoprotein E (*APOE*) [34], and vascular endothelial growth factor (*VEGF*) [35]. Above all, the discovery of genetic variants in components of the complement system indicated the potential role of local inflammation and complement regulation in the pathogenesis of AMD [36].

Given this scenario, the perspective of personalized medicine for the prevention and treatment of AMD requires a more accurate evidence-based knowledge of gene-environment interactions.

Here we provide an overview of the role of complement system in AMD and summarize the consequences of the interaction between genetic and environmental risk factors on AMD onset and progression and therapeutic response. Finally, we discuss the perspectives of current evidence in the field of genomics driven personalized medicine.

2. The Complement System

The complement system is implicated in the innate immune response, which constitutes the first-line host defense against pathogenic infections [37]. It also functions as immunoregulatory system of clear immune complexes, inflammatory products, and apoptotic cells. Complement components constitute a complex network of about 30 plasma- and membrane-associated serum proteins, designated by numerals (C1-C9) or letter symbols (e.g., complement factors H, FH), which are organized into hierarchal proteolytic cascades. The activation of complement system involves three proteolytic cascades, namely, the classical, lectin, and alternative pathways, which lead to the activation of C3 convertase, the convergence point of all complement pathways. This downstream cascade is characterized by the activation of the following effectors: the membrane attack complex (MAC), anaphylatoxins (C3a and C5a), and opsonins. The first induces cell lysis, producing a pore-like structure in the phospholipid bilayer, and stimulates the release of anaphylatoxins and growth factors from the vascular endothelium. The classical and lectin pathways are, respectively, activated by binding to complement-fixing antibodies in immune complexes or to mannose residues on the surface of microorganisms. In contrast, the alternative pathway is spontaneously activated by a constant low-rate hydrolysis of C3, which further binds to factor B (FB), allowing factor D (FD) to cleave factor B into Ba and Bb. The resulting C3 convertase initiates the terminal pathway via an amplification loop, producing more C3b and C3a from C3 (Figure 1).

3. Regulation of Complement System

The refined balance between activation and inhibition of complement system is the crucial regulatory mechanism to prevent self-tissue damage [37, 38]. Although increased complement activity may be protective against chronic low-grade

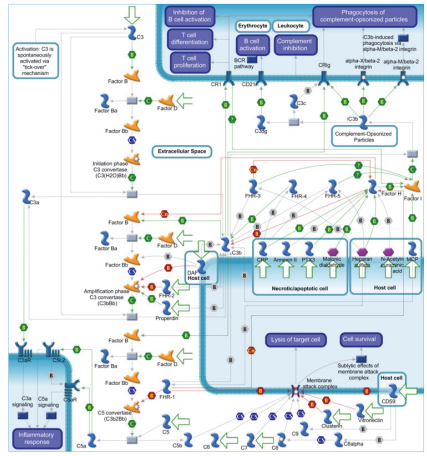

Figure 1: Complement system activation and regulation by the alternative pathway. This figure was prepared using MetaCore from Thomson Reuters.

inflammation and infection in early life [39], lack of inhibition is associated with several diseases, such as systemic lupus erythematosus [40], atypical haemolytic uraemic syndrome [41], dense deposit disease [42], and AMD [43]. Therefore, complement system activity is strictly controlled by regulatory proteins, which mainly act by degrading complement components, increasing C3 convertase decay, and modulating the MAC assembly [44–46]. The first is a function of factor I (FI), which regulates the classical and alternative pathways by cleaving C3b into inactive fragments [47]. However, to prevent nonspecific degradation of complement components, the proteolytic activity of FI requires several cofactors, including complement receptor 1 (CR1), membrane cofactor protein (MCP), and FH [47–51], which accelerate C3 convertase decay by displacing factor Bb from existing C3 convertase [52, 53].

The ability of alternative pathway to discriminate between self and potential pathogens is conferred by recognition of glycosaminoglycans (GAGs) and sialic acid glycans (i.e., heparin-sulfate and N-acetylneuraminic acid) on host cells [54–57]. Binding of FH to the surface of necrotic cells and to apoptotic particles is mediated by CRP, Annexin II, DNA, and histones [58–61]. An additional complement inhibitor is the decay-accelerating factor (DAF), which inhibits assembly of neoformed C3 convertases and accelerates the decay of pre-existing convertases [46, 62–66]. Lastly, the regulation of complement system may be also provided by inhibiting MAC formation via membrane bound (CD59) or fluid-phase (Vitronectin and Clusterin) inhibitors [67–72].

4. Complement System and AMD Pathogenesis

Although the majority of circulating complement components is produced by the liver, the retina shows extrahepatic complement synthesis [73], probably to overcome the restricted access of plasma protein to the retina through the blood-retinal barrier. Several lines of evidence demonstrated that complement dysregulation, especially the alternative

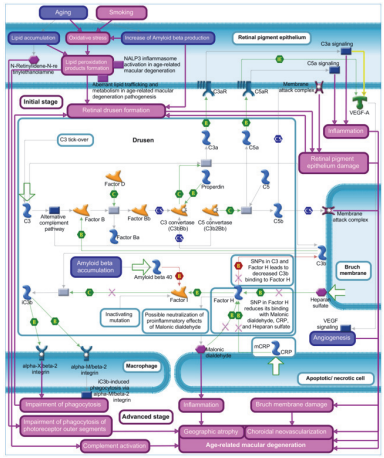

Figure 2: Complement system dysregulation in the age-related macular degeneration. This figure was prepared using MetaCore from Thomson Reuters.

pathway, is involved in the pathogenesis of AMD. The major stressors for AMD development, such as aging, smoking, and oxidative stress, have been linked to the overactivation of the complement system (Figure 2). This evidence has been also supported by immune-histological and proteomic studies, which identified complement components as constituents of drusen, suggesting the local activation of the complement pathways [30, 74–77]. Increased levels of activated complement components, which are released during the complement activation, have been also observed in peripheral blood of AMD patients [78–80]. Consistently, complement regulators, such as Vitronectin, Clusterin, and MCP, are highly expressed in drusen and RPE cells adjacent to drusen [30, 81, 82]. Drusen are especially characterized by Amyloid beta accumulation, which in turn is produced by senescent RPE cells and may induce oxidative stress [83]. Binding of Amyloid beta to FI results in complement activation and chronic low-grade inflammation [83]. During RPE aging, the accumulation of lipofuscin and bis-retinoid component N-retinylidene-N-retinylethanolamine has also been observed, which reduces the degradation of phospholipids by lysosomes [84, 85]. The accumulation of undigested lipids, combined with oxidative stress, leads to the formation of lipid peroxidation products [86], which in turn can induce apoptosis and complement activation [87, 88].

5. The Role of Common Variants in the Pathogenesis and Treatment of AMD

5.1. Complement Factor H (FH). FH is produced in the liver and secreted as a protein composed of 20 short consensus repeats (SCRs), which share homology at specific residues [89, 90]. The 1q32 region, known as the regulators of complement activation (RCA) cluster, also contains five homologous CFH-related genes (*CFHR1* to *CFHR5*), encoding FH-related proteins (FHR1-5) [91]. FH is also locally produced by RPE and contributes to C3 convertase decay, preventing the amplification of C3b deposition.

In 2005, several genetic association studies, conducted by independent research groups, identified the CFH gene on chromosome 1q32 as the first gene associated with AMD risk [76, 92–94]. The most prominent effect on AMD risk was initially attributed to rs1061170 polymorphism, which leads to an amino acid change at position 402 of the FH polypeptide (Y402H). Prevalence of the 402H risk variant varies across ethnicities [95], with an increased AMD risk of 2.5 times among heterozygous individuals and 6.0 times among homozygotes [96]. This finding was confirmed by pooled analysis in both Caucasians [95] and Asians [97–99]. A more recent meta-analysis stratified by stage of disease and ethnicity, including data of 27418 AMD patients and 32843 controls, stated that the polymorphism is significantly associated with AMD: in Caucasian the mutated allele confers a 1.44 risk of early AMD, a 2.90 risk of dry AMD and a 2.46 risk of wet AMD; in Asians, the mutated allele seems to be associated only with wet AMD [100].

The rs1061170 polymorphism has been also identified as a predictor of response to anti-VEGF treatment; homozygotes individuals were less likely to achieve a better outcome than those carrying wild type genotype, suggesting the need of more effective therapeutic strategies for this subgroup of patients [101].

Conversely to this well-known genetic risk factor, the rs800292 polymorphism, a coding variant in the SCR1 domain, has been found to be protective against AMD in both Caucasians and Asians [99, 102]. This polymorphism, which leads to an amino acid change at position 62 of the FH polypeptide (V62I), also conferred a better response to treatment of neovascular AMD [101].

Besides these polymorphisms, the impact on AMD risk of other *CFH* genetic variants is still under debate. A recent meta-analysis [103] aimed to resolve inconsistent findings from studies on distinct ethnic populations about the role of four coding and noncoding variants: two noncoding variants in intron 14 (543G>A, rs1410996) and intron 15 (3144C>T, rs1329428); a coding synonymous variant in exon 10 (A473A, rs2274700); a promoter variant, positioned 257 upstream in the *CFH* promoter region (257 C>T, rs3753394). Pooled results demonstrated that these polymorphisms are significantly associated with increased AMD risk, but none of them was related to response to treatment [104].

5.2. Complement Component 3 (C3). The *C3* gene, located on chromosome 19p13.3-13.2, consists of 41 exons encoding for 1663 amino acids and 13 functional domains. C3 protein is biologically inactive until it undergoes to conformational changes, which expose binding sites for pathogenic cell surface and other complement components [105]. Although several studies suggest the association between *C3* polymorphisms and AMD, findings are conflicting [106–110]. The rs2230199 polymorphism, leading to the R102G substitution, is the most commonly investigated, since it seems to influence C3 binding capacity and cofactor activity, thereby extending convertase lifetime [111]. Overall, this polymorphism was associated with AMD risk, even though this finding was confirmed in Caucasians but not in Asians [112]. A further meta-analysis confirmed the increased AMD risk associated with

rs2230199 polymorphism and suggested the adverse effect of rs1047286 and rs11569536 polymorphisms on the disease [113]. By contrast, the rs2250656 polymorphism has been found to be protective against AMD [113].

Lack of evidence exists about the effect of C3 genetic variants on response to AMD treatment [114–117]. Particularly, the Comparison of AMD Treatments Trials (CATT) showed no significant effect of rs2230199 polymorphism on both visual and anatomical outcomes, after anti-VEGF therapy [118].

However, analysis of changes in central macular thickness after ranibizumab treatment, showed that the minor allele of rs2250656 SNP was associated with improvement in retinal thickness and architecture [119].

5.3. Factor B and C2. The *CFB* gene is located in the major histocompatibility complex (MHC) class III region on chromosome 6p21. Several lines of evidence suggest that polymorphisms in this region are associated with reduced AMD risk. Among these, pooled results from previous meta-analyses confirmed the protective effect on AMD risk of the common rs641153 polymorphism, also known as R32Q, in Caucasians [120] and in other ethnic groups [121].

The MHC class III region also includes genes encoding for proteins involved in the regulation of the immune reaction, such as *C2* gene that is located 500 bp upstream from *CFB* gene. C2 is a serum glycoprotein that functions as part of the classical pathway of the complement system. Two polymorphisms (rs9332739 and rs547154) have been directly associated with AMD by decreasing the risk of 45% and 53%, respectively [120]. However, these variants may be indirectly linked to AMD risk due to linkage disequilibrium with *CFB*. Indeed, some common haplotypes, spanning *CFB* and *C2* genes, are considered highly protective against AMD [122]. Genetic and functional studies suggest that CFB rather than C2 polymorphisms are more likely to determine the reduced AMD risk. The rs9332739 and rs547154 polymorphisms in C2 are noncoding variant, whereas the rs641153 polymorphism in CFB results in reduced alternative pathway amplification and hemolytic activity of the CFB protein [123, 124]. Moreover, after adjustment for genetic and nongenetic risk factors, the association with rs641153 proved to be robust whereas the association with rs9332739 and rs547154 became insignificant [125].

Lack of evidence exists about the effect of CFB and C2 genetic variants on response to intravitreal anti-VEGF injections; particularly, the rs641153 polymorphism did not show any pharmacogenetics effects in patients with neovascular AMD [104, 126].

5.4. Factor I. The CFI gene, located on chromosome 4q25, consists of 13 exons encoding for a precursor protein in hepatocytes, macrophages, lymphocytes, endothelial cells, and fibroblasts. The first eight exons encode the heavy chain, and the last five exons encode the light chain, which contains the serine protease domain. To obtain the active protein, the precursor is cleaved into heavy and light chains, which form a heterodimeric glycoprotein. This heterodimer can prevent the assembly of convertase enzymes by cleaving of C4b and C3b. The association between *CFI* polymorphisms and AMD was firstly reported by Fagerness et al. [127]. Afterwards, several studies identified polymorphisms that can alter gene expression and protein production [128–131]. The association between AMD risk and rs10033900 polymorphism is the most investigated, but results are still conflicting. To date, an updated meta-analysis showed that carriers of rs10033900 polymorphism have a reduced risk of developing AMD; these results were confirmed in Caucasians, but not in Asians [132].

6. The Role of Rare Variants in AMD

Growing body of evidence supports the role of rare variants, with large effect sizes, in the pathogenesis of AMD. Accordingly, targeted genomic resequencing of selected loci pointed out the effect of nonsynonymous rare variants in four complement genes (i.e., CFH, CFI, C3, and C9). These variants and their implication for personalized treatment have been recently reviewed elsewhere [102]. The CFH rs121913059 polymorphism consists of a missense mutation in the C-terminal region of the protein, which leads to an amino acid change at position 1210 of the FH polypeptide (R1210C). The R1210C variant conferred a 47-times higher risk of developing AMD [133], independently of the common rs1061170 variant. Particularly, the R1210C variant is associated with a typical phenotype with extensive drusen accumulation, as well as with earlier age of onset of the disease [134]. Whole-exome sequencing of families with AMD allowed identifying R53C and D90G variants which accelerate activity and cofactor-mediated inactivation of FH [135]. More recently, both high penetrant splice site variant (IVS6+1G>A) and coding variants (N90G, R127H, R175P, R175G, C192F, and S193L) have been proposed to explain the high burden of disease in AMD families with unknown genetic risk factors [102, 105]. Among rare variants, the K155Q variant in C3 has been independently associated with AMD [106–109], with an overall 3-fold increased risk of developing the disease [110]. In addition, Duvvari et al. [136] identified four additional genetic variants (K65Q, R161W, R735W, and S1619R) by sequencing of all coding exons of the *C3* gene; however, none of these associations was further confirmed in independent cohorts [137]. Several rare and highly penetrant *CFI* variants have been identified in patients with AMD [108]. Particularly, the majority of mutations affect the catalytic domain of the protein, leading to secretion defect and decreasing FI-mediated cleavage of C3b. Among these, van den Ven et al. demonstrated that the missense G119R substitution conferred a 22-times higher risk of AMD [138].

7. Interaction of Genetic Variants with Environmental Risk Factors

7.1. Smoking. Evidence from candidate gene studies of AMD-associated loci suggested that smoking might be an effect modifier of genetic AMD risk. Consistently with other studies [95, 139–142], results from the Beaver Dam Eye cohort did not show significant multiplicative interaction between smoking and rs1061170 polymorphism on AMD incidence and progression [143]. However, the rs1061170 polymorphism

showed a stronger effect on AMD risk among smokers [139, 141, 142, 144–146]. Particularly, the Rotterdam Study reported that, among smokers, homozygosity for the risk variant conferred a 34-fold increased risk of late AMD compared to nonsmoking wild type subjects [147]. A study of discordant sibling pairs further specified that the combination between smoking more than ten pack-years and homozygosity for the risk variant was associated with a 144-fold increased risk of wet AMD, compared to nonsmoking heterozygous or wild type individuals [139]. Accordingly, the retrospective analysis of data from 385 eligible patients included in the European Genetic Database, a multicenter database for clinical and molecular analysis of AMD, demonstrated that the presence of homozygous risk variant among smokers was associated with earlier onset of wet AMD [148]. Moreover, the independent multiplicative effect of CFH genotype and smoking was more evident for some features of early AMD (i.e., central soft drusen, large area of soft drusen, and pericentral pigmentary abnormalities) associated with higher risk of AMD progression [149].

Overall, these findings indicate that smoking and rs1061170 polymorphism have independent multiplicative effects on AMD risk, with no significant interaction. The biological plausibility of this relationship might be explained by the well-known effects of smoking and CFH polymorphism on the activation of alternative pathway: on one hand, smoking alters binding of CFH to C3 and lowers plasma CFH levels [150, 151]; on the other hand, the presence of rs1061170 polymorphism alters the ability of CFH to bind to C3b.

7.2. Dietary Intake. In the last decades, it has been consistently demonstrated that an adequate intake of omega-3 fatty acids, lutein, zeaxanthin, and other antioxidants represents the only well-known protective factor against AMD onset and progression [19–22]. However, few studies have previously explored whether genetic susceptibility could modify this association.

While lutein and zeaxanthin supplementation clearly decreases the progression from early to advanced AMD [152], evidence on the effect of their intake through the diet is still controversial, probably due to genetic susceptibility and/or other unmeasured effect modifiers. The Rotterdam study showed a synergic biological interaction between CFH rs1061170 polymorphism and dietary intake of antioxidants, suggesting that higher intake of zinc, ω-3 fatty acids, β-carotene, lutein, and zeaxanthin might reduce the incidence of early AMD in subjects at higher genetic risk [153]. Consistently, pooled analysis of Blue Mountains Eye and Rotterdam cohorts showed that dietary intake of lutein and zeaxanthin was inversely associated with the risk of early AMD, only in concurrence with at least two risk alleles of CFH rs1061170 and ARMS2 rs10490924 polymorphisms [154]. By contrast, in absence of genetic susceptibility, higher intake of lutein and zeaxanthin was associated with greater incidence of early AMD [154]. Analysis of the Atherosclerosis Risk in Communities (ARIC) Study added to this mounting controversial evidence, demonstrating that greater lutein and zeaxanthin intake were associated with lower AMD prevalence among carriers of the heterozygous CFH genotype, higher prevalence among carriers of the homozygous risk genotype, and no statistically significant association among those with nonrisk genotype [155].

Growing body of evidence demonstrated that the anti-inflammatory and antioxidant properties of omega-3 long chain polyunsaturated fatty acids slow the progression to advanced AMD [4, 22, 156–158]. In the Age-Related Eye Disease Study (AREDS), increased intake of docosahexaenoic acid (DHA) and eicosapentaenoic acid (EPA) was associated with reduced dry AMD risk, after adjustment for behavioural factors and genetic variants, including SNPs in CFH, ARMS2/HTRA1, CFB, C2, C3, CFI, and LIPC genes [159]. In addition, the Blue Mountain Eye Study demonstrated that weekly consumption of fish was associated with lower risk of late AMD, only among subjects with the CFH homozygous risk genotype [160]. More recently, the joint effect of high-risk genotypes and vitamins intake has been also evaluated. A cross-sectional analysis of the Inter99 Eye Study suggested a significant interaction between vitamin A and rs1061170 CFH polymorphism, with a positive association between dietary intake and drusen diameter, among subjects with the homozygous risk genotype [161]. Findings from a subsample of the AREDS study also demonstrated a significant interaction between folate intake and the rs2230199 C3 polymorphism: the risk of AMD progression was lower among subjects with homozygous nonrisk genotype, but not in those carrying the risk allele. By contrast, no significant effect on AMD progression was evident for dietary intake of thiamin, riboflavin, niacin, and vitamins B6 and B12 [162]. Although foods and nutrients are consumed in combination, the abovementioned studies used single-nutrient or a single-food approach, without taking into account potential synergistic effects. To our knowledge, the study by Merle et al., including participants of the AREDS, was the first to evaluate the interaction between genetic risk factors and overall diet [163]. Particularly, the adherence to the Mediterranean diet was associated with lower risk of progression to advanced AMD among subjects with nonrisk genotype, but not among those with the homozygous risk genotype [163]. The significant association, in absence of genetic susceptibility, might be explained by the protective effect of Mediterranean diet on immune and inflammatory responses.

8. Interaction of Genetic Variants with AMD Treatments

The effect of the interaction between nutritional supplements and genetic susceptibility on the progression to advanced AMD is currently under debate. In 2008, for the first time, Klein and colleagues demonstrated that the effect of combined antioxidant and zinc supplementation on the progression to advanced AMD was greater among subjects with nonrisk genotype for the CFH rs1061170 polymorphism, compared with high-risk subjects [164]. Seddon and colleagues, investigating the progression to advanced AMD among subjects with low CFH and high ARMS2 genetic risk, reported

that antioxidant and zinc supplementation reduced the risk of progression to wet AMD, with no significant effect on dry AMD [165]. Awh et al. first reported that zinc supplementation reduced progression to advanced AMD, among subjects with no risk alleles for CFH and at least one risk allele for ARMS2 [166]. The same research group further demonstrated a distinct effect on disease progression according to the number of risk alleles for these SNPs: supplementation with zinc, alone or as a component of the AREDS formulation, was protective against the harmful effect of the ARMS2 risk allele but it increased the risk posed by CFH allele [166]. These findings are supported by current knowledge about physiologic implication of zinc binding to CFH, which might neutralize the ability to inactivate C3 convertase [167–169]. This, together with functional consequences of CFH rs1061170 polymorphism, might cause the detrimental effect associated with concurrence of CFH risk genotypes and zinc supplementation [170]. By contrast, data analysis of a larger AREDS subsample found no interaction between AREDS formulation and genetic susceptibility [171]. However, the design of this study does not allow us to exclude if the absence of interaction was caused by underpowered statistical analysis.

While the AREDS formulation may slow the progression to dry AMD by modulating complement activity [172], intravitreal injections of anti-VEGF agents are currently considered part of the standard treatment regimen for neovascular AMD, accompanied by photodynamic therapy (PDT) with verteporfin. In spite of the well-established effect of CFH rs1061170 polymorphism on AMD risk, there is still controversy about its role in the response to anti-VEGF treatment. To our knowledge, Chen et al. were the first to summarize data on the relationship between the rs1061170 polymorphism and response to treatment of neovascular AMD [32]. Pooled analysis indicated that CFH risk genotypes were weakly but significantly associated with less effective response to any form of treatment, including anti-VEGF agents, photodynamic therapy, and antioxidants/zinc supplementation [32]. This finding was further confirmed by more specific meta-analyses of studies, investigating the relationship between CFH rs1061170 polymorphism and response to anti-VEGF treatment [97, 173].

In summary, evidence on the interaction between genetic susceptibility and response to AMD treatment is currently weak and controversial, raising the need of further researches prior to applying genetic testing to personalized medicine.

9. Implications for Preventive and Personalized Medicine

Uncovering the interaction between genome and environment is one of the main challenge towards preventive and personalized medicine. The discovery of genetic variants in genes for complement proteins pointed out the role of chronic inflammation and complement regulation in AMD pathogenesis. While the effect of common and rare genetic variants is well established, our review suggests that environmental exposure could modulate the genetic-associated risk of onset and progression of AMD, as well as therapeutic response.

Since the identification of high-risk patients can improve clinical management of AMD, several prediction models of onset and progression are now widely available [174, 175]. These models, based on a small number of common genetic variants, are suitable to distinguish subjects who will and will not suffer from AMD, with an area under the curve that ranges between 0.8 and 0.9 [174, 175]. However, the evaluation of these models did not provide encouraging results, because the same subject can receive controversial forecasts from different tests [176, 177].

To date, it is difficult to evaluate the benefits of genetic testing in the context of complex diseases such as AMD [178]. To overcome this issue, prediction models should also include rare mutations, like those reviewed by Geerlings et al. [102], clinical characteristics, and environmental risk factors. Once early AMD is clinically manifested, the number and nature of risk alleles significantly influence the progression to advanced AMD. Moreover, in addition to independent risk factors (i.e., smoking) [95, 139–143], others, such as diet [163] and nutrients intake [153, 154], seem to interact with AMD-associated polymorphisms on determining the risk of progression to advanced AMD. Growing body of evidence also suggested determining the genetic risk profile prior to choosing the adequate treatment. In this context, we concluded that success of treatment of dry AMD with antioxidants and zinc relies on genetic risk variants, with a better response among subjects with no CFH risk alleles [164–166]. Similarly, the presence of CFH risk genotypes leads to worse response to anti-VEGF therapy against wet AMD [97, 173]. Despite the fact that knowledge is increasing, the perspective to guide personalized medicine through genetic testing is still under debate and further clinical studies should be encouraged.

Several lines of evidence also suggested that complement system is a promising target for the development of novel therapies, which could support the conventional treatment with anti-VEGF agents. Currently, potential candidates, such as complement component inhibitors, antibody-based compounds, and receptor antagonists, are in clinical trials or in preclinical evaluation [179]. While eculizumab, a humanized IgG antibody against complement component 5 (C5), seems to be ineffective in the management of dry AMD patients [180], treatment with lampalizumab, an antibody that inhibits complement factor D, reduced the progression of geographic atrophy lesion [181]. Since treatment with lampalizumab seems to be more effective in patients with specific CFI genotypes, a phase III trial is currently running. In this perspective, understanding the pathways involved in inflammation and neovascularization could allow the choice of proper treatment within the clinical context of disease heterogeneity.

In conclusion, our review highlighted that research behind the role of complement system in AMD has been mainly based on genome-wide and candidate gene studies. However, genomics alone does not reveal the causative relation between gene-environment interaction and AMD, and current evidence should be integrated by other "omics" disciplines which take into account the impact of exposome. However, in the forthcoming future, it is plausible that AMD

prevention and treatment will be personalized for single groups of patients, according to their genetic risk profile, clinical characteristics, and environmental exposure.

Conflicts of Interest

The authors declare that there are no conflicts of interest regarding the publication of this paper.

Acknowledgments

This research was funded by the Department of Medical and Surgical Sciences and Advanced Technologies "GF Ingrassia," University of Catania, Italy (Piano Triennale di Sviluppo delle Attività di Ricerca Scientifica del Dipartimento 2016–18).

References

[1] J. W. Miller, "Age-related macular degeneration revisited - Piecing the puzzle: The LXIX edward jackson memorial lecture," *American Journal of Ophthalmology*, vol. 155, no. 1, pp. 1–35, 2013.

[2] S. Sarks, S. Cherepanoff, M. Killingsworth, and J. Sarks, "Relationship of basal laminar deposit and membranous debris to the clinical presentation of early age-related macular degeneration," *Investigative Ophthalmology & Visual Science*, vol. 48, no. 3, pp. 968–977, 2007.

[3] J. Ambati and B. J. Fowler, "Mechanisms of age-related macular degeneration," *Neuron*, vol. 75, no. 1, pp. 26–39, 2012.

[4] J. M. Seddon, S. George, and B. Rosner, "Cigarette smoking, fish consumption, omega-3 fatty acid intake, and associations with age-related macular degeneration: the US twin study of age-related macular degeneration," *JAMA Ophtalmology*, vol. 124, no. 7, pp. 995–1001, 2006.

[5] D. Weismann, K. Hartvigsen, N. Lauer et al., "Complement factor H binds malondialdehyde epitopes and protects from oxidative stress," *Nature*, vol. 478, no. 7367, pp. 76–81, 2011.

[6] J. Thornton, R. Edwards, P. Mitchell, R. A. Harrison, I. Buchan, and S. P. Kelly, "Smoking and age-related macular degeneration: a review of association," *Eye*, vol. 19, no. 9, pp. 935–944, 2005.

[7] B. Neuner, A. Komm, J. Wellmann et al., "Smoking history and the incidence of age-related macular degeneration—results from the Muenster Aging and Retina Study (MARS) cohort and systematic review and meta-analysis of observational longitudinal studies," *Addictive Behaviors*, vol. 34, no. 11, pp. 938–947, 2009.

[8] S. C. Tomany, J. J. Wang, R. Van Leeuwen et al., "Risk factors for incident age-related macular degeneration: pooled findings from 3 continents," *Ophthalmology*, vol. 111, no. 7, pp. 1280–1287, 2004.

[9] J. R. Evans, A. E. Fletcher, and R. P. L. Wormald, "28 000 Cases of age related macular degeneration causing visual loss in people aged 75 years and above in the United Kingdom may be attributable to smoking," *British Journal of Ophthalmology*, vol. 89, no. 5, pp. 550–553, 2005.

[10] K. P. Howard, B. E. K. Klein, K. E. Lee, and R. Klein, "Measures of body shape and adiposity as related to incidence of age-related eye diseases: observations from the Beaver Dam Eye Study," *Investigative Ophthalmology & Visual Science*, vol. 55, no. 4, pp. 2592–2598, 2014.

[11] B. E. K. Klein, R. Klein, K. E. Lee, and S. C. Jensen, "Measures of obesity and age-related eye diseases," *Ophthalmic Epidemiology*, vol. 8, no. 4, pp. 251–262, 2001.

[12] J. M. Seddon, J. Cote, N. Davis, and B. Rosner, "Progression of age-related macular degeneration: association with body mass index, waist circumference, and waist-hip ratio," *JAMA Ophtalmology*, vol. 121, no. 6, pp. 785–792, 2003.

[13] C. Delcourt, F. Michel, A. Colvez et al., "Associations of cardiovascular disease and its risk factors with age-related macular degeneration: the POLA study," *Ophthalmic Epidemiology*, vol. 8, no. 4, pp. 237–249, 2001.

[14] S. C. Tomany, R. Klein, and B. E. K. Klein, "The relationship between iris color, hair color, and skin sun sensitivity and the 10-year incidence of age-related maculopathy: The Beaver Dam Eye Study," *Ophthalmology*, vol. 110, no. 8, pp. 1526–1533, 2003.

[15] S. C. Tomany, K. J. Cruickshanks, R. Klein, B. E. K. Klein, and M. D. Knudtson, "Sunlight and the 10-year incidence of age-related maculopathy: the beaver dam eye study," *JAMA Ophtalmology*, vol. 122, no. 5, pp. 750–757, 2004.

[16] E. J. Johnson, "Obesity, lutein metabolism, and age-related macular degeneration: A web of connections," *Nutrition Reviews*, vol. 63, no. 1, pp. 9–15, 2005.

[17] J. M. Seddon, G. Gensler, R. C. Milton, M. L. Klein, and N. Rifai, "Association between C-reactive protein and age-related macular degeneration," *Journal of the American Medical Association*, vol. 291, no. 6, pp. 704–710, 2004.

[18] R. Klein, Y. Deng, B. E. K. Klein et al., "Cardiovascular disease, its risk factors and treatment, and age-related macular degeneration: Women's Health Initiative Sight Exam Ancillary Study," *American Journal of Ophthalmology*, vol. 143, no. 3, pp. 473–e2, 2007.

[19] J. A. Mares-Perlman, W. E. Brady, R. Klein, G. M. Vandenlangenberg, B. E. K. Klein, and M. Palta, "Dietary fat and age-related maculopathy," *JAMA Ophtalmology*, vol. 113, no. 6, pp. 743–748, 1995.

[20] G. M. VandenLangenberg, J. A. Mares-Perlman, R. Klein, B. E. K. Klein, W. E. Brady, and M. Palta, "Associations between antioxidant and zinc intake and the 5-year incidence of early age-related maculopathy in the beaver dam eye study," *American Journal of Epidemiology*, vol. 148, no. 2, pp. 204–214, 1998.

[21] J. M. Seddon, U. A. Ajani, R. D. Sperduto et al., "Dietary carotenoids, vitamins A, C, and E, and advanced age-related macular degeneration," *The Journal of the American Medical Association*, vol. 272, no. 18, pp. 1413–1420, 1994.

[22] J. M. Seddon, B. Rosner, R. D. Sperduto et al., "Dietary fat and risk for advanced age-related macular degeneration," *JAMA Ophtalmology*, vol. 119, no. 8, pp. 1191–1199, 2001.

[23] The Age-Related Eye Disease Study 2 (AREDS2) Research Group, "Lutein + zeaxanthin and omega-3 fatty acids for age-related macular degeneration: the Age-Related Eye Disease Study 2 (AREDS2) randomized clinical trial," *The Journal of the American Medical Association*, vol. 309, no. 19, pp. 2005–2015, 2013.

[24] G.-S. Ying, J. Huang, M. G. Maguire et al., "Baseline predictors for one-year visual outcomes with ranibizumab or bevacizumab for neovascular age-related macular degeneration," *Ophthalmology*, vol. 120, no. 1, pp. 122–129, 2013.

[25] P. K. Kaiser, D. M. Brown, K. Zhang et al., "Ranibizumab for predominantly classic neovascular age-related macular degeneration: subgroup analysis of first-year ANCHOR results," *American Journal of Ophthalmology*, vol. 144, no. 6, pp. 850–857, 2007.

[26] CATT Research Group, D. F. Martin, M. G. Maguire et al., "Ranibizumab and bevacizumab for neovascular age-related macular degeneration," *The New England Journal of Medicine*, vol. 64, no. 20, pp. 1897–1908, 2011.

[27] P. J. Rosenfeld, D. M. Brown, J. S. Heier et al., "Ranibizumab for neovascular age-related macular degeneration," *The New England Journal of Medicine*, vol. 355, no. 14, pp. 1419–1431, 2006.

[28] U. Chakravarthy, S. P. Harding, C. A. Rogers et al., "Ranibizumab versus bevacizumab to treat neovascular age-related macular degeneration: one-year findings from the IVAN randomized trial," *Ophthalmology*, vol. 119, no. 7, pp. 1399–1411, 2012.

[29] J. S. Heier, D. M. Brown, and V. Chong, "Intravitreal aflibercept (VEGF trap-eye) in wet age related macular degeneration," *Ophthalmology*, vol. 119, no. 12, pp. 2537–2548, 2012.

[30] M. Nozaki, B. J. Raisler, E. Sakurai et al., "Drusen complement components C3a and C5a promote choroidal neovascularization," *Proceedings of the National Acadamy of Sciences of the United States of America*, vol. 103, no. 7, pp. 2328–2333, 2006.

[31] L. G. Fritsche, W. Chen, M. Schu et al. et al., "Seven new loci associated with age-related macular degeneration," *Nature Genetics*, vol. 45, pp. 433–439, 2013.

[32] H. Chen, K.-D. Yu, and G.-Z. Xu, "Association between variant Y402H in age-related macular degeneration (AMD) susceptibility gene CFH and treatment response of AMD: A meta-analysis," *PLoS ONE*, vol. 7, no. 8, Article ID e42464, 2012.

[33] Y. Tong, J. Liao, Y. Zhang, J. Zhou, H. Zhang, and M. Mao, "LOC387715/HTRA1 gene polymorphisms and susceptibility to agerelated macular degeneration: a huge review and meta-analysis," *Molecular Vision*, vol. 16, pp. 1958–1981, 2010.

[34] G. J. Mckay, C. C. Patterson, U. Chakravarthy et al., "Evidence of association of APOE with age-related macular degeneration - a pooled analysis of 15 studies," *Human Mutation*, vol. 32, no. 12, pp. 1407–1416, 2011.

[35] M. Barchitta and A. Maugeri, "Association between Vascular endothelial growth factor polymorphisms and age-related macular degeneration: an updated meta-analysis," *Disease Markers*, vol. 2016, 2016.

[36] M. K.Liszewski and J. P. Atkinson, "Complement regulators in human disease: Lessons from modern genetics," *Journal of Internal Medicine*, vol. 277, no. 3, pp. 294–305, 2015.

[37] P. F. Zipfel, "Complement and immune defense: from innate immunity to human diseases," *Immunology Letters*, vol. 126, no. 1-2, pp. 1–7, 2009.

[38] E. Wagner and M. M. Frank, "Therapeutic potential of complement modulation," *Nature Reviews Drug Discovery*, vol. 9, no. 1, pp. 43–56, 2010.

[39] R. S. Agbeko, K. J. Fidler, M. L. Allen, P. Wilson, N. J. Klein, and M. J. Peters, "Genetic variability in complement activation modulates the systemic inflammatory response syndrome in children," *Pediatric Critical Care Medicine*, vol. 11, no. 5, pp. 561–567, 2010.

[40] A. P. Manderson, M. Botto, and M. J. Walport, "The role of complement in the development of systemic lupus erythematosus," *Annual Review of Immunology*, vol. 22, pp. 431–456, 2004.

[41] D. Kavanagh, T. H. Goodship, and A. Richards, "Atypical hemolytic uremic syndrome," *Seminars in Nephrology*, vol. 33, no. 6, pp. 508–530, 2013.

[42] T. D. Barbour, M. M. Ruseva, and M. C. Pickering, "Update on C3 glomerulopathy," *Nephrology Dialysis Transplantation*, vol. 31, no. 5, pp. 717–725, 2016.

[43] S. Khandhadiaa, V. Ciprianib, J. R. W. Yatesb, and A. J. Loterya, "Age-related macular degeneration and the complement system," *Immunobiology*, vol. 217, no. 2, pp. 127–146, 2012.

[44] D. D. Kim and W.-C. Song, "Membrane complement regulatory proteins," *Clinical Immunology*, vol. 118, no. 2-3, pp. 127–136, 2006.

[45] A. Kopp, M. Hebecker, E. Svobodová, and M. Józsi, "Factor H: A complement regulator in health and disease, and a mediator of cellular interactions," *Biomolecules*, vol. 2, no. 1, pp. 46–75, 2012.

[46] A. Nicholson-Weller, J. Burge, D. T. Fearon, and K. F. Austen, "Isolation of a human erythrocyte membrane glycoprotein with decay-accelerating activity for C3 convertases of the complement system," *The Journal of Immunology*, vol. 129, no. 1, pp. 184–189, 1982.

[47] S. Tsukasa, O. Michiyo, M. Misako, H. Kyongsu, K. Taroh, and J. P. Atkinson, "Preferential inactivation of the C5 convertase of the alternative complement pathway by factor I and membrane cofactor protein (MCP)," *Molecular Immunology*, vol. 28, no. 10, pp. 1137–1147, 1991.

[48] T. Seya, A. Hirano, M. Matsumoto, M. Nomura, and S. Ueda, "Human membrane cofactor protein (MCP, CD46): Multiple isoforms and functions," *The International Journal of Biochemistry & Cell Biology*, vol. 31, no. 11, pp. 1255–1260, 1999.

[49] G. D. Ross, J. D. Lambris, J. A. Cain, and S. L. Newman, "Generation of three different fragments of bound C3 with purified factor I or serum. I. Requirements for factor H vs CR1 cofactor activity," *The Journal of Immunology*, vol. 129, no. 5, pp. 2051–2060, 1982.

[50] D. Mossakowska, I. Dodd, W. Pindar, and R. A. G. Smith, "Structure-activity relationships within the N-terminal short consensus repeats (SCR) of human CR1 (C3b/C4b receptor CD35): SCR 3 plays a critical role in inhibition of the classical and alternative pathways of complement activation," *European Journal of Immunology*, vol. 29, no. 6, pp. 1955–1965, 1999.

[51] R. G. DiScipio, "Ultrastructures and interactions of complement factors H and I," *The Journal of Immunology*, vol. 149, no. 8, pp. 2592–2599, 1992.

[52] J. L. McRae, T. G. Duthy, K. M. Griggs et al., "Human factor H-related protein 5 has cofactor activity, inhibits C3 convertase activity, binds heparin and C-reactive protein, and associates with lipoprotein," *The Journal of Immunology*, vol. 174, no. 10, pp. 6250–6256, 2005.

[53] J. Wu, Y.-Q. Wu, D. Ricklin, B. J. C. Janssen, J. D. Lambris, and P. Gros, "Structure of complement fragment C3b-factor H and implications for host protection by complement regulators," *Nature Immunology*, vol. 10, no. 7, pp. 728–733, 2009.

[54] P. F. Zipfel and C. Skerka, "Complement regulators and inhibitory proteins," *Nature Reviews Immunology*, vol. 9, no. 10, pp. 729–740, 2009.

[55] S. J. Perkins, K. W. Fung, and S. Khan, "Molecular interactions between complement factor H and its heparin and heparan sulfate ligands," *Frontiers in Immunology*, vol. 5, no. 126, pp. 1–14, 2014.

[56] B. S. Blaum, J. P. Hannan, A. P. Herbert, D. Kavanagh, D. Uhrín, and T. Stehle, "Structural basis for sialic acid-mediated self-recognition by complement factor H," *Nature Chemical Biology*, vol. 11, no. 1, pp. 77–82, 2015.

[57] A. Langford-Smith, A. J. Day, P. N. Bishop, and S. J. Clark, "Complementing the sugar code: Role of GAGs and sialic acid in complement regulation," *Frontiers in Immunology*, vol. 6, 2015.

[58] L. Deban, H. Jarva, M. J. Lehtinen et al., "Binding of the long pentraxin PTX3 to factor H: Interacting domains and function in the regulation of complement activation," *The Journal of Immunology*, vol. 181, no. 12, pp. 8433–8440, 2008.

[59] H. Jarva, T. S. Jokiranta, J. Hellwage, P. F. Zipfel, and S. Meri, "Regulation of complement activation by C-reactive protein: Targeting the complement inhibitory activity of factor H by an interaction with short consensus repeat domains 7 and 8-11," *The Journal of Immunology*, vol. 163, no. 7, pp. 3957–3962, 1999.

[60] M. Mihlan, M. Hebecker, H.-M. Dahse et al., "Human complement factor H-related protein 4 binds and recruits native pentameric C-reactive protein to necrotic cells," *Molecular Immunology*, vol. 46, no. 3, pp. 335–344, 2009.

[61] M. Mihlan, S. Stippa, M. Józsi, and P. F. Zipfel, "Monomeric CRP contributes to complement control in fluid phase and on cellular surfaces and increases phagocytosis by recruiting factor H," *Cell Death & Differentiation*, vol. 16, no. 12, pp. 1630–1640, 2009.

[62] W. G. Brodbeck, D. Liu, J. Sperry, C. Mold, and M. E. Medof, "Localization of classical and alternative pathway regulatory activity within the decay-accelerating factor," *The Journal of Immunology*, vol. 156, no. 7, pp. 2528–2533, 1996.

[63] M. E. Medof, T. Kinoshita, and V. Nussenzweig, "Inhibition of complement activation on the surface of cells after incorporation of Decay-Accelerating Factor (DAF) into their membranes," *The Journal of Experimental Medicine*, vol. 160, no. 5, pp. 1558–1578, 1984.

[64] C. L. Harris, R. J. M. Abbott, R. A. Smith, B. P. Morgan, and S. M. Lea, "Molecular dissection of interactions between components of the alternative pathway of complement and decay accelerating factor (CD55)," *The Journal of Biological Chemistry*, vol. 280, no. 4, pp. 2569–2578, 2005.

[65] C. L. Harris, D. M. Pettigrew, S. M. Lea, and B. P. Morgan, "Decay-accelerating factor must bind both components of the complement alternative pathway C3 convertase to mediate efficient decay," *The Journal of Immunology*, vol. 178, no. 1, pp. 352–359, 2007.

[66] D. M. Lublin, "Review: Cromer and DAF: Role in health and disease," *Immunohematology*, vol. 21, no. 2, pp. 39–47, 2005.

[67] S. A. Rollins and P. J. Sims, "The complement-inhibitory activity of CD59 resides in its capacity to block incorporation of C9 into membrane C5b-9," *The Journal of Immunology*, vol. 144, no. 9, pp. 3478–3483, 1990.

[68] S. Meri, B. P. Morgan, A. Davies et al., "Human protectin (CD59), an 18,000-20,000 MW complement lysis restricting factor, inhibits C5b-8 catalysed insertion of C9 into lipid bilayers," *The Journal of Immunology*, vol. 71, no. 1, pp. 1–9, 1990.

[69] T. Husler, D. H. Lockert, K. M. Kaufman, J. M. Sodetz, and P. J. Sims, "Chimeras of human complement C9 reveal the site recognized by complement regulatory protein CD59," *The Journal of Biological Chemistry*, vol. 270, no. 8, pp. 3483–3486, 1995.

[70] D. H. Lockert, K. M. Kaufman, C.-P. Chang, T. Husler, J. M. Sodetz, and P. J. Sims, "Identity of the segment of human complement C8 recognized by complement regulatory protein CD59," *The Journal of Biological Chemistry*, vol. 270, no. 34, pp. 19723–19728, 1995.

[71] I. Farkas, L. Baranyi, Y. Ishikawa et al., "CD59 blocks not only the insertion of C9 into MAC but inhibits ion channel formation by homologous C5b-8 as well as C5b-9," *The Journal of Physiology*, vol. 539, no. 2, pp. 537–545, 2002.

[72] Y. Huang, F. Qiao, R. Abagyan, S. Hazard, and S. Tomlinson, "Defining the CD59-C9 binding interaction," *The Journal of Biological Chemistry*, vol. 281, no. 37, pp. 27398–27404, 2006.

[73] B. P. Morgan and P. Gasque, "Extrahepatic complement biosynthesis: Where, when and why?" *Clinical & Experimental Immunology*, vol. 107, no. 1, pp. 1–7, 1997.

[74] L. V. Johnson, S. Ozaki, M. K. Staples, P. A. Erickson, and D. H. Anderson, "A potential role for immune complex pathogenesis in drusen formation," *Experimental Eye Research*, vol. 70, no. 4, pp. 441–449, 2000.

[75] L. V. Johnson, W. P. Leitner, M. K. Staples, and D. H. Anderson, "Complement activation and inflammatory processes in drusen formation and age related macular degeneration," *Experimental Eye Research*, vol. 73, no. 6, pp. 887–896, 2001.

[76] G. S. Hageman, D. H. Anderson, L. V. Johnson et al., "A common haplotype in the complement regulatory gene factor H (HF1/CFH) predisposes individuals to age-related macular degeneration," *Proceedings of the National Acadamy of Sciences of the United States of America*, vol. 102, no. 20, pp. 7227–7232, 2005.

[77] M. P. Kawa, A. Machalinska, D. Roginska, and B. Machalinski, "Complement system in pathogenesis of AMD: dual player in degeneration and protection of retinal tissue," *Journal of Immunology Research*, vol. 2014, 2014.

[78] S. Sivaprasad, T. Adewoyin, T. A. Bailey et al., "Estimation of systemic complement C3 activity in age-related macular degeneration," *JAMA Ophtalmology*, vol. 125, no. 4, pp. 515–519, 2007.

[79] H. P. N. Scholl, P. C. Issa, M. Walier et al., "Systemic complement activation in age-related macular degeneration," *PLoS ONE*, vol. 3, no. 7, Article ID e2593, 2008.

[80] A. MacHalińska, V. Dziedziejko, K. Mozolewska-Piotrowska, D. Karczewicz, B. Wiszniewska, and B. MacHaliński, "Elevated plasma levels of c3a complement compound in the exudative form of age-related macular degeneration," *Ophthalmic Research*, vol. 42, no. 1, pp. 54–59, 2009.

[81] G. S. Hageman, P. J. Luthert, N. H. Victor Chong, L. V. Johnson, D. H. Anderson, and R. F. Mullins, "An integrated hypothesis that considers drusen as biomarkers of immune-mediated processes at the RPE-Bruch's membrane interface in aging and age-related macular degeneration," *Progress in Retinal and Eye Research*, vol. 20, no. 6, pp. 705–732, 2001.

[82] J. W. Crabb, M. Miyagi, X. Gu et al., "Drusen proteome analysis: an approach to the etiology of age-related macular degeneration," *Proceedings of the National Acadamy of Sciences of the United States of America*, vol. 99, no. 23, pp. 14682–14687, 2002.

[83] R. F. Mullins, S. R. Russell, D. H. Anderson, and G. S. Hageman, "Drusen associated with aging and age-related macular degeneration contain proteins common to extracellular deposits associated with atherosclerosis, elastosis, amyloidosis, and dense deposit disease," *The FASEB Journal*, vol. 14, no. 7, pp. 835–846, 2000.

[84] S. C. Finnemann, L. W. Leung, and E. Rodriguez-Boulan, "The lipofuscin component A2E selectively inhibits phagolysosomal degradation of photoreceptor phospholipid by the retinal pigment epithelium," *Proceedings of the National Acadamy of Sciences of the United States of America*, vol. 99, no. 6, pp. 3842–3847, 2002.

[85] C. Vives-Bauza, M. Anand, A. K. Shirazi et al., "The age lipid A2E and mitochondrial dysfunction synergistically impair

phagocytosis by retinal pigment epithelial cells," *The Journal of Biological Chemistry*, vol. 283, no. 36, pp. 24770–24780, 2008.

[86] E. Kaemmerer, F. Schutt, T. U. Krohne, F. G. Holz, and J. Kopitz, "Effects of lipid peroxidation-related protein modifications on RPE lysosomal functions and POS phagocytosis," *Investigative Ophthalmology & Visual Science*, vol. 48, no. 3, pp. 1342–1347, 2007.

[87] J. Zhou, Y. P. Jang, S. R. Kim, and J. R. Sparrow, "Complement activation by photooxidation products of A2E, a lipofuscin constituent of the retinal pigment epithelium," *Proceedings of the National Acadamy of Sciences of the United States of America*, vol. 103, no. 44, pp. 16182–16187, 2006.

[88] J. Zhou, S. R. Kim, B. S. Westlund, and J. R. Sparrow, "Complement activation by bisretinoid constituents of RPE lipofuscin," *Investigative Ophthalmology & Visual Science*, vol. 50, no. 3, pp. 1392–1399, 2009.

[89] S. J. Clark and P. N. Bishop, "Role of factor H and related proteins in regulating complement activation in the macula, and relevance to age-related macular degeneration," *Journal of Clinical Medicine*, vol. 4, no. 1, pp. 18–31, 2014.

[90] A. Tortajada, T. Montes, R. Martínez-Barricarte, B. P. Morgan, C. L. Harris, and S. R. de Córdoba, "The disease-protective complement factor H allotypic variant Ile62 shows increased binding affinity for C3b and enhanced cofactor activity," *Human Molecular Genetics*, vol. 18, no. 18, pp. 3452–3461, 2009.

[91] M. Józsi and P. F. Zipfel, "Factor H family proteins and human diseases," *Trends in Immunology*, vol. 29, no. 8, pp. 380–387, 2008.

[92] R. J. Klein, C. Zeiss, E. Y. Chew et al., "Complement factor H polymorphism in age-related macular degeneration," *Science*, vol. 308, no. 5720, pp. 385–389, 2005.

[93] J. L. Haines, M. A. Hauser, S. Schmidt et al., "Complement factor H variant increases the risk of age-related macular degeneration," *Science*, vol. 308, no. 5720, pp. 419–421, 2005.

[94] A. O. Edwards, R. Ritter III, K. J. Abel, A. Manning, C. Panhuysen, and L. A. Farrer, "Complement factor H polymorphism and age-related macular degeneration," *Science*, vol. 308, no. 5720, pp. 421–424, 2005.

[95] R. Sofat, J. P. Casas, A. R. Webster et al., "Complement factor h genetic variant and age-related macular degeneration: Effect size, modifiers and relationship to disease subtype," *International Journal of Epidemiology*, vol. 41, no. 1, pp. 250–262, 2012.

[96] A. Thakkinstian, P. Han, M. McEvoy et al., "Systematic review and meta-analysis of the association between complementary factor H Y402H polymorphisms and age-related macular degeneration," *Human Molecular Genetics*, vol. 15, no. 18, pp. 2784–2790, 2006.

[97] N. Hong, Y. Shen, C.-Y. Yu, S.-Q. Wang, and J.-P. Tong, "Association of the polymorphism Y402H in the CFH gene with response to anti-VEGF treatment in age-related macular degeneration: A systematic review and meta-analysis," *Acta Ophthalmologica*, vol. 94, no. 4, pp. 334–345, 2016.

[98] M. Wu, Y. Guo, Y. Ma, Z. Zheng, Q. Wang, and X. Zhou, "Association of two polymorphisms, rs1061170 and rs1410996, in complement factor H with age-related macular degeneration in an asian population: a meta-analysis," *Ophthalmic Research*, vol. 55, no. 3, pp. 135–144, 2016.

[99] X. Wang, P. Geng, Y. Zhang, and M. Zhang, "Association between complement factor H Val62Ile polymorphism and age-related macular degeneration susceptibility: A meta-analysis," *Gene*, vol. 538, no. 2, pp. 306–312, 2014.

[100] A. Maugeri, M. Barchitta, and A. Agodi, "The association between complement factor h rs1061170 polymorphism and age-related macular degeneration: a comprehensive meta-analysis stratified by stage of disease and ethnicity," *Acta Ophthalmologica*.

[101] J. Tian, W. Yu, X. Qin et al., "Association of genetic polymorphisms and age-related macular degeneration in Chinese population," *Investigative Ophthalmology & Visual Science*, vol. 53, no. 7, pp. 4262–4269, 2012.

[102] M. J. Geerlings, E. K. de Jong, and A. I. den Hollander, "The complement system in age-related macular degeneration: A review of rare genetic variants and implications for personalized treatment," *Molecular Immunology*, vol. 84, pp. 65–76, 2017.

[103] X. Liao, C.-J. Lan, I.-W. Cheuk, and Q.-Q. Tan, "Four complement factor H gene polymorphisms in association with AMD: A meta-analysis," *Archives of Gerontology and Geriatrics*, vol. 64, pp. 123–129, 2016.

[104] F. Abedi, S. Wickremasinghe, A. J. Richardson, A. F. M. Islam, R. H. Guymer, and P. N. Baird, "Genetic influences on the outcome of anti-vascular endothelial growth factor treatment in neovascular age-related macular degeneration," *Ophthalmology*, vol. 120, no. 8, pp. 1641–1648, 2013.

[105] E. K. Wagner, S. Raychaudhuri, M. B. Villalonga et al., "Mapping rare, deleterious mutations in Factor H: Association with early onset, drusen burden, and lower antigenic levels in familial AMD," *Scientific Reports*, vol. 6, 2016.

[106] J. B. Maller, J. A. Fagerness, R. C. Reynolds, B. M. Neale, M. J. Daly, and J. M. Seddon, "Variation in complement factor 3 is associated with risk of age-related macular degeneration," *Nature Genetics*, vol. 39, no. 10, pp. 1200-1201, 2007.

[107] J. R. W. Yates, T. Sepp, B. K. Matharu et al., "Complement C3 variant and the risk of age-related macular degeneration," *The New England Journal of Medicine*, vol. 357, no. 6, pp. 553–561, 2007.

[108] J. M. Seddon, Y. Yu, E. C. Miller et al., "Rare variants in CFI, C3 and C9 are associated with high risk of advanced age-related macular degeneration," *Nature Genetics*, vol. 45, no. 11, pp. 1366–1373, 2013.

[109] H. Helgason, P. Sulem, M. R. Duvvari et al., "A rare nonsynonymous sequence variant in C3 is associated with high risk of age-related macular degeneration," *Nature Genetics*, vol. 45, no. 11, pp. 1371–1376, 2013.

[110] X. Zhan, D. E. Larson, C. Wang et al., "Identification of a rare coding variant in complement 3 associated with age-related macular degeneration," *Nature Genetics*, vol. 45, no. 11, pp. 1375–1381, 2013.

[111] N. Nishida, T. Walz, and T. A. Springer, "Structural transitions of complement component C3 and its activation products," *Proceedings of the National Acadamy of Sciences of the United States of America*, vol. 103, no. 52, pp. 19737–19742, 2006.

[112] M. X. Zhang, X. F. Zhao, Y. C. Ren et al., "Association between a functional genetic polymorphism (rs2230199) and age-related macular degeneration risk: A meta-analysis," *Genetics and Molecular Research*, vol. 14, no. 4, pp. 12567–12576, 2015.

[113] Y. Qian-Qian, Y. Yong, Z. Jing et al., "Nonsynonymous single nucleotide polymorphisms in the complement component 3 gene are associated with risk of age-related macular degeneration: A meta-analysis," *Gene*, vol. 561, no. 2, pp. 249–255, 2015.

[114] S. G. Schwartz and M. A. Brantley Jr., "Pharmacogenetics and age-related macular degeneration," *Journal of Ophthalmology*, vol. 2011, Article ID 252549, 8 pages, 2011.

[115] J. E. Grunwald, E. Daniel, G. Ying et al., "Photographic assessment of baseline fundus morphologic features in the Comparison of Age-Related Macular Degeneration Treatments Trials," *Ophthalmology*, vol. 119, no. 8, pp. 1634–1641, 2012.

[116] J. Gu, G. J. T. Pauer, X. Yue et al., "Assessing susceptibility to age-related macular degeneration with proteomic and genomic biomarkers," *Molecular & Cellular Proteomics*, vol. 8, no. 6, pp. 1338–1349, 2009.

[117] S. B. Bressler, "Introduction: understanding the role of angiogenesis and antiangiogenic agents in age-related macular degeneration," *Ophthalmology*, vol. 116, supplement 10, pp. S1–S7, 2009.

[118] S. A. Hagstrom, G.-S. Ying, G. J. T. Pauer et al., "Pharmacogenetics for genes associated with age-related macular degeneration in the comparison of AMD treatments trials (CATT)," *Ophthalmology*, vol. 120, no. 3, pp. 593–599, 2013.

[119] P. J. Francis, "The influence of genetics on response to treatment with ranibizumab (Lucentis) for age-related macular degeneration: The Lucentis Genotype study," *Transactions of the American Ophthalmological Society*, vol. 109, pp. 115–156, 2011.

[120] A. Thakkinstian, M. McEvoy, U. Chakravarthy et al., "The association between complement component 2/complement factor B polymorphisms and age-related macular degeneration: a HuGE review and meta-analysis," *American Journal of Epidemiology*, vol. 176, no. 5, pp. 361–372, 2012.

[121] X. Wang, Y. Zhang, and M.-N. Zhang, "Complement factor B polymorphism (rs641153) and susceptibility to age-related macular degeneration: Evidence from published studies," *International Journal of Ophthalmology*, vol. 6, no. 6, pp. 861–867, 2013.

[122] B. Gold, J. E. Merriam, J. Zernant et al., "Variation in factor B (*BF*) and complement component 2 (*C2*) genes is associated with age-related macular degeneration," *Nature Genetics*, vol. 38, no. 4, pp. 458–462, 2006.

[123] T. Montes, A. Tortajada, B. P. Morgan, S. R. De Córdoba, and C. L. Harris, "Functional basis of protection against age-related macular degeneration conferred by a common polymorphism in complement factor B," *Proceedings of the National Acadamy of Sciences of the United States of America*, vol. 106, no. 11, pp. 4366–4371, 2009.

[124] M.-L. Lokki and S. A. Koskimies, "Allelic differences in hemolytic activity and protein concentration of BF molecules are found in association with particular HLA haplotypes," *Immunogenetics*, vol. 34, no. 4, pp. 242–246, 1991.

[125] K. L. Spencer, M. A. Hauser, L. M. Olson et al., "Protective effect of complement factor B and complement component 2 variants in age-related macular degeneration," *Human Molecular Genetics*, vol. 16, no. 16, pp. 1986–1992, 2007.

[126] B. Kloeckener-Gruissem, D. Barthelmes, S. Labs et al., "Genetic association with response to intravitreal ranibizumab in patients with neovascular AMD," *Investigative Ophthalmology & Visual Science*, vol. 52, no. 7, pp. 4694–4702, 2011.

[127] J. A. Fagerness, J. B. Maller, B. M. Neale, R. C. Reynolds, M. J. Daly, and J. M. Seddon, "Variation near complement factor I is associated with risk of advanced AMD," *European Journal of Human Genetics*, vol. 17, no. 1, pp. 100–104, 2009.

[128] J. Wang, K. Ohno-Matsui, T. Yoshida et al., "Altered function of factor I caused by amyloid β: Implication for pathogenesis of age-related macular degeneration from drusen," *The Journal of Immunology*, vol. 181, no. 1, pp. 712–720, 2008.

[129] W. Chen, D. Stambolian, A. O. Edwards et al., "Genetic variants near timp3 and high-density lipoprotein-associated loci influence susceptibility to age-related macular degeneration," *Proceedings of the National Acadamy of Sciences of the United States of America*, vol. 107, no. 10, pp. 7401–7406, 2010.

[130] N. Kondo, H. Bessho, S. Honda, and A. Negi, "Additional evidence to support the role of a common variant near the complement factor i gene in susceptibility to age-related macular degeneration," *European Journal of Human Genetics*, vol. 18, no. 6, pp. 634-635, 2010.

[131] S. Ennis, J. Gibson, A. J. Cree, A. Collins, and A. J. Lotery, "Support for the involvement of complement factor i in age-related macular degeneration," *European Journal of Human Genetics*, vol. 18, no. 1, pp. 15-16, 2010.

[132] Q. Wang, H. S. Zhao, and L. Li, "Association between complement factor I gene polymorphisms and the risk of age-related macular degeneration: a Meta-analysis of literature," *International Journal of Ophthalmology*, vol. 9, pp. 298–305, 2016.

[133] L. G. Fritsche, W. Igl, and J. N. Bailey, "A large genome-wide association study of age-related macular degeneration highlights contributions of rare and common variants," *Nature Genetics*, vol. 48, no. 2, pp. 134–143, 2016.

[134] D. Ferrara and J. M. Seddon, "Phenotypic characterization of complement factor H R1210C rare genetic variant in age-related macular degeneration," *JAMA Ophthalmology*, vol. 133, no. 7, pp. 785–791, 2015.

[135] Y. Yu, M. P. Triebwasser, E. K. S. Wong et al., "Whole-exome sequencing identifies rare, functional CFH variants in families with macular degeneration," *Human Molecular Genetics*, vol. 23, no. 19, pp. 5283–5293, 2014.

[136] M. R. Duvvari, C. C. Paun, G. H. S. Buitendijk et al., "Analysis of rare variants in the C3 gene in patients with age-related macular degeneration," *PLoS ONE*, vol. 9, no. 4, 2014.

[137] N. T. Saksens, M. J. Geerlings, B. Bakker et al., "Rare genetic variants associated with development of age-related macular degeneration," *JAMA Ophthalmology*, vol. 134, no. 3, pp. 287–293, 2016.

[138] J. P. H. Van De Ven, S. C. Nilsson, P. L. Tan et al., "A functional variant in the CFI gene confers a high risk of age-related macular degeneration," *Nature Genetics*, vol. 45, no. 7, pp. 813–817, 2013.

[139] M. M. DeAngelis, F. Ji, I. K. Kim et al., "Cigarette smoking, CFH, APOE, ELOVL4, and Risk of Neovascular Age-Related Macular Degeneration," *JAMA Ophtalmology*, vol. 125, no. 1, pp. 49–54, 2007.

[140] E. Ryu, B. L. Fridley, N. Tosakulwong, K. R. Bailey, and A. O. Edwards, "Genome-wide association analyses of genetic, phenotypic, and environmental risks in the age-related eye disease study," *Molecular Vision*, vol. 16, pp. 2811–2821, 2010.

[141] W. K. Scott, S. Schmidt, M. A. Hauser et al., "Independent effects of complement factor H Y402H polymorphism and cigarette smoking on risk of age-related macular degeneration," *Ophthalmology*, vol. 114, no. 6, pp. 1151–1156, 2007.

[142] J. M. Seddon, S. George, B. Rosner, and M. L. Klein, "CFH gene variant, Y402H, and smoking, body mass index, environmental associations with advanced age-related macular degeneration," *Human Heredity*, vol. 61, no. 3, pp. 157–165, 2006.

[143] C. E. Myers, B. E. Klein, R. Gangnon, T. A. Sivakumaran, S. K. Iyengar, and R. Klein, "Cigarette smoking and the natural history of age-related macular degeneration: the beaver dam eye study," *Ophthalmology*, vol. 121, no. 10, pp. 1949–1955, 2014.

[144] T. Sepp, J. C. Khan, D. A. Thurlby et al., "Complement factor H variant Y402H is a major risk determinant for geographic

atrophy and choroidal neovascularization in smokers and nonsmokers," *Investigative Opthalmology & Visual Science*, vol. 47, no. 2, p. 536, 2006.

[145] S. Schmidt, M. A. Hauser, W. K. Scott et al., "Cigarette smoking strongly modifies the association of LOC387715 and age-related macular degeneration," *American Journal of Human Genetics*, vol. 78, no. 5, pp. 852–864, 2006.

[146] D. A. Schaumberg, S. E. Hankinson, Q. Guo, E. Rimm, and D. J. Hunter, "A prospective study of 2 major age-related macular degeneration susceptibility alleles and interactions with modifiable risk factors," *JAMA Ophtalmology*, vol. 125, no. 1, pp. 55–62, 2007.

[147] D. D. G. Despriet, C. C. W. Klaver, J. C. M. Witteman et al., "Complement factor H polymorphism, complement activators, and risk of age-related macular degeneration," *The Journal of the American Medical Association*, vol. 296, no. 3, pp. 301–309, 2006.

[148] Y. T. E. Lechanteur, P. L. Van De Camp, D. Smailhodzic et al., "Association of smoking and CFH and ARMS2 risk variants with younger age at onset of neovascular age-related macular degeneration," *JAMA Ophthalmology*, vol. 133, no. 5, pp. 533–541, 2015.

[149] C. Delcourt, M. Delyfer, M. Rougier et al., "Associations of complement factor H and smoking with early age-related macular degeneration: the ALIENOR study," *Investigative Ophthalmology & Visual Science*, vol. 52, no. 8, pp. 5955–5962, 2011.

[150] R. R. Kew, B. Ghebrehiwet, and A. Janoff, "Cigarette smoke can activate the alternative pathway of complement in vitro by modifying the third component of complement," *The Journal of Clinical Investigation*, vol. 75, no. 3, pp. 1000–1007, 1985.

[151] J. Esparza-Gordillo, J. M. Soria, A. Buil et al., "Genetic and environmental factors influencing the human factor H plasma levels," *Immunogenetics*, vol. 56, no. 2, pp. 77–82, 2004.

[152] N. K. Scripsema, D.-N. Hu, and R. B. Rosen, "Lutein, Zeaxanthin, and meso-Zeaxanthin in the Clinical Management of Eye Disease," *Journal of Ophthalmology*, vol. 2015, Article ID 865179, 2015.

[153] L. Ho, R. van Leeuwen, and J. C. M. Witteman, "Reducing the genetic risk of age-related macular degeneration with dietary antioxidants, zinc, and ω-3 fatty acids: the Rotterdam Study," *JAMA Ophtalmology*, vol. 129, no. 6, pp. 758–766, 2011.

[154] J. J. Wang, G. H. S. Buitendijk, E. Rochtchina et al., "Genetic susceptibility, dietary antioxidants, and long-term incidence of age-related macular degeneration in two populations," *Ophthalmology*, vol. 121, no. 3, pp. 667–675, 2014.

[155] H. Lin, J. A. Mares, M. J. LaMonte et al., "Association between dietary xanthophyll (lutein and zeaxanthin) intake and early age-related macular degeneration: the atherosclerosis risk in communities study," *Ophthalmic Epidemiology*, vol. 24, no. 5, pp. 311–322, 2017.

[156] J. M. Seddon, J. Cote, and B. Rosner, "Progression of age-related macular degeneration: association with dietary fat, transunsaturated fat, nuts, and fish intake," *JAMA Ophtalmology*, vol. 121, no. 12, pp. 1728–1737, 2003.

[157] J. P. SanGiovanni, E. Y. Chew, E. Agrón et al., "The relationship of dietary ω-3 long-chain polyunsaturated fatty acid intake with incident age-related macular degeneration: AREDS report no. 23," *JAMA Ophtalmology*, vol. 126, no. 9, pp. 1274–1279, 2008.

[158] J. P. SanGiovanni, E. Agrón, A. D. Meleth et al., "ω-3 long-chain polyunsaturated fatty acid intake and 12-y incidence of neovascular age-related macular degeneration and central geographic atrophy: AREDS report 30, a prospective cohort study from the Age-Related Eye Disease Study," *American Journal of Clinical Nutrition*, vol. 90, no. 6, pp. 1601–1607, 2009.

[159] R. Reynolds, B. Rosner, and J. M. Seddon, "Dietary omega-3 fatty acids, other fat intake, genetic susceptibility, and progression to incident geographic atrophy," *Ophthalmology*, vol. 120, no. 5, pp. 1020–1028, 2013.

[160] J. J. Wang, E. Rochtchina, W. Smith et al., "Combined effects of complement factor H genotypes, fish consumption, and inflammatory markers on long-term risk for age-related macular degeneration in a cohort," *American Journal of Epidemiology*, vol. 169, no. 5, pp. 633–641, 2009.

[161] I. C. Munch, U. Toft, A. Linneberg, and M. Larsen, "Precursors of age-related macular degeneration: associations with vitamin A and interaction with CFHY402H in the Inter99 Eye Study," *Acta Ophthalmologica*, vol. 94, no. 7, pp. 657–662, 2016.

[162] B. M. J. Merle, R. E. Silver, B. Rosner, and J. M. Seddon, "Dietary folate, B vitamins, genetic susceptibility and progression to advanced nonexudative age-related macular degeneration with geographic atrophy: A Prospective Cohort Study," *American Journal of Clinical Nutrition*, vol. 103, no. 4, pp. 1135–1144, 2016.

[163] B. M. J. Merle, R. E. Silver, B. Rosner, and J. M. Seddon, "Adherence to a Mediterranean diet, genetic susceptibility, and progression to advanced macular degeneration: a prospective cohort study," *American Journal of Clinical Nutrition*, vol. 102, no. 5, pp. 1196–1206, 2015.

[164] M. L. Klein, P. J. Francis, B. Rosner et al., "CFH and LOC387715/ARMS2 Genotypes and Treatment with Antioxidants and Zinc for Age-Related Macular Degeneration," *Ophthalmology*, vol. 115, no. 6, pp. 1019–1025, 2008.

[165] J. M. Seddon, R. E. Silver, and B. Rosner, "Response to AREDS supplements according to genetic factors: survival analysis approach using the eye as the unit of analysis," *British Journal of Ophthalmology*, vol. 100, no. 12, pp. 1731–1737, 2016.

[166] C. C. Awh, S. Hawken, and B. W. Zanke, "Treatment response to antioxidants and zinc based on *CFH*and *ARMS2*genetic risk allele number in the age-related eye disease study," *Ophthalmology*, vol. 122, no. 1, pp. 162–169, 2015.

[167] R. Nan, I. Farabella, F. F. Schumacher et al., "Zinc binding to the Tyr402 and His402 allotypes of complement factor H: possible implications for age-related macular degeneration," *Journal of Molecular Biology*, vol. 408, no. 4, pp. 714–735, 2011.

[168] R. Nan, J. Gor, I. Lengyel, and S. J. Perkins, "Uncontrolled zinc- and copper-induced oligomerisation of the human complement regulator factor H and its possible implications for function and disease," *Journal of Molecular Biology*, vol. 384, no. 5, pp. 1341–1352, 2008.

[169] S. J. Perkins, A. S. Nealis, and R. B. Sim, "Oligomeric Domain structure of human complement factor H by X-ray and neutron solution scattering," *Biochemistry*, vol. 30, no. 11, pp. 2847–2857, 1991.

[170] B. Bao, A. S. Prasad, F. W. J. Beck et al., "Zinc decreases C-reactive protein, lipid peroxidation, and inflammatory cytokines in elderly subjects: a potential implication of zinc as an atheroprotective agent," *American Journal of Clinical Nutrition*, vol. 91, no. 6, pp. 1634–1641, 2010.

[171] E. Y. Chew, M. L. Klein, T. E. Clemons et al., "No clinically significant association between CFH and ARMS2 genotypes and response to nutritional supplements: AREDS report number 38," *Ophthalmology*, vol. 121, no. 11, pp. 2173–2180, 2014.

[172] Y. Tian, A. Kijlstra, R. L. P. van der Veen, M. Makridaki, I. J. Murray, and T. T. J. M. Berendschot, "Lutein supplementation

leads to decreased soluble complement membrane attack complex sC5b-9 plasma levels," *Acta Ophthalmologica*, vol. 93, no. 2, pp. 141–145, 2015.

[173] G. Chen, R. Tzekov, W. Li, F. Jiang, S. Mao, and Y. Tong, "Pharmacogenetics of complement factor H Y402H Polymorphism and treatment of neovascular AMD with anti-VEGF agents: a meta-analysis," *Scientific Reports*, vol. 5, Article ID 14517, 2015.

[174] G. H. S. Buitendijk, E. Rochtchina, C. Myers et al., "Prediction of age-related macular degeneration in the general population: The three continent AMD consortium," *Ophthalmology*, vol. 120, no. 12, pp. 2644–2655, 2013.

[175] F. Grassmann, L. G. Fritsche, C. N. Keilhauer, I. M. Heid, and B. H. F. Weber, "Modelling the genetic risk in age-related macular degeneration," *PLoS ONE*, vol. 7, no. 5, Article ID e37979, 2012.

[176] G. H. S. Buitendijk, N. Amin, A. Hofman, C. M. van Duijn, J. R. Vingerling, and C. C. W. Klaver, "Direct-to-consumer personal genome testing for age-related macular degeneration," *Investigative Ophthalmology & Visual Science*, vol. 55, no. 10, pp. 6167–6174, 2014.

[177] R. R. J. Kalf, R. Mihaescu, S. Kundu, P. De Knijff, R. C. Green, and A. C. J. W. Janssens, "Variations in predicted risks in personal genome testing for common complex diseases," *Genetics in Medicine*, vol. 16, no. 1, pp. 85–91, 2014.

[178] B. Simone, W. Mazzucco, M. R. Gualano et al., "The policy of public health genomics in Italy," *Health Policy*, vol. 110, no. 2-3, pp. 214–219, 2013.

[179] R. Troutbeck, S. Al-Qureshi, and R. H. Guymer, "Therapeutic targeting of the complement system in age-related macular degeneration: a review," *Clinical & Experimental Ophthalmology*, vol. 40, no. 1, pp. 18–26, 2012.

[180] Z. Yehoshua, C. A. D. A. G. Filho, R. P. Nunes et al., "Systemic complement inhibition with eculizumab for geographic atrophy in age-related macular degeneration: The COMPLETE study," *Ophthalmology*, vol. 121, no. 3, pp. 693–701, 2014.

[181] W. Rhoades, D. Dickson, and D. V. Do, "Potential role of lampalizumab for treatment of geographic atrophy," *Clinical Ophthalmology*, vol. 9, pp. 1049–1056, 2015.

Hindawi
BioMed Research International
Volume 2018, Article ID 3148137, 8 pages
https://doi.org/10.1155/2018/3148137

Research Article

Polymorphisms of TNF-α -308 G/A and IL-8 -251 T/A Genes Associated with Urothelial Carcinoma: A Case-Control Study

Chia-Chang Wu,[1,2,3] Yung-Kai Huang,[4] Chao-Yuan Huang,[5] Horng-Sheng Shiue,[6] Yeong-Shiau Pu,[5] Chien-Tien Su,[1,7] Ying-Chin Lin,[8,9,10] and Yu-Mei Hsueh[10,11]

[1] *School of Public Health, College of Public Health and Nutrition, Taipei Medical University, Taipei 110, Taiwan*
[2] *Department of Urology, School of Medicine, College of Medicine, Taipei Medical University, Taipei 110, Taiwan*
[3] *Department of Urology, Shuang Ho Hospital, Taipei Medical University, New Taipei City 235, Taiwan*
[4] *School of Oral Hygiene, College of Oral Medicine, Taipei Medical University, Taipei 110, Taiwan*
[5] *Department of Urology, National Taiwan University Hospital, College of Medicine, National Taiwan University, Taipei 100, Taiwan*
[6] *Department of Chinese Medicine, Chang Gung Memorial Hospital and Chang Gung University, College of Medicine, Taoyuan 333, Taiwan*
[7] *Department of Family Medicine, Taipei Medical University Hospital, Taipei Medical University, Taipei 110, Taiwan*
[8] *Department of Family Medicine, School of Medicine, College of Medicine, Taipei Medical University, Taipei 110, Taiwan*
[9] *Department of Health Examination, Wan Fang Hospital, Taipei Medical University, Taipei 116, Taiwan*
[10] *Department of Family Medicine, Shuang Ho Hospital, Taipei Medical University, New Taipei City 235, Taiwan*
[11] *Department of Public Health, School of Medicine, College of Medicine, Taipei Medical University, Taipei 110, Taiwan*

Correspondence should be addressed to Yu-Mei Hsueh; ymhsueh@tmu.edu.tw

Received 5 February 2018; Revised 1 April 2018; Accepted 10 April 2018; Published 21 May 2018

Academic Editor: Sajib Chakraborty

Cigarette smoking and exposure to environmental tobacco smoke are well-known risk factors for urothelial carcinoma (UC). We conducted a hospital-based case-control study involving 287 UC cases and 574 cancer-free controls to investigate the joint effects of cigarette smoking and polymorphisms of inflammatory genes on UC risk. Tumor necrosis factor alpha (TNF-α) -308 G/A and interleukin-8 (IL-8) -251 T/A polymorphisms were determined using a polymerase chain reaction-restriction fragment length polymorphism method. People who had ever smoked and those who were exposed to environmental tobacco smoke had significantly increased UC odds ratios (ORs) of 1.65 and 1.68, respectively. Participants who had smoked more than 18 pack-years had a significantly increased UC OR of 2.64. People who had ever smoked and who carried the A/A genotype of the *TNF-α* -308 G/A polymorphism had a significantly higher UC OR (10.25) compared to people who had never smoked and who carried the G/G or G/A genotype. In addition, people who had ever smoked and who carried the *IL-8* -251 T/T genotype had a significantly increased UC OR (3.08) compared to people who had never smoked and who carried the T/A or A/A genotype. In a combined analysis of three major risk factors (cumulative cigarette smoking, the *TNF-α* -308 A/A genotype, and the *IL-8* -251 T/T genotype), subjects with any one, any two, and all three risk factors experienced significantly increased UC ORs of 1.55, 2.89, and 3.77, respectively, compared to individuals with none of the risk factors. *Conclusions*. Our results indicate that the combined effects of cumulative cigarette exposure and the *TNF-α* -308 A/A genotype and/or the *IL-8* -251 T/T genotype on UC OR showed a significant dose-response relationship.

1. Introduction

The bladder is the most common site of urothelial carcinoma (UC), a multifactorial malignancy influenced by exogenous exposure to environmental risk factors and molecular variations in metabolism-related genes [1]. Cigarette smoking is the major risk factor for bladder cancer, and epidemiological studies have indicated that cigarette smokers have a 2~4-fold increased risk of bladder cancer [2]. Cigarettes contain approximately 60 chemical carcinogens, including polycyclic

aromatic hydrocarbons, aromatic amines, and N-nitroso compounds, which are associated with the development of bladder cancer [3]. Cigarette smoke contains free radicals and induces oxidative stress, which is associated with the development of bladder cancer [4, 5].

Oxidative stress can induce proinflammatory cytokines such as tumor necrosis factor alpha (TNF-α) and interleukin-8 (IL-8), which are involved in the development of various malignancies [6, 7]. Exposure to cigarette smoke can enhance TNF-α expression through upregulating the activator protein, AP-1 [8]. TNF-α is involved in the immune response during the intravesical instillation of bacillus Calmette-Guerin [9]. Previous studies reported that cigarette smoking can induce inflammation that is characterized by increased levels of cytokines such as TNF-α and IL-8 [10, 11]. IL-8 is a proinflammatory chemokine that is secreted by various cell types. Studies showed the chronic inflammation is involved in various tumorigenesis steps. TNF-α initiates signaling pathways that activate proinflammatory gene expression via the transcription factor; nuclear factor-kappa B (NF-κB) is also produced by tumors and acts as an endogenous tumor promoter. Cytokines, like IL-6 and IL-8, are also involved in transformation and angiogenesis, respectively [12]. Environmental-genetic associations with tobacco smoke combined with genetic polymorphisms of inflammation-related genes provide additional bladder cancer risk.

The polymorphism of *TNF-α* gene (-308 G/A, rs1800629) is located in promoter and has functional impact on the TNF-α expression [13–15]. Compared to SNPs of TNF-α, -308 G/A polymorphism was investigated and found to be related to several cancers, including breast, gastric, and bladder cancers [13, 16–18]. However, results from previous studies were inconsistent. The *IL-8* gene is located on chromosome 4q13-q21, and several polymorphisms were identified in this gene [19]. A common polymorphism at the promoter region (-251 T/A, rs4073) was reported to influence the transcriptional activity of *IL-8*, and it was identified to be associated with various cancer risks in Asian group [6]. Therefore, these findings raise the possibility that genetic variations in the *TNF-α* and *IL-8* genes may modify the risk of UC.

To investigate the effects of *TNF-α* -308 G/A and *IL-8* -251 T/A polymorphisms on the UC risk, we conducted a hospital-based case-control study. We also examined the combined effects of cumulative cigarette exposure, the *TNF-α* -308 A/A genotype, and the *IL-8* -251 T/T genotype on UC risk.

2. Material and Methods

2.1. Study Population. This study involved 861 participants enrolled from the Departments of Urology and those undergoing a general health examination at National Taiwan University Hospital, Taipei Medical University Hospital, and Taipei Municipal Wan Fang Hospital between September 2002 and May 2009. In total, 287 UC cases were included (with a mean age of 62.95 ± 13.62 years). Each case was diagnosed with histopathological confirmation, which was performed using routine urological practices and verified by board-certified pathologists. In total, 574 age- and gender-matched cancer-free controls (with a mean age of 62.56 ± 13.50 years) were recruited from a hospital-based pool. All participants provided informed consent before the questionnaire interview and biospecimen collection. The Research Ethics Committee of National Taiwan University Hospital (Taipei, Taiwan) approved this study, and this study complied with the World Medical Association *Declaration of Helsinki*.

2.2. Questionnaire Interview and Biospecimen Collection. Well-trained investigators interviewed each patient using a structured questionnaire. Information collected by the questionnaire included demographic characteristics and lifestyle habits such as cigarette smoking, secondhand smoke exposure, betel nut chewing, alcohol, tea, and coffee consumption, exposure to occupational and environmental carcinogens such as pesticides, and a family history of disease. Study subjects who had smoked more than 100 cigarettes during their lifetime were regarded as people who had ever smoked, while those who had smoked fewer than 100 cigarettes were defined as people who had never smoked. Environmental tobacco smoke (secondhand smoke exposure) was assessed through a questionnaire asking participants whether anyone had ever smoked around them. A 6~8-ml sample of venous blood was drawn from each participant for genotype determination.

2.3. Genotyping of the TNF-α -308 G/A and IL-8 -251 T/A Polymorphisms. Genomic DNA was extracted from the buffy coat of peripheral blood using standard methods and stored at −80°C. Genotyping was completed using a polymerase chain reaction-restriction fragment length polymorphism (PCR-RFLP) method modified from a study by Duarte et al. [20]. Briefly, the following primer sets were designed for the *TNF-α* -308 G/A polymorphism: 5′-TCCTCCCTGCTCCGATTCCG-3′ (sense) and 5′-AGG CAATAGGTTTTGAGGGCCAT-3′ (antisense). The thermal PCR conditions were as follows: one cycle at 95°C for 5 min; 35 cycles of 95°C for 30 s, 58°C for 30 s, and 72°C for 45 s; and a final extension at 72°C for 10 min. After complete digestion with the NcoI restriction enzyme, the resulting DNA fragments, which represented the *TNF-α* -308 G/A polymorphism, were determined (G/G: 87 and 20 bp; G/A: 107, 87, and 20 bp; and A/A: 107 bp). PCR-RFLP genotyping and sequencing of *TNF-α* -308 G/A are shown in Figure 1(a). For the *IL*-8 -251 T/A polymorphism, the following primers were used: 5′-ATCTTGTTCTAACACCTGCCACTC-3′ (sense) and 5′-TAAAATACTGAAGCTCCACAATTTGG-3′ (antisense) [21]. The PCR conditions were as follows: one cycle at 94°C for 5 min; 35 cycles of 94°C for 50 s, 61°C for 60 s, and 72°C for 55 s; and a final extension at 72°C for 5 min. The genotypes were determined after digestion with the MfeI restriction enzyme for the *IL*-8 -251 T/A polymorphism (T/T: 121 bp; T/A: 121, 82, and 39 bp; and A/A: 82 and 39 bp). PCR-RFLP genotyping and sequencing of *IL*-8 -251 T/A are shown in Figure 1(b). For quality control, genotyping was repeated on a random 10% of the samples.

2.4. Statistical Analysis. A goodness-of-fit Chi-squared test was used to test for Hardy-Weinberg equilibrium (HWE) among the cancer-free controls. Study subjects who had smoked more than 100 cigarettes during their lifetime were

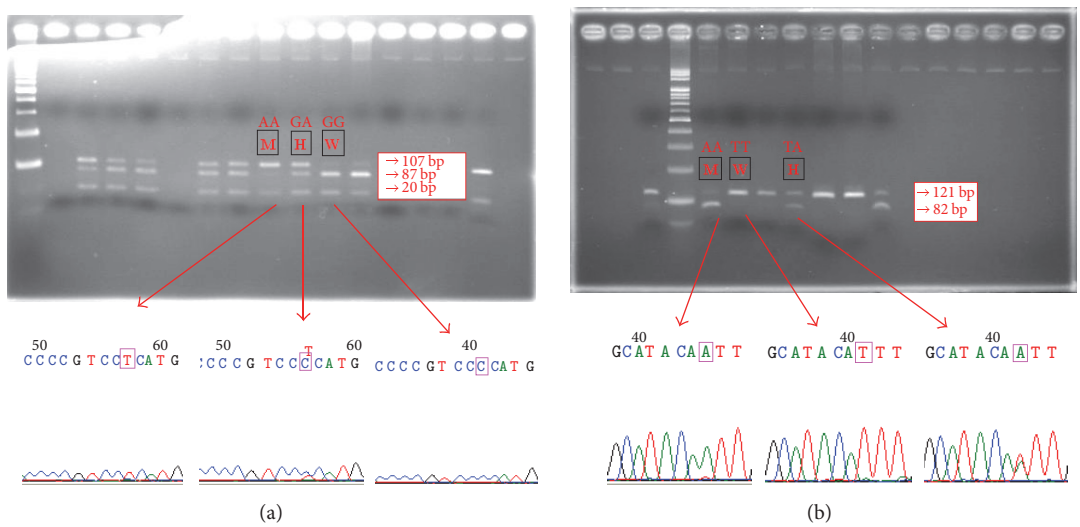

FIGURE 1: PCR-RFLP genotyping and sequencing of *TNF-α* -308 G/A and *IL*-8 -251 T/A. (a) Genotyping of *TNF-α* -308 G/A. Arrows indicated location of AA, GA, and GG. (b) Genotyping of *IL*-8 -251 T/A. Arrows indicated location of AA, TT, and TA.

regarded as people who had ever smoked, while those who had smoked fewer than 100 cigarettes were defined as people who had never smoked. The pack-years of cigarette smoking were calculated using the formula: pack-years = (cigarettes per day ÷ 20) × (number of years smoked). Because of dependent variable (UC) is binary, logistic regression is used to assess the association between UC and related risk factors. The combined effects of cumulative cigarette exposure, the *TNF-α* -308 A/A genotype, and the *IL-8* -251 T/T genotype on the UC risk were estimated by odds ratios (ORs) and associated 95% confidence intervals (CIs) using a multivariate-adjusted logistic regression. All data were analyzed using the Statistical Analysis Software for Windows, ver. 9.2 (SAS Institute, Cary, NC). p values of < 0.05 were considered statistically significant.

3. Results

No significant differences were found in age or gender between the UC cases and cancer-free controls. Occasional alcohol drinkers had a significantly lower OR for UC than people who had never consumed alcohol. After adjusting for age, gender, educational level, alcohol consumption, and other risk factors, people who had ever smoked had a significantly higher UC OR of 1.65 (95% CI: 1.19~2.27) compared to people who had never smoked. Individuals who were exposed to environmental tobacco smoke had a significantly higher UC OR (1.68, 95% CI: 1.22~2.30) than those with no exposure. Frequencies of the *TNF-α* -308 A/A genotype and the *IL-8* -251 T/T genotype among controls fit HWE (χ^2 = 0.99, $p > 0.05$; χ^2 = 1.27, $p > 0.05$, resp.). The genotype distribution of the control did not show significant difference from the Hardy-Weinberg equilibrium values. Subjects who carried the *TNF-α* -308 A/A genotype had a significantly increased OR for UC (3.56, 95% CI: 1.03~12.28) compared to those with the G/G or G/A genotype. Subjects who carried the A/A genotype of the *IL-8* -251 T/A polymorphism had a significantly lower OR for UC (0.52, 95% CI: 0.27~0.99) than those carrying the T/T genotype (data not shown).

After stratification by the *TNF-α* -308 G/A and *IL-8* -251 T/A genotypes, individual characteristics, including age, gender, educational level, cigarette smoking, environmental tobacco smoke exposure, and alcohol consumption, displayed no significantly different distributions in either of the polymorphism strata (Table 1). In terms of the effect of the cigarette smoking profile on the OR for UC, we found significantly increased ORs (95% CI) for UC of 2.33 (1.52~3.55), 2.74 (1.77~4.24), and 2.64 (1.75~3.99) for subjects who had smoked more than 1 pack per day, individuals who had smoked for more than 31 years, and those who had smoked more than 18 pack-years, respectively (Table 2).

The joint effects of cigarette smoking, the *TNF-α* -308 A/A genotype, and the *IL-8* -251 T/T genotype on the OR for UC after multivariate adjustment are shown in Figure 2. People who had ever smoked and who carried the A/A genotype of the *TNF-α* -308 G/A polymorphism had a significantly higher UC OR of 10.25 than people who had never smoked and who carried the G/G or G/A genotype. In addition, people who had ever smoked who carried the T/T genotype of the *IL-8* -251 T/A polymorphism had a significantly increased UC OR of 3.08 compared to those who carried the T/A or A/A genotype.

Furthermore, we included three major risk factors (cumulative cigarette smoking, the *TNF-α* -308 A/A genotype, and the *IL-8* -251 T/T genotype) in a combined analysis (Table 3). Compared to individuals who did had none of these risk factors, significantly increased ORs (95% CI) for UC were 1.55 (1.03~2.35), 2.89 (1.70~4.93), and 3.77 (2.16~6.56) for study subjects with any one, any two, and all risk factors, respectively; these risk factors showed a significant dose-response relationship (p for trend < 0.0001).

Table 1: Sociodemographic characteristics of 287 urothelial carcinoma cases and 574 matched noncancer controls, stratified by *TNF-α* and *IL-8* genotypes.

Variable	TNF-α			IL-8		
	GG/GA	AA	*p* value	TT	TA/AA	*p* value
Age (years)	62.82 ± 13.56	59.18 ± 9.45	0.38	60.83 ± 13.55	65.59 ± 12.99	<0.0001
Gender						
Male	591 (69.53)	10 (90.91)	0.19	357 (69.89)	244 (69.71)	0.96
Female	259 (30.47)	1 (9.09)		154 (30.14)	106 (30.29)	
Educational level						
Illiterate or elementary school	229 (27.00)	1 (9.09)	0.41	124 (24.31)	106 (30.37)	0.05
Junior or senior high school	304 (35.85)	5 (45.45)		181 (35.49)	128 (36.68)	
College or university	315 (37.15)	5 (45.45)		205 (40.20)	115 (32.95)	
Cigarette smoking						
No	526 (61.88)	5 (45.45)	0.35	329 (64.38)	202 (57.71)	0.05
Yes	324 (38.12)	6 (54.55)		182 (35.62)	148 (42.29)	
Environmental tobacco exposure						
No	411 (51.31)	6 (54.55)	0.65	250 (51.98)	167 (50.45)	0.10
Yes	290 (36.20)	5 (45.45)		182 (37.84)	113 (34.14)	
Alcohol consumption						
No	497 (58.47)	5 (45.45)	0.68	297 (58.12)	205 (58.57)	0.11
Yes	167 (19.65)	3 (27.27)		111 (21.72)	59 (16.86)	
Occasional	186 (21.88)	3 (27.27)		103 (20.16)	86 (24.57)	

Educational level and environmental tobacco smoke were unavailable for two and 149 of the *TNF-α* GG/GA genotypes, respectively. Educational level and environmental tobacco smoke were unavailable for one and 79 of the *IL-8* TT genotypes, respectively. Educational level and environmental tobacco smoke were unavailable for one and 70 of the *IL-8* TA/AA genotypes, respectively.

Table 2: Dose-response relationship between cigarette smoking profiles and the odds ratio (OR) for urothelial carcinoma (UC).

	UC cases	Controls	Age/sex-adjusted OR (95% CI)	Multivariate-adjusted OR (95% CI)
Cigarette smoking (packs/day)				
0	152	379	1.00	1.00
0~1	108	169	1.69 (1.10~2.61)*	1.90 (1.19~3.03)*
>1	27	26	2.39 (1.62~3.54)*	2.33 (1.52~3.55)*
Cigarette smoking (years)				
0	153	379	1.00	1.00
0~31	49	101	1.46 (0.93~2.27)	1.49 (0.92~2.39)
>31	85	94	2.59 (1.74~3.86)*	2.74 (1.77~4.24)*
Cigarette smoking (pack years)				
0	153	379	1.00	1.00
0~18	35	81	1.19 (0.73~1.94)	1.30 (0.78~2.19)
>18	99	114	2.62 (1.80~3.81)*	2.64 (1.75~3.99)*

Multivariate ORs were adjusted for age, gender, educational level, and alcohol consumption. * $p < 0.05$. CI: confidence interval.

Table 3: Adjusted odds ratios (ORs) of urothelial carcinoma risk by cumulative cigarette exposure, the tumor necrosis factor (*TNF*)-α -308 A/A genotype, and the interleukin (*IL*)-8 -251 T/T genotype.

Risk factors	Age/sex-adjusted OR (95% CI)	Multivariate-adjusted OR (95% CI)
None	1.00	1.00
Any one risk factor	1.47 (0.99~2.19)	1.55 (1.03~2.35)*
Any two risk factors	2.69 (1.63~4.43)*	2.89 (1.70~4.93)*
All three risk factors	3.61 (2.15~6.07)*	3.77 (2.16~6.56)*
	$p_{trend} < 0.0001$	$p_{trend} < 0.0001$

The three risk factors were cumulative cigarette exposure,the *TNF*-α -308 A/A genotype, and the *IL*-8 -251 T/T genotype. Multivariate ORs were adjusted for age, gender, educational level, and alcohol consumption. * $p < 0.05$. CI: confidence interval.

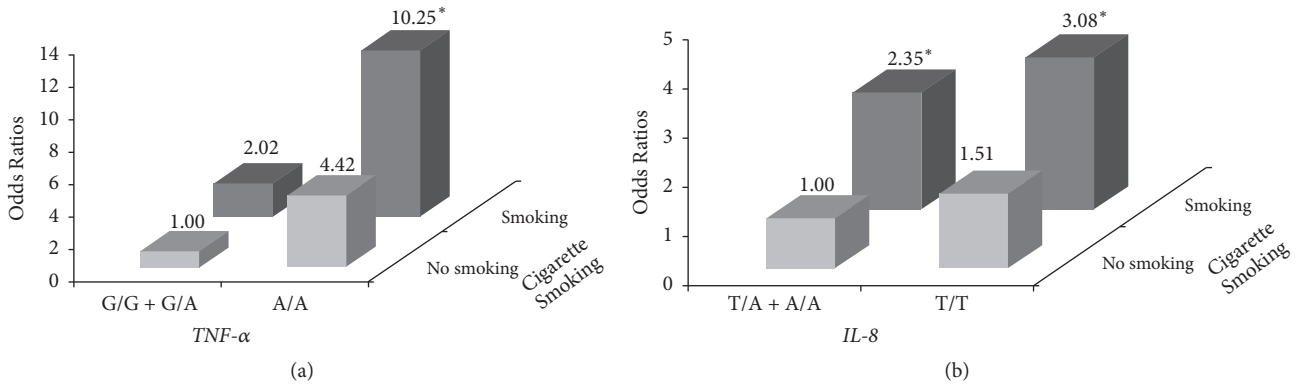

Figure 2: Joint effects of (a) the tumor necrosis factor α (TNF-α) genotype and cigarette smoking and (b) the interleukin 8 (IL-8) genotype and cigarette smoking on the urothelial carcinoma (UC) risk after adjusting for age, gender, educational level, and alcohol consumption. * $p < 0.05$.

4. Discussion

In this study, the risk of UC in smokers was 2~2.5-fold compared to nonsmokers. This result was consistent with a previous study [22]. In our previous study, there were no significant differences in the association of age and gender between UC cases and controls. UC conventional risk factors such as status smoking carried 1.65-fold risk [23]. Smokers or people who had ever smoked and carried *TNF*-α -308 A/A genotype and the *IL-8* -251 T/T genotype had a higher risk of UC compared to nonsmokers. Gene-environment interactions are a potential way to identify individuals' risk. This study analyzed the combined effect of three major risk factors (high cumulative cigarette smoking, the *TNF*-α -308 A/A genotype, and the *IL-8* -251 T/T genotype) and found dose-response relationships for UC risk in study subjects with

any one risk factor, any two risk factors, and all three risk factors.

Functional polymorphisms of inflammatory genes can affect cytokine production. A previous study reported that the *TNF-α* -308 G/A polymorphism contributes to carcinogenesis and that the variant A allele was associated with increased TNF-α expression [14]. A Korean study also reported that the *TNF-α* -308 G/A polymorphism was significantly associated with the tumor stage and grade of bladder cancer [24]. In this study, subjects who carried the A/A genotype of the *TNF-α* -308 G/A polymorphism had a significantly higher OR for UC than those with the G/G or G/A genotype. These results suggest that the *TNF-α* -308 G/A polymorphism might regulate angiogenesis, which plays a role in the invasion and metastasis of various tumors. However, another study did not report the same findings in urinary stone diseases or bladder cancer in Taiwan [25].

Compared to previous studies, differences in genotype frequencies may have been due to ethnic variations. The A/A genotype frequency of TNF-α in the case and control groups of this study was 2.23% and 0.67%, respectively, and the TNF-αA/A genotype carried a 3.56-fold risk of UC. A meta-analysis study showed that the A/A genotype frequency of TNF-α in cervical cancer cases and controls was 0.97%~7.33% and 0%~6.78%, respectively. The TNF-α A/A genotype significantly elevating risks of cervical cancer was found in a Caucasian population (OR: 2.09, 95% CI: 1.34~3.25) [26]. Although the TNF-α A/A genotype frequency was very low in Japanese (141 bladder cancer patients and 173 control subjects), the allelic frequency of patients (3.5%) was higher than that in controls (0.6%) [27]. A previous study indicated that cigarette smoking activates systemic inflammation and upregulates TNF-α expression in an animal model [8]. Another study also found that the circulating TNF-α level was higher in people who had ever smoked compared to people who had never smoked [17]. A study also showed that the A allele polymorphism of TNF-α -308 genotypes was associated with HCC risk in Taiwan males who were exposed to cigarette and alcohol [28]. In the present study, we observed a significant combined effect of cigarette smoking and the A/A genotype of the *TNF-α* -308 polymorphism on the OR (10.25) for UC. This finding suggests that the *TNF-α* -308 G/A polymorphism can modify the OR for UC, especially in people who had ever smoked.

IL-8 plays a critical role in inflammation. A common single-nucleotide polymorphism at the -251 position of the *IL-8* promoter region can influence its expression and may increase one's susceptibility to bladder cancer [29]. In the present study, subjects who carried the A/A genotype had a significantly decreased OR for UC. Previous studies explored the association between the *IL-8* -251 T/A polymorphism and various cancer risks, but the findings were inconsistent [29, 30]. Some researchers reported that the *IL-8* -251A allele has significantly higher promoter activity than the -251T allele [31]. However, another study reported that the *IL-8* -251T allele had significantly higher transcriptional activity than the -251A allele of the *IL-8* gene [32]. In addition, previous studies indicated that cigarette smoking causes chronic inflammation characterized by increased levels of cytokines, such as IL-8 [10, 11]. IL-8 plays a role in assisting cancer cells to eschew stress and induce apoptosis and is also involved in angiogenesis, tumor growth, and metastasis [33]. A meta-analysis showed that IL-8 -251A/T polymorphism has significantly elevated risks of cancer in Asian population [34]. It is possible that the increased IL-8 expression induced by cigarette smoking may modify the carcinogenesis of UC. In the present study, we found a significant joint effect of cigarette smoking and the T/T genotype of the -251 T/A polymorphism on the OR for UC (OR = 3.08). This suggests that the -251 T/A polymorphism can modify the UC risk, especially in people who have ever smoked.

Single-nucleotide polymorphisms of genes can increase disease susceptibilities via affect gene expression. Silico analysis is a novel computational approach to identify potential SNPs causing transcription factor binding affinities to change and influence regulatory functions of genes [35]. Since polymorphisms have been identified and their transition is considered to be an important enhancer of transcriptional activation associated with elevated levels genes expression, structural analysis study showed that TNF-α protein stability was impacted by amino acid residue substitutions of P84L (rs4645843) and A94T (rs1800620) [36]. The effect of IL-8 SNPs and protein structure in disease risk was also conducted by silico analysis [37]. Although the level of confidence is too high in some cases, it is still too low for clinical purpose, which is a main limitation of silico analysis programs [38].

Our study has some limitations. We only investigated one polymorphism located in the promoter region, which might not entirely account for the functions of the *TNF-α* and *IL-8* genes. More functional polymorphisms of the *TNF-α* and IL-8 genes should be included in future analyses with larger samples to validate our findings. Other proinflammatory cytokines such as NF-κB also need to be further investigated. In addition, interactions of cigarette smoking and other cytokines on the UC risk should be explored in the future.

5. Conclusions

We found a dose-response relationship between the number of risk factors and the OR for UC. These findings suggest that individuals who carry high-risk genotypes, including the *TNF-α* -308 A/A genotype and the *IL-8* -251 T/T genotype, and who experience cumulative cigarette smoking have a significantly increased OR for UC in a dose-response manner.

Data Availability

The data used to support the findings of this study are included within the article.

Conflicts of Interest

The authors have disclosed all financial and interpersonal relationships that present potential conflicts of interest.

Authors' Contributions

Dr. Chia-Chang Wu and Dr. Yung-Kai Huang contributed equally to this work.

Acknowledgments

This study was supported by Grants (NSC90-2320-B-038-021, NSC91-3112-B-038-0019, NSC92-3112-B-038-001, NSC93-3112-B-038-001, NSC94-2314-B-038-023, NSC95-2314-B-038-007, NSC96-2314-B038-003, NSC97-2314-B-038-015-MY3, NSC100-2314-B-038 -026, and NSC101-2314-B-038-051-MY3) from National Science Council, Taiwan, and by Grants (MOST103-2314-B-038-021-MY2 (1-2), MOST103-2314-B-038-021-MY2 (2-2), and MOST 105-2314-B-038-082) from Ministry of Science and Technology, Taiwan, to YM-H.

References

[1] D. Volanis, T. Kadiyska, A. Galanis, D. Delakas, S. Logotheti, and V. Zoumpourlis, "Environmental factors and genetic susceptibility promote urinary bladder cancer," *Toxicology Letters*, vol. 193, no. 2, pp. 131–137, 2010.

[2] C. Samanic, M. Kogevinas, M. Dosemeci et al., "Smoking and bladder cancer in Spain: Effects of tobacco type, timing, environmental tobacco smoke, and gender," *Cancer Epidemiology, Biomarkers & Prevention*, vol. 15, no. 7, pp. 1348–1354, 2006.

[3] S. S. Hecht, "Tobacco carcinogens, their biomarkers and tobacco-induced cancer," *Nature Reviews Cancer*, vol. 3, no. 10, pp. 733–744, 2003.

[4] S. S. Hecht, "Human urinary carcinogen metabolites: Biomarkers for investigating tobacco and cancer," *Carcinogenesis*, vol. 23, no. 6, pp. 907–922, 2002.

[5] IARC, *Monographs on the Evaluation of the Carcinogenic Risk of Chemicals to Humans: Tobacco Smoking*, WHO, Lyon, France, 1986.

[6] N. Wang, R. Zhou, C. Wang et al., "−251 T/A polymorphism of the interleukin-8 gene and cancer risk: a HuGE review and meta-analysis based on 42 case-control studies," *Molecular Biology Reports*, vol. 39, no. 3, pp. 2831–2841, 2012.

[7] P. Zhou, G.-Q. Lv, J.-Z. Wang et al., "The TNF-Alpha-238 polymorphism and cancer risk: a meta-analysis," *PLoS ONE*, vol. 6, no. 7, Article ID e22092, 2011.

[8] Y.-T. Li, B. He, and Y.-Z. Wang, "Exposure to cigarette smoke upregulates AP-1 activity and induces TNF-alpha overexpression in mouse lungs," *Inhalation Toxicology*, vol. 21, no. 7, pp. 641–647, 2009.

[9] K. Taniguchi, S. Koga, M. Nishikido et al., "Systemic immune response after intravesical instillation of bacille Calmette-Guerin (BCG) for superficial bladder cancer," *Clinical & Experimental Immunology*, vol. 115, no. 1, pp. 131–135, 1999.

[10] S. E. Tanni, N. R. Pelegrino, A. Y. Angeleli, C. Correa, and I. Godoy, "Smoking status and tumor necrosis factor-alpha mediated systemic inflammation in COPD patients," *Journal of Inflammation*, vol. 7, article 29, 2010.

[11] H.-Y. Wang, Y.-N. Ye, M. Zhu, and C.-H. Cho, "Increased interleukin-8 expression by cigarette smoke extract in endothelial cells," *Environmental Toxicology and Pharmacology*, vol. 9, no. 1-2, pp. 19–23, 2000.

[12] B. B. Aggarwal, S. Shishodia, S. K. Sandur, M. K. Pandey, and G. Sethi, "Inflammation and cancer: how hot is the link?" *Biochemical Pharmacology*, vol. 72, no. 11, pp. 1605–1621, 2006.

[13] H. P. Marsh, N. A. Haldar, M. Bunce et al., "Polymorphisms in tumour necrosis factor (TNF) are associated with risk of bladder cancer and grade of tumour at presentation," *British Journal of Cancer*, vol. 89, no. 6, pp. 1096–1101, 2003.

[14] D. Ahirwar, P. Kesarwani, P. K. Manchanda, A. Mandhani, and R. D. Mittal, "Anti- and proinflammatory cytokine gene polymorphism and genetic predisposition: association with smoking, tumor stage and grade, and bacillus Calmette-Guérin immunotherapy in bladder cancer," *Cancer Genetics and Cytogenetics*, vol. 184, no. 1, pp. 1–8, 2008.

[15] K. M. Kroeger, J. H. Steer, D. A. Joyce, and L. J. Abraham, "Effects of stimulus and cell type on the expression of the -308 tumour necrosis factor promoter polymorphism," *Cytokine*, vol. 12, no. 2, pp. 110–119, 2000.

[16] C. Shen, H. Sun, D. Sun et al., "Polymorphisms of tumor necrosis factor-alpha and breast cancer risk: A meta-analysis," *Breast Cancer Research and Treatment*, vol. 126, no. 3, pp. 763–770, 2011.

[17] J. J. Yang, K.-P. Ko, L. Y. Cho et al., "The role of TNF genetic variants and the interaction with cigarette smoking for gastric cancer risk: a nested case-control study," *BMC Cancer*, vol. 9, article 238, 2009.

[18] A. Loktionov, "Common gene polymorphisms, cancer progression and prognosis," *Cancer Letters*, vol. 208, no. 1, pp. 1–33, 2004.

[19] S. K. Ahuja, T. Özçelik, A. Milatovitch, U. Francke, and P. M. Murphy, "Molecular evolution of the human interleukin−8 receptor gene cluster," *Nature Genetics*, vol. 2, no. 1, pp. 31–36, 1992.

[20] I. Duarte, A. Santos, H. Sousa et al., "G-308A TNF-α polymorphism is associated with an increased risk of invasive cervical cancer," *Biochemical and Biophysical Research Communications*, vol. 334, no. 2, pp. 588–592, 2005.

[21] E. Vairaktaris, C. Yapijakis, Z. Serefoglou et al., "The interleukin-8 (-251A/T) polymorphism is associated with increased risk for oral squamous cell carcinoma," *European Journal of Surgical Oncology*, vol. 33, no. 4, pp. 504–507, 2007.

[22] P. Vineis, G. Talaska, C. Malaveille et al., "DNA adducts in urothelial cells: Relationship with biomarkers of exposure to arylamines and polycyclic aromatic hydrocarbons from tobacco smoke," *International Journal of Cancer*, vol. 65, no. 3, pp. 314–316, 1996.

[23] C.-C. Wu, Y.-K. Huang, C.-J. Chung et al., "Polymorphism of inflammatory genes and arsenic methylation capacity are associated with urothelial carcinoma," *Toxicology and Applied Pharmacology*, vol. 272, no. 1, pp. 30–36, 2013.

[24] P. Jeong, E.-J. Kim, E.-G. Kim, S.-S. Byun, C. S. Kim, and W.-J. Kim, "Association of bladder tumors and GA genotype of -308 nucleotide in tumor necrosis factor-alpha promoter with greater tumor necrosis factor-alpha expression," *Urology*, vol. 64, no. 5, pp. 1052–1056, 2004.

[25] F.-J. Tsai, H.-F. Lu, L.-S. Yeh, C.-D. Hsu, and W.-C. Chen, "Lack of evidence for the association of tumor necrosis factor-alpha gene promoter polymorphism with calcium oxalate stone and bladder cancer patients," *Urolithiasis*, vol. 29, no. 6, pp. 412–416, 2001.

[26] F. Pan, J. Tian, C. Ji et al., "Association of TNF-α-308 and -238 Polymorphisms with Risk of Cervical Cancer: A Meta-analysis," *Asian Pacific Journal of Cancer Prevention*, vol. 13, no. 11, pp. 5777–5783, 2012.

[27] N. Nonomura, T. Tokizane, M. Nakayama et al., "Possible correlation between polymorphism in the tumor necrosis factor-beta gene and the clinicopathological features of bladder cancer in Japanese patients," *International Journal of Urology*, vol. 13, no. 7, pp. 971–976, 2006.

[28] M. D. Yang, C. M. Hsu, W. S. Chang et al., "Tumor Necrosis Factor-alpha Genotypes Are Associated with Hepatocellular Carcinoma Risk in Taiwanese Males, Smokers and Alcohol Drinkers," *Anticancer Res*, vol. 35, no. 10, pp. 5417–5423, 2015.

[29] D. K. Ahirwar, A. Mandhani, and R. D. Mittal, "IL-8 -251 T > A Polymorphism is associated with bladder cancer susceptibility and outcome after BCG immunotherapy in a northern Indian cohort," *Archives of Medical Research*, vol. 41, no. 2, pp. 97–103, 2010.

[30] L.-B. Gao, X.-M. Pan, J. Jia et al., "IL-8 -251A/T polymorphism is associated with decreased cancer risk among population-based studies: Evidence from a meta-analysis," *European Journal of Cancer*, vol. 46, no. 8, pp. 1333–1343, 2010.

[31] M. Ohyauchi, A. Imatani, M. Yonechi et al., "The polymorphism interleukin 8 - 251 A/T influences the susceptibility of Helicobacter pylori related gastric diseases in the Japanese population," *Gut*, vol. 54, no. 3, pp. 330–335, 2005.

[32] W.-P. Lee, D.-I. Tai, K.-H. Lan et al., "The -251T allele of the interleukin-8 promoter is associated with increased risk of gastric carcinoma featuring diffuse-type histopathology in Chinese population," *Clinical Cancer Research*, vol. 11, no. 18, pp. 6431–6441, 2005.

[33] D. J. Waugh and C. Wilson, "The interleukin-8 pathway in cancer," *Clinical Cancer Research*, vol. 14, no. 21, pp. 6735–6741, 2008.

[34] Z. Wang, Y. Liu, L. Yang, S. Yin, R. Zang, and G. Yang, "The polymorphism interleukin-8 -251A/T is associated with a significantly increased risk of cancers from a meta-analysis," *Tumor Biology*, vol. 35, no. 7, pp. 7115–7123, 2014.

[35] R. Li, D. Zhong, R. Liu et al., "A novel method for in silico identification of regulatory SNPs in human genome," *Journal of Theoretical Biology*, vol. 415, pp. 84–89, 2017.

[36] B. Dabhi and K. N. Mistry, "In silico analysis of single nucleotide polymorphism (SNP) in human TNF-α gene," *Meta Gene*, vol. 2, pp. 586–595, 2014.

[37] T. C. Dakal, D. Kala, G. Dhiman, V. Yadav, A. Krokhotin, and N. V. Dokholyan, "Predicting the functional consequences of non-synonymous single nucleotide polymorphisms in IL8 gene," *Scientific Reports*, vol. 7, no. 1, article no. 6525, 2017.

[38] D. Tchernitchko, M. Goossens, and H. Wajcman, "In silico prediction of the deleterious effect of a mutation: Proceed with caution in clinical genetics," *Clinical Chemistry*, vol. 50, no. 11, pp. 1974–1978, 2004.